DEFENCE R&D ORGANISATION
MINISTRY OF DEFENCE

Solid Propellant Chemistry

Condensed Phase Behaviour of Ammonium Perchlorate-Based Solid Propellants

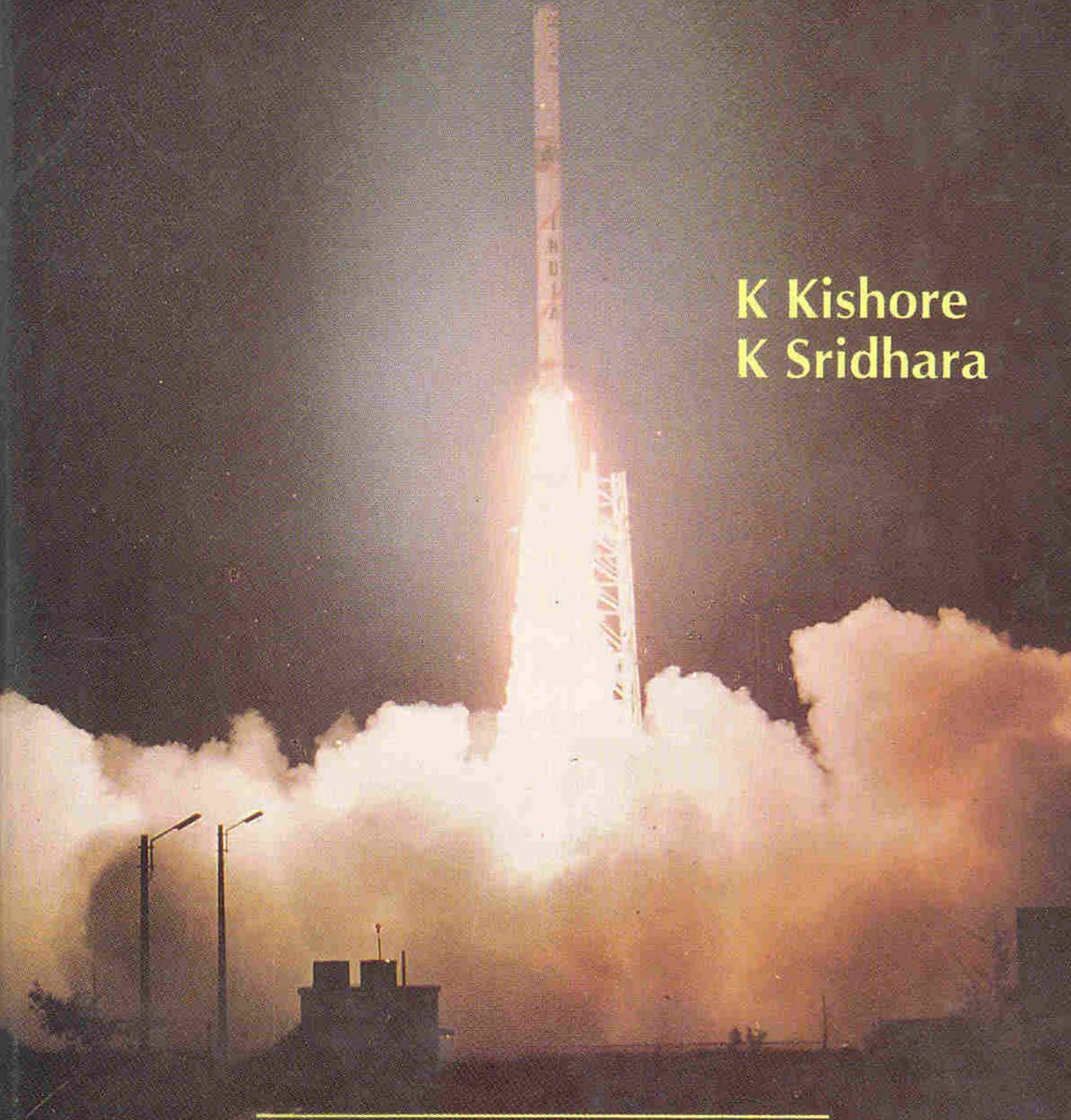

K Kishore
K Sridhara

SOLID PROPELLANT CHEMISTRY

Condensed Phase Behaviour of Ammonium Perchlorate-Based Solid Propellants

SOLID PROPELLANT CHEMISTRY

Condensed Phase Behaviour of Ammonium Perchlorate-Based Solid Propellants

K Kishore & K Sridhara

Foreword by

Dr APJ ABDUL KALAM
Scientific Adviser to Raksha Mantri

DEFENCE RESEARCH & DEVELOPMENT ORGANISATION
MINISTRY OF DEFENCE
NEW DELHI-110 011
1999

DRDO Monographs/Special Publications Series

SOLID PROPELLANT CHEMISTRY: CONDENSED PHASE BEHAVIOUR OF AMMONIUM PERCHLORATE-BASED SOLID PROPELLANTS

K Kishore & K Sridhara

Production

Printing	*Cover Design*	*Marketing*
SB Gupta	SK Saxena	RK Dua

ISBN: 81-86514-02-6

Printed and published by Director, DESIDOC, Metcalfe House, Delhi-110 054.

Dedicated to

Indian Scientists and Engineers
working on Propellants

CONTENTS

FOREWORD

Despite rapid growth and developments in different areas of advanced solid rocket propellants such as composite modified double base (CMDB), fuel rich propellants (FRP) for IRR applications, ammonium dinitramide (ADN) and hydrazinium nitroformate (HNF) based propellants, during last few decades, composite propellants (CP) are still widely used for different military and space applications. A number of research groups are engaged in the basic and applied research on the combustion of composite solid propellants. Although the literature on various aspects of combustion of CP is enormous, but it is scattered. There has been considerable interest in understanding the role and importance of condensed phase and flame zone reactions in controlling the burning process. The combustion behaviour of CP is characterised by the steady linear regression rate of the burning surface and is regarded as the most important and critical performance parameter for the rocket designer.

While Chapter 1 of the present monograph introduces the subject of combustion of CP, Chapter 2 deals with the effect of particle size and its distribution on condensed phase reactions, measurement of burning rates, and the factors affecting the burning behaviour. In addition, the combustion of CP in low, medium and high pressure domains has also been discussed. The effect of other variables affecting burning rate like oxidizer, shape, size, size distribution and purity, fuel and metal content, shape and particle size of metals, type and ratio of binder-plasticizer and total solid content (solid loading), influence of catalysts and additives, initial pressure and initial temperatures, effect of processing parameters, and ageing behaviour are also discussed. The oxidizer content not only affects the energy in terms of specific impulse (I_{sp}), but also the mechanical properties of the resultant propellant, safety and cost. While comparing the properties of the various oxidizers namely, ammonium perchlorate (AP), cyclo-1,3,5 trimethylene-2,4,6 trinitramine (RDX), octahydro-1,3,5,7-tetranitro-1,3,5,7, tetrazocine (HMX), ADN, ammonium nitrate (AN), one must look for higher performance, good compatibility and stability, adaptability to tailor a wide burning rate range, and relative insensitivity, low cost and availability.

Chapter 3 essentially reviews the thermal decomposition behaviour of AP (proton transfer, electron transfer) and effect of pressure on the thermal decomposition behaviour. Various binders (polyesters, polyethers, polyurethanes, polybutadienes, etc.) have been used in CP formulations. Chemical and structural characteristics of the binder and its role in the overall combustion of CP is very important. This aspect has been brought out in Chapter 4 including salient features of fuel-binder pyrolysis and condensed phase and gas phase combustion behaviour of fuel-cum-binder. The authors have also covered the modelling studies in each subchapter, the importance of which does not need overemphasis. Ferrocene compounds, which have been used to increase burn rates (100-150 per cent) of CP are prone to migration and affect the ageing process. The authors have covered these aspects in Chapter 5. Ageing is a very important aspect that has to be considered when formulating propellants for various missions. Various factors that affect the safe and useful life of the propellants, kinetics and mechanism of ageing, estimation of safe-life, and ways and means to increase the life of CP are considered by the authors in Chapter 6.

To obtain higher energy (I_{sp}), superior mechanical properties, new and more energetic binders and oxidizers are being searched continuously. Oxetanes—bis-azidomethyl oxetane (BAMO) and azidomethyl methyl oxetane (AMMO)—and their derivatives are attracting considerable attention due to their low polydispersity, low glass transition temperature (T_g), higher energy and easy handling characteristics. Glycidyl azide polymer (GAP) is finding applications in CP, low vulnerability ammunition (LOVA) propellants for guns, and plastic bonded explosives (PBX). Chapter 7 is therefore devoted to high energy binders, oxidizers and advanced propellants. To overcome the limitations of AP-based propellants, various other environment-friendly oxidizers like ADN and HNF are being evaluated. The properties of these two oxidizers are explained in detail in Chapter 7. The authors' views on the future directions of research in the area of combustion of composite propellants are covered in Chapter 8.

This monograph is the most comprehensive review of condensed phase behaviour of AP-based solid propellants and covers all important aspects of AP-based CP. The language is very lucid and easy to understand. Prof. K Kishore is a well known propellant and polymer chemist and a renowned teacher and has incorporated his wide and rich experience both as a researcher and a teacher in the form of this monograph. It was indeed a delightful experience for me to work with Prof. Kishore during the preparation of the monograph. I am confident this monograph will serve as a trustworthy reference book in the field of CP to all scientists/ engineers of aerospace engineering.

APJ Abdul Kalam

(APJ Abdul Kalam)
SA to RM and Secretary Defence R&D
Ministry of Defence

PREFACE

There are about half a dozen books dealing with propellant chemistry but much of the information available therein is rather old and none of them discusses the condensed phase combustion chemistry of solid propellants in detail. The present monograph is the first of its kind in which the material accumulated over several decades has been sifted from literature and articulated to highlight the importance of condensed phase chemistry which seems to be vital for understading the key phenomena like burning rate modulation and ageing. Besides, the subtle roles of binders, oxidizers and catalysts have been brought out. It has also been demonstrated as to how condensed phase chemistry is vital in understanding the commonly observed phenomena in solid propellants like extinction, intermittent, plateau and flameless combustions.

In defence and space laboratories and also in some private companies, a large number of scientists and engineers are involved in work on propellants. This monograph will be extremely useful for this large community, not only in helping them to assess the progress made in AP-based composite solid propellants but also to grasp the key phenomena in an organised manner. It will also serve as a useful information source for those who wish to enter the fascinating field of solid propellant combustion. Besides, there are many academic institutions and universities where propellant chemistry is taught either as an independent subject or under the general courses in combustion or fuel science and technology. This monograph will serve as a good reference book not only for those opting for these courses but also for those engaged in basic research in propellant chemistry. This monograph is aimed at catering to the information needs of readers at postgraduate and research levels. The readers of course are required to have some exposure in propellants.

The authors are extremely thankful to the Indian Space Research Organisation (ISRO), Bangalore and ISRO-Indian Institute of Science-Space Technology Cell for providing funds for writing this monograph. The authors are also thankful to ISRO for agreeing for the open publication of the monograph by DRDO and to have no claim on its copyright from DRDO. They are also thankful to Mr S Vasudeva Murthy for the assistance rendered in the preparation of the manuscript.

Bangalore
January 1999

K Kishore
K Sridhara

CHAPTER 1

INTRODUCTION

Man's desire to explore outer space and build a strong defence edifice has culminated in the development of space vehicles and missiles in which composite solid propellants (CSP) are the major source of chemical energy[1,2]. Being complex mixtures, their combustion behaviour too is quite complex and is not yet fully understood. CSP[3-6] are heterogeneous mixtures consisting of a large proportion of oxidizer, usually ammonium perchlorate (AP), and a fuel-cum-binder, generally hydroxy-terminated polybutadiene (HTPB) or carboxy-terminated polybutadiene (CTPB). In addition, they contain curing agents, plasticizers and bonding agents for improving their mechanical properties, and metallic fuel additives and burning rate modifiers for improving specific impulse and burning rate, respectively. A typical CSP composition is given in Table 1.1.

Table 1.1. Typical composition of CSP[6]

Ingredients	*Weight, %*
Ammonium perchlorate	60 - 84
Butadiene polymer	12 - 16
Aluminium	2 - 20
Curing agent(s)	0.2 - 1.0
Stabilizers	0 - 1.0

The chemistry of a CSP formulation and its combustion is an engrossing complex phenomenon and has been the subject of many studies[7-14]. The combustion profile of the propellant can be classified into several zones, such as heated zone, chemical reaction zone, burning surface zone and porous zone, all in the condensed phase, and fragment flowing zone and product zone in the gas phase[15]. The combustion of CSP occurs to varying degrees in both condensed and gas phases[16]. There are two schools of thought regarding the combustion of CSP. According to one school, the gas phase processes are believed to control the burning of the propellant; the gaseous species emanating from the pyrolyzing surface are considered to intermix and react exothermally in the gas phase to form final products, liberating heat and establishing an equilibrium flame temperature. Part of the heat generated in the flame is transferred to the surface to be used up in pyrolyzing and gasifying the surface layer, so that the combustion process recurs steadily. In modelling gas phase combustion processes, the reactions occurring therein are considered to be fast and the heat transfer from the flame to the surface is considered to be the rate-controlling step.

The other school of thought[16-18], which also includes the Bangalore group[19-26], believes that the condensed phase reactions occurring at or just below the burning surface are important. The decomposition/degradation in addition to the gas phase reactions of the oxidizer and the binder, and the cross-reactions between their products are exothermic in nature and contribute significantly to the total energy of the propellant. Condensed phase processes also include melting and gasification phenomena at the surface. Knowledge about the chemistry of condensed phase reactions, which is a key process, will facilitate understanding of vital phenomena like burning rate modulation and ageing. An organized comprehension of the condensed phase chemistry will also provide a better insight into the extinction phenomenon and intermittent, plateau and flameless combustion.

Kishore and coworkers[19-27] demonstrated both qualitatively and quantitatively the existence of condensed phase reactions. In AP/polystyrene (PS) model propellant[19-26], mass spectroscopic analyses have indicated that the mass spectrum of CSP is different from the additive spectra of AP and PS individually. Likewise, the enthalpy of propellant decomposition, which is a nucleation-controlled phenomenon[28], is larger compared to the additive enthalpies of the individual components[29,30]. This excess enthalpy of the condensed phase is about one third of the calorimetric value (total heat of combustion)[18,23,24,31]. This is corroborated by a master plot of the thermal decomposition rate against the burning rate of propellants, which suggests that the burning rate increase/decrease is about one third of the order by which the rate of thermal decomposition increases/decreases in the presence of additives[21,22,25]. Separation of the binder portion from the quenched propellant surface and analysis by thin layer chromatography have shown a number of spots, suggesting complex nature of the condensed phase reactions[25,32]. The largest proportion of the intermediate was found to have peroxy linkages in the polymer backbone. Spectral and chemical analyses confirmed the existence of poly(styrene peroxide) (PSP) in AP/PS propellant system[32,33]. Both partially decomposed propellant residue and an aged propellant show the presence of this intermediate, which was later used as a natural catalyst for burning rate modification[34,35]. This has led to detailed investigations on the syntheses of several polyperoxides of styrene[36-43], methyl methacrylate[44], vinylnaphthalene[45], divinylbenzene[46], vinylacetate[47], α-methyl styrene[48,49], copolyperoxides[50,51], terpolyperoxides[52] and on several aspects of their physicochemical behaviour[53,54].

Thermochemical calculations of exothermic degradation of polymeric peroxide have led to the unique discovery that polymers of this class undergo "autopyrolysis" and these are highlighted as special fuels[55]. The critical AP concentration in CSP for just sustaining its combustion is considerably reduced in the presence of PSP due to its high pyrolytic exothermicity[56] not only in the combustion of propellant but also in the ageing process. It has been demonstrated that the condensed phase reactions are important. In this laboratory, the rate controlling step for the ageing process has been shown to be proton transfer in oxidizer decomposition, which has led to the use of ammonium salts for increasing the longevity of propellants[57-66].

The literature on various aspects of the process of combustion of CSP is enormous and fragmentary. In this book, an attempt has been made to present various facets of propellant combustion, focusing attention on the importance of condensed phase reactions, hitherto unattempted in this fashion. The subtle role of the binder, which has so far remained latent, compared to that of the oxidizer, is also brought into prominence and its impact on combustion parameters has been presented. While maintaining the above objectives, this book begins with a brief introduction about CSP in this chapter followed by a discussion on the influence of non-chemical factors, such as pressure and initial temperature in Chapter 2. Chapters 3, 4, 5 and 6 are devoted to CSP, oxidizer, fuel-binder, catalyst and ageing, respectively. Chapter 7 describes recent developments in the area of high performance binders, oxidizers and propellants. These aspects are briefly highlighted below.

The combustion behaviour of CSP is generally characterized by the steady linear regression rate of the burning surface, known as the burning rate *($\dot{r}$)*, and is regarded as one of the most important performance parameters. It strongly depends on the nature of the condensed phase and gas phase reactions and on other variables[2,7]. But its dependence on pressure *(P)* and initial temperature *(T_0)* is the most important and well recognized aspect[67,68]. Although information on these aspects is available in literature, important features of empirical relationships of $\dot{r}$ with P and T_0 are discussed in this book to get an overall comprehensive picture as to how $\dot{r}$ is primarily influenced by the oxidizer, nature of the fuel-binder, catalyst, heat release rate, etc. Some of these features are helpful in understanding plateau and extinction phenomena as well.

The combustion behaviour of CSP also depends on the burning behaviour of its major component[69]—the oxidizer AP - which happens to be the most commonly used oxidizer in CSP formulations. AP is a unique oxidizer, which is capable of supporting its own combustion (i.e., monopropellant) also and has been the subject of vast investigations for a long time to understand its decomposition and deflagration behaviour. AP deflagration has also been used as a prelude to the development of a suitable model for CSP combustion. Despite the existence of extensive literature on AP, its decomposition mechanism is still a matter of debate, while the deflagration process is intriguing in its various facets, making their mechanistic understanding more elusive as much it is pursued. For example, a clear understanding of the low pressure deflagration limit (LPL) has remained an elusive goal. Literature has been organised to clearly comprehend the decomposition and deflagration processes, emphasis being laid on the analysis of LPL. Although the oxidizer happens to be the largest ingredient in CSP, it is the binder which is the key fuel in solid propellant formulations, controlling their energetics, but it has not received adequate attention[70]. The impact of structural and other physical features of the binder has largely been ignored in literature. The subtle role of the binder, which has so far remained latent compared to that of AP, has also been brought into prominence, and its impact on combustion parameters has been discussed. Chemistry of AP decomposition/deflagration and binder degradation/combustion has been presented separately to assess their relative performance in CSP.

A lot has been said in literature about various kinds of catalysts and additives for controlling the $\dot{r}$ of CSP and AP. The most effective and commonly used catalysts are transition metal oxides (TMO)[71]. The present book overviews the existing knowledge in the field of catalysts and discusses the mechanism of their action on AP and binder decomposition. Currently, ferrocene derivatives are receiving considerable attention and much of the available information is patented. In this book, information on various ferrocene derivatives used in CSP has been consolidated; their advantages and multifunctional role[72] have also been highlighted.

The useful life of a propellant is extremely important from the point of view of its flawless performance during the stipulated usable period. Various chemical reactions that occur and lead to changes in characteristics of the oxidizer and the binder are presented. Strategies for remedial measures, which have emerged from such studies, have been pointed out.

There has always been interest to develop high energy binders and oxidizers which could not only provide high specific impulse but should also be safe to handle and should produce pollution-free combustion plumes. High energy polymers based on oxetanes and their derivatives are attracting considerable attention and appear to be the most suited binders in this regard. A separate chapter has been presented on various high energy binders and oxidizers.

CHAPTER 2

COMBUSTION OF COMPOSITE SOLID PROPELLANTS

2.1 DETERMINATION OF BURNING RATE

The combustion behaviour of a CSP is generally characterized by the steady linear regression rate of the burning surface known as the burning rate ($\dot{r}$) and is regarded as one of the most important performance parameters. It strongly depends on the nature of the condensed phase and gas phase reactions and on a host of other variables[2,7]. It is expressed as:

$$\dot{r} = f(P, T_0, O_p, \phi, C\text{-}F, U_g, G_p) \qquad (1)$$

where P is the pressure; T_o, the initial grain temperature; O_p, the oxidizer particle size; ϕ, the oxidizer-fuel mixture ratio; C-F, the chemical formulation of the propellant; U_g, the transverse velocity of the combustion gases wetting the burning surface and G_p, the propellant grain shape factor. Although $\dot{r}$ depends upon a large number of physicochemical factors, its dependence on P and T_o is very important and is well recognized[67,68].

The most convenient and common method employed to measure $\dot{r}$ is the strand burning technique developed by Crawford, *et al*[73] and Grune, *et al*[74]. Thin fuse wires are embedded through the propellant strand at accurately measured distances. The fuse wires are connected to an electronic timer and the strand is mounted in a closed chamber pressurized by an inert gas like nitrogen (N_2) or argon (Ar). The desired constant pressure in the bomb is maintained during combustion by the use of a large surge tank of an inert gas. The propellant is ignited at the top by means of a hot wire and the value of $\dot{r}$ is calculated from the distance between the wires and the burning time elapsed between the fuse wires. Though this method is simple, its drawback is that gas flow is not the same as encountered in rocket motors.

$\dot{r}$ has been measured on the basis of simulated motor burning conditions described by Osborn, *et al*[75]. This method, involves photographing the moving burning surface in a ventilated chamber and computing the distance from the photographs for a known time interval. Though this method yields reliable $\dot{r}$ data and does not disturb the flow field, data reduction is tedious and time-consuming. Another method reported by Osborn[76] involves a servo mechanism, which moves the propellant sample in a direction opposite to that of the receding burning surface with a velocity which will be equal to $\dot{r}$, such that the surface of the propellant is maintained at a fixed position.

$\dot{r}$ has also been measured by the acoustic technique. The propellant is dipped in water with a small portion protruding above the water surface at the top of which a nichrome wire is contacted for achieving ignition. This method is known to give very accurate results. An acoustic emission technique having 94 per cent accuracy has been reported by Caveny, *et al*[77]. Ultrasonic method[78] is made use of to check the $\dot{r}$ of uncured propellant prior to casting and the feasibility of this method has been demonstrated. Change in electrical capacitance of the propellant sample during combustion has also been used for the determination of $\dot{r}$. A method which involves continuous measurement of such resistance has been proposed by Osborn, *et al*[79].

One of the most widely used techniques[80] is the closed bomb technique. In this method, pressure variation with time is measured. The pressure is allowed to build up, thereby accelerating combustion. The pressure is recorded as a function of time. At any time, t, the value of $\dot{r}$ is determined by the instantaneous pressure prevailing therein at that time. $\dot{r}$ is calculated using the following empirical relationship:

$$\ln (dP/dt) = \ln (q\, a_1 / LC_pT_o) + (1+n) \ln P \qquad (2)$$

where L is the length of the cylindrical sample; q, the heat of combustion in cal/g; n, the number of moles of the gas; and a_1 is a constant. Thus, a plot of $\ln (dP/dt)$ vs $\ln P$ will give a straight line with a slope of $(1+n)$ and intercept of $\ln (qa_1/LC_pT_o)$, where C_p is the specific heat. From the intercept, a_1 could be calculated, since other parameters, q, L, C_p and T_o are known. The value of $\dot{r}$ is calculated at a desired pressure. Recently, a closed bomb device[81] which provides direct measure of $\dot{r}$ combining the advantages of conventional Crawford bomb and a closed bomb is described. The closed bomb method of Richard[82] involves the principle of microwave interferometry. An advantage of this method is that the contact of foreign substances, such as wire probes, etc. with the sample is avoided and the pressure could go up to 1000 atm.

2.2 INFLUENCE OF PRESSURE ON BURNING RATE OF CSP

Of all the variables, pressure is the most important parameter on which $\dot{r}$ depends[67]. Generally, as the pressure is increased, $\dot{r}$ is accelerated (Fig.2.1); efforts have been made to develop laws relating $\dot{r}$ with *P*. Various empirical relationships proposed (Eqns, 3-15) are summarized in Table 2.1. Their adequacy in satisfactorily fitting the experimental data in different pressure domains and the associated physicochemical processes are discussed below.

The most popular and commonly used empirical relationship for CSP[4] and AP[83] is Vieille's law (Eqn. 3, Table 2.1) in the pressure domain up to around 100 atm in rocket motors. Constant *'a'* in

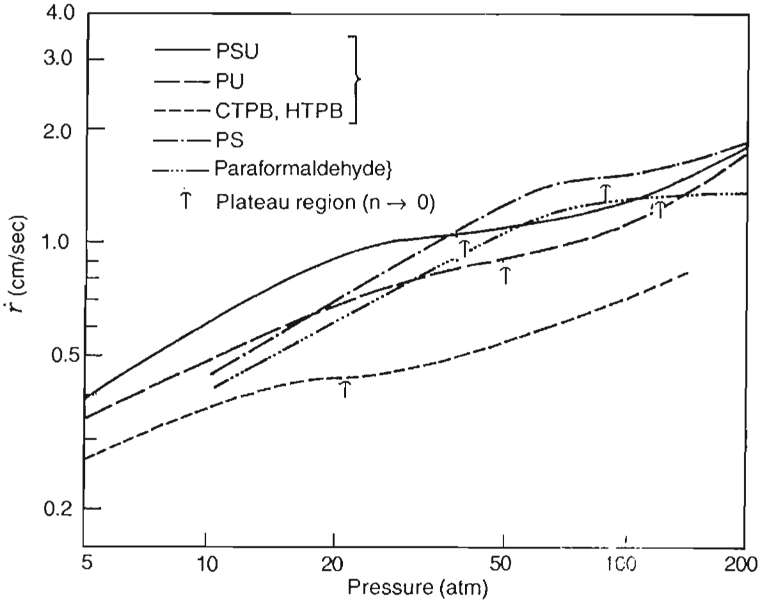

Figure 2.1. Burning rate of CSP as a function of pressure.

Source : Cohen, N., *et al.* Role of binders in solid propellant combustion. *AIAA. J*, 1974, p.12-18. (Reproduced with permission from Aerospace Access, American Institute of Aeronautics & Astronautics, New York).

Eqn (3) is dependent on T_o, whereas the pressure exponent (n) is related to the characteristics of the components[3,98]. The influence of n is significant for a stable operation and its magnitude provides an important diagnostic of the effect of pressure on the combustion process.

Physical significance of the n value in Eqn (3) is discussed below.

$\underline{n \to 0}$, $\dot{r}$ approaches a constant value and becomes less sensitive to P, resulting in plateau burning. It is desirable that $\dot{r}$ should have the least influence on P and for this purpose it is usually preferred to have as low an n value as possible.

$\underline{n \to 1}$, A linear relationship is acquired between $\dot{r}$ and P. However, the consequence under this condition in the actual motor performance is disastrous, as the chamber pressure (P_c) tends to infinity when n approaches unity, as shown[99] by Eqn (16).

Table 2.1. Empirical relationships of the pressure dependence of $\dot{r}$

Eqn No.	*Relationship*	*Features*	*Ref*
3.	$\dot{r} = ap^n$ (Vieille's Law)	Fits CSP data; $n < 1$; P = 20-80 atm. Fits AP combustion data; $n = 0.77$; P = 20-80 atm. Fits Gun propellant data; $n = 1$ *a:* constant, T_0-dependent. *n:* pressure exponent, composition-dependent.	3,4 83
4.	$\dot{r} = a + bP$ (Muraor)	Fits CSP combustion data; P< 1 atm. Fits DB propellant data; P<70 atm. a, *b:* constants	84
5.	$\dot{r} = a + bp^n$	Fits CSP at higher *P* up to 80 atm.; $n = 0.45$-0.6 Fits DB propellant data; $P > 70$ atm. *a, b:* constants	85
6.	$\left(\frac{1}{\dot{r}}\right) = \frac{a}{P} + \frac{b}{P^{1/3}}$ (Summerfield)	Fits CSP combustion data; *P* = 1-100 atm. *a* and *b* are empirical constants; *'a'* is known as the chemical reaction time parameter. Chemical kinetics controls the overall rate at low pressure and governs the premixed flame. *b:* diffusion time parameter	4 5 86

Contd...

Eqn No.	Relationship	Features	Ref
		and has particle size effect related to diffusion coefficient. High pressure behaviour not well understood.	
7.	$\left(\frac{1}{\dot{r}}\right)^2 = \left(\frac{a^*}{P}\right)^2 + \left(\frac{b^*}{p^{1/3}}\right)^2$ (Penner)	Fits CSP data; P = 1-136 atm. a^* and b^* are constants; b^* varies with particle size. In obtaining this relationship mass burning rate for combined diffusion and gas phase reaction is considered and is, therefore, better motivated than Summerfield's equation, which considers a separate mass burning rate. With the same physical model, Penner has obtained this rate law which fits Summerfield's data satisfactorily.	87
8.	$\left(\frac{1}{\dot{r}}\right) = \frac{a}{P} + C$ (Von Elbe)	Fits CSP data; $P <$ 100 atm. a and C are constants; a depends upon chemical reaction rate, while C depends upon diffusional mixing rate.	88
9.	$\left(\frac{\dot{r}}{a}\right) \alpha \left(\frac{p}{b}\right)$ (Rosen)	Fits CSP data in the range 1-136 atm a: prefactor of the pyrolysis law and is a constant related to the propellant composition. b: a parameter with the dimension of pressure.	89
	$\left(\frac{\dot{r}}{a}\right) \alpha \left(\frac{p}{b}\right)^{1/3}$ (Rosen)	Fits high pressure behaviour in the range 1-136 atm.	89
	$\frac{\dot{r}}{a} \rightarrow exp(-n_s) = const$ (Rosen)	This limiting factor relationship is asymptotically constant for very high pressures (1360 atm.), indicating that the pyrolysis law with T_s = T_f provides the maximum $\dot{r}$. But additional high pressure measurements are needed to test this theory. n_s is the index for surface decomposition, which is same as the activation temperature.	89
10.	(Hermance)*	Fits CSP data; P = 1-400 atm. Surface reaction energetics have a significant role. a_1, b_1, c_3, d_1 are constants, m is the	90

$$^*\dot{r} = a_1\, exp\left(\frac{-E_f}{E\theta_s}\right) + \frac{b_1 P^{\delta}}{\theta_s^{1/2}}\left(\frac{C_3}{\dot{r}} - \frac{d_1}{P^m}\right) exp\left[\frac{-(E_{ox} + E_s}{E\theta_s}\right]$$

Contd...

Eqn No.	*Relationship*	*Features*	*Ref*
		diameter exponent for particle ignition and δ is the reaction order.	
		Ingredient parameters : Activation energies for gas phase reaction *(E)*, oxidiser pyrolysis *(E_{ox})*, fuel pyrolysis *(E_f)*, and surface reaction *(E_s)* are considered. θ_s is the dimensionless temperature at the surface.	90
11.	$\dot{m} = P^s A x^* \exp(-E / RT)$ or $\dot{m} = p^{\delta/2}(k\lambda\xi^* / C_p)^{1/2}$ (Beckstead-Derr-Price Triple Flame Model)	Fits CSP data and predicts $\dot{r}$ - *P* curve well; *P* < 70 atm. Vapour phase considered. At low *P*, premixed flame controls $\dot{r}$. At high *P*, diffusion flame controls $\dot{r}$.$\dot{r}$, is the mass burning rate, *A:* pre-exponential factor, δ: arbitrary reaction order, *E:* activation energy, x^*: flame stand off distance, *T:* temperature, *k:* pseudo-rate constant, C_p: the mean specific heat of the solid and gas, λ: the thermal conductivity, ξ^*: the non dimensional stand off distance.	91
12.	$\dot{r} = \dfrac{P}{A_f + B\dot{r}\, p^{(2-\delta)/2}}$ (Fenn's Phalanx Model)	Fits CSP data; *P* < 100 atm. δ : gas phase chemical reaction order, B: constant; A_f a parameter related to T_s, T_f and the enthalpy difference per unit mass between the solid and gas phases. This model considers the flame as occurring at the interfacial region between streams of fuel and oxidant produced by rapid vaporization of the components.	92
13.	(Kumar)*	Fits CSP data; *P* = 1-50 atm. Considers the condensed phase processes. φ: interfacial reaction layer thickness, which is considered as the melt layer thickness on AP crystals in the propellant. For AP/CTPB (75/25), φ is 5 μm, *'a'* is oxidiser particle size taken as 90 μm for the above propellant. *(6φυ/a)* is the volume fraction of AP undergoing degradation and *'υ'*, the volume fraction of the oxidiser loading . Fragment size vaporizing (FSV) for binder is taken based on the	93 94

$$* \quad \dot{r} = \left[\frac{(6\varphi\upsilon / a)(k / \rho_c)(B_o P)\exp(-E / RT_w)}{(E / RT_w)\left(\dfrac{T_w - T_o}{T_w}\right)\left[\left(\dfrac{D}{C(T_w - T_o)} + 1\right)\ln\left(\dfrac{FSV}{FSV - 1}\right) - \dfrac{D}{C(T_w - T_o)FSV}\right]}\right]$$

Contd...

Eqn No.	*Relationship*	*Features*	*Ref*
		consideration that $\dot r$ *(AP)* = $\dot r$ (binder). *D*: heat degradation of the binder to monomer units. E: activation energy for the thermal degradation, C_p : specific heat, T_w: wall temperature, ρ_c: the density of CSP , B_0 the pre-exponential factor for the degradation process.	
14.	$\left(\frac{\dot r}{P}\right)^2 = \frac{a''}{P} - b''$ (Rastogi)	This model fits CSP combustion data (P = 1 - 95 atm.) and gives a better correlation than Summerfield's equation. *a*" and *b*" are constants. *a*" is a function of temperature, while *b*" is related to the volume of activation. The value of *b*" is also determined by the type of oxidizer and its mechanism of thermal decomposition in CSP. For KNO_3 or $NaNO_3$, *b*" is negative, while for perchlorates, it is positive.	95 96
15.	$\dot r = ap^s + \left(b/p + cd_{ox}/p^{1/3}\right)^{-1}$ (Miller)	Fits CSP data for 68 < P < 340 atm. This relationship possesses 'qualitative' exponent break information. *a, b, c, s* are constants, d_{ox} is the oxidizer particle size. *a* and *s* are identified with AP for CSP containing endothermally degradable binders. For reactive binders that sustain rapid deflagration, they are identified with the binder.	97
	$\dot r = ap^s + gp^{1/3}$ (Miller)	This relationship fits CSP data for P >340 atm as $(b/p) <<< (cd_{ox}/P^{1/3})$ in the above relationship. *'g'* is a constant inversely proportional to d_{ox}.	97

$$P_c = \left\{\frac{k_m \rho a C^*}{a}\right\}^{\frac{1}{1-n}} \qquad 16$$

where k_m is the grain area to nozzle throat area ratio, *'a'*, a constant, ρ, the propellant density, C^*, the characteristic velocity, and *g*, acceleration due to gravity. The above condition may lead to explosion and motor failure.

n > 1: $\dot{r}$ becomes more sensitive to pressure. However, its consequence in Eqn (16) is that P_c becomes much less, which has no practical meaning.

n < 1: $\dot{r}$ becomes inversely proportional to pressure. Its consequence in Eqn (16) is that P_c decreases and this condition leads to unstable combustion, known as 'chuffing' and 'extinction'. Propellants with negative exponents are known, but they are rare[100-102].

Generally, *n* is 0.7 and 0.4 for double base (DB) propellants and CSP[1], respectively.

2.2.1 Combustion Behaviour of CSP in Different Pressure Domains

2.2.1.1 Low pressure domain (< 1 atm)

At low pressures, Eqn (4) adequately describes the behaviour of CSP. The constant *'a'* is governed by thermal conductivity and is independent of pressure in the condensed phase[103-106]. At 1 atm, with $a = 0$ and $n = 1$, Eqn (5) tends itself to Eqn (3) and offers ballistic calculations in gun propellants with some accuracy; however, it fails to describe the CSP behaviour.

2.2.1.2 Moderate pressure domain (1 - 100 atm)

At moderate pressures, the dependence of $\dot{r}$ on P can be represented adequately by Eqns (3) and (4), but more precisely by Eqn (5), which is almost a combination of Eqns (3) and (4) describing the behaviour of CSP and DB propellants, respectively [107]. With $a = 0$, Eqn (5) tends to Eqn (3) and has been verified to describe the behaviour of CSP. Summerfield's equation Eqn (6) is also applicable to CSP, but it breaks down when the oxidizer particle size is < 250 μm. This is because the flame is no longer unidimensional, as assumed in the theory. Eqns (7) and (8) have been verified on the basis of experimental data; they are as good as Summerfield's equation (Eqn 6).

2.2.1.3 High pressure domain (> 100 atm)

At higher pressures, the flame passes from a homogeneous to heterogeneous structure[108,109]. The plateau effect (Fig.2.1) depends on the nature of the fuel binder and particle size of the oxidizer; *n* decreases when ϕ decreases. If the particle size is in the intermediate range of 200-250 μm, Eqn (6) breaks down for a reason similar to that mentioned in the previous section. In fact, due to this weak effect of the oxidizer particle size on $\dot{r}$, the effects of high pressure on *n* and binder are not well predicted either by

Eqn (3) or Eqn (6). Incorporating some of these effects, not understood by the empirical laws relating $\dot{r}$ and P, the importance of surface heterogeneity has been recognised. Considering various effects, several laws have been proposed (Table 2.1). Equations (9),(10),(13),(14) and (15) consider the importance of surface heterogeneity, oxidizer decomposition and binder degradation characteristics. Equations (11) and (12) consider the gas phase chemical reactions.

The above discussion of the combustion of CSP, as influenced by pressure in different domains[110] implies that it is not possible to present a unique mechanism for the combustion of CSP in the entire pressure range of interest in rocket motors.

2.2.2 Surface Heterogeneity and Thermal Decomposition of CSP

The burning surface of CSP, with the complex decomposition and pyrolysis reactions of the dispersed oxidizer and the inter-dispersed binder is highly heterogeneous in nature and is markedly influenced by the flow fields[90]. Although surface heterogeneity has been recognized as important in the formulation of empirical laws, its nature is not fully understood. Surface features like microstructure, particularly the oxidizer particle size effect have been studied[111], which indicates that $\dot{r}$ and n may change as the cross-flow velocity increases for oxidizer particle size >10 μm. It has also been found[112] that for an oxidizer mixture of different particle sizes, the experimental $\dot{r}$ *vs* P behaviour agrees well with the theoretical observations. The effect of particle size and its distribution in the steady and non-steady burning rate and pressure exponent has been studied[113,114]. Concomitant with changes in the composition (i.e., ϕ), the propellant material ablating from the surface affects the surface heat release and causes fluctuation in the burning process[108,109,115-117]. Damping of these fluctuations has been found to result in the extinction phenomenon[118]. Shannon[119] has studied the photomicrographs of PBAN, PU and CTPB - based AP propellants prior to ignition. In all cases, polymer melting and flowing were observed and the large particles of AP were found to protrude from the surface. The surface showed a pebbled structure and was found to be coated with molten polymer. Such protrusion has been confirmed by Lengelle, *et al*[120] from SEM studies on polybutadiene propellants. Furthermore, study of the surface structure has revealed that the protruding AP particles at low pressure recessed at higher pressures where plateau is observed. Boggs, *et al*[121] also confirmed that at 6.8 atm, AP particles protruded on the surface, suggesting that the $\dot{r}$ of AP was lower than that of the binder, but at 54.4 atm, the reverse situation was observed. At still higher pressures, regression of the binder was slower than that of AP and the binder melt covered AP crystals, bringing about extinction.

Apart from surface heterogeneity, the heat transferred from the flame to the unburnt solid[122] results in thermal stresses and increases the thermal gradient in the burning surface layer. This induces microcracks[123], thus increasing the surface area; propagation of microcracks activates the condensed phase reactions[124,125].

There has been a lot of interest in understanding the role of condensed phase reactions during the combustion of solid propellants[30,70]. For instance, in NH_4ClO_4-$NaNO_3$ eutectic formation, the flux growth of NH_4NO_3 and cooperative rearrangement of the ions to $NaClO_4$ occurs, leading to reduction in the $\dot{r}$ of magnesium-based fuel-rich propellants[126]. Quantitative contribution of the condensed phase reaction at ambient pressure is known[21]. As a logical consequence, it would be of interest to show the contribution of condensed phase reaction at elevated pressures; such studies are, however, very few. In a PVC-AP propellant, plateau effect is observed in a given pressure range. When $KClO_4$ is used as oxidizer, no plateau effect is observed due to high combustion temperature and KCl does not participate in the chain termination mechanism[127].

According to Bouck, *et al.*[127] the temperature for the onset of runaway exothermic reaction of solid propellant is a function of pressure and heating rate. Waesche, *et al*[128] studied the thermal decomposition of AP/polybutadiene acrylic acid (PBAA) propellant at ambient 17 atm pressure to examine the effect of particle size and catalyst. A close examination of their results showed that pressure sensitizes thermal decomposition of the propellant. The heat of reaction of DB propellant was found to depend on pressure. The work of Eisenreich and Pfeil[129] reveals that below 30 atm, there is a strong dependence of heat of reaction on pressure; above 30 atm, however, this effect is less pronounced. Although correlation of $\dot{r}$ and thermal decomposition rate in the propellant at higher pressures has been indirectly shown through similarity in the exponent of thermal decomposition rate and $\dot{r}$, the exact contributions of the condensed phase at higher pressure is not known precisely. It is believed that propellants with higher

$\dot{r}$'s will have a diminished contribution from condensed phase reaction since the residence time available in the condensed phase gets reduced successively as the pressure is increased. The same holds good for the effect of particle size with respect to the depth of heat penetration, when the contribution of the condensed phase reaction becomes smaller.

To obtain a realistic picture about the contribution of the condensed phase reactions at elevated pressures, more investigations may be necessary.

2.3 INFLUENCE OF TEMPERATURE ON BURNING RATE OF CSP

2.3.1 Basic Analysis

Generally, $\dot{r}$ increases with T_o[98,99,130,131], but the magnitude of the variation is much less pronounced compared to that of $\dot{r}$ variation with pressure. However, it is significant to consider it from the point of view of its influence on propellant storage under varied climatic conditions. The change in value of $\dot{r}$ with T_0, at a constant P, is defined as temperature sensitivity (σ_p) of the burning rate[1,3,113]

$$\sigma_p = \left(\frac{\partial \ln \dot{r}}{\partial T_0}\right)_p = \frac{1}{\dot{r}}\left(\frac{\partial T}{\partial T_0}\right)_p \tag{17}$$

σ_p is a basic propellant characteristic and is expressed as %/°C. Attempts to explain temperature dependence of $\dot{r}$ have been reviewed by Cohen and Flanigan[132]. Schoyer and Korting[133,134] observed that the coefficient and exponent in Vieille's burn rate law Eqn (3) vary with T_0; he suggested that σ_p varies as a function of temperature according to the equation:

$$\sigma_p = \left(\frac{\partial \ln a}{\partial T_0}\right)_p + \ln P\left(\frac{\partial n}{\partial T_0}\right)_p \tag{18}$$

In Eqn (18), the variation in values of a and n with T_0 accounts for its influence on the propellant composition and thus σ_p depends on the propellant formulation as well[135-138]. To predict the effect of the main parameters influencing σ_p, fuel-rich propellant and non-fuel-rich propellant containing the same ingredients have been studied[120]. Kubota and Miyazaki[139] found that σ_p obeys the equation:

$$\sigma_p = \left(\frac{\partial ln\ y}{\partial T_0}\right)_p - \left(\frac{\partial ln\ z}{\partial T_0}\right)_p \qquad (19)$$

where $y=(dT/dx)_{s,g}$ is the temperature gradient and $z=[T_s-T_0-(Q_s/C_p)]$, where T_s and Q_s are the surface temperature and surface heat release, respectively. Thus, σ_P consists of two parameters and Eqn (19) is written as:

$$\sigma_p = Y+Z \qquad (20)$$

where Y is the gas phase reaction parameter and Z is the condensed phase reaction parameter. Temperature sensitivity of the solid phase reactions is found to play a more dominant role in σ_p than that of the gas phase reaction in the pressure range tested.

2.3.2 Initial Temperature Effect and Condensed Phase Considerations

During combustion, a thin zone beneath the burning surface is conceived to be effectively heated from T_0 to its reaction temperature[140], depending upon ϕ and chemical nature of the propellant[139,141]. When combustion of the oxidizer and the fuel takes place in stoichiometric amounts, σ_p assumes a minimum value[142]. The existing analyses of $\dot{r}$ *vs* T_0 data for CSP are fragmentary and do not adequately explain various physicochemical processes and their mechanistic implications[143]. Literature data on the effect of T_0 are compiled in Table 2.2 and important conclusions are presented in Table 2.3. Experimental and theoretical studies on the effect of T_0 on $\dot{r}$ of CSP, summarized in Table 2.3, suggest that σ_P is influenced by oxidizer particle size, additives, metallic fuel, condensed phase processes, nature of the fuel-binder and pressure.

σ_p is generally observed to increase with increase in oxidizer particle size[91,139,155]. It also increases with oxidizer loading[91]. For very low particle size range (< 10 µm), σ_p is almost constant, but beyond 101 µm, σ_p increases with particle size and particle size distribution[150]. However, this trend is reversed if the propellant burning is erosive[153].

At a given pressure, CC increases σ_p for CTPB propellant both in the presence and absence of Al, but for PU-containing CSP, it decreases in the presence of Al[102]. It could, therefore, be inferred that the chemical nature of the binder influences σ_p. Even as a function of pressure, the effect of CC in the presence of Al

Table 2.2. Dependence of $\dot{r}$ on T_0 of CSP

System	*p(atm)*	*T_0(°C)*	*$\dot{r}=f(T_0)$ (cm/sec)*	*σ_p and important observations (%/°C)*	*Ref*
AP(70%)/polysulfide (30%)	1-1000	-20,0-60	0.06-6.00	(i) σ_p (predicted) = 0.0015 (ii) σ_p (reported) = 0.0005 (iii) Since the predicted value is higher than the experimental value reported; it does not provide a satisfactory model in this aspect.	90
80% AP/20% styrene crosslinked polyester resin (Bimodal AP mean particle size 147(μm))	2-108 2-108 2-108 9-82	89-94 36-44 1-3 -75 to -65	0.16-0.96 0.15-0.82 0.15-0.74 0.26-0.60	(i) GDFM*and Phalanx* model represent the data more closely. (ii) As T_o is lowered, low and high pressure limits appear.	144
AP(60-70%)/ polysulphide AP bimodal	68	not given	—	(i) σ_p (exptl) = 0.0064 - 0.0075 (ii) σ_p (calctd)=0.0064 and 0.0168 for 20 and 200 μm oxidizer particle size respectively. Calculations indicate that σ_p increases with increasing pressure, particle size and oxidizer content.	91
AP cocrystalized with $(NH_4)_2HPO_4$ (82%) CTPB/curing agents	34	-15,24 and 65	0.56-0.64	σ_p=0.0062	145
AP recrystallized (82%)/ CTPB/curing agents	34	-15,24 and 65	0.57-0.64	σ_p=0.0055	145
AP cocrystallized with $KClO_3$ (82%)/	34	-15,24 and 65	0.55-0.61	(i) σ_p=0.00561 (ii) Effect of low temperature	145

Contd...

System	*p(atm)*	*$T_0(^oC)$*	*$\dot{r}=f(T_0)$ (cm/sec)*	*σ_p and important observations (%/^oC)*	*Ref*
CTPB/curing agent				decomposition of AP on σ_p is realised.	
AP(70%)/ PBAA (30%) AP 80μm	14-35	21,38 and 55	0.13-0.43	(i) Intermittent burning is observed and GDFM can not predict the pressure at which it occurs. (ii) Increase in $\dot{r}$ does not follow the predicted trend and σ_p=0.00011	146
AP(69.4%)/PBAA(29.4%) /CC (1.2%) AP 80μm	14-35	21,38 and 55	0.17-0.70	$\dot{r}$ follows the predicted value; σ_p = 0.00013	146
AP (68.8%)/PBAA(28.8%)/ CC(2.4%)AP 80μm	14-55	21, 38 and 55	0.18-0.70	$\dot{r}$ follows the predicted trend σ_p =0.00016	146
AP(68.8%)/PBAA (28.8%)/CC(2.4%)	14-55	21,38 and 55	0.38-1.00	σ_p not given	146
AP(65%)/Polysulfide	2-10	27-73	0.10-1.00	(i) Modified GDFM** gives σ_p as 0.0008 (ii) No definite conclusions are arrived at regarding the merits and demerits of modified GDFM.	147
AP(80%)/CTPB(20%)	10-70	0-140	0.60-2.50	σ_p is studied as a function of pressure. At P =10 and 70 atm, σ_p(0.0034) seems to be independent of P and its value is approximately equal to that of pure AP.	148
AP(80%)/CTPB (19%) CC(1%)	10-70	0-140	0.90-2.30	(i) CC catalyzes AP decomposition and increases the $\dot{r}$ of the propellant at low P, while preheating leads to small increase in $\dot{r}$ at high P.	148

Contd...

System	p(atm)	T_0(^{0}C)	$\dot{r}=f(T_0)$ (cm/sec)	σ_p and important observations (%/^{0}C)	Ref
				(ii) At $P=10$ atm, $\sigma_p=0.0045$ and at $p=70$atm, $\sigma_p=0.0007$. While at low P, σ_p shows an increase with CC, it significantly decreases at higher pressures. This can be explained by considering the fact that at low P, the diffusional phenomena are rapid and $\dot{r}$ is controlled by the chemical reaction rate influenced by the catalytic effect of CC.	
AP(80%)/CTPB (19%)/LIF(1%)	10-70	0-140	0.45-1.90	(i) At $P=10$atm, $\sigma_p=0.0013$ and at $P=70$atm, $\sigma_p=0.0022$ (ii) with LiF, σ_p is an increasing function of pressure.	148
AP(70%)/CTPB (20%)Al(10%)				(i) At $P=1$ atm, $\sigma_p=0.0018$ and at $P=40$ atm $\sigma_p=0.0022$ and at $P=70$ atm, $\sigma_p=0.0017$. (ii) σ_p depends on P. σ_p decreases compared to non-metallized propellant; this may be attributed to an increase in T_s caused by melting of Al at the burning surface of the propellant.	148
AP(70%)/CTPB (19%)/Al(10%)/CC (1%)	10-70	0-140	0.80-2.50	At $P=10$ atm, $\sigma_p=0.0029$ and at $P=70$ atm also σ_p is same, thereby indicating that this system is independent of P. The data, however, satisfy Summerfield's equation.	148
AP(70%)/CTPB (19%)/Al (10%)/LiF(1%)	10-70	0-140	0.60-1.80	AP $=10$ atm, $\sigma_{p*}=0.0026$. σ_p is almost same as CC containing aluminized propellant. This must be due to the heat released at the surface by Al combustion.	148

Contd...

System	*p(atm)*	*T_0(°C)*	*$\dot{r}=f(T_0)$ (cm/sec)*	*σ_p and important observations (%/°C)*	*Ref*
AP(80%)/PU(20%)	10-70	0-140	0.20-1.00	Fuel type profoundly affects $\dot{r}$ behaviour; $\dot{r}$ values at high T_o (60°C) are very inaccurate and scattered due to unstable combustion and, therefore, probably σ_p is not reported. $\dot{r}$ *Vs* P dependence shows marked tendencies of plateau, mesa and intermediate presssure extinction effects. Also, extinction occurs at higher binder proportions.	148
AP(80%)/PU (19%)/CC(1%)	10-70	0-140	0.20-2.00	(i) With CC, plateau and unstable combustion is eliminated. σ_p is large compared to AP/CTPB and an increasing function of pressure; σ_p=0.0061-0.0090. (ii) Increases the upper pressure limit of the non-catalyzed propellant from 68 to 80 atm, when catalyzed by CC.	148
AP(80%) /PU (19%)/LiF(1%)	10-70	0-140	not given	LiF provokes extinction more and more as pressure increases due to decrease in T_f.	148
AP(70%)/PU (20%)/Al(10%)	10-70	0-140	0.10-0.80	σ_p is lowered from 0.0064 to 0.0014, since introduction of Al into the propellant moderates the burning process. It also enables study of variation of $\dot{r}$ as a function of P at all T_0 values up to 40°C.	148
AP/(70%) /PU (19%)/Al(10%)/CC(1%)	10-70	0-140	0.16-1.80	CC tends to reduce σ_p from 0.0045 to 0.0032 with increase in pressure.	148
AP(70%)/PU (19%)/Al(10%)/LiF(1%)	10-70	0-140	0.13-1.90	LiF also tends to reduce σ_p from 0.0040 to 0.0021 as a function of pressure.	148

Contd...

System	p(atm)	T_0(°C)	$\dot{r} = f(T_0)$ (cm/sec)	σ_p and important observations (%/°C)	Ref
Mg(60%)/$NaNO_3$(40%)	1-10	—	—	(i) σ_p varies from 0.0021 to 0.0026. (ii) JANAF*** composite solid propellant illustrates the same trend.	149
AP(80.4%)HTPB(19.6%)	68	11-31	5.50-0.50	(i) For AP particles in the range 1-1000 μm, σ_p=0.001- 0.005. (ii) For AP < 10 μm, σ_p is constant and for AP > 10 μm, σ_p increases as a function of particle size distribution.	150
Bimodal AP propellant	68	11-31	2.00-3.50	(i) For coarse (400 μm)/fine bimodal AP in CSP, σ_p=0.001-0.004. (ii) Unimodal propellant behaviour influences the σ_p value.	150
JANAF*** standard composite propellant	3-58.8	0, 21 and 54	0.20-0.90	σ_p has been calculated for four different models andfound to be in the range 0.0007-0.0045.	151
AP(68%)/CTPB (12.83%)/Al(16%)	34, 68 and 102	-10, 10 71, 150	—	σ_p=0.0064 152	
AP(65%)/Binder (18%)/Al(17%)	28-41	-26,16,38	0.97-0.91 (expt) 0.95-1.22 (theor)	(i) Experimental data for $\dot{r}$ and σ_p have shown the same trend as indicated by theory. (ii) For non-erosive burning at low P, σ_p (exptl) = 0.0024, while σ_p (theor) = 0.0014 and increases with oxidizer particle size, monopropellant flame controls the burning mechanism. (iii) Erosive burning has little or no effect on σ_p but depends on the oxidizer particle size. σ_p decreases with increase in particle	153

Contd...

System	p(atm)	T_0(°C)	$\dot{r}=f(T_0)$ (cm/sec)		σ_p and important observations (%/°C)	Ref
					size due to the turbulent boundary layer at the burning surface.	
				(iv)	In both the cases, σ_p decreases with pressure.	
AP(73.8%)/Binder (23.2%); Binder is Styrene/butadiene	0.2-14	-40, 25 and 50	0.02-0.10 Vielle's law is applicable		σ_p=0.0012-0.003; σ_p appears large and seems to depend on the composition and strongly on the temperature.	154
dAP(80%)/HTPB (20%)/Fe_2O_3	15-50	-30,70	$\dot{r}$ increases		σ_p decreases with Fe_2O_3	154
AP(80%)/HTPB(20%)/LiF	15-50	-30,70	$\dot{r}$ decreases		σ_p increases with LiF.	154
AP(80%)/HTPB (20%) (Fine AP particles)	15-50	-30	0.65-1.30		σ_p = 0.0032	139
AP(80%)/HTPB(20%)/ (coarse AP particles)	15-50	-30	0.25-0.48		σ_p =0.0036	139
AP(80%)/HTPB(20%)/ BEFP****1%)					σ_p increases with AP particle size and decreases in the presence of BEFP**** catalyst. T_s plays an important role.	139

* GDFM: Granular Diffusion Flame Model of Summerfield[5]
Phalanx Model of Fenn[92]

** Modified GDFM ; CC: Copper chromite ;

*** JANAF CSP: AP(75%)/PBAN(19.1%)/CC(1%)/Carbon black(0.5%)/epoxy curative (4.4%);

**** BEFP: 2,2'-Bis (ethyl ferrocenyl) propane

Table 2.3. Effect of various variables on σ_p

Oxidizer particle size/loading	σ_p increases with oxidizer particle size	85, 121, 137
	σ_p increases with oxidizer loading.	85
Additives	Catalyst copper chromite (CC) increases σ_p of CTPB propellant. Catalyst CC decreases σ_p of PU propellant	130
	Catalysts (CC, Fe_2O_3, BEFP) decrease σ_p with increase in P for CTPB and PU propellant	130,136
Al fuel	Inhibitor LiF brings about an increase in σ_p vs P dependence for CTPB, HTPB CSP, but it decreases for PU CSP and moderates burning behaviour. Melting of Al decreases σ_p.	130-136
	Metal combustion overshadows the effect of catalysts and σ_p remains unaltered in the presence of catalysts/inhibitors	130
Condensed phase processes	Surface structure is considered in combustion analysis.	128, 130
	Parametric study of the surface features made to predict $\dot{r}$ and σ_p	
Type of fuel binder	Analysis of σ_p revisited, induces intermittent and extinction phenomena. Analysis of the surface structure attempted	128, 130
Pressure	σ_p (Exptl) is invariant with pressure. As per theoretical predictions, σ_p should increase with pressure.	130,136, 85

shows no significant effect on σ_p for CTPB propellant. This is somewhat strange, since CC, in the absence of Al, shows decrease in σ_p with pressure[148], thereby suggesting significant influence of metal on catalytic reactions. For variation of σ_p with pressure, in PU-based CSP, both $\dot{r}$ catalyst (CC) and inhibitor (LiF) follow the same trend, i.e., σ_p decreases with increase in P[148]. On the other hand, for HTPB and CTPB-based propellants, catalysts like BEFP (for coarse AP particles only)[129], CC[148], Fe_2O_3[154], and an inhibitor like LiF[148,154] show an opposite trend. It may be generalized that σ_p, as a function of P, decreases for catalysts and increases for inhibitors.

Melting and combustion of Al influence σ_p at a given pressure. For instance, in CTPB propellant, decrease in σ_p is attributed to Al melting, resulting in increase in T_s. However, σ_p is not affected by CC or LiF in the presence of Al. Interestingly, in Al-containing PU CSP, the magnitude of the effect of catalysts/inhibitors remains the same, although reduction in σ_p values is influenced by the binder characteristics. Thus, combustion of Al overshadows the effect of the catalyst or the inhibitor[102]. Al also suppresses the plateau effect observed in propellants[156]. Al has low propensity to react on the surface and in the condensed phase, and hence it is more sensitive for radiative feedback. Mg and B, on the other hand, react readily on the surface and in the condensed phase and hence are more sensitive to condensed phase heat release[157].

Analytical models of combustion of CSP have shown much concern for the condensed phase processes[158]. Some of the models consider surface heat release on account of condensed phase reactions. If the surface heat release falls below a certain critical value, the predicted performance parameters do not match with the experimental values, thereby showing the significance of condensed phase reactions. Generally, condensed phase heat release occurs at or just below the burning surface. Consequently, it affects T_s and the kinetics of surface pyrolysis, which is reflected in E_s (surface activation energy). Some of the models, where Q_s, T_s and E_s are considered as surface features, are briefly discussed below. Depth profile studies on the burned propellant samples by IR microscopy reveal that chemical reactions occur within 10 μm[159] from the surface.

In the model of Beckstead, *et al*[91], oxidizer decomposition occurs at the surface and its associated heat release is regarded as an important parameter. It is realized that a critical value of heat release in the range 100-200 cal/g is necessary to predict the $\dot{r}$ for its T_0 dependence. This is borne out by the fact that if the heat release is less than the critical value, σ_p becomes very much lower than the experimental value. Ewing and Osborn[146] studied the effect of surface feature parameter *(u)* on $\dot{r}$ and suggested the following relationship:

$$\left(\frac{\dot{r}_0}{\dot{r}}\right) = \left(1 - \frac{T_0}{u}\right)^{\frac{1}{2}} \tag{21}$$

where u is defined as $u = T_s - T_0 - (Q_s / C_s)$; and $\dot{r}_0$ is the burning rate at some reference temperature, T_0. The predicted and experimentally observed effect of u on $\dot{r}$ of four AP/PBAA propellants, shown in Fig. 2.2, suggests that the catalyzed (CC) propellants follow the predicted trend in $\dot{r}$. On the basis of Summerfield's GDF model, Cohen Nir[148] derived an expression for σ_p, which is essentially based on the parameters T_s, Q_s and E_s. His results of analysis of σ_p agree with the experimental observations; the expression for σ_p is as follows:

$$\sigma_p = \frac{1}{2\left(T_s^* + \left\{\frac{Rt_s\sigma_p^2\Delta T_o}{E_s} - T_o\right\} - \left(\frac{Q_s}{C_s}\right)\right) + \left(\frac{R}{E_s}\right)\left(T_s^* + Rt_s^2\sigma_p\frac{T_o}{E_s}\right)^2} \tag{22}$$

where σ'_p is the temperature coefficient of $\dot{r}$ used in iteration, E_s, the surface activation energy, T_s, the surface temperature corresponding to some reference temperature, T_0, C_s, the heat capacity of the solid; and R the gas constant.

It has already been noted in the foregoing discussion that in CTPB and PU CSP, the chemical nature of the fuel-binder affects the σ_p significantly both in the absence and presence of a catalyst[148]. Furthermore, when the extinction phenomena for different binders in a propellant are considered, varied behaviours are observed, suggestive of a strong influence of the fuel binder characteristics. CTPB or HTPB propellants do not show extinction in the usual pressure range of interest, whereas PBAA and PU propellants exhibit intermittent burning[146] and extinction[148], respectively. For PBAA propellant, intermittent burning occurs in the pressure range 15-35 atm. The intermittent burning and extinction phenomena could be explained by Summerfield's granular diffusion flame model (GDFM)[5], which considers that binder melt covers oxidizer particles to bring about local extinction. However, in PBAA-based propellant, the binder does not melt in

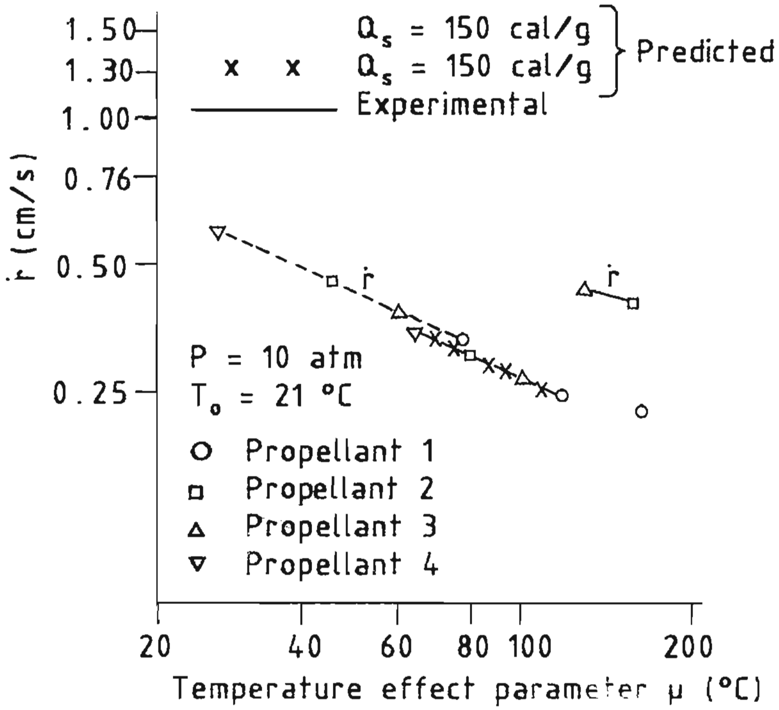

Figure 2.2. Effect of parameter *u* on the burning rate.

Source : Ewing, *et al.* Burning rate temperature sensitivity of composite solid propellants. *Journal of Spacecraft and Rockets,* 1971, **8**(3), p. 290-92. (with permission from Aerospace Access, AIAA, New York).

this pressure range, and therefore, GDFM is inadequate to explain intermittent burning in PBAA propellant; the predicted pressure range for extinction from GDFM theory does not tally with the experimental observations. PU-based propellants, at low percentage of the binder (20%), undergo self-extinction above 70 atm. At higher percentage of PU (30%), self-extinction occurs at all pressures in the range1-80 atm, except at 7-12 atm. Scanning electron microscopic observations of the extinguished surface (70 atm burning) revealed that the PU binder forms extensive char covering AP particles. From these observations, it is inferred that the carbonized layer on the oxidizer particles strongly perturbs ϕ, causing local self-extinction; this perturbation in ϕ is dependent on pressure[160].

Now, we consider another aspect, which exemplifies the influence of chemical nature of the binder, namely, effect of binder on the burning behaviour. Unlike in the case of CTPB, where a steady increase in $\dot{r}$ is observed with T_0, in a PU-containing propellant, a large scatter is observed for $\dot{r}$ at T_0's beyond 60 ^{0}C. This is attributed to deflagration along the faces of the burning strand[102]. This kind of burning behaviour is usually moderated by the addition of metal fuels like Al. Another important aspect is the effect of pressure on the σ_P of CSP. In AP/CTPB or of HTPB propellant, σ_P is almost invariant with pressure[102,109]. However, a theoretical study[91] on AP/polysulfide propellant suggested that σ_P should increase with pressure. Perhaps more studies are needed to understand this aspect to arrive at some useful generalised conclusions.

CHAPTER 3

SUBLIMATION, THERMAL DECOMPOSITION & DEFLAGRATION BEHAVIOUR OF AMMONIUM PERCHLORATE

3.1 AN OVERVIEW

AP is the principal ingredient and the most practical oxidizer in CSP[16]. It is also used in explosives[161,162]. The available literature indicates that it is one of the most studied molecules in respect of various facets, especially its decomposition and combustion behaviours[163-165]; studies on decomposition outnumber those on combustion. Recently, considerable interest has been evinced in porous AP, it is promising for obtaining increased $\dot{r}$ of the propellant[166]. The decomposition of porous AP is faster than that of fresh AP, it decomposes at a temperature 50 °C below that at which fresh AP decomposes[167]. But heat of decomposition is not affected[167]. In the propellant, the binder diffuses into the pores of porous AP and as a result, elongation of the propellant decreases[168]. It also affects the cross-linking density of the binders[169].

AP in a propellant can be reliably estimated by titrating with tetra-butyl ammonium perchlorate using pyridine as the solvent[170]. It has also been found that $\dot{r}$ of the propellant increases by using freeze-dried AP[171].

AP can undergo either sublimation or decomposition or decomposition and sublimation simultaneously, depending upon the temperature and pressure conditions[172-175]. Under deflagration conditions, whether sublimation occurs or not is a debatable point. Studies on the decomposition characteristics of AP are of prime importance and give valuable information regarding the actual species emanating from the propellant surface that mix and react in the gas phase, and on the phenomenon[176] of ageing of CSP etc.

Studies by Kishore, *et al.*[61,177,178] have revealed that changes in propellant $\dot{r}$, thermal decomposition rate and the extent of ageing, get reduced as the oxidizer loading increases. It has also been observed[176] that ammonium salts like $(NH_4)_2HPO_4$, NH_4F, NH_4Cl and NH_4Br desensitize the thermal decomposition of AP to increase the thermal stability and hence the longevity of the propellants[179]. Thus, the ageing characteristics are directly related to the thermal stability of the oxidizer.

In this chapter, the decomposition characteristics of AP, as affected by temperature, purity and pressure are presented. The reactions initiated at the solid surface leading to 30 % decomposition in the low temperature region, and the high temperature decomposition characteristics are discussed. Theoretical and experimental aspects of enthalpy and activation energy for the decomposition processes and their mechanisms are discussed.

AP is a unique oxidizer and functions as a monopropellant too, since it self-deflagrates above its low pressure limit (LPL, 20 atm)[163]. The deflagration rate of AP is of the same order as that observed for many AP-based CSP's at typical pressures and since it is present in large proportions it may control the combustion of CSP. Deflagration of AP is considered as a prelude to the understanding of the more complex processes of combustion of CSP. Many models like the Hermance model[90] and multiple flame model[91] consider AP monopropellant flame as the key step in the condensed phase and gas phase combustion of CSP. Studies on deflagration of AP also help in understanding the mechanism of catalyst action on the burning rate[16,163] of CSP. In this chapter, various physicochemical processes operative in the condensed phase are described. Results of studies on the self-deflagration characteristics of AP influenced by P and T_0 are presented. The existence of LPL, its dependence on physicochemical characteristics of the solid phase and interrelationships with $\dot{r}$ and σ_p are discussed. Variations in σ_p with pressure as evidenced by condensed phase processes, are also discussed.

3.1.1 Physical Properties of Ammonium Perchlorate

There have been a lot of studies on the determination of heat capacity (C_p), density (ρ), thermal conductivity (k) and thermal diffusivity (α) of AP. The results are summarized in Tables 3.1 and 3.2. k and α values for AP in the cubic region have been obtained by extrapolation of the reported data.

Table 3.1. Specific heat *(C_p)* and density *(ρ)* data for AP

Source of data	*Specific heat (cal g^{-1} K^{-1})*			
	Ortho	*Cubic*	*Melt*	*Gas*
Guirao and Williams[180]	0.309	0.365	0.328	0.300
Hall and Pearson[85]	0.308	0.365	—	—
Beckstead, Derr and Price[91]	0.300	0.300	—	0.305
Manelis and strunin[181]	0.300	0.300	—	0.306
Price, Boggs and Derr[182]	0.332* (473K)	0.432(673K)	—	—
Sohn[183]	—	—	—	0.312
Hertzberg[184]	0.370	0.370	—	—
Rosser, Inami and Wise[185]	0.333	—	—	—
Experimental work	0.340	0.340	—	—

	Density (g cm^{-3})		
	Ortho	*Cubic*	*Melt*
Guirao and Williams[180]	1.95	—	1.71
Hall and Pearson[85]	1.95	1.71	—
Beckstead, Derr and Price[91]	1.80	—	—
Jacobs and Whitehead[163]	1.95	1.76	—
Hertzberg[184]	1.95	—	—
Sohn[183]	1.95	—	—
Caveny and Pittman[186]	—	—	1.71

* C_p (Orthorhombic) = 0.13626 + 0.000414T
C_p (Cubic) = 0.15309 + 0.000414T

Table 3.2. Thermal conductivity (k) and diffusivity (α) data for ammonium perchlorate

Source of data	*Thermal conductivity (cal cm^{-1} s^{-1} K^{-1})*		
	Solid	*Melt*	*Gas*
Guirao and Williams[180]	—	0.9 x 10^{-3}	0.1 x 10^{-3}
Hall and Pearson[85]	1.112 x 10^{-3}	—	—
Manelis and Strunin[181]	—	—	1 x 10^{-3}
Price, Boggs and Derr[182]	f(T)	(0.3 to 1)x10^{-3}	—
Beckstead, Derr and Price[187]	—	—	0.3 x 10^{-3}
Sohn[183]	0.16 x 10^{-3}	—	—

Contd...

Source of data	*Thermal conductivity (cal cm^{-1} s^{-1} k^{-1})*		
	Solid	*Melt*	*Gas*
Caveny and Pittman[186]	0.97×10^{-3}	—	—
Rosser, Inami and Wise[185]	0.90×10^{-3}(673K) (extrapolated)	—	—
	Thermal diffusivity (cm^2 s^{-1})		
Hall and Pearson[85]	2.17×10^{-3}	—	—
Kumar[94]	1.50×10^{-3}	1.5×10^{-3}	—
Rosser, Inami and Wise[185]	—	—	—
Price, Boggs and Derr[182]	2.5×10^{-3}	—	4.55×10^{-6} T
Rosser, Inami and Wise[185]	0.7×10^{-3} $(673K)^{*}$	—	—
Calculation from k, and C_p	1.5×10^{-3} $(673K)^{**}$	—	—
Experimental work	$1.1 \times 10^{-3***}$	1.77×10^{-3}	

* Value extrapolated from data.

** Calculated from k=0.9 cal cm^{-1} s^{-1} K^{-1}; ρ =1.76 g cm^{-3} and C_p = 0.34 cal g^{-1} K^{-1} :

*** In solid AP it is a mean of 0.7×10^{-3} and 1.5×10^{-3} cal s^{-1} K^{-1}; C_p = 0.33 cal^{-1} g^{-1} K^{-1} and ρ = 1.71 g cm^{-3}

3.2 SUBLIMATION FEATURES OF AMMONIUM PERCHLORATE

AP undergoes phase transition from orthorhombic to cubic structure at 240 °C due to the rotation of perchlorate ion[163]. From data given in Table 3.3, an average value of 20 cal g^{-1} may be

Table 3.3. Enthalpy data for AP phase transition, sublimation, decomposition and melting

Process	*Enthalpy (cal/g)*
Phase transition	+19.57[188], +22.98[85], +21.28[180] +21.28[189], +19.50[186], +20.30[180] +20.00[191], +19.60[182]
Sublimation	+497.0[180], +500.4[192], +480.0[91] +500.0[120], +493.6 ±17 (Exptl)[193] + 497.9[194]
Decomposition	-260.0 (Exptl)[195], -270.64[181] -300[197], -385[193], -800[189] -326.55[196], -277.4[190]
Melting	+59.6[180.182]

assigned for the enthalpy of phase transition of AP. AP also undergoes sublimation and decomposition under appropriate pressure conditions[172-174]. Sublimation of AP strongly depends on its purity[198]. It is also affected by additives[199]. It has been shown[172,191] that below 20 torr, AP undergoes dissociative sublimation and above 60 torr and up to 250 atm, AP only decomposes with a heat release of 260 cal g^{-1} and with little or no sublimation. However, Kraeutle[200] has reported that the residue obtained on decomposition undergoes sublimation quantitatively even at 1 atm pressure. Boldyrev, *et al*[196] have shown by mass spectroscopy that at 1 to 50×10^{-6} torr and 280 °C-500 °C, AP dissociates to NH_3 and $HClO_4$. As regards the mechanism, it is generally believed that proton transfer is the rate-controlling step in sublimation[198,201,202].

$$NH_4ClO_4 \rightleftharpoons NH_3(ads) + HClO_4(ads) \rightleftharpoons NH_3(g) + HClO_4(g)$$

3.2.1 Enthalpy

The dissociative sublimation process gives rise to a broad endotherm after phase transition. Figure 3.1 shows a typical differential thermal analysis (DTA) curve. The heat of endothermic dissociative sublimation (Table 3.3) was measured by Inami, *et al*[193] while other authors reported only calculated values. An experimental value of 494 cal g^{-1} has been considered by Price, *et al*[182]. and Guirao and Williams[180]. Kishore, *et al*[194] calculated the heat of sublimation to be 497.9 cal g^{-1}. Considering the theoretical and experimental

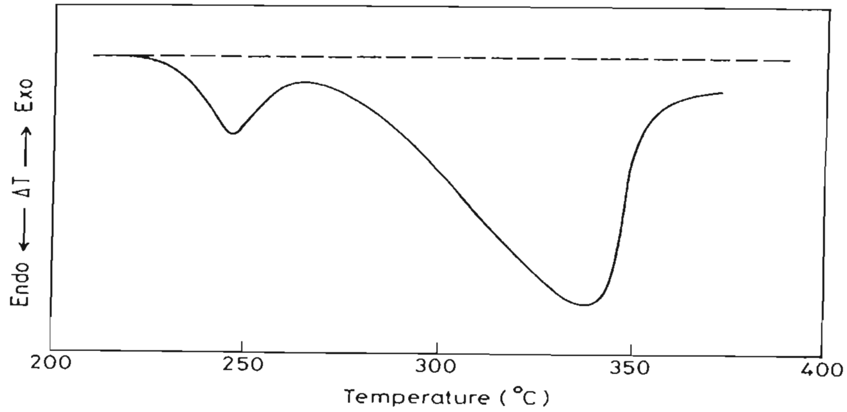

Figure 3.1. DTA trace of AP phase transition and sublimation under reduced pressure[174].

values, a mean value of 496 cal g^{-1} could be assigned for the endothermic sublimation of AP.

3.2.2 Activation Energy

Bircumshaw and Phillips[203] studied the vacuum sublimation rate by the weight-loss technique in the temperature range 260-320 °C. For the observed activation energy (E) of 22.0 kcal/mole, they advocated the proton transfer mechanism. Jacobs and Jones[204] reported a high E value of 30.0 kcal/mole. Pai Verneker, *et al*[172] studied thermal decomposition and sublimation in the temperature range 220-320 °C and reported a value of 18.2 kcal/mole, thereby resolving the discrepancy in the high value observed by Jacobs and Jones[204]. More appropriately, Kishore and Pai Verneker[194], based on the thermodynamic interpretation of the process, simplified activation energy (E) dependence on enthalpy of sublimation to the following form.

$$E = \left[\Delta H_{s(NH_3)} + \Delta H_{s(HClO_4)}\right] \qquad (23)$$

where $\Delta H_{s(NH_3)}$ and $\Delta H_{s(HClO_4)}$ are the enthalpies of sublimation of NH_3 and $HClO_4$ components. E value for AP sublimation calculated from Eqn (23) has been found to be 16.3 kcal/mole.

3.3 DECOMPOSITION OF AMMONIUM PERCHLORATE

Decomposition of AP strongly depends on the prevailing experimental conditions of pressure, temperature and whether it occurs in an open or a closed system. Depending upon the pressure, sublimation and decomposition occur simultaneously to some extent in an open system, while in a closed system the sublimation process is overtaken by decomposition[205]. The chemical reactivity is influenced by active volume, surface of the sample container and temperature distribution prevailing in it[206]. In aqueous solution, AP decomposes at a much slower rate than in neat form[207]. But in methanol, it decomposes at the same rate as neat AP[207].

Thermal decomposition of AP has been studied widely at atmospheric pressure[85,163,190,208-210]. A typical DTA curve (Fig. 3.2b) shows phase transition endotherm at 240 °C and decomposition exotherms at about 300 °C and 400 °C, which we shall term as low temperature decomposition (LTD) and high temperature decomposition (HTD) exotherms, respectively. Decomposition of AP often depends on the degree of purity[211]. A typical differential

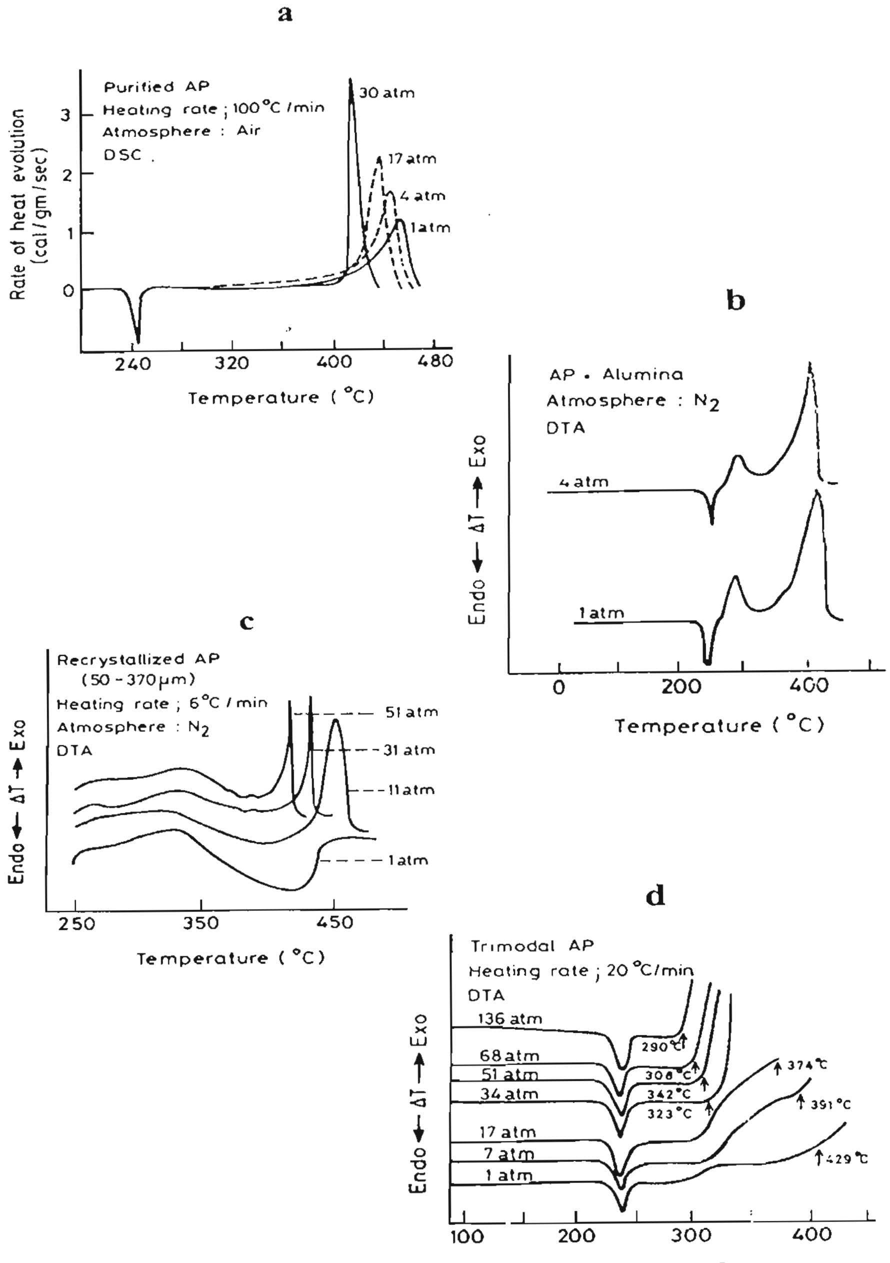

Figure 3.2. Effect of pressure on DSC and DTA thermograms of AP[195, 208, 209 & 210].

scanning calorimeter (DSC) thermogram of AP of different purity levels is shown in Fig. 3.3. Commercial AP shows a large exotherm around 300 °C which is less pronounced in the case of AP crystals

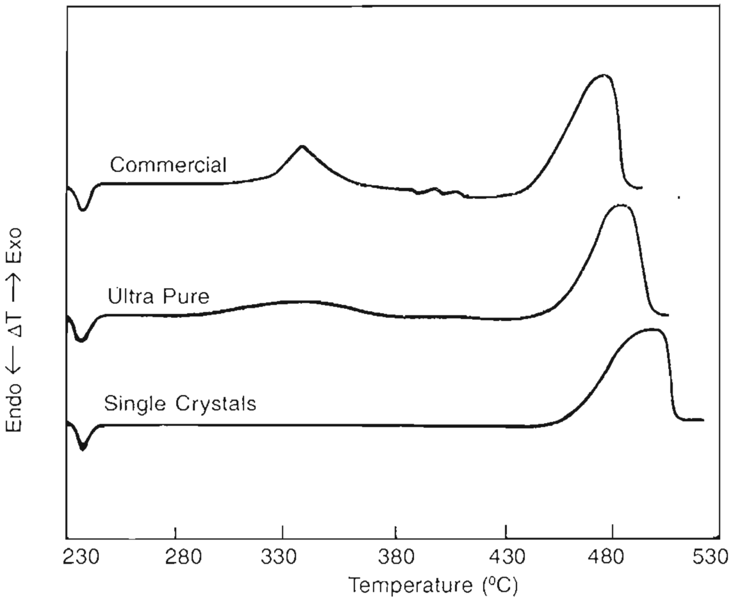

Figure 3.3. Effect of purity on DSC thermograms of AP[211].

of the highest purity and is absent in the case of single crystals. However, it undergoes 30% decomposition when it is held isothermally at 230 °C (below its phase transition temperature) for several hours[212]. Crystals, when ground and heated, exhibit the first exotherm due to the formation of perchloric acid or generation of more defects[213]. Several views have been expressed[214] as to the cause of the first exotherm. One view is that transition metal impurities, such as copper salts, catalyse the thermal decomposition of AP to produce the exotherm. Another view is that it could arise from excess $HClO_4$ trapped with AP crystals. As per still another view chlorate could be present in AP as an impurity. Rajeshwar, *et al*[215] observed that the decomposition temperature of AP is lowered by as much as 100 °C in the presence of electric field.

A plausible explanation for AP to undergo decomposition in two temperature regimes[216,217] is based on the fact that at low temperatures (~300 °C), decomposition occurs to only about 30% and is incomplete; above this temperature it decomposes to completion. When AP is kept isothermally in the orthorhombic region, it also decomposes, but at a much slower rate. LTD occurs below 300 ^{0}C and covers both orthorhombic (240 ^{0}C) and cubic (240-300 ^{0}C) AP. Even thermogravimetric (TG) studies show a break at 30% weight loss around the temperature of the first exotherm. In the low temperature region, the reaction is initiated on the surface and does not penetrate into the interior, as it is limited by the intermosaic block of AP crystal and only 30% decomposition occurs. The residual porous solid from LTD was found to contain a loose aggregate of crystallites with a few imperfections and with a total surface area greater than that of the original sample[163,188]. According to Maycock and Pai Vernekar[217], the $ClO_4^{\bullet}$ radical formed by electron transfer from ClO_4^- to interstitial NH_4^+ requires fresh surface to decompose and to oxidize NH_3. Formation of a Frenkel defect does not lead to fresh surface, and, therefore, the decomposition terminates at 30%. Boldyrev, *et al*[218] found that the $HClO_4$ formed in the primary stage of LTD accumulates and combines with NH_3 before it has a chance to decompose and oxidize NH_3 and thereby the reaction comes to a halt at 30% weight loss. Pai Verneker, *et al*[219] have shown that accumulation of acid in the solid phase takes place during the thermal decomposition of orthorhombic AP at 230 ^{0}C. However, Davies *et al*[220] found that loss in weight of AP occurs even after 30% decomposition when it is left for several days; they argued that it happens due to sublimation. But the questions are; (i) whether sublimation or decomposition or both occur and (ii) whether orthorhombic AP decomposes to completion? It has been found that LTD is not incomplete, but goes to completion with an activation energy of 20 kcal/mole and the process is exothermic[219]. The fact that it is a decomposition reaction and not sublimation is supported by the *IR* analysis done by Varadaraju[221]; the process seems to be akin to the low temperature decomposition of cubic AP.

Jacobs[163] extended the mechanism for the decomposition of orthorhombic AP to explain the decomposition of cubic AP; at high temperatures, both $HClO_4$ and NH_3 desorb into the gas phase (details given in Section 3.3.3). If the ambient pressure is increased, diffusion of the products decreases and the usual dissociation of $HClO_4$ and oxidation of NH_3 occur. According to Pearson and Jacobs[222], the chemistry of high temperature decomposition (HTD) of AP is dominated by the decomposition reactions of $HClO_4$ and by the oxidation of NH_3. The formation and decomposition of $HClO_4$ have been monitored at some distance above the surface and the decomposition kinetics is found to depend on the temperature[223]. Koroban and Guk[224] found that the gaseous products of decomposition of deuterated AP influence the decomposition rate, which is more in the cubic region compared to normal AP. Unlike the Frenkel defect, Schottky type of defects, formed in the cubic region, are known to produce a new surface and the decomposition proceeds to completion[217].

3.3.1 Enthalpy

There is a lot of controversy about the enthalpy value for the exothermic decomposition of AP, as seen in Table 3.3. One can see that the values range from 260 cal g^{-1} to 800 cal g^{-1}. Waesche, *et al*[195] reported 260 cal g^{-1} from DSC measurements. They compared the experimental value with the theoretical value calculated by product distribution[128], for which no details are given. Based on DSC experiments, Kishore *et al*[190] obtained a value of 277 cal g^{-1}, which is the net enthalpy of the LTD and HTD exotherms. Considering the theoretical value of 260 cal g^{-1} from the reaction energies of the decomposition products and the experimental values of 260 cal g^{-1} and 277 cal g^{-1}, an average value of 265 cal g^{-1} could be assigned for the exothermic decomposition of AP.

3.3.2 Activation Energy

Activation energy measurements have been made in different temperature regimes. Studies[225] on thermal decomposition in the presence of electric field have shown that the activation energy in the range 140-190 °C (orthorhombic) is around 15 kcal/mole which compares reasonably well with the value of 20.0 kcal/mole obtained from electrical conduction studies; charge-carrying species, such as H^+ and NH_4^+ are known to be involved.

In the range 190-240 °C, the extent of decomposition *vs* time curve of orthorhombic AP is sigmoidal with an induction period, an acceleration region and finally a deceleration region. Activation energy in this region is found to be 30 kcal/mole and decomposition goes up to only 30%. While studies stress the decomposition to be a proton-transfer process, some authors argue that decomposition proceeds by the initial destruction of NH_4^+ interstitials.

In the range 240-350 °C (cubic AP), decomposition goes to completion. However, a break occurs at 30% decomposition. The extent of decomposition *vs* time curve for this range is characterized by a short induction period, the main reaction being deceleratory in nature. Two activation energy values (30 kcal/mole for the proton transfer process and 20 kcal/mole for diffusion in Schottky type defect structure) have been reported in this range.

Above 350 °C (cubic AP), decomposition exhibits a total deceleratory curve and is associated with fastness and completeness of decomposition. Two values of 30 kcal/mole and 60 kcal/mole have been reported for the decomposition, and the mechanism has been argued in terms of proton transfer process, electron transfer process and Cl-O bond dissociation.

Although activation energy measurements made for the sublimation and decomposition processes point to proton transfer as the rate-determining step, the activation energy values for the two processes differ. This does not give a unified picture of the mechanism operative in the decomposition of AP.

3.3.3 Mechanism of Ammonium Perchlorate Decomposition

Several studies have been made to understand the mechanism of decomposition of AP[226-228]. Reviews by Hall and Pearson[85], Jacobs and Whitehead[163], and Kishore and Sunitha[71] give good accounts of the mechanism of thermal decomposition of AP, but it still remains a matter of debate. Three important decomposition mechanisms are discussed below.

3.3.3.1 Proton transfer mechanism

Bircumshaw and Newman[229-231], Jacobs and Whitehead[163] and Isaev, *et al*[232] proposed proton transfer from cation to anion, resulting in adsorbed ammonia and perchloric acid on the surface of AP, followed by evaporation of NH_3 and $HClO_4$ into the gas phase, depending upon the prevailing temperature and pressure conditions.

Proton Transfer Process

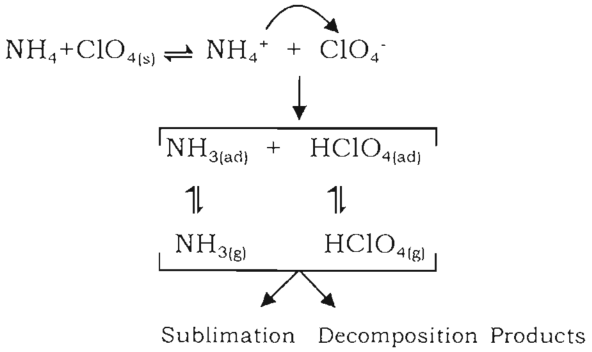

These authors have argued that LTD being faster than the rate of sublimation in vacuum must involve the adsorbed species, viz., NH_3 and $HClO_4$. Confirming the proton transfer mechanism of decomposition of AP over a wide range of temperature, Boldyrev, *et* *al*[233] and Khairetidinov[234-236] showed that the proton transfer process includes reorientation of the protonated anion:

$$\overset{+}{H}\,Cl\overset{-}{O_4} \longrightarrow Cl\overset{-}{O_4}\,\overset{+}{H}$$

for which the frequency is 10^3 sec^{-1}, and proton jumps to a neighbouring anion for which also the frequency is $10^{13} sec^{-1}$.

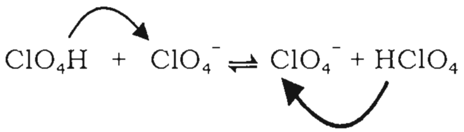

$$ClO_4H + ClO_4^- \rightleftharpoons ClO_4^- + HClO_4$$

These two steps are believed to be responsible for migration of the proton to the anion in the lattice. The main contribution to the value of the activation energy for the migration is made by reorientation of the protonated anion. According to this mechanism, which is widely accepted[237], both sublimation and decomposition could occur, depending upon the experimental conditions like pressure and temperature.

Tang and Fenn[238] observed that the vapours subliming from the surface of the single crystal of AP were of NH_3 and $HClO_4$. The decomposition, according to the proton transfer mechanism, could be a direct bimolecular reaction between NH_3 and $HClO_4$ or could proceed via bimolecular decomposition of $HClO_4$. This gets support from the fact that decomposition of AP[239-241] is accelerated by $HClO_4$ and retarded by NH_3[240].

3.3.3.2 Electron transfer mechanism

Maycock and Pai Verneker[217,242], based on a careful kinetic analysis of the decomposition products and electrical conductivity studies, have argued in terms of a point defect model. They have assumed a Frenkel structure in orthorhombic AP with NH_4^+ ions in the interstitial position. They have pointed out that the decomposition proceeds via the initial destruction of the NH_4^+ interstitials, which is expressed as follows[4] :

$$Cl_4^- + NH_4^+ \rightarrow ClO_4^- + NH_4^\bullet$$

$$NH_4^\bullet \rightarrow NH_3 + H^\bullet \quad (26\pm1.0\ \text{kcal/mole})$$

$$ClO_4^\bullet + 2H^\bullet \rightarrow H_2O + ClO_3$$

The $ClO_4^\bullet$ radical formed in the body of the crystal will be stable because of the crystalline force fields. However, it is probable that $ClO_4^\bullet$ radical can effectively migrate to the surface by an electron transfer process from ClO_4^- to $ClO_4^\bullet$ radical. Break-up of $ClO_4^\bullet$ radical on the surface and subsequent oxidation of NH_3 will give rise to a decomposition nucleus, which will then grow into the crystal. Decomposition on the inner face of the nucleus will not occur readily, because electron transfer will be more difficult in a disorganized lattice. Gamma-irradiated AP also decomposes by an electron-transfer mechanism. NH_4^+ and ClO_4^-, in the interstitial site, react to form $NH_4^\bullet$ and $ClO_4^\bullet$ radicals which decompose to NH_3 and ClO_3[243].

A very important feature of this mechanism is the requirement of a fresh surface for the decomposition to proceed. The formation of Frenkel defects does not lead to the production of a fresh surface and hence the decomposition terminates at 30%. The defect structure in the temperature range 250-350 °C is of the Schottky form. The creation of a new Schottky pair produces a new surface and hence decomposition proceeds to completion. In the temperature range 350-440 °C, AP is shown to exhibit electronic conduction due to electronic transition.

3.3.3.3 *Mechanism via formation of nitryl perchlorate intermediate*

Bircumshaw and Newman[230,231] suggested that ammonium nitrate may be a product of decomposition of all ammonium salts of sufficiently oxygenated acids. Kishore, *et al*[244] observed that there is flux growth of ammonium nitrate from a eutectic mixture of AP-$NaNO_3$ at 233 °C in which ClO_4^- is stabilized by a metathetical reaction. Solymosi[245] suggested that the stability of the ClO_4^- ion gets reduced on covalent bond formation.

Galwey and Mohamed[246-248] confirmed the qualitative results of Pai Verneker, *et al*[249] that oxidized nitrogen species (NO_3^-) are formed in partially decomposed AP. They proposed that the oxygenated nitrogen must be in the form of nitrylperchlorate intermediate in the low temperature decomposition of AP in the range 187-237 °C wherein the reactions pertain to the orthorhombic AP. It is believed that the formation and rapid decomposition of NO_2ClO_4 is the rate-controlling step in AP decomposition. This mechanism is valid in the orthorhombic region represented in the following scheme.

The highly active disintegration product of ClO_4^- ion formed by decomposition of AP oxidizes NH_4^- and/or NH_3 to yield NO_2^+, which combines with the ClO_4^- ion and forms nitrylperchlorate (NO_2ClO_4) and they exist in a dynamic equilibrium. It is observed that NO_2ClO_4 is volatile and is confined within the pores of the reaction zone in the molten phase. NO_2ClO_4 being unstable, rupture of the covalent bond to $[O_2N^+O]$ and ClO_3^- ion occurs more readily than that of the ionic perchlorate[250]. The $[O_2N^+O]$ formed subsequently disintegrates to (N^+O) and O_2 (or 2O) which combine with ClO_3 to form NO^+ClO_3 and O_2 (or 2O). This species capable of oxidizing NH_4^+ and/or NH_3 to N^+O_2, thereby regenerating the intermediate; the cycle recurs. The ClO_3^- ion is capable of oxidizing NH_3 and/or NH_4^+ to form NH_4NO_3. This is also supported by the fact that NH_4ClO_3 on decomposition forms NH_4NO_3[230].

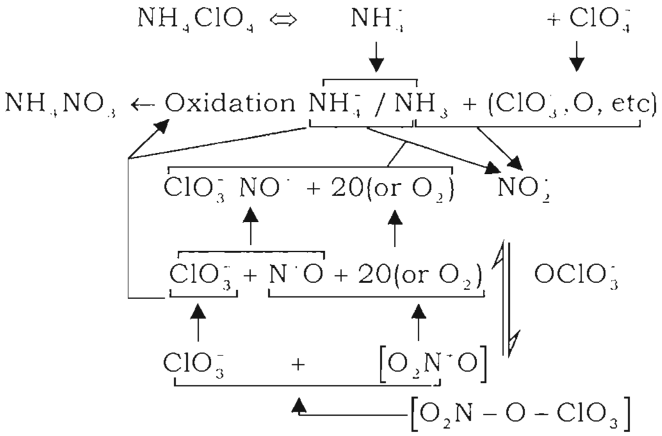

Covalently bonded nitryl perchlorate intermediate

Evidence supporting this mechanism includes analytical detection of the NO_2ClO_4 intermediate. The activation energy for AP decomposition is close to that reported for NO_2ClO_4, which is 31.0 kcal/mole, indicating that the same rate-controlling process operates in both the decomposition reactions. Evaluation of the time required to complete LTD by extrapolation of the kinetic data for AP has suggested that the decomposition of NO_2ClO_4 is a rate-controlling step. Addition of NH_4NO_3 or $Mg(NO_3)_2.6H_2O$ reduces the induction period. The additives do not change the mechanism; this is consistent with the view that the promotion of decomposition involves the conversion of NO_3^- to NO_2^+, which participates in the reaction, as mentioned in the above scheme.

3.3.4 Stoichiometry of Ammonium Perchlorate Decomposition

Chemical analysis of the decomposition products of AP is rather complex. The basic chemistry of the exact reaction involved is not yet clear. Simchen[206] has reviewed the chemical, thermochemical and stoichiometric aspects of the results of this reaction. Several equations are proposed which are stoichiometrically correct and chemically wrong, as some of the products identified do not account for the proposed reaction scheme.

Dode[251] did chemical analysis of the gaseous products of vacuum decomposition of AP, after condensing them in a liquid air trap, and proposed equations for LTD and HTD. At temperatures in the range 200-230 °C, the stoichiometry is expressed[252] as:

$$NH_4ClO_4 \rightarrow 2H_2O + 0.5Cl_2 + 0.75O_2 + 0.5N_2O$$

and for the temperature range 300-420 °C, the stoichiometry is[85] :

$$NH_4ClO_4 \rightarrow 2H_2O + 0.5Cl_2 + 0.5O_2 + NO$$

Bircumshaw and Newman[229] and Rosser *et al*[253] confirmed Dode's[251] observation of temperature-sensitive product distribution.

In order to identify the primary products of decomposition of AP and minimize the interference of secondary reactions in product analysis, mass spectroscopic technique has been employed[85]. Detailed investigations by Pellet and Saunders[254] have established the following product composition in the temperature range 140-240 °C:

$$NH_4ClO_4 \rightarrow 1.83H_2O+0.33HCl+0.6O_2+0.33Cl_2+0.33N_2O+0.33NO_2$$

They also found that the product composition changes above 240 °C.

Since the nature and relative proportions of the products formed depend on temperature, pressure, and sampling technique employed, Jacobs and Pearson[252], on the basis of analysis of major products reported by several workers, have given a typical average representation of the stoichiometry of decomposition of AP in the temperature range 160-380 °C:

$$NH_4ClO_4 \rightarrow 1.88H_2O + 0.24HCl + 0.6O_2 + 0.38Cl_2 + 0.264N_2O + 0.323NO_2 + 0.07N_2 + 0.01NO$$

It may be seen from the above two equations that in the wider temperature range of 140-400 ^{0}C, except for a relatively small proportion of N_2 and NO at higher temperatures, the major products and their compositions are almost same, unlike the stoichiometry reported by Dode[251].

3.3.5 Effect of Pressure on Thermal Decomposition of Ammonium Perchlorate

The first report on the study of thermal decomposition of AP as a function of pressure was by Stone[208] (Fig. 3.2). The author[195, 208-210] has not discussed much about the pressure dependence of decomposition of AP, but an examination of the DTA curves clearly indicates that decomposition of AP is accelerated as the pressure is increased. Waesche and Wenograd[195] recorded DSC thermogram of decomposition of AP up to 30 atm and observed that when pressure is increased, the high temperature peak becomes sharper and occurs at lower temperatures, but the phase transition temperature is unaffected. This may be due to the negligible volume change taking place during phase transition. Similar results were obtained by Morisaki and Komamiya[209] who obtained DTA of AP in N_2 and O_2 at various pressures (Fig. 3.2). Schmidt[210] obtained DTA thermogram of AP up to 136 atm. He has not reported the complete thermograms, but it is possible to identify the temperature at which the onset of the fast decomposition in the high temperature region occurs (Fig. 3.2). This temperature gets lowered as the pressure is increased. The data of Schmidt[210] were plotted against the above temperature and linear dependence was obtained, suggesting a correlation between $\dot{r}$ and thermal decomposition of AP at higher pressures. Similar to the effect of thermal decomposition, the ignition of AP is also sensitized with pressure[255,256]. Demazeu, *et al*[257] studied the effect of pressure on the thermal decomposition of AP+Cr_2O_3 at 350 ^{0}C; at 2000 atm pressure, CrO_2, a magnetic material, is obtained.

3.4 SALIENT FEATURES OF AMMONIUM PERCHLORATE DEFLAGRATION

The deflagration of AP has been studied as a function of various parameters, such as pressure[258,259], initial temperature[258,260-263] and particle size[258,260,262]. The effects of catalysts as well as inhibitors have also been the subject of many studies[258,260,264-266]. One of the unique and elusive features of deflagration of AP is the existence of LPL (20 atm) below which AP does not undergo deflagration.

Although there are several interesting characteristics of deflagration of AP, the main emphasis here is on the condensed phase behaviour, influence of *P* and T_o, existence of LPL and its interrelationship with other parameters[267].

3.4.1 Condensed Phase Characteristics during Ammonium Perchlorate Deflagration

Deflagration of AP is depicted schematically in Fig. 3.4, phase transition occurs in the subsurface region[268-270]. The thickness of the phase transition layer in quenched single crystals of AP was measured by Beckstead and Hightower[271]. According to McGurk[272,273], orthorhombic and cubic phases coexist over a time-dependant 50 μm zone in the surface layer, which becomes an advancing combustion surface. Melting of AP is not observed during decomposition conditions. DTA curve (Fig. 3.2b) shows that the decomposition goes to completion at 400 °C at atmospheric pressure and gets sensitized at higher pressures; however, it does not undergo melting. Hightower and Price[268] and other investigators[77,243] obtained evidence that the surface of deflagrating AP is covered with a liquid phase; the quenched samples show the existence of melt.

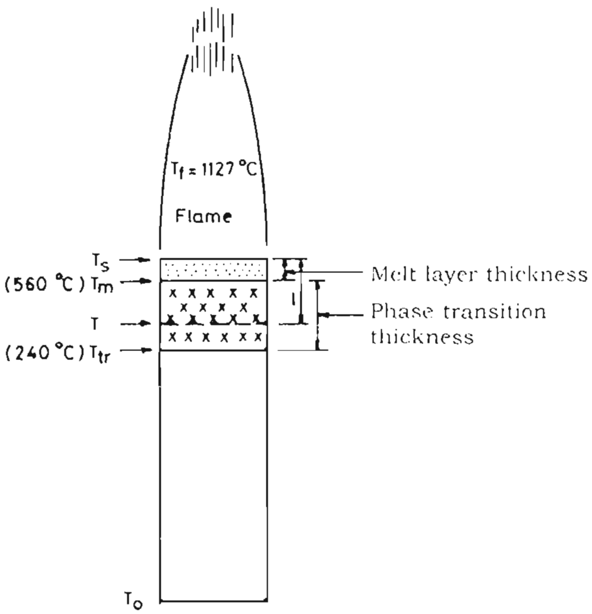

Figure 3.4. Schematic representation of ammonium perchlorate deflagration.

As mentioned earlier, at and above 1 atm pressure, AP undergoes only decomposition. However, whether decomposition alone or decomposition with sublimation occurs during deflagration is not known for certain and it is difficult to confirm the occurrence of sublimation under combustion conditions. Conflicting views regarding the occurrence of sublimation are available in literature. According to Lengelle, *et al*[120], rapid decomposition and sublimation of AP occur during deflagration. The work of Waesche and Wenograd[195] showed that AP does not undergo any sublimation at P>1 atmosphere. Hightower and Price[268] and Boggs[121] also argued against the occurrence of sublimation.

As in CSP, condensed phase reactions have been found to occur in AP too[267.274,275]. The heats of phase transition, sublimation, decomposition and melting are taken into account (Table 3.4) and the condensed phase heat release has been obtained by a simple thermodynamic approach :

$$\text{Heat released in the condensed phase} = \frac{(1-\beta)\,\Delta H_d}{431.5 + \beta \Delta H_s} \qquad (24)$$

where β is the fraction of AP sublimed, ΔH_d the heat of decomposition, and ΔH_s is the heat of sublimation. Sublimation during deflagration may be considered to occur somewhere between 0 and 30%[202]. Even with 30% sublimation, significant condensed phase heat release occurs just below the surface and thus it plays an important role in deflagration of AP. Derivation of Eqn (24) is based on the energy balance during the steady state deflagration

Table 3.4. Data on AP

Phase transition temperature (T_{tr})	240 °C
Melting temperature (T_m)	560 °C
Surface temperature (T_s)	T_s = f(p)
Flame temperature (T_f)	1127 °C
Heat of Phase transition (ΔH_{tr})	+20 cal g^{-1}
Heat of Sublimation (ΔH_s)	+496 cal g^{-1}
Heat of Decomposition (ΔH_d)	-265.0 cal g^{-1}
Heat of Melting (ΔH_m)	+60 cal g^{-1}
Specific heats of	
a) Orthorhombic solid (Cp_o)	0.34 cal g^{-1} C^{-1}
b) Cubic Solid (Cp_c)	0.34 cal g^{-1} C^{-1}
c) Melt (Cp_m)	0.33 cal g^{-1} C^{-1}
d) Gaseous products (C_{pg})	0.30 cal g^{-1} C^{-1}

process. It is considered that AP, on complete combustion, releases heat *(ΔH)*, which is adiabatically used to raise the temperature of the product gases to the adiabatic flame temperature, T_f. In order to calculate the enthalpy changes at various stages in the combustion process, Hess's cycle is used. Accordingly, the energy released to raise the temperature of AP from T_o to a diabatic flame temperature T_f is given by

$$\Delta H = \beta \Delta H_s + (1-\beta)\,\Delta H_d = \{Cp_o(T_{tr}-T_o) + \Delta H_{tr} + Cp_c(T_m-T_{tr}) + \Delta H_m + Cp_m(T_s-T_m) + Cp_g(T_f-T_s)\} \qquad (25)$$

where Cp_o, Cp_c, Cp_m and Cp_g are the specific heats of orthorhombic, cubic, melt and the gaseous products of combustion, respectively; T_{tr}, T_m and T_s are the phase transition, melting and surface temperatures, respectively; and ΔH_{tr}, ΔH_m and ΔH_r are the heats of phase transition, fusion and gas phase reaction, respectively (Table 3.4)[188]. Evidences in favour of the occurrence of condensed phase reactions in deflagration of AP are as follows. A correlation of $\dot{r}$ with the temperature of decomposition of AP has been obtained from the data of Schmidt[210], which indicates that $\dot{r}$ depends on the rate of thermal decomposition of AP at higher pressures[70]. Kinetic analysis[274], which is primarily based on the proton transfer mechanism is outlined below:

$$NH_4ClO_4 \underset{k_2}{\overset{k_1}{\Leftrightarrow}} NH_3 + HClO_4 - 58\ kcal \qquad (26)$$

$$NH_3 + HClO_4 + xN_2 \overset{k_3}{\Leftrightarrow} \text{Decomposition products} + xN_2 + \Delta H_d \qquad (27)$$

is consistent with the observation that the decomposition of AP is sensitized with increase in pressure[195,209,210].

3.4.2 Chemical Reactions in the Gas Phase

In the gas phase, Korobeinichev and Kuibida[276] detected $HClO_4$, which is the basic product of condensed phase gasification. A general scheme for the chemical reactions associated with the self-sustained combustion of AP has been formulated[163]. According to this scheme, $HClO_4$ decomposes in the gas phase producing initially $ClO_3^{\bullet}$ and $^{\bullet}OH$ radicals:

$$HOClO_3 \rightarrow {}^{\bullet}OH + {}^{\bullet}ClO_3$$

$^{\bullet}ClO_3$ radical is very unstable and decomposes either bimolecularly to ClO_2 and O_2 or unimolecularly to ClO_2 and oxygen atom, or to $ClO^{\bullet}$ radical and O_2 :

$$2{}^{\bullet}ClO_3 \rightarrow 2ClO_2 + O_2$$

$$^{\bullet}ClO_3 \rightarrow ClO_2 + O^{\bullet}$$

$$^{\bullet}ClO_3 \rightarrow {}^{\bullet}ClO + O_2$$

The next stage is attacked by radicals on the ammonia molecules, principally by $ClO^{\bullet}$ radicals and possibly by $^{\bullet}OH$ radicals and by oxygen atoms, to form $^{\bullet}NH_2$:

$$NH_3 + {}^{\bullet}ClO \rightarrow {}^{\bullet}NH_2 + ClOH$$

$$NH_3 + O^{\bullet} \rightarrow {}^{\bullet}NH_2 + OH$$

$$NH_3 + {}^{\bullet}OH \rightarrow {}^{\bullet}NH_2 + H_2O$$

ClOH can further react with oxygen atoms or with $^{\bullet}OH$ radicals to regenerate $ClO^{\bullet}$ radicals:

$$ClOH + O^{\bullet} \rightarrow ClO^{\bullet} + OH$$

$$ClOH + {}^{\bullet}OH \rightarrow ClO^{\bullet} + H_2O$$

Reaction of NH_2 with O_2 gives NO, which then reacts as follows :

$$NH_2 + NO \rightarrow N_2 + H_2O$$

Ermolin, *et al*[277-279] substantiated direct and reverse rate constants for a large number of reactions involving several species in the AP flame. By mass probing, concentration profiles of the reacting species and temperature profile of AP flames have also been obtained. The mechanism of combustion of AP changes in the presence of fuels and additives[71].

3.4.3 Influence of Pressure on Ammonium Perchlorate Deflagration

Most of the existing combustion data relate to pressures well above 1 atm. Some representative atmospheric pressure data for the combustion of AP, assisted by preheating, are also available[255]. AP undergoes self-sustained combustion only in a certain pressure range, giving rise to pressure limits; it burns only above LPL[280]. The value of $\dot{r}$ at LPL for single crystals or high density discs is 2-3 mm/s. LPL is attributed to the radiant heat loss to the surroundings[183,281] and to the dependence of heat of decomposition of NO on pressure[109]. At LPL, sufficient amount of NO is observed in the final product of decomposition of AP while little is observed at higher pressures. This indicates that NO fails to decompose below a certain pressure and its persistence lowers the net energy release and contributes to LPL. LPL can be reduced to atmospheric pressure by increasing T_o, by incorporating additives, by adding fuels or by changing its particle size[280,282]. LPL of AP is affected by catalysts. Fe_2O_3 and copper chromite reduce it, while LiF and $CaCO_3$ increase it[283].

Considerable data exist on the dependence of $\dot{r}$ of AP on pressure. Several workers[83,284,285-290] have studied AP deflagration as a function of pressure. For a given T_o, the deflagration rate curve is divided into four pressure-dependent regimes based on the characteristics of burning surface structure, subsurface profile and energy transfer mechanism. Figure 3.5 shows the $\dot{r}$ *vs* P plot taken from the paper of Boggs, *et al*[284]. The data of other investigations have also been added.

Regime I (20-55 atm): Dependence of $\dot{r}$ on P is represented by Eqn (3) with n = 0.77. The value of $\dot{r}$ lies between 0.13 and 0.34 cm/s depending on *P*. The value of $\dot{r}$ increases with pressure. The regression is smooth and planar and the surface contains a thin layer of liquid over it. This regime is of importance in propellant combustion.

Regime II (64-138 atm): The value of *n* is found to be less than 0.77 and the $\dot{r}$ lies between 0.34 and 0.48 cm/s. Melt is observed in this region too. The surface exhibits a conspicuous intricate pattern of ridges and valleys, where reaction sites are localized.

Regime III (138-275 atm): The value of $\dot{r}$ lies in the range 0.48-1.0 cm/s. In this region, *n* is found to have a negative value and $\dot{r}$ decreases when pressure is increased, this is accompanied by a sporadic uneven surface. Quenched samples have indicated the formation of some needle-shaped crystals on the surface.

Regime IV (>275 atm): The value of $\dot{r}$ increases again as the pressure is increased. In this region, no melt is observed. The surface is found to be covered entirely by needle-shaped crystals. The upper pressure limit (UPL; 300 atm) up to which deflagration can be maintained and beyond which steady deflagration becomes difficult also exists[281,288]

In both III and IV regimes, Glaskova[289] observed irregular combustion and found the value of $\dot{r}$ to increase at pressures beyond 350 atm.

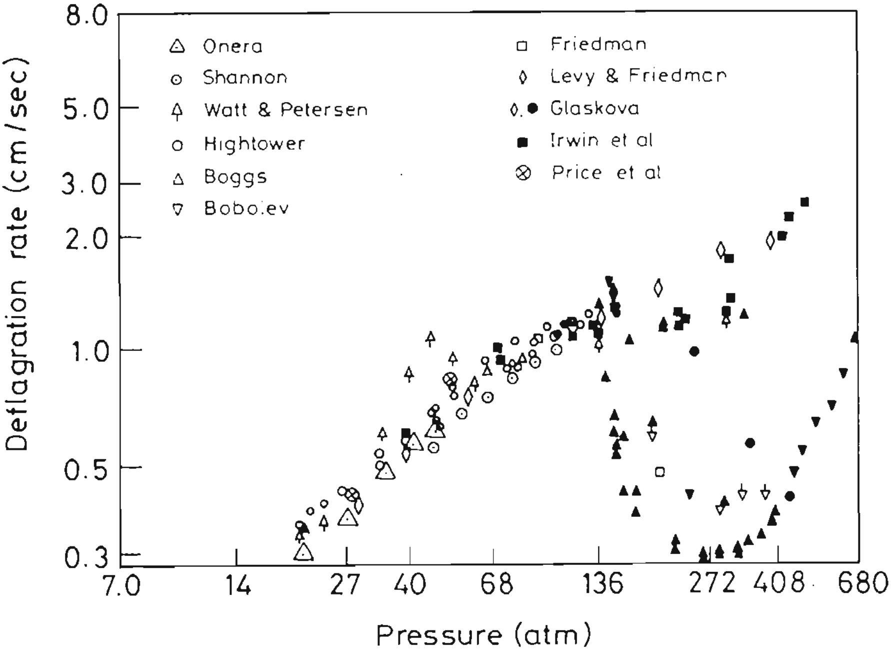

Figure 3.5. Dependence of burning rate of AP on pressure (ref. 284 and data added from ref. 85, 182, 268, 285-290).

Source : Boggs, T.L. Deflagration rate, surface structure and sub surface profile of self-deflagrating single crystals of ammonium perchlorate. *AIAA. J*, 1970, **8**(5), P.867-73. (with permission from Aerospace Access AIAA, New York).

3.4.4 Melting of Ammonium Perchlorate

Several studies[187,258,268] have revealed the presence of a melt on the surface of AP during deflagration. The melting temperature (T_m) has been reported to be in the range 442-592 ± 20 ^{0}C [186,271,291,292]. Based on the theory of corresponding states, Cordes[291] has obtained the T_m of AP by extrapolating both T_m and vapour pressure data for various ammonium salts as a function of inter-ionic distance (λ), as shown in Fig 3.6. Using Eqn (28) and setting the values for the

$$\log (P_m/P_{0.8}) = (6283.7/T_m)(0.25) \tag{28}$$

ratio of the vapour pressure by extrapolation, T_m of AP has been found to be 592±20 ^{0}C. Here P_m and P_0 are the vapour pressures of the salts at some fixed fraction of T_m. Through microscopic studies, Beckstead and Hightower[271] showed that the surface is not planar and the phase transition thickness was taken at the bottom of the depression. The ups on the surface seem to be due to solidification of molten AP and, therefore, the temperature measured at the bottom of the depression could be considered as the liquid-solid cubic AP interface temperature. The temperature reported as 560±35 °C could be taken as the T_m of AP. From electrical conductivity studies, Melik-Gaikazov and Marshakov[293], found that the hypothesis of liquid AP cannot explain the low value of equivalent conductivity and suggested that the liquid layer on the surface during combustion at 1 atm pressure is due to the eutectic of the decomposition products, such as $HClO_4$ and NH_4ClO_4.

No experimental data are available in literature on the enthalpy of AP melting. However, Guirao and Williams[180] and Price, *et al*[182] used 59.6 cal g^{-1} (Table 3.3 and 3.4) as the heat of melting (ΔH_m) of AP, which is actually the heat of fusion of $LiClO_4$. In the absence of experimental data on melting of AP, this value is used as the heat of melting of AP.

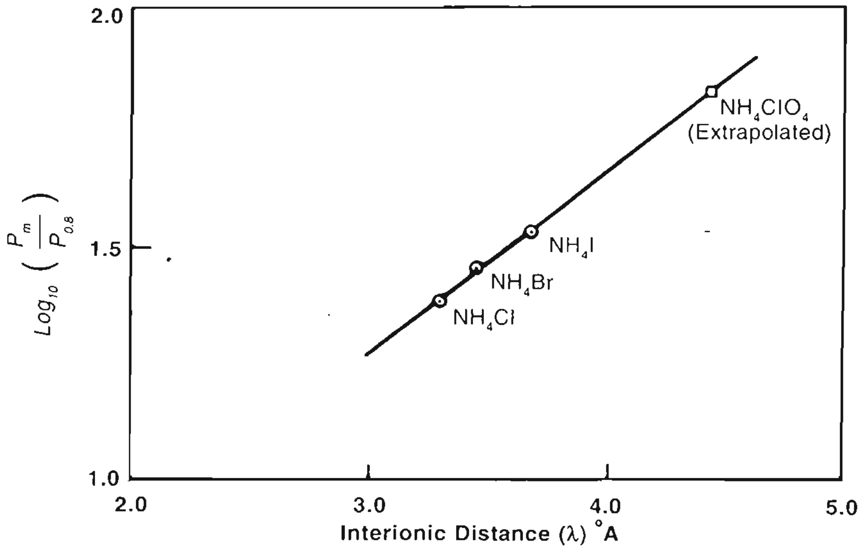

Figure 3.6. Dependence of reduced pressure ratio on inter-ionic distance in ammonium salts[291].

Source : Cordes, H.F. Estimate of the melting point of ammonium perchlorate. *AIAA. J*, 1969, **7**(6), P.1193-95.

3.4.5 Temperature at the Burning Surface

Several investigators have measured T_s of AP[271,281,294-297] using thermocouples. However, the accuracy of measured values of T_s also depends on the heat capacity and bead size of the thermocouple[109,281]. Optical methods have also been used[294,295] and the associated uncertainties have been discussed in detail by Price, *et al.*[182].

The T_s values for deflagration of pure AP are presented as a function of P in Fig. 3.7. It is seen that the value of T_s increases with pressure; the values reported by of Price, *et al*[182] are higher than those of Guirao and Williams[180] and Lengelle[120]. From knowledge of T_s of CSP (which could be higher than that of AP), it appears that the values of T_s reported by Price, *et al*[182] are on the higher side and, therefore, the data of Guirao and Williams[180] and Lengelle[120] could be taken as authentic values of T_s.

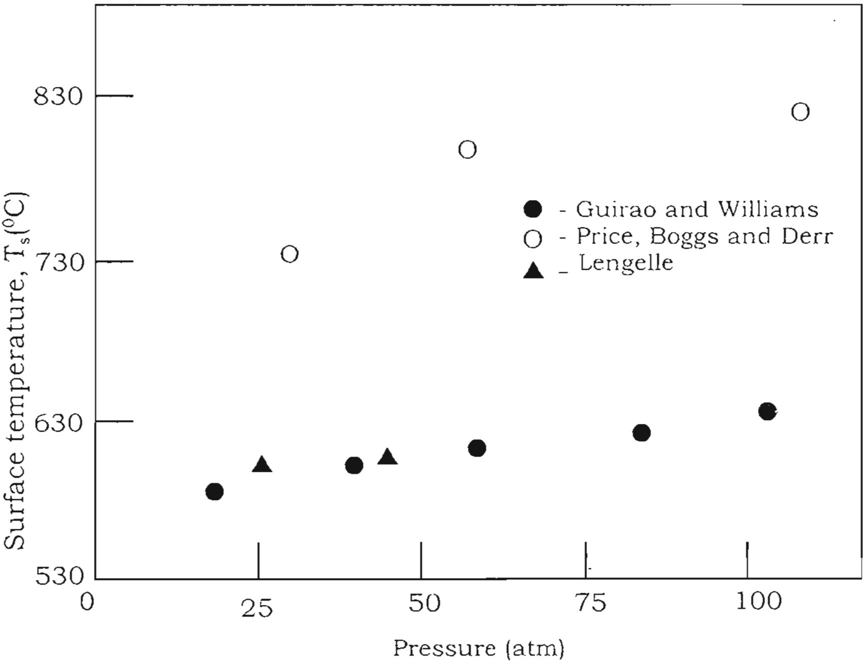

Figure 3.7. Dependence of T_S on pressure in AP deflagration[120,180, 1820].

3.4.6 Temperature of Ammonium Perchlorate Flame

In literature, two sets of data (Fig. 3.8) on T_f seem to exist, one in the range 930-980 °C while the other in the range 1130-1180 °C.

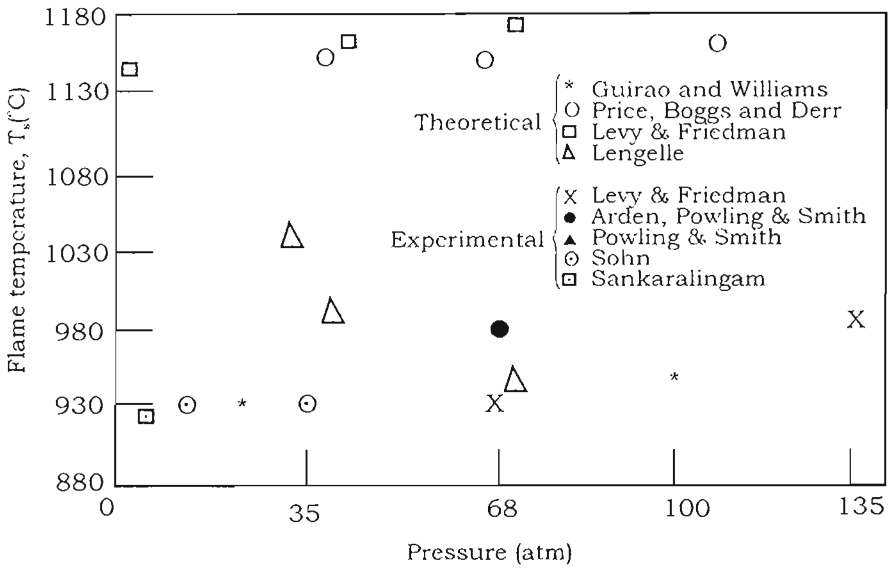

Figure 3.8. Dependence of flame temperature on pressure in AP deflagration.[109, 120, 180, 182, 267, 288, 294].

The lower values of T_f are the ones obtained experimentally while the higher values are theoretical. The lower value of T_f is the one obtained from the experiments while the higher value is obtained theoretically. The theoretical values of T_f is in the range 1110-1180 °C (T_o=25 °C) for the following combustion process:

$$NH_4ClO_4 \rightarrow 0.5N_2+1.33H_2O+HCl+1.25O_2 \ ; \ \Delta H = -38.4 \text{ kcal/mole}$$

The experimental values of T_f are well below the theoretical adiabatic T_f. This difference could be due to error in the experimental measurements or due to heat losses.

3.5 INFLUENCE OF INITIAL TEMPERATURE (T_0) ON DEFLAGRATION OF AMMONIUM PERCHLORATE

Dependence of deflagration of AP on T_o is as significant as that observed in CSP. The salient observations from various observations (Table 3.5) are outlined in Table 3.6.

Table 3.5. Dependence of $\dot{r}$ on T_o of AP monopropellant

System	*P (atm)*	*T_o (°C)*	*$\dot{r} = f(T_o)$ (cm/sec)*	*σ_p and important observations (/°C)*	*Ref.*
Pellets	upto150	21	0.5 - 1.3	(i) At 21°C, both LPL and upper pressure limits exit. However, increase in T_o to 70° C lowers LPL to 20 atm and raises UPL (ii) Rigorous conclusions regarding pressure limits are not reached.	284
	150-300	21	1.3 - 1.15		
	upto 200	70	0.3 - 1.5		
	200-300	70	1.5 - 0.4		
Pellets	upto 350	20-150	—	(i) Increase in T_o increases, $\dot{r}$, lowers LPL and raises UPL. (ii) Critical pressure below which $\dot{r}$ becomes pulsating has been found to increase with T_c	262
Pellets	50-200	50-150	—	(i) σ_p Changes with P. σ_p initially increases and then decreases as the pressure increases to 100 atm. (ii) σ_p=0.001-0.003	262
	upto 350	20-150	—	(i) Increase in T_o leads to increase in $\dot{r}$ and decrease in LPL at which combustion begins	298
		room	—	(i) LPL is 30 atm.	298
		temp		(ii) LPL is 15 atm	298
	30-150	150	—	(i) Combustion mechanism important in the solid phase.	261
		20-100		(ii) T_s increases with T_o	
Pellets	20-140	20-120	.30-1.20	(i) Limiting pressure of	299

Contd...

System	*P (atm)*	*T_o (°C)*	*$\dot{r} = f(T_o)$ (cm/sec)*	*σ_p and important observations (/°C)*	*Ref.*
(AP particle size)				combustion decreases with increase in T_0 and mean particle size.	
(50 µm)	40-100	20-120	—	σ_p=0.013-0.005	
(100-160 µm)	20-80	20-120	—	σ_p= 0.0094-0.003	
(250-315 µm)	20-80	20-120	—	σ_p= 0.0053-0.0028 (ii) σ_p decreases with increase in pressure and particle size. (iii) Softening or coalescence of AP particles leads to decrease in LPL (iv) Combustion of AP is determined by the reaction in the condensed phase and by its dispersion. (v) Sublimation of AP also needs to be considered	
Crystals/ pellets	14 - 29	-40 to +50	0.30	A linear relationship exists between LPL and T_0; LPL decreases linearly from 26 to 15 atm. (ii) Single crystals (LPL = 19 atm) and pellets (LPL = 22 atm) have almost similar LPL. Therefore, LPL is a property of AP and is not influenced by inter-particle processes in pellets, as was thought previously.	300
		50	—	LPL asymptotically approaches a minimum.	300

Contd...

System	*P (atm)*	*T_o (°C)*	*$\dot{r} = f(T_o)$ (cm/sec)*	*σ_p and important observations (/°C)*	*Ref.*
AP single crystals	LPL to 82 and 340	89, 23 and-28	—	(i) Consistent shape of the variation of $\dot{r}$ *vs P* curve is observed as T_o decreases.	287
		23 and 89 23 to -28	—	(ii) $\dot{r}$ initially increases and the deflagration mechanism seems to change as the pressure is increased. (iii) This provides an opportunity for gaining further understanding of the deflagration process.	287
	28-38.5	-28	—	An apparent froth is observed at the surface	287
	136-306	-28	—	Deflagration of AP occurs normally, However, discontinuity in the burning behaviour at high pressure is not described, which may explain the high pressure limit observed for AP pellets.	287
		-28	—	High pressure asymptote is reached.	258
	14	20-180	0.19-2.30	(i) $\dot{r}$ is not zero at LPL. (ii) σ_p=0.0064-0.0020; it decreases as a function of pressure	258
AP strands	18-32	20, 60	0.17-0.19	(i) $\dot{r}$ is not zero at LPL. (ii) LPL decreases with increasing strand density, burning surface area and T_o.	301

Contd..

System	*P (atm)*	*T_0 (°C)*	*$\dot{r} = f(T_0)$ (cm/sec)*	*σ_p and important observations (/°C)*	*Ref.*
				(iii) Maintenance of combustion is difficult due to heat loss, if void fraction increases or density decreases.	
				Observation of the burning surface at LPL indicates that it is not uniform; the surface is flatter at 50 atm than at 22 atm.	301
Rectangular AP strands	10-26	20-200	limit $\dot{r}$ = 0.17-0.19	(i) $LPL = k/[\exp 2\sigma_p (T_0 - T^*)]$ and gives $\sigma_p = 0.0018$ close to an experimental value of 0.002. (ii) LPL drops from 24 to 13 atm.	301
Cylindrical strands	10-26	20-200	—	LPL drops from 20 to 11 atm	
AP	Pressure in dimensionless form	T_0 parameter as θ_0 = 0.2-0.3	—	(i) The model proposed considers exothermic decomposition in the condensed phase and and the calculated value of $\sigma_p = 0.00283$ validates the model. (ii) At low P, $1/(T_s - T_0)$ accounts for the decrease in σ_p. (iii) At high P, $E/2L(T_m - T_s)$ accounts for the increase in σ_p.	302
	150			(iv) σ_p falls when P is replaced by its growth.	
Single crystals	3-102	26-150	0.38-1.35	$\dot{r}$ is same for single crystals and for AP of different particle sizes(300-500 μm) and there is no discernible particle size effect.	259

Table 3.6. Effect of various parameters on LPL, UPL and T_S

T_o	Increase in T_o decreases LPL	262, 281, 298-301
	Increase in T_o increases UPL	262, 281
	Increase in T_o increases T_s	261
Strand density	Increase in strand density decreases LPL	301
Burning surface area	Increase in burning surface area decreases LPL	301
Particle size	Increase in particle size decreases LPL	303, 301
LPL, $\dot{r}$ and σ_p	$\dot{r}$ is not zero at LPL but acquires a critical value.	258-301
	Relationship between LPL and σ_p exists and predicts σ_p value and the general agreement is that T_o increases $\dot{r}$ and decreases LPL	301
	The experimental observation of σ_p vs P is highly controversial in literature; With increase in P	
	(I) σ_p decreases	258, 259, 263
	(ii) σ_p increases and decreases	281, 299, 298, 300
	(iii) σ_p increases	258,301

Maksimov, *et al.*[299] found that coalesence of AP particles occurs and this reduces the LPL with rise in T_o. Investigations of Shannon[263] and Friedman. *et al*[280, 282] also support this hypothesis[299]. With increase in T_o, the UPL increases[262,281].

Combustion of AP is considered to be determined by reactions in the condensed phase leading to increase on T_s with T_o[261]. The parametric relationship between T_s and T_o is expressed as[300]

$$(T-T_o)/(T_s-T_o) = Exp\,\{- x/(\dot{r}\alpha)\} \tag{29}$$

where T_o is the initial temperature; T_s the surface temperature, '*x*' the distance from the burning surface into the solid at which temperature is T, and α, the thermal diffusivity. In deflagration of AP, condensed phase reactions are very significant, which also accounts for the increase in T_s with T_o. The importance of condensed phase process is further revealed through σ_p calculations based on a model[302] that considers exothermic decomposition in the condensed phase. Manelis and Strunin[181] obtained σ_p values based on condensed phase considerations. Price, *et al.*[182] considered the condensed phase reactions as an important energy source for self-deflagration of AP and their model appears to predict σ_p. Although Guirao and Williams[180] have considered exothermic condensed phase reactions in a liquid layer, equilibrium dissociative vaporization and gas phase combustion have not predicted the effects of T_o.

LPL is observed for both compressed pellets and single crystals which is regarded as a characteristic property of AP[268,300]. Occurrence of a common LPL for pellets and single crystals is attributed to the presence of molten AP on the burning surface. LPL decreases with increase in strand density[301]. Compared to a single crystal, pressed pellets of a certain particle size contain voids. Pellet density decreases as the particle size increases, and the same way the void fraction is more for a pellet of larger particle size. At low pellet densities, void fraction is higher and heat losses occur in the pores. Consequently, it becomes difficult to maintain combustion and as a result LPL increases. But with increase in density, the void fraction decreases, so that combustion occurs easily and LPL decreases. Also, as the particle size decreases, the density of the pellet increases and ultimately approximates the density of a single crystal. The burning surface is observed to be nonuniform with apparent froth formation at LPL[287,301]. With increase in the burning surface area from 10 mm^2 to 500 mm^2, LPL reduces by 4-7 atm. This decrease is also significantly affected by strand density[301].

LPL increases with decreasing particle size[299,301]; from a very large particle size up to 80 μm, change in LPL is marginal from 20 to 23 atm. LPL of a single crystal of AP (19 atm) is also very close to 20 atm. However, a drastic increase in LPL is observed for very fine particles (below 19 μm)[299,301]. The change in LPL here is from 23 atm to more than 75 atm. Similarly, Maksimov, *et al.*[299] found that LPL increases to an alarmingly high value of 110 atm for particle size below 50 μm. These observations are at T_o of 20 ^{0}C. Interestingly, at higher T_o, LPL change is marginal (14-17 atm) and is almost independent of particle size.

Isothermal $\dot{r}$ data[286] for AP single crystal at low pressures have indicated that transition of $\dot{r}$ occurs from the low pressure mechanism to the high pressure mechanism. Extrapolation of $\dot{r}$ data[302] to LPL is not zero, but 0.2 mm s^{-1}. If this is a critical value between temperature conditions for deflagration and non-deflagration, a different mechanism may be involved in the deflagration process, as reported by Friedman and Levy[303] and theories will have to account for this. Confirming the idea that $\dot{r}$ does not approach zero at LPL, Cohen Nir[258,301], based on the criterion of critical burning rate at LPL, has given the following empirical equation for the dependence of LPL on T_o:

$$LPL = k^{1} / [\, exp \,\{2\ \sigma_p (T_o - T_o^{*})\}] \tag{30}$$

where T_0^{*} is the reference initial temperature and k^{1} is a constant. This equation predicts σ_p and there is general agreement that $\dot{r}$ increases with T_o and that it decreases with LPL. However, the rationale for considering 'n 'value as 0.5, in deriving the above equation, has not 'been given by Cohen Nir[301] Beckstead, *et al.*[187] also examined the σ_p by differentiating the governing equations.

A plot of σ_p *vs* P behaviour, observed by several investigators, is presented in Fig. 3.9. It is evident that the variation of σ_p as a function of P is highly controversial; in a majority of cases however, a decrease is observed. A plausible explanation[304] for the differences in reports of different authors may be due to the potassium impurity present at different levels in the sample used. Strunin and Manelis[302] found that $\dot{r}$ is determined by the condensed phase reactions and σ_p is expressed as

$$\sigma_p = \frac{E_g}{2L}\left(\frac{1}{T_m^{'} - T_s}\right) + \left(\frac{1}{T_s - T_o}\right) \tag{31}$$

where E_g is the activation energy of the gas phase reaction; L, a parameter that represents the saturated vapour pressure of AP, T_m is the maximum temperature given by $T'_m = T_o + Q/C$ (Q is the heat of decomposition and C is the specific heat). At low pressures, the variation in σ_p is determined by the second term and the decrease in σ_p depends considerably on T_o and only slightly on the decomposition. At low pressures, the variation in σ_p is determined by the second term and the decrease in σ_p depends considerably on T_o and only slightly on the decomposition and vaporization activation energies. At high pressures, $T_s \rightarrow T_m$, and σ_p is given as

$$\sigma_p \rightarrow (\, E_s / 2RT_s^{2}\,) \tag{32}$$

However, variation of s_p as a function of pressure would remain unclear until a more concerted mechanism for the physicochemical factors operative is accounted for.

3.6 MODELLING STUDIES

A number of modelling efforts have been made to describe the deflagration of AP for its T_0 and P dependence on $\dot{r}$[180,181,187]. Here, an attempt is made to cover in brief as to how the effects of P and T_0 have been visualized by various theories and the importance of condensed phase reactions realised.

Johnson and Nachbars model[305] includes an arbitrary heat loss term in order to explain the existence of LPL. Theoretical $\dot{r}$ *vs* P curves have been presented for different values of E_s in the range 5-60 kcal/mole. Although its effect on $\dot{r}$ is not much at pressures of 3 and 100 atm, there is slight variation in $\dot{r}$ at intermediate pressures. Waesche and Wenograds theory[195,306] of AP combustion

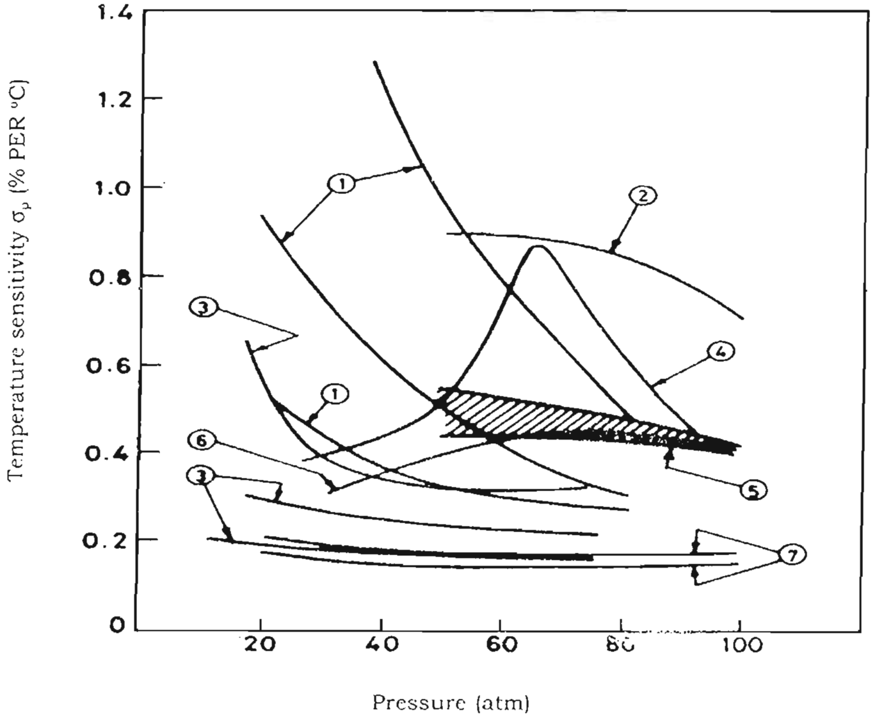

Figure 3.9. Effect of pressure on temperature sensitivity of burning rate of AP [1(ref 299); 2(ref 282); 3(ref 258); 4(ref 287); 5(ref 263); 6 (ref 298); 7(ref 259)].

Source : *Combustion Science and Technology*. 1972, **4**, 227-32. (with permission from Gordon & Breach Publishers, World Trade Centre, Switzerland and I. Glassman, Editor, CST).

differs from the other theories in that the combustion reactions occur in the condensed phase prior to vaporization. The velocity of propagation is determined by the chemical kinetics and thermophysical properties of the combustible material. From the steady-state equation, the expression for the mass burning rate ($\dot{m}$) is:

$$\dot{m} = \left[\frac{2kT_s^2 \rho \omega (T_s)}{C_p^2 E (T_s - T_o)^2} \right]^{1/2} \tag{33}$$

where k is the thermal conductivity, T_s, the surface temperature ρ, density, ω, the volumetric rate of energy release which is a function of surface temperature governed by Arrhenius expression, C_p, the specific heat and E, the activation energy of the driving reaction. Dependence of T_s on P is taken from the data of Inami, *et al.*[193] and Powling and Smith[294]. The same approach has been applied to CSP also[286].

Beckstead-Derr-Price's model[187], originally developed to describe CSP, essentially reduces to the following three equations for AP deflagration:

(i) Surface regression is described by:

$$\dot{m} = A \, exp \, (-E_d \, / \, RT_s) \tag{34}$$

where $\dot{m}$ is the mass burning rate; A is the pre-exponential factor, R is the gas constant; and E_d is the activation energy for AP decomposition.

(ii) Surface temperature resulting from energy balance at the surface is expressed as:

$$T_s = T_o - (Q_s / C_p) + (Q_g / C_p) \, exp \, (\xi^*) \tag{35}$$

where Q_s is the condensed phase energy release at the surface and the last term is the energy transferred from the flame to the surface, and ξ^* is the non-dimensional flamestand off distance given by

$$\xi^* = (Cp / \kappa') \, (m^2 / kP \, \delta) \tag{36}$$

where k' is the average gas phase thermal conductivity, k, is the gas phase rate constant which is a function of T_f and Q_g is the heat released in the flame; and δ is the reaction order.

(iii) Heat release in the flame is expressed as:

$$Q_g = C_p \, (T_f - T_o) - \Delta H_d \tag{37}$$

where ΔH_d is the heat of AP decomposition. An effective way of looking at LPL in this model is to obtain the value of n when the slope of the $\dot{r}$ *vs* P curve becomes infinite and the rate zero.

The pressure exponent is given by

$$n = \frac{d\ ln\ \dot{m}}{d\ ln\ P} = \frac{\delta}{2 + \{(CpRT_s^2)/E_d Q_g \xi^* \exp(-\xi^*)\}}$$

which is obtained by differentiating Eqns (34-36) and solving for n. It can be seen that n is dependent on T_s and ξ^*, which are variables. The value of σ_p has also been obtained by differentiating Eqns (34) - (37) with respect to T_o and is evaluated as a function of P with ΔH_d and E_d as parameters for the decomposition of AP.

The principal features of Guirao and Williams' model[180] are the introduction of the reactions of AP undergoing exothermic condensed phase reactions in a liquid layer and consideration of the fact that the overall gasification process is exothermic. They have also assigned the key reaction rates and the overall reaction activation energies for the gas phase reactions in an attempt to predict $\dot{r}$ of AP. It has been found that LPL occurs when the T_s falls below the melting point of AP (560 °C). The initial temperature sensitivity appears to be a simple energy consequence and is probably not related to any details of chemistry and this theory does not predict the effect of T_o.

Price, *et al.*[182] in their NWC model considered various processes of phase transition, melting, vaporization, condensed phase reactions and gas phase combustions. The overall enthalpy change, ΔH_{solid}, for the solid phase heated from T_o to T_m is given as:

$$\Delta H_{solid} = \int_{T_o}^{T_{tr}} C_{po} dT + \Delta H_{tr} + \int_{T_{tr}}^{T_m} C_{pc} dT \qquad (39)$$

where C_{po} and C_{pc} are the specific heats of orthorhombic and cubic AP respectively and ΔH_{tr} is the heat of phase transition from orthorhombic to cubic form. A simple expression for σ_p is obtained from the governing equations. It is believed that such expressions are useful in correlating experimental data to evaluate floating parameters, which otherwise get frozen. The E value of 15 kcal/mole, used to predict T_f, is considered to be a floating parameter. This model predicts σ_p and considers the condensed phase reactions as an important energy source for self-deflagration of AP.

Manelis and Strunin[181] describe combustion as condensed phase and gas phase processes. Dependence of σ_p for the condensed phase is given as:

$$\sigma_p = \left(\frac{\partial \ln \dot{r}}{\partial T_0}\right)_p = \left(\frac{\partial \ln \dot{r}}{\partial T_s}\right)_p \left(\frac{\partial T_s}{\partial T_0}\right)_p \qquad (40)$$

and for the gas phase as:

$$\sigma_p = \left(\frac{\partial \ln \dot{r}}{\partial T_0}\right)_p = \frac{E_g}{2R\,T_s^2} \qquad (41)$$

where E_g is the activation energy of the gas phase reaction.

Incorporating the experimentally observed microstructure at the burning surface, Sohn[307] formulated a unified theory explaining ignition and $\dot{r}$ as a function of P, T_o and LPL (at various T_o's) by a single framework, the $\dot{r}$ - T_s relationship is given by:

$$\dot{r} = \dot{r}_s^* \exp\{E_s / R(1/T_s^* - 1/T_s)\} \qquad (42)$$

where $\dot{r}_s^*$ is the burning rate at reference surface temperature, T_s^*.

According to Kumar's[93.94] condensed phase model, $\dot{r}$ as a function of P is given by:

$$\dot{r} = \Psi\,(FSV\text{-}1/2)\,B_o(P/P_o)\,\exp(-E_s / RT_s) \qquad (43)$$

where Ψ is the thickness of the surface melt layer on the oxidizer; B_o, the pre-exponential factor in the Arrhenius law for thermal degradation; P_o, the ambient pressure; and FSV is the fragment size vaporizing taken as 8 for AP. The FSV concept which describes the size of the fragment coming out from the surface may be realistic for binder species where size larger than that of the monomer (FSV>1) is justified but extension of this to AP is highly debatable.

Based on surface heating by conduction and pyrolysis, Gordan[308] developed an analytical model of combustion of AP for the calculation of propellant $\dot{r}$ from P and T_f. Recently, Kishore and Sridhara[275] proposed a novel thermodynamic model of deflagration of AP based on the partial differentiation of $\dot{r}$ as a function of P and T_o. Considering other governing equations for surface regression, pressure and temperature sensitivity of burning rate, the expression obtained for the overall surface activation energy, (E_s) is:

$$E_s = \frac{\sigma_p R T^2}{(dT_s/dT_o)_p} + \frac{(n/P)RT_s^2}{(dT_s/dP)_{To}} \qquad (44)$$

where R is the gas constant, σ_p the temperature sensitivity of burning rate, $(dT_s/dT_o)_p$ and $(dT_s/dP)_T\ T_o$, the surface temperature sensitive parameters for the physicochemical changes occurring in the condensed and gas phases, respectively; n, the pressure exponent and P, the pressure. Thus, E_s comprises the true surface activation energy of reactions in the condensed phase occurring just below the surface ($E_{s,c}$) and the true activation energy for gas phase reactions occurring just above the surface ($E_{s,g}$), Eqn. (44) could be written as:

$$E_s = E_{s.c} + E_{s.g}$$

This kind of a situation, where condensed and gas phase reactions occur just below and above the burning surface, has been visualized in the combustion of CSP[309]. This thermodynamic model can also be applied to any other self-deflagrating system and, therefore, appears to be universal in character. This model has been critically scrutinized to understand the subcritical (1-20 atm, hereby called regime I') deflagration of AP; a low value of $E_{s,c}$ (5.3 kcal/mole) is attributed to the acid catalyzed decomposition[310] of AP, which is further authenticated by the following observations:

(1) The value of $E_{s,c}$ has been estimated directly using Arrhenius equation and T_s data obtained at different T_o values (180 °C-260°C) and pressures in regime I' and found to be 5.8 kcal/mole.

(2) It has been shown that AP recrystallized from acids, such as HCl, HNO_3[310,311] and $HClO_4$, undergoes catalyzed decomposition.

(3) The quenched surface shows the presence of a liquid; pH measurements and chemical analysis of the liquid show acidic nature of the surface in regime I', which is attributed to the formation of $HClO_4$. Acid formation is not observed either in the case of virgin AP or in the sample quenched above LPL (above 20 atm, regime I).

(4) Microscopic observations of the extinguished surface of AP in regime I' reveal porous structure formed by the cluster of microdents. They are perhaps formed by the faster rate of decomposition of catalyzed AP, as compared to the uncatalyzed AP. Surface features of samples quenched in regime I (at 30 atm) do not exhibit any such dent formation, whereas samples quenched close to LPL exhibit the combined features of regimes I' and I representing transition of the surface features from I' to I.

(5) Electrical conductivity data[293] on the combustion of AP have suggested that the burning surface consists of a eutectic of AP with $HClO_4$, forming charged species, such as $NH_4^+.HClO_4$, and $H_3O^+.HClO_4$. An observed activation energy of 5-6 kcal/mole has been ascribed to such a reactive liquid layer on the burning surface, which is in excellent agreement with $E_{s,c}$. This provides strong support for the thermodynamic approach for deriving the true surface activation energy for deflagration of AP.

A thermochemical approach[274,275] has been adopted to gain further understanding of critical phenomenon of LPL and to find the surface heat release in both regimes I' and I. According to Hess cycle, the total heat (ΔH) required to raise the temperature of AP from T_o to T_f is given by $\Delta H = \Delta H_1 + \Delta H_2$ where $\Delta H_1 = [C_{po}(T_{tr}-T_o) + (\Delta H_{tr} + C_{pc}(T_m-T_{tr}) + \Delta H_m + C_{pm}(T_s-T_m)]$ is the heat required to raise the temperature of AP from T_o to T_s and $\Delta H_2 = C_{pg}(T_f-T_s)]$ is the heat required to raise the temperature from T_s to T_f. Substituting appropriate values of the physical constants (Table 3.4) in Eqn. (45), it is found that at LPL (under adiabatic conditions of deflagration), the total heat (ΔH = 432 kcal/g) must be self-generated by the condensed phase (ΔH_1= 263cal g^{-1}) and gas phase (ΔH_2 = 169.0 cal g^{-1}) heat releases, which are sufficient to support the combustion in their respective regimes. In regime I' (below LPL) at 1 atm, the total surface heat release is 274 cal/g and accounts for 21% sublimation; it decreases with increase in pressure up to LPL, where it is zero. This is also realized from the temperature profile analysis of the heat release rate from deflagrating AP at various initial temperatures at 1 atm. Above LPL, the surface is covered with molten AP and $E_{s,c}$=35 kcal/mole is attributed to the melt state decomposition of AP; excess heat is transferred from the gas phase to the condensed phase, which goes to increase the melt layer thickness in the condensed phase. Thus, thermochemical and temperature profile analyses of the deflagrating surface in regimes I' and I are different, suggestive of the different physicochemical phenomena operative in regimes I' and I. We can now examine the condensed phase heat release, ΔH_1 = 105 cal/g (at 1 atm), which corresponds to 21% sublimation. Heat release data computed by other investigators (Table 3.7) show a large variation, which may be attributed to (i) variance in the value of ΔH_d and ΔH_s of AP, and (ii) variance in the proportion of decomposition/sublimation of AP. From Table 3.7 one could assign the most accepted value as

Table 3.7. Net AP gasification heat release during deflagration in the condensed phase

Net heat release J/kg x 10^{-3}	Ref
-502.4	133
-418.7	180
-167.5	181
-544.3	310
-314.0	91
-142.4	295
-335.0	297
-502.4	297
-774.6	202

350-550 J/g. This could lead to the consideration of sublimation.

From this thermodynamic model, the dependence of σ_p on P has been verified as follows. Rearranging Eqn (44), σ_p may be written as,

$$\sigma_p = \frac{E_{s,c}}{R\,T_s^2}\left(\frac{dT_s}{dT_0}\right)_p \tag{45}$$

Substituting the values of $E_{s,c}$ and T_s obtained at various pressures[312] in regime I', σ_p decreases with pressure which is due to the steep decrease in $(dT_s/dT_o)_p$ and it turns out to be 0.5 at LPL (Fig 3.10). Consequently, Eqn (45) at LPL becomes

$$\sigma_p = E_{s,c}/2RT_s^2$$

which is similar to the equation based on Belayaev-Zeldovich model[313], suggesting that calculation of σ_p using above equation is valid only at LPL. At other pressures, it is likely to give erroneous values. Variation of σ_p with pressure has also been examined[314] by differentiating, with respect to P, the following expression, which is the modified form of the equation given in reference 135:

$$\sigma_p = 1/(T_s - T_o)$$

$$\frac{d\sigma_p}{dP} = -\sigma_p^2\left(\frac{dT_s}{dP}\right)_{T_0} \tag{46}$$

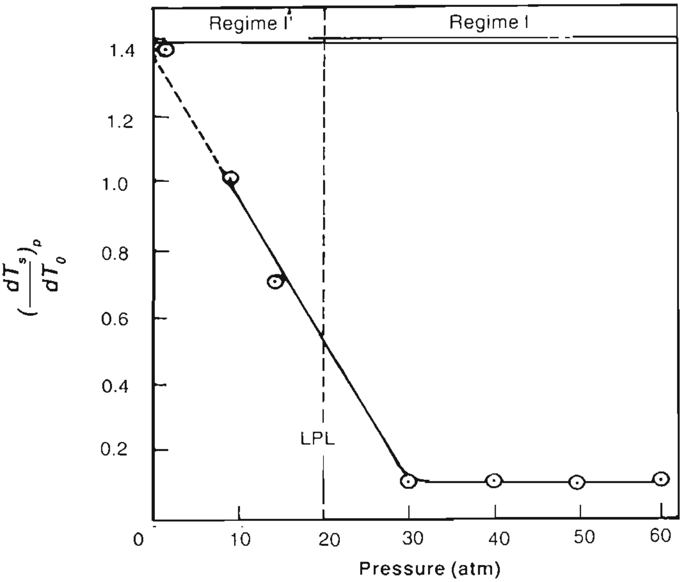

Figure 3.10. **Variation of $\left(\frac{dT_s}{dT_o}\right)_p$ as a function of pressure[31,40].**

It is apparent from Eqn (46) that σ_p should decrease with pressure, since both σ_p and $(dT_s/dP)\ T_o$ are positive quantities. Experimentally, σ_p has been found to decrease with increase in pressure in both regimes I' and I.

At pressures above LPL (beyond 30 atm), it may be seen from Fig. 3.10 that $(dT_s/dT_o)_p$ is almost constant, having a value of 0.1 in regime I and, therefore, σ_p can be written as:

$$\sigma_p = (10RT_s^2)$$

Above equation has been verified for the data of Guirao and Williams[180], Lengelle[120], Cohen Nir[258] and Boggs[315]. It is found that Cohen Nir's data[258] give a better dependence of T_s on P.

CHAPTER 4

ROLE OF POLYMERIC FUEL-CUM-BINDER DURING BURNING OF COMPOSITE SOLID PROPELLANTS

4.1 AN OVERVIEW

In CSP, the binder is a continuous phase and begins as a liquid prepolymer, mixing easily with the particulate oxidizer, and constitutes the second important ingredient after the oxidizer. These prepolymers generally contain reactive groups, which can be chain-extended or cross-linked during cure to a solid[98] in the binder matrix. Polymer chains of different molecular weights, M_1, M_2, M_3 etc., as depicted in Fig. 4.1, not only provide structural

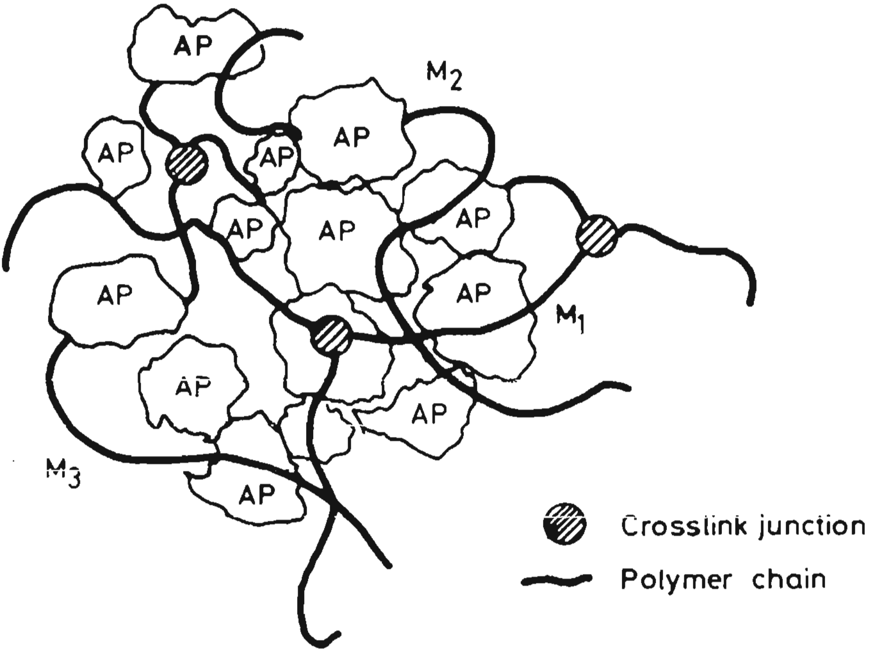

Figure 4.1. Binder-matrix holding the ingredients.

integrity for imparting sufficient mechanical strength to the propellant by holding the ingredients tightly but also function as a fuel. The molecular structures of some typical prepolymers and their curing agents are given in Table 4.1; molecular weight of a semi-fluid viscous prepolymer is usually in the range 2000-5000. Depending on the functionality of the reactive groups and their molecular weight, a crosslinked network (Fig. 4.1) is built up and a significant increase in molecular weight takes place in presence of 80-90% particulate ingredients during propellant curing. The molecular weight of the finally cured polymer influences the properties of a CSP significantly[316]. Crosslinks invariably increase the mechanical strength[6] of the propellant, which also depends on how the reactive functional groups are located in the prepolymer. If random, as in PBAA, curing (Table 4.1) gives rise to free dangling chain ends which are not effective in providing desirable and reproducible physical properties. By locating the functional groups at the chain ends (e.g., telechelic polymers, such as HTPB or CTPB; Table 4.2), improved tensile strength with good elongation characteristics, besides batch-to-batch reproducibility of the formulation, has been achieved[111, 115].

The most widely used polymers are HTPB (cured with isocyanates) and CTPB (cured with aziridines or epoxy compounds). HTPB crosslinking agents, isophorone diisocyanate (IPDI), toulene diisocyanate (TDI), hexamethylene diisocyanate (HMDI) and diiphynylmethane diisocyanate (MDI), show gel time in the following order: IPDI > TDI > HMDI >MDI, suggesting low reactivity of IPDI, MDI-cured propellant gave 15-24% higher $\dot{r}$ and three times higher tensile strength than IPDI. TDI and HMDI cured composites have intermediate values [317]. HTPB and CTPB also have excellent low temperature properties due to their low glass transition temperature (-60 ^{0}C)[318]. In addition to the effect of factors like functionality, molecular weight, etc. of prepolymers on the mechanical properties of the cured propellant[319-321], it has also been recognized that the chemical nature and structure of the binder affect the ballistic properties, such as specific impulse and $\dot{r}$[322-326]. Table 4.2, for example, indicates that the contribution of the binder to specific impulse and $\dot{r}$ is also determined by the structure of the binder.

Table 4.1. Typical polymers and curing agents

Polymer	*Curing agent*	*Binder structure*
$HO-[-CH_2-CH=CH-CH_2-]_n-OH$ Hydroxy-terminated polybutadiene	OCN-R-NCO Diisocyanate	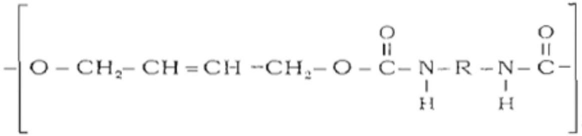 $-\left[O-CH_2-CH=CH-CH_2-O-\overset{O}{\overset{\parallel}{C}}-\underset{H}{N}-R-\underset{H}{N}-\overset{O}{\overset{\parallel}{C}}-\right]_n$
$HOOC-[-CH_2-CH=CH-CH_2-]_n-COOH$ Carboxy-terminated polybutadiene (CTPB)	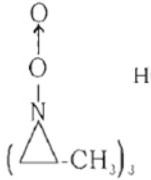 Tris 1-(2 methyl) aziridinyl phosphine oxide	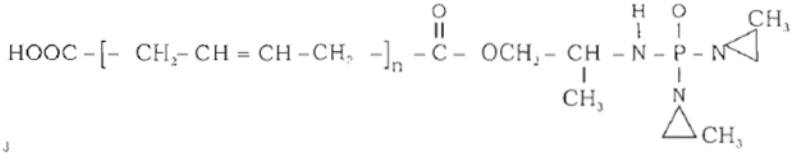
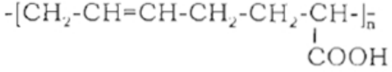 $-[CH_2-CH=CH-CH_2-CH_2-\underset{COOH}{CH}-]_n$ Polybutdiene acrylic acid (PBAA)	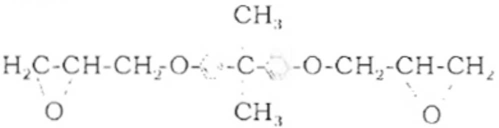 Diglycidyle ether of Bisphenol-A (Diepoxide)	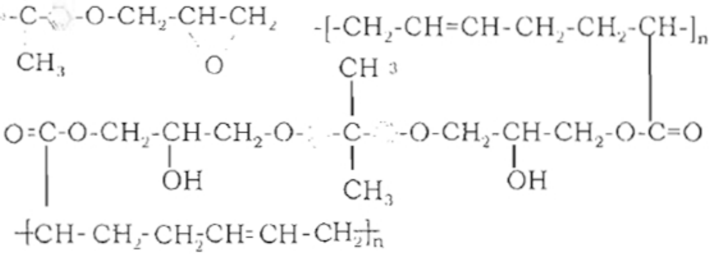

Contd....

Polymer	Curing agent	Binder structure
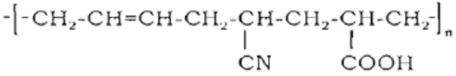 $-[-CH_2-CH=CH-CH_2-\underset{CN}{CH}-CH_2-\underset{COOH}{CH}-CH_2-]_n$ Polybutadiene-acrylic acid-acrylonitrile (PBAN)	Diepoxide	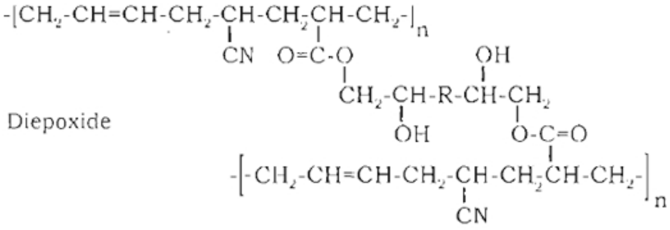
$-[CH_2-CH_2-CH_2-CH_2-O-CH_2-CH_2-CH_2-CH_2-S-S-]_n$ Butyl ether polysulfide (PSU)	 p-Quinone dioxime	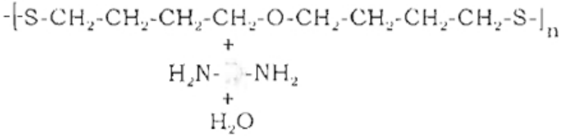 $-[-S-CH_2-CH_2-CH_2-CH_2-O-CH_2-CH_2-CH_2-CH_2-S-]_n$ + H_2N- $-NH_2$ + H_2O

Table 4.2. Performance data for CSP containing different fuel binders[98]

Property	*NH_4ClO_4 Polyester*	*NH_4ClO_4 Poylvinyl chlorde*	*NH_4ClO_4 Polyurethane/ aluminium*	*NH_4ClO_4 Polybutadiene*
Process	Cast	Cast	Cast	Cast
Density (g/cm^3)	1.88	1.64	1.72	1.74
Chamber pressure (kg/cm^2)	30-140	1-120	1-140	1-140
Specific impulse (s)	180-200	225	240	250
Burning rate (cal/s)	1.75	0.65-1.30	0.50-1.00	1.20
Pressure exponent (n)	0.60-0.59	0.40-0.30	0.50-0.40	0.24-0.21
Mechanical properties	Excellent	Excellent	Excellent	Excellent

Although fuel binder happens to be an important ingredient controlling the mechanical properties and the energetics of a propellant, it is surprising that enough attention has not been paid to understand its chemical nature and structural characteristics that influence the CSP behaviour. However, there has been a realization that the importance of the binder cannot be neglected and that its role in the overall combustion of CSP is important. The available literature on the pyrolysis of fuel binders used in propellants pertains mostly to individual polymers. These studies were carried out with the main objective of obtaining information on the energetics and pyrolysis kinetics with the hope that it explains the role of the binder in propellant combustion. But propellant being an exotic mixture of ingredients, it affects the binder pyrolysis kinetics and energetics significantly. Much less is known about the decomposition mechanisim of the fuel binder during propellant burning. It is, therefore, necessary that the enthalpic changes and the surface pyrolysis of the fuel binder be viewed in an actual combustion environment. Such an attempt has not been made hitherto. In this chapter, we discuss the role of chemical nature and structure of the fuel binder from the point of view of condensed phase reactions to understand its role in CSP models.

4.2 SALIENT FEATURES OF FUEL BINDER PYROLYSIS

Pyrolysis of fuel binders in CSP has been a subject of continued interest [327, 238]. Of the various techniques used in polymer pyrolysis studies, DSC has provided information on the energetics of polymer degradation/decomposition brought about by endothermic or exothermic processes. DSC thermograms for some of the important polybutadiene polymers are given in Fig. 4.2; polymer degradation/decomposition is affected by the heating rate. According to Varney and Strahle[329], at low heating rates up to 5 °C/min, in N_2, CTPB exhibits slow outgassing in the range 340°C-420°C. A melt is observed at 420 °C, which is followed by rapid endothermic decomposition beyond 420 °C, completing at 500 °C. However, at higher heating rates (33 °C/s), Bouch, *et al*[330] observed that the decomposition process becomes exothermic beyond 380 °C. From TG studies, Thomas and Krishnamurthy[326] found that CTPB degrades in two stages in the heating rate range 1-110 °C/min. The first stage is primarily due to partial degradation and

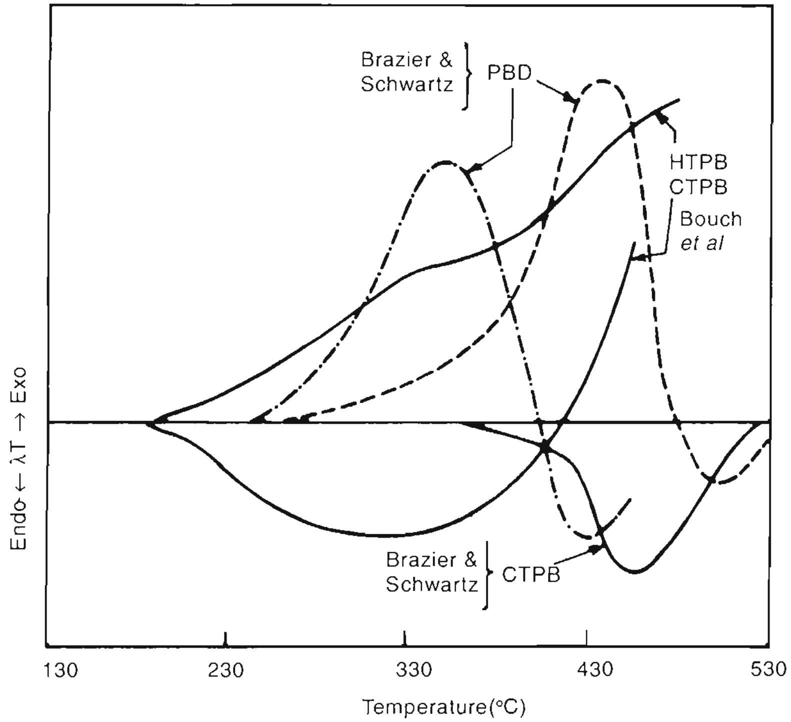

Figure 4.2. DSC traces of degradation of polymeric binders in N_2[329-331].

cyclization, while the second stage is due to the subsequent depolymerization of the undegraded polymer. This kind of two-stage degradation behaviour had been observed earlier by Brazier and Schwartz[331] for polybutadiene. They have shown that the exothermic decomposition of polybutadiene occurs not only at higher heating rates (100 °C/min) but at lower heating rates as well. Significant exothermic decomposition has also been observed for HTPB polymer[330]. In diisocyanate-cured HTPB, the first step is the cleavage of urethane crosslinks. It then crosslinks exothermally and cyclizes and also depolymerizes to give butadiene and its oligomers and formaldehyde [332]. The overall exothermic degradation/decomposition may be due to the precursor reactions, leading to depolymerization, cyclization and crosslinking[331]. According to the free-radical degradation/decomposition scheme shown in Fig. 4.3, there is primarily a hydrogen abstraction, leading to cyclization or crosslinking (200 °C) in addition to fragmentation of the main chain to low molecular weight species. Subsequently, up to 350 °C, depolymerization leads to gasification of the products. The solid residue that remains due to crosslinking and cyclization, decomposes at higher temperatures (above 45 °C) to the main products, such as butadiene, 1,5-hexadiene, 1,3-cyclohexadiene, cyclopentene and vinylcyclohexane.

The events that take place before volatilization of pyrolyzed products constitute condensed phase reactions of the binder, which can be visualized as follows. The binder in its original state has a large molecular weight and very low vapour pressure; it cannot volatilize. Hence, it undergoes bond breakage when heat is supplied. The long chain undergoes bond scission until a requisite mean fragment size is reached, the vaporization of which becomes more economical than the bond breakage process. These small fragments are actually involved in gas phase combustion. Sometimes, the small fragments which interact in the binder matrix could also undergo condensed phase reactions. Generally, the bond breakage process is endothermic. But recently we have shown in this laboratory that special polymers like polyperoxides degrade exothermally[55].

The mean fragment size volatilizing at the surface has been explained through various models. Kumar[94] has defined the mass burning rate in terms of fragment size vaporizing (FSV), which directly relates to the number of unbroken bonds during vaporization. Rabonovich [333] has defined the volatile fragments in terms of critical fragment size (CFS), which is the ratio of the C-C bond energy to the heat of vaporization of the monomer. Kishore, *et al.*[334] defined these

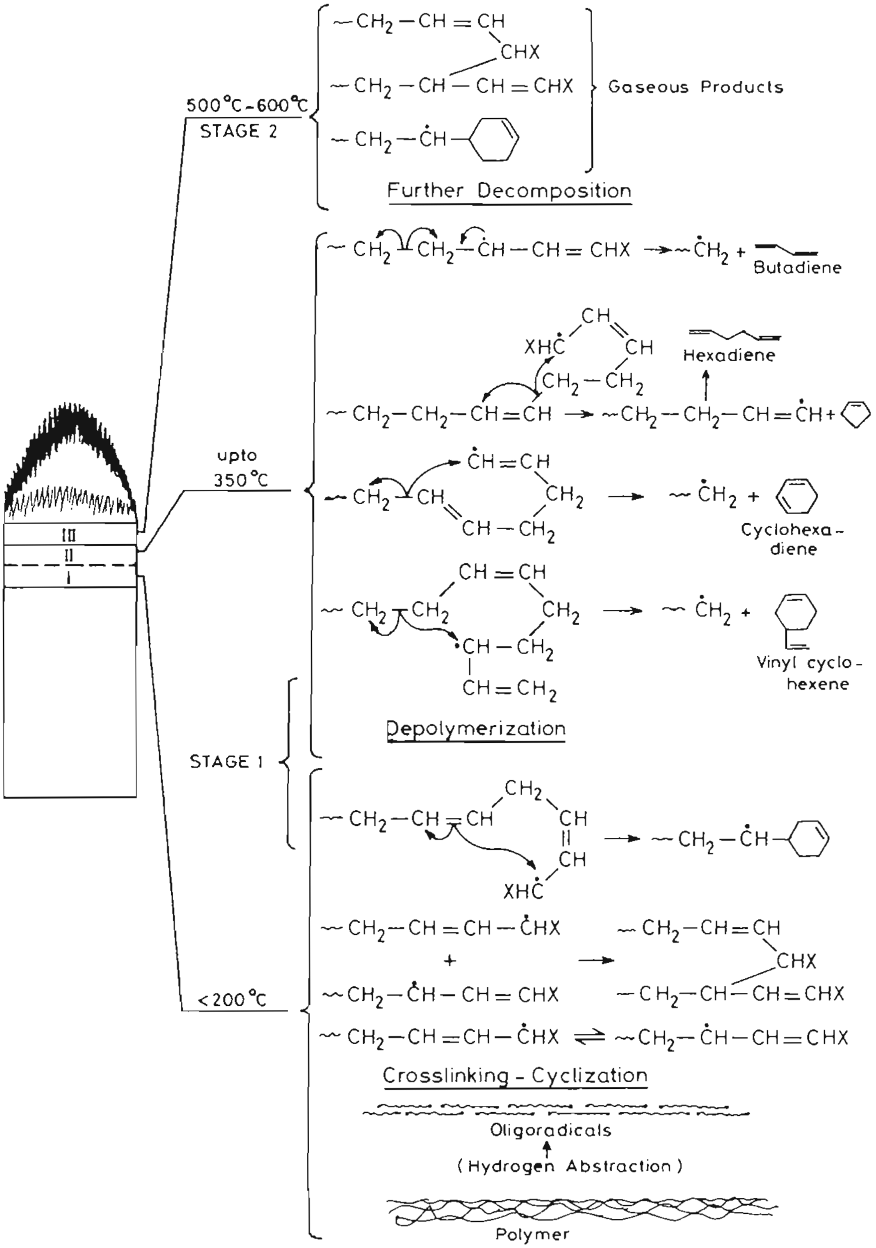

Figure 4.3. A model for polybutadiene burning.

fragments in terms of mean fragment size (MFS), which is the statistical average emerging from the surface and is obtained from thermodynamic considerations. A discussion on MFS is given below.

Mean Fragment Size (MFS)

The MFS of the polymer is defined as the average size of the species as a multiple of the fundamental repeating unit leaving the pyrolyzing surface of the polymer during gasification. Consider a unit weight of the polymer heated to a certain temperature at which it gasifies rapidly. The total heat expended is the sum of the heat required to raise the temperature of the polymer from the ambient temperature (T_a) to the gasification temperature (T_{gas}) plus the heat of gasification. For crystalline polymers, heat of melting has to be included.

If the heating rate at which the sample temperature is rapidly raised to T_{gas} is high enough, negligible degradation may be assumed to occur in the process. From the energy balance, the total heat (ΔH_t) absorbed during gasification of 1g of the polymer is given by:

$$\Delta H_t = \int_{T_a}^{T_{gas}} C_p dT + Q_g$$

where Q_g, the heat of gasification, is the heat absorbed by the sample at T_{gas} to volatilize into products. Gasification of the polymer involves pyrolysis of the polymer and subsequent volatilization of the products. So, the term Q_g can be visualized as the sum of two terms, heat of depolymerization (Q_p) and heat of vaporization (Q_v) of the pyrolyzed fragments.

$$Q_g = Q_p + Q_v$$

Formation of a polymer molecule, $(M)_n$, where M represents the monomer and n, the degree of polymerization, can be represented as:

$$nM \longrightarrow (M)_n + \Delta H_p$$

where ΔH_p is the heat of polymerization from monomer to polymer. If the polymer, on pyrolysis, is completely depolymerized into the monomer, then

$$\Delta H_p = Q_p$$

Evidently, the MFS in this case equals unity. For example, in poly(methlylmethacrylate) (PMMA), the MFS is unity in the temperature range 400-600 °C, because this polymer is well known to pyrolyze exclusively into monomers. But such a situation arises only in a few polymers, hence MFS will be given by the direct relationship:

$$MFS = \Delta H_p / Q_g \tag{47}$$

which says that when the average size of the fragments is equal to that of the dimer, the heat of pyrolysis is half of the heat of polymerization, for the trimer, the heat of pyrolysis is one third of the heat of polymerization, etc. It may be noted that we are considering only those polymers, like, for example, polystyrene, PMMA, poly (α-methylstyrene), polypropylene (PP), PE, etc., which on degradation mostly yield monomer, dimer, trimer, etc. Understandably, the reliability of MFS values will be less in cases where other pyrolysis products are also formed in addition to monomer, dimer, etc. Such a situation will be particularly more pronounced when the monomer itself undergoes pyrolysis at relatively higher temperatures; in such cases, MFS will be lowered considerably.

It can be conveniently assumed that after pyrolysis, the total heat of vaporization is independent of the sizes of the fragments and depends only on the total amount of the sample. This assumption requires the heat of vaporization to be linearly proportional to the size of the number of carbon atoms present in the molecule. Literature data justify this assumption for homologous compounds, like, for example, n-alkanes. Hence, in the present situation, Q_v in the equation $Q_g = Q_p + Q_v$ above can be replaced by vaporization energy of the monomer (ΔH_v). Combining with Eqn. (47), we get.

$$Q_g = \Delta H_p / MFS + \Delta H_V \tag{48}$$

In Eqn. (48), all the energy terms are with respect to the quantity of the monomer unit in the chain. MFS is a dimensionless quantity and (DH_p) is the heat of depolymerization of the solid polymer, which is equivalent to the heat of polymerization of the monomer. On rearrangement, Eqn. (48) becomes:

$$MFS = \Delta H_p / (Q_g - \Delta H_q) \tag{49}$$

From the data on DH_p, Q_g and DH_V, MFS can be calculated; Q_g can be measured from block calorimetric experiments using isothermal DTA principle[334]. The value of Q_g increases with temperature, which indicates that more and more pyrolysis occurs as the temperature is raised. This leads to lower values of MFS at higher temperatures.

The MFS values were further verified from the gas composition data obtained by the pyrolysis gas chromatograph technique using the following expression:

$$MFS = \frac{\sum_{i=1}^{n} X_i}{M \sum_{i=1}^{n} X_i / M_i} \tag{50}$$

where X_i and M_i respectively represent the weight fraction and the corresponding molecular weight of the pyrolysis products, and M the molecular weight of the monomer. Both Q_g and gas composition data provide concordant values in MFS. Though MFS is not a substitute for a complete analysis of the pyrolysis products, which is much more difficult to carry out, it certainly provides a considerable insight into the gasification process.

Merits of FSV and MFS are discussed below. CFS is a limiting parameter for a particular polymer. It only indicates that during pyrolysis any fragment could vaporise, provided its size is equal to CFS. The value of CFS is constant for a particular polymer and, therefore, it does not vary with temperature. CFS can be considered only under ideal situations, since it does not involve the kinetics of vaporization and the bond-breaking process or the pyrolysis condition that would drastically alter the size of the volatilizing fragments. The quantity FSV proposed by Kumar and Stickler[335,336] gives a better picture of the actual gasification than CFS. But FSV was computed from the vaporization data for hydrocarbons. Although the physical concept is admirable in enabling identification of the gasification of a polymer as a boiling phenomenon, the inevitable pyrolysis that occurs before the gasification is ignored. In place of the physical binding between the vaporizing molecule in the liquid phase, the fragments vaporizing during the gasification of a polymer are originally bound with strong chemical bonds. In the case of FSV also, the values appear to indicate the limiting size of the vaporizing species.

On the other hand, the MFS values indicate the average size of the species volatilizing from a polymer at any temperature. Each MFS value represents a particular set of pyrolysis conditions. Any polymer can have a wide range of MFS values from very low (at very high temperature) to high, depending on the experimental conditions and chemical characteristics of the polymer. MFS appears to give a better picture of pyrolysis and gasification of a polymer.

Data on heat of formation of the binder is essential for the computation of condensed phase energy changes in propellants. Compared to AP, thermophysical data for the binder are very scarce. No consistent value of heat of formation of CTPB is reported in literature. Considering the basic structure of the binder to be similar to that of polybutadiene, the ΔH_f^0 of CTPB/PBD was obtained[139] from the following thermochemical cycle:

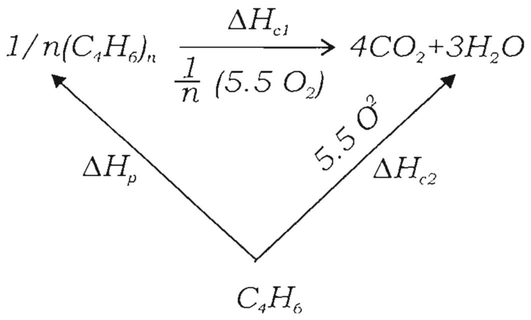

The experimental ΔH_{Cl} for CTPB is -551.82 kcal/mole and from this value, ΔH_f^0 values for CTPB were calculated using ΔH_f^0 of CO_2 and H_2O. The heat of combustion, ΔH_{c2}, for butadiene (-607.9 kcal/mole)[337] and ΔH_p^0 for butadiene polymerization[338] were obtained from literature. From ΔH_p^0 and ΔH_{c2}, the value of ΔH_f^0 of CTPB was calculated. In yet another way, ΔH_f^0 for CTPB was obtained from ΔH_p^0 and ΔH_f^0 of butadiene (26.33 kcal/mole)[339]. Using all the above methods, an average ΔH_f^0 4.94 kcal/mole was assigned for CTPB. The calorific value of the polymer is an important factor as far as propellant energy is concerned. It is also logical to expect the degradation kinetics to have a significant influence on $\dot{r}$. However, very little effort has been made to understand binder degradation relevant to propellant combustion.

4.2.1 Activation Energy

Several investigators[236,239,331,340-342] have obtained values for various polymers in the hope that the results will suggest and resolve whether physical or chemical properties of a binder are important in propellant combustion. It can be seen from Table 4.3 that the activation energy values for pyrolysis depends upon the technique and heating rate employed. In bulk pyrolysis methods, such as DSC and DTG, the heating rate usually employed (1-100 °C/min) is regarded low compared to that for linear pyrolysis methods (i.e. layer by layer burning in propellant) where very high heating rates

Table 4.3. Activation energies for pyrolysis of typical binders[327]

Binder(s)	*Experimental method*	*Temperature range (°C)*	*Heating rate (°C min^{-1})*	*E_a (k cal mol^{-1})*	*Ref.*
CTPB	DTG (b)	317-557	2-100	25-39	326
PBD	DTG/ DSC (b)	317-577	2-100	60/40	331
CTPB, PBAA	DSC(b)	177-477	1-80	28	329
HTPB, CTPB PBAA, PBAN, PIB	Focussed source method	127-527	3000-18000	10-15	330
CTPB, HTPB	DTG(b)	Not given	1-100	30-45	340
PMMA	Hot plate (l)	277-627	-	11-29	343
PMMA	O_2/N_2jet(l)	447-587	-	37	344
PS	Rocket exhaust (l)	477-727	-	40-50	345
CTPB, HTPB PBAN	Arc image furnace(l)	327-777	300 cal $cm^{-2}s^{-1}$ (h)	-	192
PVC			29-32	-	346

Note : PBD=Polybutadiene; PIB=Polyisobutylene; b=bulk method; l=linear pyrolysis method; h=heat flux

exist. It has been observed that for CTPB, bulk pyrolysis methods give higher *E* values in the range 24-45 kcal/mole at heating rates of 1-100 °C/min[326,326,340] However, for higher heating rates (3000-18,000 °C/min), the *E* values are lower (10-15 kcal/mole)[311] A similar behaviour is observed for HTPB polymer also[330,340]. Degradation of HTPB and PBAN in the presence of AP gives an activation Energy of 12.4 kcal/mol[347-348]. Different binders exhibit a range of kinetic parameters; the E values for surface decomposition lie in the range 10-30 kcal/mole (Fig. 4.4), depending on the nature of the polymer and the decomposition temperature[120]. Although some workers[120,349], have considered breaking of the C-C bond to be the rate-determining step, the low

E values obtained at high heating rates and surface temperature conditions cannot represent any such specific chemical processes; they represent physical processes; like vaporization of fuel at the burning surface[350]. Activation energies for the gasification of polymers like polyethylene, polyisobutylene, polyvinyl alcohol, polyvinyl pyridine and PVC are low (20 to 50 kcal/mole), which is attributed to volatilization of the degraded products.

These low values for gasification, their similarity in various polymers and CSP[334] and the fact that the *E* value for the bond breakage process is very high support the view that the ignition phenomenon is controlled by gasification. The low activation energy values obtained at high heating rates/fluxes also suggest the invalidity of low heating rate data to propellant combustion conditions, where high heat fluxes exit[330]. According to Price[351], the bulk pyrolysis data obtained by using low heating rates in the range 1-100 ^{0}C/min are questionable when extrapolated to propellant combustion conditions where the surface heating is several times the order used in such techniques. Therefore, there

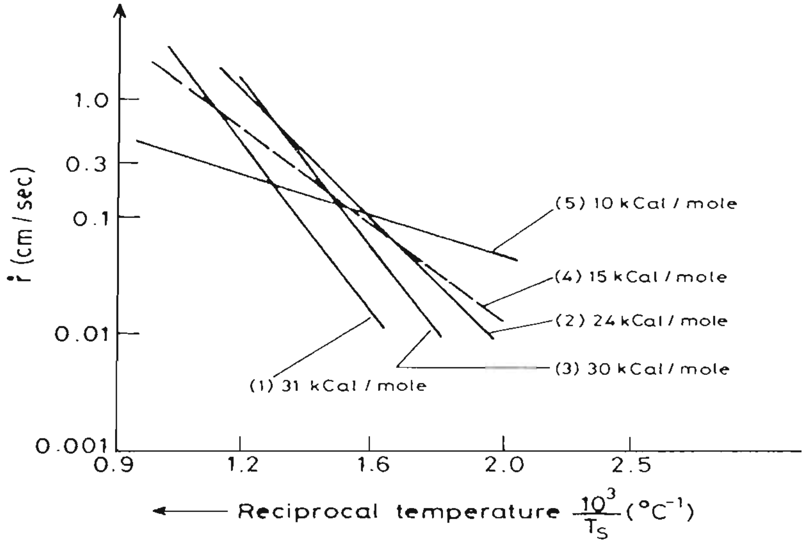

Figure 4.4. Arrhenius plot for the pyrolysis of various binders [(1) CTPB, (2) Polyoxymethylene, (3) Polystyrene, (4) Polymethyl-methacrylate, and (5) Polyurethane[120].

Source : Lengelle, *et al.* combustion mechanisms of composite solid propellants. Sixteenth Symposium (Int: on Combustion. Pittsburgh. 1976 P. 1257-69. (Reproduced with permission from Executive Administrator. The Combustion Institute, Pittsburgh and Dr Lengelle, D.E.G., ONERA, France).

is a strong general opinion[310] that binder pyrolysis studies should be carried out under conditions approximating actual propellant combustion.

4.3 ROLE OF FUEL BINDER IN COMPOSITE SOLID PROPELLANT COMBUSTION

Combustion of polymeric binders has been of importance in view of the understanding of their role in CSP combustion. According to the reviews by Kishore[70,352] and Yano, *et al.*[353], in a typical CSP burning, polymer sustains combustion, depending on the flammability and the heat fed back to the polymer. The combustion rate depends on several physical factors like melting, diffusion, volatility, conductive heat flow, etc. Polymer combustion is also viewed as a solid phase reaction forming hydrocarbon fragments; the gas phase flame is considered to be similar to the flames obtained on gaseous hydrocarbon burning. However, the polymer behaviour in CSP combustion seems to be complicated in view of the vast physico-chemical processes that occur in the condensed and gaseous phases. In the multitude of processes involved, it is difficult to extract a single hypothesis for the role of fuel binder in the overall combustion process. Study of the effects of 10 binder on the $\dot{r}$ value of the propellant show that it is strongly dependant on binder decomposition temperature[354]. The temperature of initial decomposition of the propellant is controlled by the binder[355].

In order to obtain an understanding of the main features of the effect of chemical nature and structure of the fuel binder affecting the $\dot{r}$ value of CSP, features related to condensed and gas phase behaviours are given.

4.3.1 Condensed Phase Behaviour of Fuel Binders

During propellant combustion, the binder surface regresses as a result of heat transfer from the gas phase flame to the surface. In the process, the binders actually get heated at low heating rates in the subsurface region to high heating rates at the burning surface. The reactions proceed extensively, modifying the virgin polymer before high temperatures are reached[330,356]. It has been proposed[357-359] that degradation of the binder occurs at the weak link, which generally exists at the crosslink junctions (Fig. 4.1). In aziridine-cured CTPB, the weak link is the P-N bond, whereas in isocyanate-curred HTPB, the weak link is the urethane linkage. This weak link degradation mechanism renders the binder once again in the liquid form, which gets accumulated at the burning surface. The thickness of the molten fuel layer decreases as the heating rate increases and the polymeric fuel is known to break down to chain fragments of varying sizes (as in Fig. 4.3). monomers, dimers, trimers, etc. Also, light hydrocarbons are obtained due to the degradation of the monomer and side chain scission[310,346,360]. It is suggested that any mechanism of polymer degradation at the burning surface must also take into account the physical processes of melting, boiling, vaporization, etc[350].

Studies have shown that almost all pyrolyzed binders have a molten surface layer with varying amounts of char[192]. The molten binder over the oxidizer surface interferes with the AP decomposition process in the vicinity of the binder[192,361]. Thus, the propellant burning surface gets complicated by a mixture of the molten fuel and char. Smith[362] has proposed a model based on the heterogeneous gas-solid reactions primarily occuring at the propellant surface. Such reactions may involve fuel gases and solid oxidizer, or oxidizer gases and solid fuel. In fact, several workers[306,363,364] have taken into account the occurrence of interactions among the constituents and this offers an opportunity to explore the possible oxidative degradation effects of the oxidizer. The products of oxidizer decomposition and fuel pyrolysis formed at the oxidizer-binder interface within the solid fuel matrix are considered to be important[360]. McAlevy and Hansel[350] have found that Cl_2 and NO_2 which are the products of breakdown of AP, influence the rate of pyrolysis of PS and are of much relevance to studies on PS-containing propellants. Kishore, *et al*[365] have found the occurrence of condensed phase interactions in potassium perchlorate (KP)/PS propellants, the $\dot{r}$ being correlated to the thermal decomposition of KP.

Fishman[366], from his arc-image furnace experiment on the ignition of CSP, observed that exothermic reactions occur at the propellant surface prior to ignition. This exotherm at the surface seems to be associated with heterogeneous decompostion of $HClO_4$ and heterogeneous oxidation of the fuel. The ignition and extinction characteristics of CSP also depend upon the nature of the binder and on its decomposition characteristics[367,368]. Kishore, *et al*[369-373] found that in the case of fuel binders such as CTPB, PS and PVC, ignition occurs when the polymer gasification rate reaches a critical value, which varies with the type of binder. It may be noted that oxidation of the binder with $HClO_4$ becomes more pronounced in the condensed phase compared to that with O_2 and hence brings about faster ignition of the propellant. Furthermore, studies on the propellant weight loss prior to ignition, ignition temperature and high pressure decomposition of AP and binders in the presence of oxygen, clearly show that ignition of the propellant follows the trend of the binder ignition suggesting thereby that the ignition of the propellant is governed by gasification of the binder[370]. Thus, the role of the binder in terms of its effect on ignition and $\dot{r}$[374] is manifested by the process of its degradation or decomposition in the condensed phase[375-377].

The combustion wave structure of AP-based CSP has been studied and the effect of binder, such as HTPB and hydroxy-terminated polyester (HTPE), on $\dot{r}$ has been examined[378]. Actually, the physical state of the binder near the burning surface of the propellant[315, 326] affects the surface structure and thereby the combustion wave. This is evidenced by the changes in $\dot{r}$ and structure of the burning surface and is explained by the pyrolysis law of certain binders which differs, depending upon the layer size and chemical nature of the fuel binder[360,379-381].

4.3.1.1 *Influence of microscopic features of the fuel on the burning rate of model composite mixtures*

Not much parametric information is available on CTPB/HTPB gumstock[382] as to how molecular weight, its distribution, functionality, *cis-trans* isomerism, etc. influence the properties of CSP, particularly, $\dot{r}$. Hence, it is necessary to gain some knowledge about the structure-property relationships. For simple polymeric systems, it is necessary only to know the molecular weight or chain length to predict the properties of the polymer[383]. Thus, one needs polymeric samples of varying molecular weight, with other properties remaining constant. Realizing that only simple organic model fuels with definite molecular weights could be examined without much difficulty, a system of aliphatic dicarboxylic acids was chosen with the hope that it provides some insight into the characteristics of the binder and its impact on the ultimate ballistic behaviour.

The influence of molecular weight on the $\dot{r}$ value of AP +aliphatic dicarboxylic acid (n=1-8) has been studied[384] by varying the molecular weight of the acid fuel and keeping other dependent factors constant. The $\dot{r}$ values of AP/CTPB and AP/HTPB have also been obtained. Fig. 4.5 indicates that the value of $\dot{r}$ increases exponentially with increase in molecular weight. The $\dot{r}$ values of AP/CTPB and AP/HTPB fall on the extrapolated curve, suggesting that the influence of molecular weight of the acid fuels could be extended to polymeric fuels as well. In fact, Fig. 4.5 provides an idea of the average size of the fragment resulting from degradation of CTPB or HTPB, which eventually participates in the combustion process. Extrapolating the MFS data[334] at different temperatures of a structurally close polymer like polythylene to the T_s of burning AP/CTPB system, an average size which emanates from the surface is realized to be 200, which is close to the molecular weight of sebacic acid. It is, therefore, interesting to note that the dependence of $\dot{r}$ on molecular weight provides very useful information on the average size of the fragment emanating from the surface during combustion. The thermal cyclization of HTPB residue depends on its molecular weight and not on its hydroxy content[385]. Thus, studies on AP+sebacic acid mixture seem to provide information which could be extrapolated to CTPB or HTPB propellants. The dependence of $\dot{r}$, at constant P and T_0, on the molecular weight (M) of a fuel of a particular class is defined as the molecular weight sensitivity of burning rate (σ_m) and is defined as[384].

$$\sigma_m = (\partial ln\dot{r} \ / \ \partial M)_{P,T} \tag{51}$$

and expressed as fractional change in $\dot{r}$/g mole^{-1} of the molecular weight of the repeat unit. From the plot of ln $\dot{r}$ *vs* M, three different

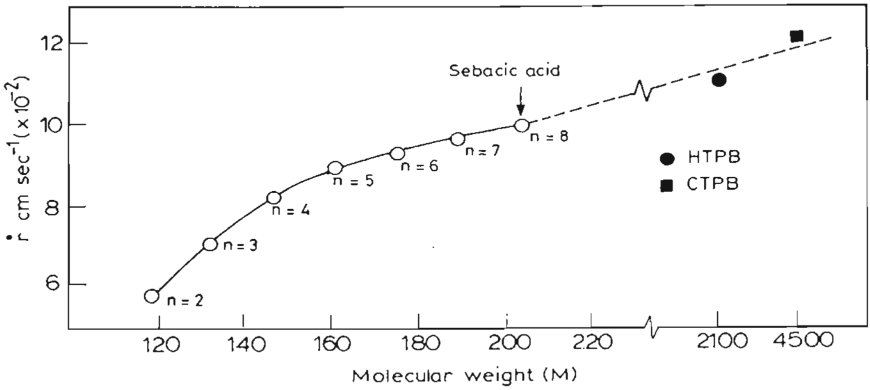

Figure 4.5. **Dependence of burning rate of AP+dicarboxylic acids on the molecular weight of the acids[384].**

values of σ_m have been obtained from the slope corresponding to three intersecting lines, I, II and III (Fig. 4.6). Up to adipic acid, σ_m is 12.8 x 10^{-3} g/mole^{-1} of the molecular weight of the repeat unit (Slope I). The slope becomes 2.9 x 10^{-3} for acids beyond adipic acid up to sebacic acid for Slope II. Corresponding to Slope III, for high molecular weight fuels, such as CTPB or HTPB, σ_m (=0.05 x 10^{-3}) becomes least sensitive. This anomaly in the transition of σ_m values from I to III with increase in molecular weight of the fuel arises due to the microstructural differences in the planarity of the molecules, proximity and interaction between the end groups, chemical structure of the backbone and size of the fragments emanating from the burning surface. Consequently, σ_m turns out to be a representative parameter significant of the changes the fuel component undergoes during solid-melt-gaseous transitions of the entire combustion profile.

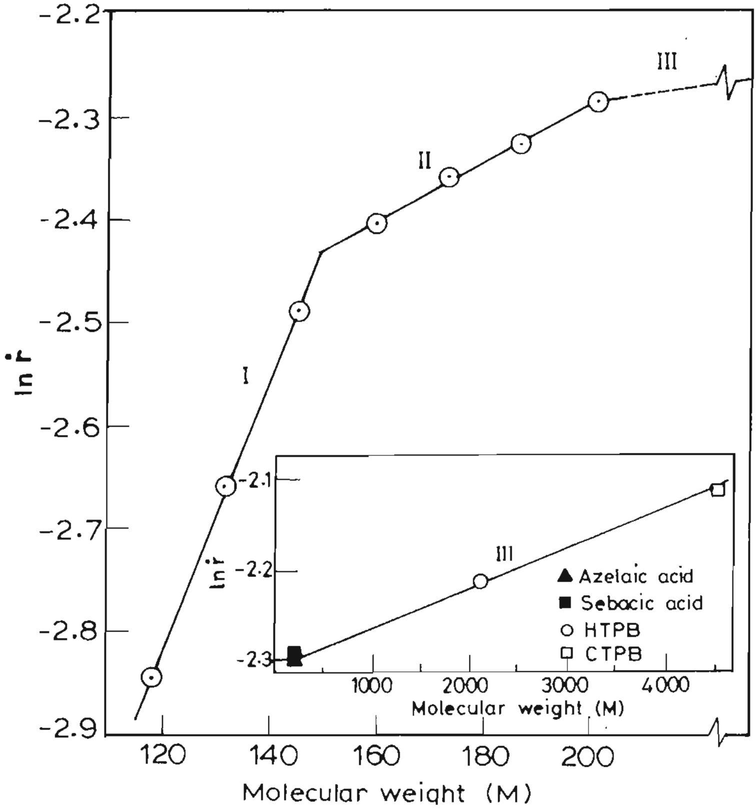

Figure 4.6. Plot of in $\dot{r}$ *vs M* of dicarboxylic acids, HTPB and CTPB with AP[384].

Further, condensed phase analysis of the quenched surface of the burning mixtures suggests anhydride formation in the case of acids represented by Slope I, while no anhydride formation is observed for systems represented by Slope II. Structural sensitivity is also apparent from the differences in the volatility of the acid fuel/gasification product in the two regions, as evidenced by simultaneous DTA-TG-DTG analysis. Accordingly, the study of temperature profiles of the burning mixtures of the model composite systems reveal that the burning surface reaction is uneven with irregular temperature jumps in the region of Slope I and smooth for acids in Region II. A clearer interpretation of the temperature profile and of the physico-chemical processes in the condensed phase is made by transforming the temperature profile into heat release rate profiles. In fact, the DTA-TG-DTG profiles turn out to be complementary to these profiles and are helpful in the identification of the processes which may occur in the condensed phase. From the heat release rate profiles, ratio of the condensed phase enthalpy to gas phase suggests that the extent of condensed phase enthalpy increases linearly up to adipic acid and deviates thereafter up to sebacic acid with less variation as a function of molecular weight. The heating rate at the burning surface of AP-sebacic acid mixture (470 ^{0}C/s) was found to be almost of the same order as expected in real CSP systems[348]. Thus, the surface and subsurface seem to be the zone wherein the physico-chemical characteristics of the acid fuel sensitize the burning behaviour.

The effect of different end groups on $\dot{r}$ has been studied by measuring the $\dot{r}$ values of AP-sebacic acid derivatives with varied end groups. From a knowledge of the Taft constant (σ_I) of the end group substituents, the plot of $\dot{r}$ *vs* σ_I suggests that the $\dot{r}$ decreases (Table 4.4) become more and more electron withdrawing. This trend of the effect of end groups on $\dot{r}$, visualized in model fuel molecules, could also be realized in practical telechelic polymers containing similar end groups[384]. This correlative study is suggestive of the manner in which microscopic changes in the fuel binder at the molecular level bring about macroscopic changes[385] in gross phenomenon like $\dot{r}$. *Cis/trans* and vinyl contents in HTPB affects the mechanical property and viscosity significantly, but not the ballistic property[386]. The $\dot{r}$ values of maleic acid-AP and fumaric acid-AP mixtures were found to be only marginally different, only 6 per cent more for the trans isomer[384]. Polymer viscosity increases on increasing the 1,2 vinyl content[386]. The tensile strength and elongation increase on increasing the trans content and decrease on decreasing the 1.2 vinyl content[386]. But the ballistic properties of HTPB propellant with different microstructures were more or less of the same order[386].

Table 4.4. $\dot{r}$ data for AP/sebacic acid derivatives and Taft constants (σ_I) for acid derivatives[384]

Derivative	*M*	σ_I	$\dot{r}$ *(cm/s)*
HO-C-X-C-OH	202.3	+0.34	0.101
H_2N-C-X-C-NH_2	200.3	+0.21	0.118
Cl-C-X-C-Cl	239.2	+0.39	0.093
H_3CO-C-X-C-OCH_3	230.3	+0.30	0.102
N_3-C-X-C-N_3	252.3	-	0.140
HO-X-OH	146.3	+0.25	0.121
Cl-X-Cl	183.0	+0.47	0.083
Br+X-B_r	272.0	+0.45	0.087
N_3-X-N_3	196.0	+0.43	0.107

Note : X = $(CH_2)_8$

4.3.2 Gas Phase Behaviour of Fuel Binders

Gasification of the propellant surface layer involves polymer degradation, and the gas phase reactions are similar to those occurring in the diffusion flames of gaseous hydrocarbons[70,309,360]. The methane-oxygen diffusion flame can be considered as a model for the more complex polymer flames. Beackstead-Derr-Price (BDP) model.

[91] considers the input parameters in terms of ClO_2-CH_4 reactions. However, the gas phase reactions also depend on the kind of products being gasified from the condensed phase and the nature of fuel binder present therein. In fact, the mass transfer numbers of such combustible fuels are classified on the basis of their structural characteristics as aromatic, aliphatic, etc. and are related to the apparent heat of gasification of the fuels[387]. Thus, the heat of gasification is not an independent parameter, but is related to the chemical structure of the fuel. It has also been found that the feedback of heat from the gas

phase to the condensed phase, which decides the linear pyrolysis rate of the binder and heat release at the burning surface, depends on the structure of the fuel binder[388].

Although both condensed and gas phase behaviours of the fuel binder point to the fact that its chemical nature and structure affect the combustion behaviour of the propellant, yet there is no direct relationship between $\dot{r}$ and chemical structure of the fuel[389].

4.4 MODELLING STUDIES AND ROLE OF FUEL BINDER

Many idealizations to rationalise the effect of variables, such as P and T_0, on the combustion of CSP have resulted in various combustion models which have been reviewed by Kishore[70] and Cohen[390]. These theories have been developed largely to predict $\dot{r}$ values; they are primarily based on the condensed phase details and gas phase considerations. It would, however, be worthwhile to draw attention to the role of fuel binder implicit in structuring these theories of CSP combustion.

4.4.1 Condensed Phase Considerations

The main feature of condensed phase theories, in the light of various models, is that the solid phase has been primarily treated as a source for the gaseous material to support the flame[70]. Considering that the major condensed phase reactions occur at

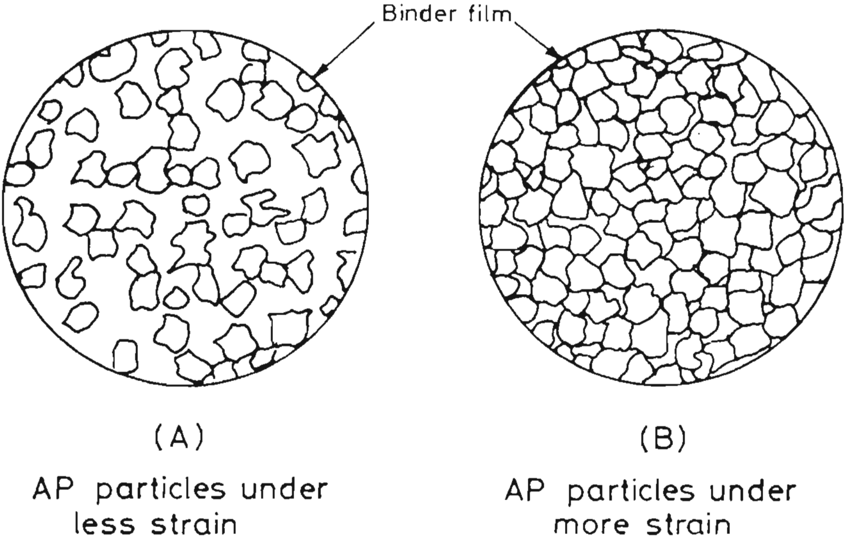

Figure 4.7. Propellant (A) with lower AP loading and (B) with higher AP loading [26, 27].

the surface, followed by diffusion of the reaction products to undergo secondary combustion in the gas phase, a reasonable correlation of the data of Summerfield[5] has been made purely on the basis of surface reaction and convective transport[362].

According to the model proposed[26,27] at this laboratory (Fig. 4.7), AP particles are surrounded by a thin polymer film. As the AP concentration increases (i.e., at higher AP loading), the film imparts strain on the AP particles; higher the AP loading, the higher is the strain. The behaviour of strained AP particles in the propellant can be examined by studying their decomposition in the orthorhombic and cubic regimes. It is observed that decomposition of the propellant, where AP particles exist under strain, is desensitized in the orthorhombic region and the propellant can be examined by studying its decomposition in the orthorhombic and cubic regimes. It is observed that decomposition of the propellant, where AP particles exist under strain, is desensitized in the orthorhombic region and sensitized in the cubic region. This behaviour is analogous to the thermal decomposition of pure AP as a function of precompression pressure, which induces strain on AP particles[27,391]. Further support for this model is afforded by results of initial pyrolysis of AP/PS propellant sample[26]. The initial decomposition products that emanate are those from PS degradation. Mass spectroscopic studies on growth and decay of styrene and benzene confirm this. Chemical analysis of KP/PS propellant[365] also supports the view that the initial decomposition product is styrene. As the decomposition proceeds further, the binder film surrounding the AP particles is ruptured and the decomposition products from the oxidizer and the reaction products of the binder and oxidizer species are observed. These degradation studies support the view that AP particles, surrounded by the binder film, experience strain.

Several investigators[24,392] have obtained evidence supporting the contribution of heterogeneous condensed phase reaction during propellant combustion. According to Pantoflicek and Lebr theory[393]. $\dot{r}$ is influenced by the reactions occurring during melting and gasification of the propellant surface layer. Melting is found to have a destabilizing effect on the propagation of the reaction front in the combustion of the condensed phase[394], but the mechanism is not clear.

Sammons[18] has proposed a model (Fig. 4.8) for CSP exhibiting the occurrence of condensed phase reactions. AP and binder both decompose in the solid phase in such a way that the products mix and interact in the interstices between the AP particles. At higher heating rates encountered during combustion, finer AP particles are assumed to be completely decomposed in the liquid binder layer, resulting in large exothermic condensed phase reactions.

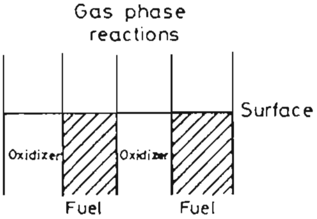

Sandwich columnar diffusion model (ref. 398)

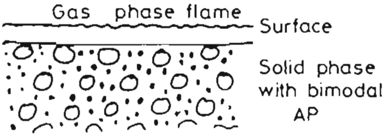

Condensed phase model (ref. 18)

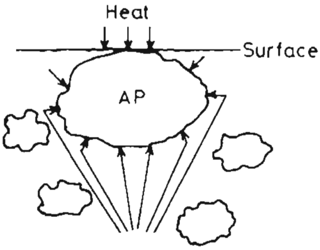

Site for possible heterogeneous reactions

$O_2 + (CH_2)_n \longrightarrow$ products + heat

$Cl_2 + (CH_2)_n \longrightarrow$ products + heat

$N_2O + (CH_2)_n \longrightarrow$ products + heat

$Cl_2O_7 + (CH_2)_n \longrightarrow$ products + heat

$HClO_4 + (CH_2)_n \longrightarrow$ products + heat

Condensed phase model (ref. 396)

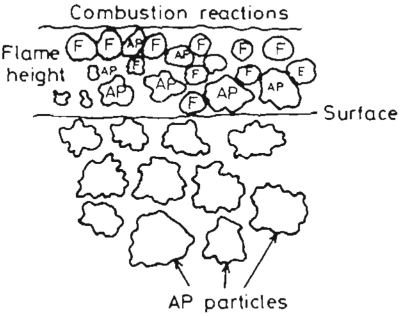

Granular diffusion flame model (ref. 5)

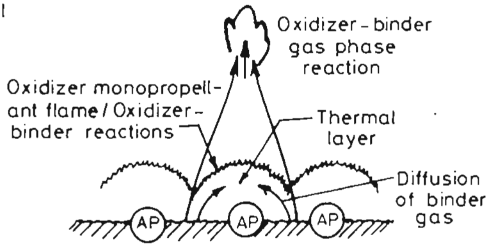

Thermal layer theory (ref. 400)

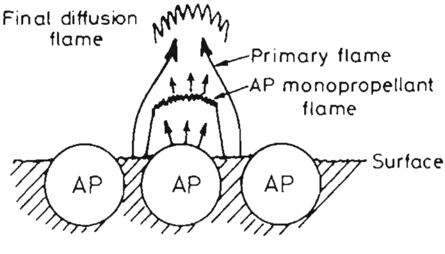

Multiple flame model (ref. 91)

Figure 4.8. Schematic representation of various models of CSP combustion.

Waesche, *et al.*[128] observed an intense and energetic exothermic condensed phase reaction to occur in CSP, which points to the degree of interaction between the oxidizer and the binder. Such condensed phase interactions are strong functions of the chemical nature of the binder used. Polysulfide-based propellant shows a low temperature exotherm and results in 'flameless combustion'. PU propellant is characterized by lesser interaction between the oxidizer and the binder and lesser energy release. Study of PBAA propellant shows that both low and high temperature decomposition of AP occur with a significant heat release to maintain the combustion wave of the propellant. However, this model does not explain 'intermittent burning'[146] of the propellant. The key ingredient of Hermance model[90] is heterogeneity of the burning surface. The physico-chemical processes considered are: surface processes of endothermic pyrolysis of the binder, exothermic oxidizer decomposition, exothermic chemical reaction between the fuel binder and the oxidizer and gas phase combustion of the products of decomposition of the fuel and the oxidizer. This model envisages a very large exotherm near the surface. In the relationship developed for linear $\dot{r}$ (Table 2.1), activation energies for fuel binder pyrolysis, surface reactions and gas phase reactions are considered in addition to the activation energy of oxidizer decomposition. This model predicts T_s and heat generated in the condensed phase. However, the effect of chemical nature of the fuel binder is not clearly understood[4].

Kumar[93,94] considering the overall rate determining step to be the condensed phase reaction, has predicted $\dot{r}$ values (Table 2.1) based on the thickness of the melt layer on the oxidizer crystals and fragment size vaporizing (FSV) of the fuel from the surface. The FSV varies from polymer to polymer which was also observed by Braginskii and Bakhman[395].

Theories have been developed to predict $\dot{r}$ as a function of T_s and condensed phase details of polymer combustion[16,396,397]. Brown, *et al.*[16,396] suggest significant interfacial reaction between decomposition products of the fuel and the oxidizer much below T_s (400-700 °C). It is believed that highly reactive $HClO_4$ and O_2 are capable of attacking typical binders during combustion. Several possible heterogeneous reactions are proposed (Fig. 4.8) to occur at the oxidizer-polymeric binder interface. It is interesting to note that the binder-structure dependent factor '*Z*' is related to the heat generated at the surface (Q_s) and in the subsurface region (Q_{ss}) as:

$$Z = Q_s/[(LX_0)^n] \exp(E_s/RT_s) \qquad (53)$$

$$Z = Q_{ss}/[MX_0] \exp (E_s/RT) \tag{54}$$

where T_s and T are the temperatures at the surface and in the subsurface, n, the order of surface reaction, L and M the constants and X_0 the mole fraction of the oxidizer species. The above two expressions have been used to obtain the energy balance around the solid phase reaction zone.

Although the structure of the fuel binder is recognized, no model has yet proposed any unique parameter representative of the effect of fuel characteristics on the overall burning of a propellant.

4.4.2 Gas Phase Considerations

The major feature of a gas phase theory is that the heat produced by exothermic reaction of the gaseous products of decomposition/degradation of the oxidizer and the binder is important in determining values of $\dot{r}$[61]. The role of fuel is quite apparent in many of the gas phase models and is discusseed below.

In 'Sandwich Columnar Diffusion Flame' model, Nachbar and Parks[398] (Fig. 4.8) consider conversion of thin plates of fuel and oxidizer (sandwiched as a two-dimensional array) into gas phase from the dry solid-gas interface. This theory does not take into account the condensed phase details and predicts $\dot{r}$ to be independent of pressure.

The Two-Temperature Postulate developed by Shultz and Decker[399] states that the oxidizer and the binder decompose more or less independently. Although the physico-chemical properties of the two are quite different, the T_s of each adjusts itself in such a way that the rate of consumption becomes equal to $\dot{r}$ of the propellant.

Chaiken's Thermal Layer Theory[400] is based on the two-temperature postulate and considers decomposition of the oxidizer separately from that of the binder. It is assumed that a thermal layer or flame zone adjacent to the oxidizer particle size exists (Fig. 4.8) and heat transfer occurs from this layer to the condensed phase. Thermal layer thickness (δ) during steady state burning is found to be sensitive to ϕ and pressure, δ is given as:

$$\delta = r_0 / (1 + \phi P) \tag{55}$$

where r_0 is the average oxidizer particle radius and δ is the mixture ratio. The heat affected zone of about 0.025 cm is found to extend into the solid phase. Although satisfactory prediction is made for

AP propellant, the model is not completely in accordance with the experimental findings.

Rosen[89] obtained the following relationship for $\dot{r}$:

$$\dot{r}/a = P/b\left[F\left(\frac{n_S}{\ln(a/\dot{r})} - \frac{C_p T_o + \Delta H_d}{\Delta H_g}; n\right)\right]^{1/2} \tag{56}$$

which incorporates the solid phase heat release (ΔH_d) due to the decomposition occurring at the surface, ΔH_g is the heat of reaction in the gas phase; n_s, index for surface decomposition; and n, index for the chemical reactions in the gas phase. Constants *'a'* and *'b'* are related to propellant decomposition, thereby revealing the importance of condensed phase also; *F* is a function.

Summerfield[5] proposed an elaborate model known as the Granular Diffusion Flame Model (GDFM), which is shown in Fig. 4.8. According to this model, a steady gaseous flame just over the burning surface is considered. The oxidant and/or the fuel are believed to leave the surface directly by sublimation or pyrolysis in the form of tiny packets of a certain mass without undergoing any chemical reaction among them in the solid phase. The only chemical process of any significance at the surface, according to this model, is gasification of the propellant. The oxidant and/or fuel pockets mix in the gas phase and undergo combustion to form the final products. The pockets are considered to be consumed at a rate controlled by diffusional mixing and chemical reaction. With the above assumptions, the following expression for $\dot{r}$ is obtained;

$$\frac{1}{\dot{r}} = \left[\frac{\rho_p\left[C_s(T_s - T_o) - Q_s\right]}{\lambda_g\left[T_f - T_s\right]}\right]^{1/2}\left[\frac{f_1}{\rho_g\left(A\exp - E_f / RT_f\right)} + \frac{f_2\lambda^{1/3}}{D_g^{1/2} r_g^{5/6}}\right] \tag{57}$$

where, ρ_p and ρ_g are the densities of the propellant and the gas phase respectively; λ, the mass of the fuel vapour as packets; f_1 and f_2 are factors associated with flame length when it becomes chemical reaction controlled and diffusion controlled, respectively; λ_g, thermal conductivity in the gas phase; D_g the intermolecular diffusion coefficient, and Q_s , the net heat release (positive) for gasification of the propellant. Summerfield considered Q_s of the binder as "probably negative" and for AP it is taken as endothermic (256 cal/g). The average Q_s for both binder and AP is considered as +100 cal/g.

Although Chiken's model[400] considers the importance of the thermal layer in the gas phase, basically it is a gas phase model. Nevertheless, it considers decomposition of AP in the condensed phase as exothermic in contrast to GDFM theory[5], where both AP and binder gasify independently and endothermally. The endothermic gasification of AP can be only due to its dissociative sublimation. It may be noted that the average enthalpy for dissociative sublimation of AP is 496 cal/g (Table 3.3). Further, it may be noted that this model does not consider that factors such as heat of gasification, mass transfer (related to D_g) and heat transfer from the gas phase to the condensed phase are dependent on the structure of the fuel[388,389,395]

According to Summerfield's model[5], pressure dependence of $\dot{r}$ is given by Eqn (6) (Table 2.1), where constants a and b are related to the chemical reaction time and diffusion time parameters respectively. Ebenezer, *et al.*[401] found that b would be somewhat sensitive to the mixture ratio as well as to the oxidizer particle size. Bernard, *et al.*[402,403], explained the satisfactory fit of the experimental data of Summerfield on the basis of the dissociative process and phase changes. Considering the fact that the fuel-oxidizer gases emerge from the regressing propellant surface, Rice[404] and Von Elbe, *et al.*[88] obtained Eqns. (7) and (8) (Table 2.1).

Fenn[92], in his phalanx model, has provided a detailed description of the flame zone and diffusion flame burning at the interface between streams of fuel and oxidant vapours emitted from the propellant surface. The $\dot{r}$-P relationship is represented by Eqn (12) (Table 2.1). Assuming an effective and rate-determining reaction layer between the decomposition and flame zones, Hur and Mok[405], developed theoretical relationship for predicting $\dot{r}$.

According to Arden, *et al.*[109], volatility of the fuel is found to affect the vlaue of $\dot{r}$. With very volatile fuels, propagation is normal to the surface and the flame appears to be homogeneous. As the fuel becomes less volatile, the mode of flame propagation becomes abnormal and shows some progressive changes, and departure from one-dimensional model becomes obvious; the consumption of the burning surface by wave reactions across the burning area becomes pulsating or rhythmic. This is believed to be fundamental in all solid propellants. Even in small proportions, the binder has been shown to profoundly influence steady state combustion[329] as well as oscillatory combustion[406]. Combining the concept of perturbation of vapour diffusion with AP decomposition flame, Ebenezer *et al.*[401] have modified Summerfield's GDMF which is referred to as the modified granular diffusion flame model (MGDFM). MGDFM incorporates intermixing of fuel vapour into the AP decomposition flame and an additional reaction with AP decomposition flame is also considered to occur and the effects of pressure, AP particle size, mixture ratio and T_0 and $\dot{r}$ are predicted. The compositional dependence of $\dot{r}$ of propellants is described by a percolation model of propellant combustion[470].

The BDP model[91] shown in Fig 4.8 proposes three different flames, namely, the primary flame due to the decomposition products of the initial fuel and the oxidizer, AP monopropellant flame above the oxidizer and the final diffusional flame due to AP and fuel decomposition. Depending upon the pressure, these flames assume different levels of importance. This model considers preheating of the components and exothermic condensed phase reaction between the decomposition products of the oxidizer and the binder. Based on the kinetics of a series of chemical reactions, a relationship is developed to predict the dependence of $\dot{r}$ on T_0, mean T_s etc. The model developed by Beckstead and McCarty[408] indicates that the decomposition characteristics of the binder are important in the burning process. In their more general approach, the binder and the oxidizer are allowed to have independent T_s values. The concept of burn through time, which represents the unsteady nature of binder pyrolysis in a propellant environment is introduced and indicates that the fuel binder has a more significant influence than was previously thought. Attempts are also made to explore as how the binder is proportioned to the various oxidizer fractions in the gas phase. It is found that the flame appears at stoichiometric conditions, while some portion of the binder is left over. For AP propellant, most of the binder reacts, but the extent depends on the energy fed back from the primary flame over the binder. It appears to be related to T_0 and possibly the stoichiometry. However, quantitiave data are not available to allow estimation of the fraction of the binder that does not react. More fundamental work is perhaps needed on binder behaviour[409].

The binder regression rate determined using Arrhenius equation is used to understand the surface structure in the BDP model[91]. This equation, according to Cohen and Strand[410] is inconsistent, since it utilizes T_s of AP, which is assumed to be uniform. The criticism is that the binder is given too subordinate a role, as it is made to simply exhibit AP regression behaviour. A related problem is that there is no mechanism for heating the binder directly; the heat fed back from the flame is apportioned between AP and the binder. This looks too simple and a separate energy balance is given[410] such that the energy required to heat the binder to its T_s, including the heat of decomposition, is equal to the fraction of primary diffusion flame energy utilized to heat the binder. This treatment suggests that the portion of the diffusion flame over the binder does not seem to be a part of the usual BDP flame. Incorporation of this treatment however, has improved the $\dot{r}$ model in predicting high pressure burning behaviour, such as prediction of propellant T_s and also a better understanding of the surface. Combustion regimes of volatile substances decomposing in the condensed and gas phases are, however, analyzed and this appears to be a good beginning[411].

The thermodynamic model of deflagration of AP proposed by Kishore and Sridhara[274], besides considering both condensed and gas phase processes, has a universal character and could be applied to other self-deflagrating systems. This equation was used in the case of combustion of stoichiometric mixture of AP-sebacic acid model fuel system and later of AP/CTPB propellant. The $E_{s,c}$ and $E_{s,g}$ values for the atmospheric pressure burning of AP-sebacic acid system were obtained by substituting the values of the input parameters of σ_p, T_s, n, $(dT_s/dT_o)_p$ and $(dT_s/dP)_T$ in Eqn. (5) of reference 274.

$$E_{s,c} = \sigma_p R T_s^2 \,/\, (dT_s/dT_0)_p = 6.2 \text{ kcal/mole} \tag{58}$$

$$E_{s,g} = (n/P) R T_s^2 \,/\, (dT_s/dP)T_0 = 65.4 \text{ kcal/mole} \tag{59}$$

The low $E_{s,c}$ value of 6.2 kcal/mole has been ascribed to the decomposition of pure AP, because sebacic acid being a fusible fuel vaporizes at much lower temperatures, leaving behind AP in the condensed phase, so that essentially the decomposition of AP occurs at the burning surface. The similarity of $E_{s,c}$ in deflagration of AP-sebacic acid mixture and AP suggests[274] that the condensed phase chemistry is more or less similar in the two systems. From the temperature profile analysis of the heat release rate, the gas phase heat release per g of AP in AP+sebacic acid mixture is found to be 1162 cal/g, which is larger than that observed for pure AP (169 cal/g).

Unlike AP+sebacic acid systems, the situation completely changes in the case of AP/CTPB propellant, where the fuel cannot volatilize prior to its degradation and, therefore, extensive interplay in the condensed phase is expected. Thus, the polymeric nature of the fuel brings about a substantial contribution in the condensed phase. Upon extending this model to a real fuel system comprising CTPB/AP, it provides valuable insight into the polymeric nature of the fuel. Substituting all the input values of the parameters in Eqns (58), (59), $E_{s,c}$= 1 kcal/mole and $E_{s,g}$ = 30 kcal/mole were obtained. Unlike in AP+sebacic acid fuel system with $E_{s,c}$ = 6.0 kcal/mole, the low $E_{S,c}$value observed for AP/CTPB propellant is attributed to the softening of CTPB, which occurs by overcoming the secondary interactions, such as Van der Waal forces and dipole-dipole interactions. This energy may, be of the order of 1 kcal/ mole the softening of CTPB, which subsequently covers the AP particles to promote reactions in the condensed phase, could be the rate-controlling step.

Since the oxidizer happens to be present in a large proportion, viz., in stoichiometric amounts (>75%), it is reasonable to consider the gas phase reactions just above the surface to be predominantly of the AP flame reactions. Thus, the gas phase activation energy of $E_{s,g}$ = 30 kcal/mole can be assigned for the gas phase flame reactions of AP deflagrating as a monopropellant; this is in accordance with the BDP model[85] (Fig 4.8), where 30 kcal/mole has been considered to represent the AP monopropellant flame extending from the surface rather than occurring at the propellant surface.

Thus, the thermodynamic model applied to AP, AP+sebacic acid mixture and AP/CTPB systems illustrates that the $E_{s,c}$ values and condensed phase reactions operative in AP and AP+sebacic acid systems are similar, although $E_{s,g}$ values differ widely. In AP and AP/CTPB systems, the $E_{s,g}$ values are similar, but the $E_{s,c}$ values differ considerably.

The thermodynamic model also provides some basis for explaining some special combustion features, such as intermittent burning, flameless combustion and plataeu burning. The main controlling factors in Eqn (5) (ref 274) are n and $(dT_s/dP)_T$ and, therefore, $E_{s,g}$ may be written as:

$$E_{s,g} \; \alpha \; n/(dT_s/dP)T_0 \qquad (60)$$

In practice, in CSP, the variation of n (0.4-0.8) compared to $(dT_s/dP)_T$ will be much smaller and it is rarely > 1. Hence $E_{s,g}$ is primarily controlled by $(dT_s/dP)_{T_0}$ so that

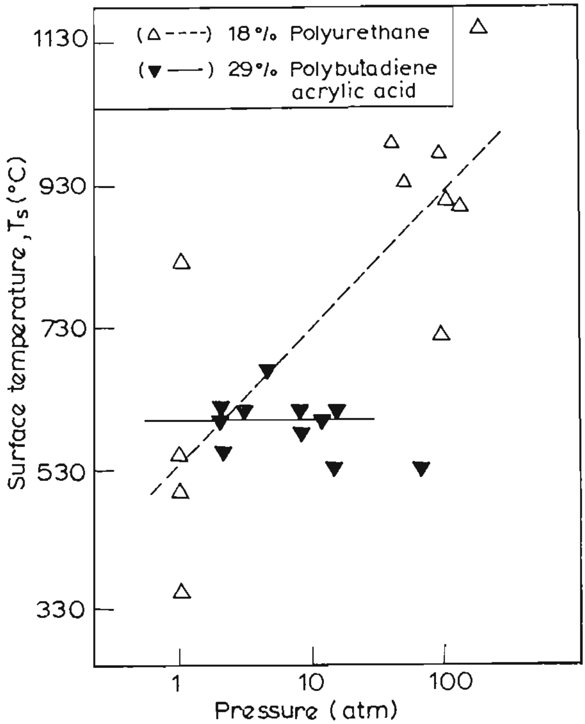

Figure 4.9. Surface temperatue for AP-based propellants as a function of pressure[275].

$$E_{s,g} \alpha 1 / (dT_s / dP)T_o \qquad (61)$$

In PBAA propellant, intermittent burning and extinction have been observed[146]. In this particular case, $(dT_s/dP) \longrightarrow 0$ (Fig 4.9). As a result, according to Eqn (61) $E_{s,g}$ becomes so high that the gas phase reactions do not take place and condensed phase reactions predominate. Waesche, *et al.*[128] observed that extensive condensed phase reactions occur in PBAA propellants. Even in flameless combustion, which is primarily supported by condensed phase reactions, the second term in Eqn (5)[274] has no contribution. Unlike in PBAA propellant, PU propellant exhibits plateau burning[148] (1-80 atm), $(dT_s/dP)_T$ is very large (Fig 4.9) and $n \longrightarrow 0$, such that the gas phase reactions could be favoured over the condensed phase reactions. This behaviour of PU propellant of gas phase-controlled combustion is further corroborated by the work of Waesche, *et al.*[128] who observed lesser interaction between the fuel and the oxidizer in PU propellant in the condensed phase. Similarly, the behaviour of polyisobutylene-based propellant, which also exhibits plateau burning[86], can be explained by this thermodynamic model.

Thus, the modelling studies reveal that solid phase considerations have the potential to predict the heat release in the solid phase, temperature sensitivity of $\dot{r}$ and catalyst action. Although gas phase considerations identify the role of binder as significant, the effect of changes in the binder characteristics on the regression rate has neither been analyzed nor predicted[69].

4.5. EFFECT OF FUEL BINDER STRUCTURE

The structure-property relationships of fuel binders are important not only in propellant combustion, but also in pyrotechnics[412], explosives[413] and fire extinguishers[414]. In pyrotechnic compositions, the binder induces a new exotherm and reduces the ignition temperature[415]. The reaction between the binder and the nitrate in Mg-$NaNO_3$ and Mg-$Sr(NO_3)_2$ compositions appears to be important. Such chemical reactions of the ingredients changes the ignition temperature[416].

CHAPTER 5

EFFECT OF BURNING RATE MODIFIERS ON COMPOSITE SOLID PROPELLANTS & THEIR COMPONENTS

5.1 AN OVERVIEW

Additives are known to affect the combustion of CSP and its components–the oxidizer and the binder. It is a vast subject and has been reviewed by Hall and Pearson[85], Jacobs and Whitehead[163], and Kishore and Sunitha[71]. Additives generally are of two types, namely, those which enhance the $\dot{r}$ value of propellants (catalysts) and those which decrease their $\dot{r}$ value (inhibitors)[163].

Effective catalysts, known to modify the decomposition and combustion rate of CSP and its constituents, are transition metal oxides (TMO), such as Fe_2O_3, MnO_2, Ni_2O_3, copper chromate, etc.[71]. The concentration of these catalysts is another important aspect in their effectiveness[417]; the concentration should be such that it does not alter the propellant composition and must be as low as possible, so that the propellant energetics is not affected. Kishore, *et al.*[418] found that the decomposition and $\dot{r}$ value of AP/PS propellant increase up to a certain catalyst (Fe_2O_3) concentration beyond which the effect either levels off or decreases. Although Fe_2O_3 is an effective catalyst and is used widely, the catalysts currently in vogue are ferrocene-based compounds which possess better processing characteristics than Fe_2O_3 and they increase $\dot{r}$ by over 20%[419-421].

Some of the important aspects that serve to explain the mechanism of catalyst action are summarized below[16].

(i) Metal components in TMO can exhibit variable valence or oxidation states and hence TMO's are effective decomposition and $\dot{r}$ catalysts.

(ii) Additives which are electron donors or acceptors can modify oxidation/decomposition products.

(iii) Catalytic activity results from physical contact; the reaction ceases when particles no longer have an oxidizer-additive interface.

(iv) Gaseous product distribution may be altered by some catalytic agents.

(v) Iron compounds are common catalysts for AP propellant systems; a redox-cycle involving the ferric-ferrous couple may be the key mechanism in combustion catalysis by iron compounds.

(vi) $\dot{r}$ depends on catalyst concentration, surface area and state of aggregation.

Not many studies have been reported on the additives which decrease the $\dot{r}$ of CSP and decomposition of its components. However, LiF is known to inhibit $\dot{r}$ of CSP, probably due to the formation of NH_4F through the formation of an LiF-NH_4ClO_4 eutectic mixture[348]. NH_4F and other easily decomposable ammonium salts, such as NH_4Cl, NH_4Br, etc, are versatile inhibitors for AP decomposition/deflagration and CSP combustion[422]. Thus, LiF reduces the $\dot{r}$ of CSP by reducing the thermal effect in the condensed phase to 15-20%[313]. The available literature mostly concerns mechanistic studies on the action of the catalyst on the decomposition and combustion behaviours of AP and CSP. Such studies are important from the standpoint that propellants may be formulated to give predetermined $\dot{r}$[71,252]. In this chapter, the present status of the catalyzed decomposition of AP, binder, CSP and their combustion is presented to understand the mechanism of their action. Widely used catalysts, such as TMO and copper chromite have been covered in the present discussion. Shortcomings in the use of Fe_2O_3 have led to the use of ferrocene derivatives for improving the performance. While discussing these aspects, emphasis is laid on the condensed phase processes and on identification of the site of catalyst action.

5.2 EFFECT OF CATALYSTS/INHIBITORS ON DECOMPOSITION AND DEFLAGRATION OF AMMONIUM PERCHLORATE

Catalyzed thermal decomposition[195,230,423,424-426,9,17] and deflagration[249] of AP in the presence of TMO, such as Fe_2O_3, MnO_2, CuO, Cu_2O, Cr_2O_3, $CuCrO_3$, $CuCrO_4$ etc. have been a subject of wide interest. However, the exact mechanism of catalyst action on the decomposition of AP is still not clear, it has been broadly explained on the basis of the mechanism of decomposition of AP. Catalyzed decomposition of AP into NH_3 and $HClO_4$ by proton transfer[427] and subsequent oxidation of NH_3 (adsorbed on the catalyst surface) by $HClO_4$ at the catalyst site has been reported[428,429]. Diffusion of ClO_4^- into the catalyst surface in close contact with AP is considered[430] to be an important feature; Decomposition of ClO_4^- via Cl-O bond cleavage is believed to be the rate-controlling step.

Apart from the proton transfer mechanism, electron transfer mechanism has also been proposed. TMO is understood to provide a sort of bridge in the electron-transfer process facilitating low temperature decomposition of AP[230,431], and this is considered to be the rate-controlling step[432]. Kishore, *et al.*[433] proposed an electron transfer mechanism for the catalytic action of MnO_2 on decomposition of AP:

$$\begin{aligned} Mn^{4+} + ClO_4^- &\rightarrow {}^{\bullet}ClO_4 + Mn^{3+} \\ Mn^{3+} + NH_4^+ &\rightarrow {}^{\bullet}NH_4 + Mn^{4+} \end{aligned} \qquad (62)$$

The activation energy is observed to correspond to the electron transfer process[434]. The ${}^{\bullet}NH_4$ and ${}^{\bullet}ClO_4$ radicals further decompose into NH_3 and oxides of chlorine[196], the products of catalyzed decomposition seem to be different from those of pure AP[435,436]. Calcining of a TMO like Fe_2O_3 has little effect on its activity[437].

Rastogi, *et al.*[438,439] described the following equation which applies not only to catalyzed decomposition of AP but also to its inhibition:

$$d\alpha/dt = (a\alpha - b\alpha^2)/(1+h\alpha) \qquad (63)$$

where α is the fraction decomposed at time t; a, b and h are constants, a being associated with the nucleation process and h with the adsorption of $HClO_4$ on the catalyst surface. h is large for catalysts and zero for inhibitors.

Like decomposition, catalyzed deflagration of AP[440] depends on the catalyst concentration[264], particle size[441] and its distribution[442,443]. Catalyst concentration, for example, has an important bearing on the LPL of pure AP. CuO, Cr_2O_3, Fe_2O_3, MnO_2 and $KMnO_4$ increase LPL at low concentrations and decrease the same when present at higher concentrations[442]. At low concentrations (~3 wt%), the endothermic step and heat loss are dominant and LPL increases. At higher concentrations, the rate of exothermic reaction becomes predominant and heat feedback to the solid surface outweighs the heat loss; consequently, LPL is lowered[282,441]. Catalysts are known to act in both condensed and gas phases[442]. In the condensed phase, catalysts alter the surface features in AP combustion; the influence of AP melt and its enhancement is profound in increasing $\dot{r}$ and is affected by T_o[173]. Actually, it has been found[444] that there is an inherent instability of deflagration of the condensed phase; the effects of preheating, external heat flux and catalysts on LPL have been explained.

According to Boggs, *et al.*[264] the catalytic action of Cu, CuO and Cu_2O in the condensed phase is responsible for accelerating the deflagration of AP. The observed T_s (~630 °C), temperature gradient at surface and concentration gradient of the catalyst due to surface inhomogeneity are such that the catalyst action, under these combustion conditions, cannot be equated to their behaviour under decomposition conditions. Boggs, *et al.*[264] are, therefore, of the opinion that direct application of low temperature decomposition studies in deflagration conditions may be deceptive[445].

Generally, the inhibition of deflagration of AP is achieved by the addition of (i) readily decomposable ammonium salts, such as NH_4F, NH_4Cl, NH_4Br, NH_4HPO_4, $NH_4H_2PO_4$, etc, (ii) salts which bind $HClO_4$ or its decomposition products into less reactive

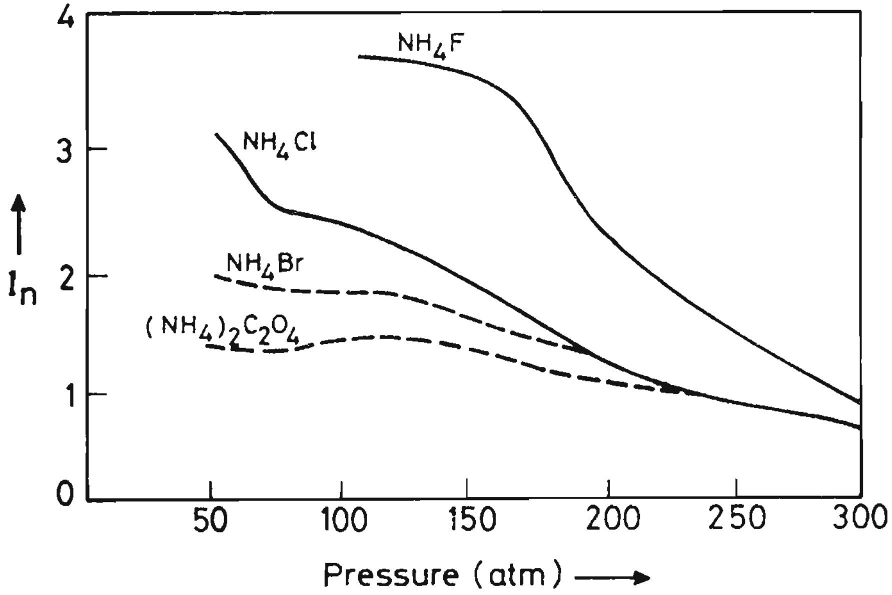

Figure 5.1. Effect of ammonium salts on deflagaration of AP[265].

compounds like CdF_2, and $PbCl_2$, ZnF_2, etc., and (iii) compounds like urea, oxamide, etc. which inhibit the decomposition of $HClO_4$. Alfakir, *et al*[446,447] studied the inhibitory effect of readily decomposable salts of ammonia like NH_4Cl, NH_4F, etc. on the combustion of AP. Ammonium salts are highly effective, because they shift the dissociative equilibrium towards the reactants due to the excess NH_3 generated. Glaskova[265] determined the effectiveness of inhibition in terms of coefficient of inhibition I_n as:

$$I_n = \frac{\dot{m} \text{ of pure AP}}{\dot{m} \text{ of AP with an inhibitor}} \tag{64}$$

where $\dot{m}$ is the mass burning rate. The inhibitory effect of ammonium halides (Fig. 5.1) decreases with reduction in the quantity of NH_3 generated during decomposition. I_n decreases from 3.7 to 1.9 for salts (1.0 wt.%) from NH_4F to NH_4Br. NH_4F is the most effective inhibitor; AP begins to burn only at 100 atm (LPL) and the deflagration rate is 3.7 times slower than that of pure AP. Salts like $PbCl_2$, PbF_2, CdF_2, and ZnF_2 are also equally effective, but they act by their exchange reaction with AP, resulting in more stable perchlorates of the metals. Reduction in the completeness of the oxidation reaction of NH_3 alters heat release in the condensed phase and decreases the $\dot{r}$ value.

5.3 CATALYZED DECOMPOSITION & COMBUSTION OF BINDERS

Not many studies have been reported on catalyzed decomposition of the binders. TMOs are known to catalyze hydrocarbon oxidation reaction by inducing free radical decomposition of hydroperoxides formed by the reaction of oxidizer and hydrocarbons[448].

$$ROOH + M^{n+} \rightarrow RO^{\bullet} + HO^{-} + M^{(n+1)+}$$

$$ROOH + M^{(n+1)+} \rightarrow RO_2^{\bullet} + H^{+} + M^{n+}$$

In hydrocarbon oxidation, metal salts like cupric stearate have been found to act as accelerators by lowering the activation energy for hydroperoxide decomposition. This depends upon the redox potential of the metal ion, which is further correlated with the catalytic activity[449].

Kishore[450] found that TMO's, such as Fe_2O_3, Ni_2O_3, Co_2O_3 and MnO_2 decrease the $\dot{r}$ of polymer combustion. These oxides affect the condensed phase reactions by suppressing the gasification and subsequent gas phase reactions by radical recombination on the oxide surface. Fe_2O_3 affects the decomposition of the binder[355,426] and lowers its decomposition temperature[425]. It is found to affect the kinetics of the first stage of isophorone diisocyanate-cured HTPB and also its exothermicity[348]. The liquid catalyst, 2,2-bis(ethyl ferrocenyl) propane, activates decomposition of the binder[426]; it also decreases the ignition delay and activation energy of the propellant[451]. Similarly, butyl ferrocene and carborane also decrease the ignition delay and activation energy of the propellant[451]. Ammonium phosphate suppresses polymer combustion[70], it primarily acts in the condensed phase, and flame retardation is due to extensive char formation at the burning surface, which acts as a barrier for effective heat transfer from the flame to the condensed phase. Combustibility of polymers is compared in terms of a laboratory test parameter, 'limiting oxygen index' (LOI)[452]. LOI is the minimum fraction of O_2 in an O_2/N_2 mixture, which is required to maintain the burning of a polymer sample of defined dimensions after it has been ignited by a pilot flame. A conspicuous example of study of catalyst action exclusively from binder considerations in CSP is that of the action of metal phthalocyanine complexes. These complexes are known to catalyze thermal decomposition of the binder resulting in the breaking of urethane linkages producing liquid or molten binder phase on the propellant surface; condensed phase reactions are believed to be the rate-controlling step[358,453].

Some examples demonstrate the importance of condensed phase reactions. Martin and Rice[454] observed that $Al_2O_3.3H_2O$, beyond 40% loading in epoxy resin increased the LOI, while anhydrous Al_2O_3 acted as an inert filler supporting the occurrence of condensed phase reactions with $Al_2O_3.3H_2O$. Fennimore and Jones[455] found that LOI vastly differs for PVC and poly 3,3-bis(chloromethyl)oxetane with similar Cl_2 content, indicative of the fact that the structure of the polymer in the condensed phase is important. Chlorine, when chemically bound to polyethylene and other plastics, retards the combustion more effectively than when it is added to the atmosphere around the burning polymer.

5.4 CATALYZED DECOMPOSITION & COMBUSTION OF CSP

The effect of TMO on the $\dot{r}$ of CSP has been studied[456-458] and reviewed by Kishore and Sunitha[71,459]. Apart from TMO, ferrocene and its derivatives are also known[424,427,428] to enhance the of CSP[419-421]. Kishore, *et al.*[418] made a systematic study of decomposition of AP and propellant burning as a function of catalyst concentration. Effectiveness of the catalyst for increasing propellant burning rate *($\dot{r}_b$)* and thermal decomposition rate *($\dot{r}_d$)* of AP was estimated on the basis of the following relationship:

$$\frac{\dot{r}_{bc}}{\dot{r}_{bu}} = \frac{\dot{r} \text{ of catalyzed propellant}}{\dot{r} \text{ of uncatalyzed propellant}} \tag{65}$$

and

$$\frac{\dot{r}_{dc}}{\dot{r}_{du}} = \frac{\text{rate of thermal decomposition of catalyzed AP}}{\text{rate of thermal decomposition of uncatalyzed AP}} \tag{66}$$

and they are plotted as a function of catalyst concentration in Fig. 5.2. The $\dot{r}$ value of the catalyzed propellant increases as the catalyst concentration is increased and reaches a maximum value around 1% of the catalyst, except for cobalt oxide. After the maxima, $\dot{r}$ either levels off or decreases. At low concentrations, $\dot{r}$ increases without significantly affecting the calorimetric value of the propellant. With increase in catalyst concentration, the calorimetric value is found to decrease, since the catalyst not only reduces the weight of the propellant but also takes away some heat to raise its temperature in the flame and hence reduces $\dot{r}$. Similar observations have been made in respect of thermal decomposition of catalyzed AP (Fig. 5.2). Effective catalyst concentration on the binder surface seems to provide adequate contact with the fuel vapour, bringing the flame closer to the surface[460,461]. Catalysts accelerate the initial decomposition by reducing the decomposition temperature of CSP, leading to shorter ignition delays depending on the catalyst concentration[462].

Salts of aromatic carboxylic acids (salicylates and resorcylates) have been widely used as effective $\dot{r}$ modifiers in DB propellants[463-467]; they exert plateau and mesa effects. However, these salts have not been tried in CSP. Kishore, *et al.*[468] demonstrated that these metal salicylates significantly affect degradative ignition and combustion of polymers. They also enhance the $\dot{r}$ and T_s of CSP. The condensed phase heat release was found to be very significant in the presence of these salicylate additives, which in fact, explains sensitization of the ignition of CSP. Iron salicylate brings about the highest increase in the condensed phase heat release. Consequently, $\dot{r}$ is the highest for iron salicylate as compared to other salicylates.

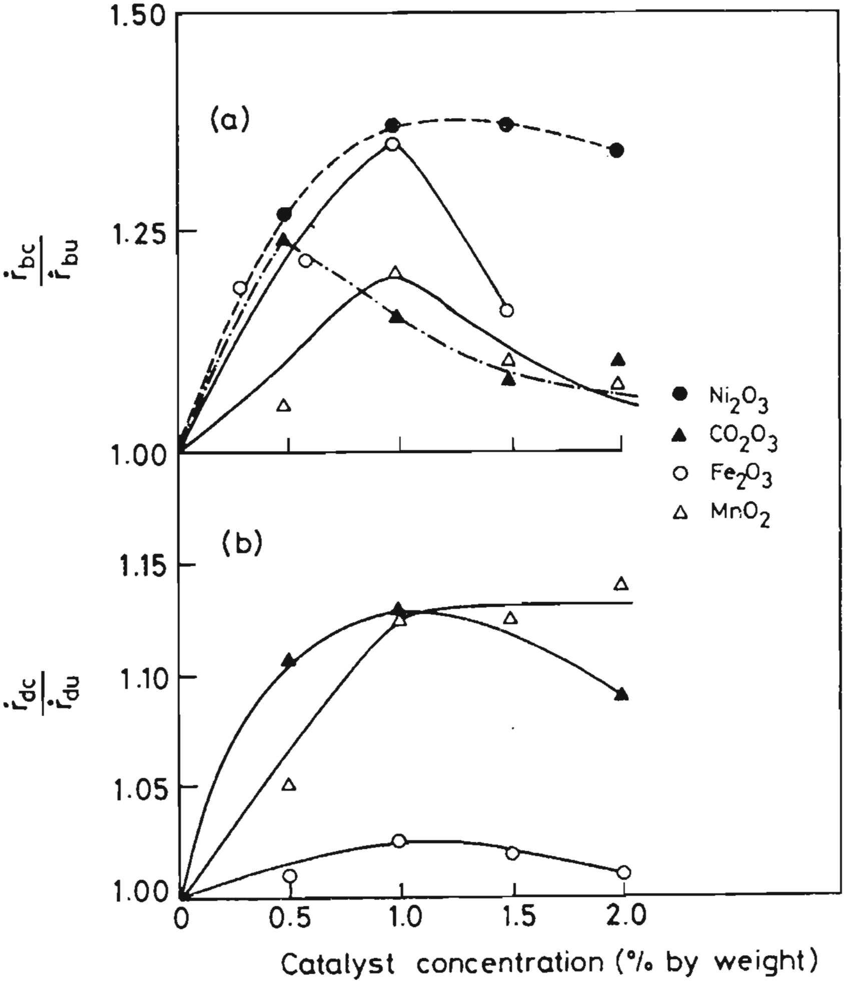

Figure 5.2. Dependence of burning rate ratio and thermal decomposition ratio on catalyst concentration in PS/AP propellant[418].

Very few studies have been reported on high temperature degradation relevant in ignition and combustion of CSP. Since polymer degradation is oxidative in nature, particularly in the ignition process, Kishore, et al[469] have shown that the activation energy for the oxidative degradation of polystyrene is 28-30 kcal/mole corresponding to O-O bond scission, which gets incorporated in the main chain during degradation. Studies on oxidative degradation in the presence of several metal salicylates, especially iron salicylate have shown no change in *E* value, suggesting that the metal ions do not interact during the initiation step. However, there is sensitization of degradation of poly(styrene peroxide), where O-O bond intentionally incorporated in the backbone follows a different order (Fe > Co > Ni > Mn) compared to the oxidative degradation of PS: (Ni > Co > Mn > Fe). This opposing trend once again reaffirms that metal ions do not interact in the initiation step. Kishore, *et al.*[470] have shown that the metal ions affect the propagation step.

The mechanism of action of catalysts on the decomposition and combustion of CSP is not clearly understood. However, it is believed that the reaction between NH_3 and $HClO_4$ (initial dissociation products of AP) and between $HClO_4$ and fuel enhances heat release on the catalyst surface[460,471]. Consequently, the activation energy of the primary flame reaction decreases, and as a result $\dot{r}$ value increases[472].

Attempts have also been made to ascertain whether the catalysts act in the condensed phase or the gas phase; yet there has been no definitive study on the regime of catalyst action during propellant combustion. Caveny and Pittman[186] have shown that at higher pressures, the subsurface temperature is large enough, so that the transient reactions occurring in it have no contribution to the $\dot{r}$ of the propellant. However, Pearson[473], considering the concept of melt layer on the surface, believes the catalyst to be operative in the heterogeneous surface region. Doping and coating of AP with the catalyst have been found to be less effective in altering the burning behaviour of CSP; gas phase decomposition mechanism is considered to be important. Nadaud[474], on the basis of the results of AP/polybutadiene sandwich experiments, concluded that the catalysts do not operate in the condensed phase, but probably act in the gas phase increasing the reaction rate of $HClO_4$ and its initial decomposition products. According to Zhang[475], the catalysts increase the heat of condensed phase reactions and raise the $\dot{r}$ of the propellant. Although several studies regarding the role of catalysts have been reported, unfortunately no clear-cut knowledge on the site of catalyst action in CSP combustion is available at present. Variable surface and subsurface heat release have been incorporated into BDP model to explain the catalytic effect[476].

It may be worthwhile to examine the effect of additives on CSP in the light of their action on the combustion of the polymer and AP. Fe_2O_3 accelerates the deflagration of AP, besides augmenting its decomposition and the overall effect of Fe_2O_3 in CSP is its enhancement in the value of $\dot{r}$[71]. Fe_2O_3, however, decelerates combustion of the binder[150]. This shows that the effect of the catalyst of the combustion of AP is dominant over its effect on combustion of the binder. Interestingly, ammonium phosphate, unlike Fe_2O_3, lowers the $\dot{r}$ of both polymer and AP, besides decelerating the decomposition of AP. The effects of catalysts and inhibitors can be examined more quantitatively from Table 5.1. Fe_2O_3 clearly shows that the effect of the catalyst on the deflagration of AP is predominant and is reflected in the propellant. Fe_2O_3 is more effective in augmenting $\dot{r}$ than Fe_3O_4[479]; it also brings about plateau and mesa burning characteristics. Such an effect of Fe_2O_3 on pressure sensitivity indicates that condensed phase chemistry plays an important role in the mechanism of catalysis[480]. The shape of Fe_2O_3 particle also affects the $\dot{r}$ of the propellant. Among spheroidal and acicular particles, the latter show higher $\dot{r}$ of the propellant[479]. The opposite effect of Fe_2O_3 on binder combustion in altering the overall combustion of CSP is very little. In short, it could be said that the effect of the catalyst on the deflagration of AP, which is present in larger proportions in CSP, overshadows the effect of the same catalyst on the binder in the combustion of the propellant.

Table 5.1. Effect of catalyst/inhibitor on $\dot{r}$ value of AP/PS CSP

Catalyst/Inhibitor	*wt.%*	*% change in $\dot{r}$*			*Ref.*
		AP	*PS*	*AP/PS*	
Fe_2O_3	1	+68	-9.4	+64.0	21,450,456
$(NH_4)_2HPO_4$	1/4	-72*	-20.0	-15.0	21,265,477
NH_4Cl	1/3	-70*	+4.0	-5.0	177,265,478
NH_4Br	1/5	-47*	+14.0	-3.4	177,265,478

\+ Increase
\- Decrease
* % change in $\dot{r}$ was calculated on the basis of effectiveness of the inhibitor and the burning rate law constants[265]

Examining the effect of inhibitors (e.g. ammonium salts), it may be observed in a qualitative fashion that the decrease in the $\dot{r}$ of AP too is reflected in the propellant. The extent to which one would have expected retardation in the combustion of the propellant is, however, far too low. This goes to show that the influence of the inhibitor on combustion of the binder is significantly involved.

Unlike the less reactive Fe_2O_3, which augments $\dot{r}$ by a physical electron transfer process in the decomposition of AP, ammonium salts decompose to give acids which may react with the binder and change the decomposition or combustion behaviour significantly. Whereas HCl and HBr basically desensitize polymer combustion by the gas phase mechanism[476], H_3PO_4 produces significant quantity of char in the condensed phase and acts as a barrier for the transfer of heat from the flame to the virgin polymer[478]. The pronounced effect of ammonium phosphate among the ammonium salts may perhaps be due to significant char formation[481], which once again sufficiently demonstrates the importance of condensed phase reactions. $SrCO_3$, $LiCO_3$, $BaCO_3$, LiF, oxamide and catocene reduce $\dot{r}$ of the of AP-HTPB propellant[481-484]. Oxamide was found to suppress pressure oscillations at the end of combustion[483]. $CaCO_3$ enhances the combustion of AP at low pressures (< 1.96 MP_a) and depresses the same at pressures above it (> 1.96 MP_a). $CaCO_3$ reacts with AP to produce $CaCl_2$ and promotes the melting of AP on the burning surface. The concentration of $CaCl_2$ on the quenched surface is increased with increase in pressure[485].

It may, therefore, be concluded that the effects of catalysts/ inhibitors may not follow any definitive mechanism and hence a generalized picture cannot be given for their action. Each case, perhaps, has to be examined on its own merit.

5.4.1 Effect of TMO

The effect of TMO on the decomposition or combustion of CSP has been reviewed by Kishore, *et al*[71]. Based on the linear dependence of increase in $\dot{r}$ on the redox potential of metal oxide and the associated heat of reaction, an electron transfer process is found to promote the thermal decomposition and $\dot{r}$ value, besides lowering[486] the pressure exponent.

TMO is also known to act via the formation of thermally stable metal perchlorate amines[456]. The relative effectiveness in enhancing the $\dot{r}$ in TMO follows the order:

$Ni_2O_3 \sim Fe_2O_3 > Co_2O_3 > MnO_2$

It is observed that Ni_2O_3 is as effective as Fe_2O_3. However, recently Cr_2O_3 has been reported to be more effective than Fe_2O_3 in the primary propellant flame with low value for the pressure exponent, which decreases with increase in Al content[487]. In another study, the $\dot{r}$ of HTPB-AP propellant was found to decrease in the order[488]:

$CuO > Fe_2O_3 > CrO_3 > C_2O_5 > TiO_2$

Calcining of CrO_3 and CuO at high temperture increases their catalytic action on the deflagration of AP[434]. Calcining of Fe_2O_3 at higher temperatures has negligible effect on its catalytic properties[437].

Kuratani[431] found no correlation between $\dot{r}$ and thermal decomposition and suggests that gas phase processes are important in catalytic control of $\dot{r}$. The results of Hermoni and Salmon[489] indicate that the catalysts influence the reaction in both solid and gas phases. No definitive evidence about the site of catalyst action is as yet available.

5.4.2 Effect of Copper Chromite and Copper Chromate

Copper chromite (CC) and copper chromate are excellent catalysts for increasing the $\dot{r}$ of CSP[5,423,490-492]. The effect of CC and copper chromate was studied by Pearson[493]; he has suggested a electron transfer process. CC alters the low temperature decomposition of AP and its catalytic activity is destroyed since it is oxidized to chromate by the products of decomposition of catalysed AP. The products of decomposition of catalysed AP have been found[494] to be different from those obtained on decomposition of neat AP in several ways. It is envisaged that the enhancement of $\dot{r}$ is due to an exothermic redox cycle between cupric oxide/ cuprous oxide/Cu formed at high temperatures at the burning surface of the propellant. However, the exact route by which these catalysts act is not clear. The dual role of these catalysts in accelerating the decomposition of AP and promoting oxidation of the fuel by heterogeneous reaction in the condensed phase has been considered[462,492]. However, investigations of Jones and Strahle[495] have indicated that CC possibly promotes the gas phase reactions.

5.4.3 Effect of Iron Oxide

Fe_2O_3 is the most widely used catalyst in practical applications of CSP[230]. Burnside[417] found that $\dot{r}$ of the propellant depends on catalyst concentration, particle size and surface area. In AP-HTPB-Al propellant, the values of $\dot{r}$ and pressure exponent were found to increase with Fe_2O_3 content. The catalytic activity of Fe_2O_3 was found to be dependent on its particle size and surface area[496]. In AP/HTPB sandwich system[492,497], Fe_2O_3 has been found to catalyze the gas phase reaction and consequently increase the heat release rate at the interface between the oxidizer and the binder undergoing heterogeneous reactions. Significant aggregation of FeO and Fe_3O_4-

Fe_2O_3 solid solution, on the burning surface, has been observed[498]. Since the catalyst will have to mix with the propellant in the melt layer than in the subsurface solid, catalyst action is believed to be at the surface layer[335]. However, Powling and Smith[499] observed that the Fe_2O_3 does not alter the T_s of the propellant and, therefore, they put forth the opinion that it does not accumulate on the burning surface. Wang, *et al.*[500] found that Fe_2O_3 increases $\dot{r}$ and the total heat release while decreasing T_s. Bobolev, *et al.*[501] concluded that Fe_2O_3 influences both the condensed and gas phase reactions. There has been no definite study on the regime of catalyst action so far.

5.5 FERROCENE AND ITS DERIVATIVES

Most of the catalysts discussed so far and which are in use are in the solid form. They have certain disadvantages such as their large particle size, surface area, etc. and they introduce a certain degree of inhomogeneity and thus alter the effective catalyst concentration leading to erratic burning of the propellant[502]. According to Wang, *et al.*[503], migration is an important factor affecting the $\dot{r}$ value more than volatility in terms of catalytic activity. The most widely used catalyst, Fe_2O_3, for example, is migration resistant, but is known to build viscosity during processing[504,505]. In order to overcome some of these disadvantages, considerable research is being done on iron-containing compounds.

Ferrocene is used as an additive for modifying the $\dot{r}$ of AP[506] or CSP[420,421]. During combustion, ferrocene decomposes to hydrocarbons and Fe gets oxidized to Fe_2O_3, releasing substantial amount of energy. Besides being a good energy supplier, ferrocene functions as an effective catalyst in enhancing $\dot{r}$, because Fe_2O_3 formed *in situ* is of finer particle size than that obtainable by mechanical grinding. Besides the use of ferrocene, much of the current work is being directed towards the synthesis of ferrocenyl-substituted compounds[507], which may be binder soluble, or may exist as liquids or binder-cum-catalysts (Table 5.2) possessing specific functional groups. These catalysts with different groups impart improved processability (without adversely affecting the slurry viscosity[534]) and offer a multifunctional role as burning rate modifiers, curing agents, bonding agents, etc., which ferrocene alone cannot afford. However, not much mechanistic information is available on these aspects, as most investigations are patented.

Table 5.2. Ferrocene derivatives/binder-ferrocene catalysts used in CSP

System	*State*	*Advantages*	*Ref*
Ferrocene	S	$\dot{r}$ modifier	420
4,4-diferrocenyl-1-pentanol	S	$\dot{r}$ modifier	502
1,1'-(1,1-)ferrocenedyldiethylidene) tris(thiocarbonahyrdide)	S	$\dot{r}$ modifier	508
1,1'-diacetylferrocene disemicarbazone	S	$\dot{r}$ modifier	508
1,1'-diacetylferrocene benzoylhydrazone	S	bonding agent	508
1,1'-diacetylferocene-p-nitrobenzoylhydrazone	S	$\dot{r}$ modifier	508
1,1'-bis (trimethylsiloxymethyl) ferrocene	S	$\dot{r}$ modifier bonding agent, energy supplier	509
Triferrocenyl methyl perchlorate	S	improved processability and mechanical strength	510
Cyclopentadienyl [2-(1-hydroxyethyl) cyclopentadienyl] iron	S	compatible	511
Vinyl magnesium chloride : diacetylferrocene adduct	S	curable and co-curable	512
1-pyrrolidinyl methyl ferrocene	S	$\dot{r}$ modifier, processing and bonding agent ; better mechanical properties	513 514
1,1'-carbonyl bis ferrocene	S	$\dot{r}$ modifier, stable burning	515
Diferrocenyl piperazine	S	AP coatable $\dot{r}$ modifier	516
2-ferrocenyl tetrahyrofuran	—	$\dot{r}$ modifier	517
2-ferrocenyl-2-(3-hydroxypropyl) tetrahydrofuran	—	$\dot{r}$ modifier	518

Contd...

System	*State*	*Advantages*	*Ref*
1,1'-bis(glycidoxymethyl) ferrocene	L	$\dot{r}$ modifier, curing agent, bonding agent	519
Epoxy ethyl ferrocene	L	$\dot{r}$ modifier, curing agent	520
n-butylferrocene	L	$\dot{r}$ modifier	505
Dimethylferrocene	L	accelarates thermal decomposition	521
Dibutyl ferrocene	L	accelarates thermal decomposition	522
,3-diferrocenyl-1-butene	L	reduces activation energy, decreases pot life, volatile; so not superior	523
2,2-diethyl ferrocenyl propane (Catocene)	L	$\dot{r}$ modifier	504
,1'-bis(1-glycidoxy alkyl) errocene	L	$\dot{r}$ modifier, curing agent, bonding agent, crosslinking agent, plasticizer	524
Vinyl-ferrocene-butadiene opolymer	P	AP coatable $\dot{r}$ 20% higher than butadiene binder	525 526
Butadiene-ferrocenyl methyl methacrylate copolymer	P	$\dot{r}$ 20% higher than butadiene binder	527
entaerythritol methacrylate diferrocenoate-Butadiene opolymer	P	no processing and storage problems	528 529
errocenyl methyl acrylate - HTPB copolymer	P	$\dot{r}$ modifier, plasticizer	530
erroceny; methyl acrylate - HTPB copolymer	P	$\dot{r}$ modifier, binder catalyst	531 532
-ferrocenylethanethiol-HTPB	P	$\dot{r}$ modifier, stable burning binder-catalyst.	533

ote: S= Solid; L= Liquid; P= Polymer.

Kishore, *et al*[508,509,519] synthesized certain ferrocene-based derivatives and silicon-containing compounds which possess promising performance characteristics (Table 5.2). Some of these compounds, which may be solids or liquids, function as curing agents, bonding agents, burning rate modifiers, etc. For example, 1,1-bis(glycidoxymethyl)ferrocene, besides being a burning rate modifier and bonding agent, also serves as a curing agents[510]. 1,1'-bis(trimethyl siloxymethyl) ferrocene performs as a bonding agent and energy supplier. The bonding of this molecule with both AP and HTPB is shown (Fig. 5.3) to be at the silicon centre by both solubility measurements and IR peak shifts. Because of the presence of silicon, this compound also acts as a very good energy supplier and burning rate modifier[509]. 1,1'(1,1'-ferrocenedyldiethylidene) bis-(thiocarbonohydrazide); 1,1-diacetyl-ferrocene disemicarbazone; 1,1'-diacetyl ferrocene benzoyl hydrazone and 1,1'-diacetylferrocene-p-nitrobe-nzoyl hydrazone, synthesised in this laboratory, are solids and are binder soluble. Besides, they are good bonding agents too[508]. The bonding ability is also seen in the SEM photomicrographs[534]. To further examine the bonding ability, UV experiments were performed on the solution in which a pellet of AP and the bonding agent dissolve increasingly with time. A definite quantity of the solution was

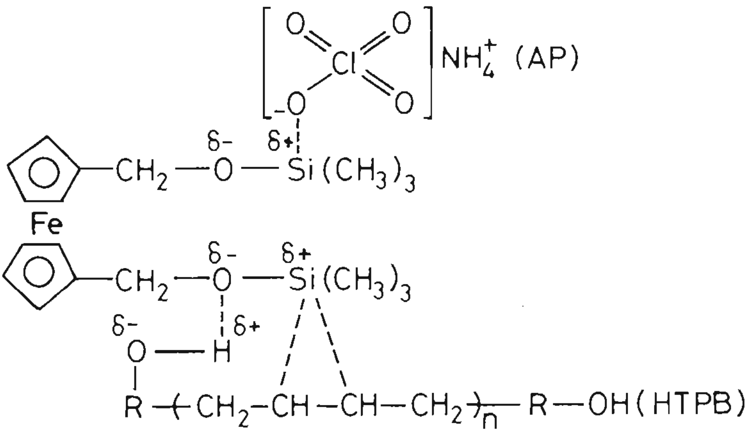

Figure 5.3. Bonding sites of 1,1'-bis(trimethyl siloxymethyl) ferrocene with AP and HTPB[509].

withdrawn and absorbance recorded. The first order rate constant for the dissolution of bonding agent into acetone was obtained from the optical density *vs* time plot, which is a direct measure of the bonding ability of the compound with AP. The lower the rate constant, greater is the bonding. The plot of optical density as a function of time at different temperatures gives a straight line, from the slope of which the rate constant (k) is obtained. The Arrhenius log k *vs* 1/T plot yielded an activation energy value of 10.5 kcal/mole, which corresponds to the energy required to break ion-dipole interactions, suggesting that bonding agent-AP interactions are of the ion-dipole type. The bonding agent containing the polar sulfone group yielded higher rate constants[534].

Liquid ferrocene derivatives, such as 2,2-bis (ethyl ferrocenyl) propane (catocene)[504], butylferrocene[521] and 1,3-diferrocenyl-1-butene[522], are finding use in solid propellants[533,535]. Catocene is hazardous if it becomes volatile at the mixing temperature[517,535], Liquid ferrocene compounds, such as butyl ferrocene, dimethyl ferrocene and dibutyl ferrocene[521,522] are as effective as Fe_2O_3, but act through a different mechanism. Whereas ferrocene compounds reduce the activation energy for decomposition of CSP, Fe_2O_3 lowers the decomposition temperature.

The location of catalytic site during actual combustion is a matter of interest, but it is difficult to locate it, because the rate controlling combustion zone at the surface is very thin involving both condensed and gas phase regimes with a large thermal gradient across them. Pittman[419] attempted to locate the site of catalyst action in propellant-containing n-butyl ferrocene. It was found to be an effective catalyst when AP loading in the propellant was high. Decomposition of the binder, in fact, is not enhanced by n-butylferrocene or Fe_2O_3. Experiments have been carried out to ascertain whether catalyzed subsurface reactions control $\dot{r}$, CSP-containing AP coprecipitated with ferrocene salts burnt slightly faster than the propellants containing binder with ferrocene salt. The marginal increase was not suggestive of any subsurface decomposition of AP and AP-binder reactions. In order to assess whether these reactions really occurred, AP was coated with ferrocenyl ethylamine liquid catalyst. It was found that the close AP-catalyst and also AP-catalyst-binder contact did not show any increased catalytic effect in enhancing $\dot{r}$. Yet, in another experiment, AP encapsulated with a fluoropolymer was used in the propellant-containing binder mixed with n-butylferrocene or Fe_2O_3. Despite the loss of AP-catalyst contact due to encapsulation, enhanced $\dot{r}$ was observed. The above results suggest the importance of gas phase reactions for catalytic activity. It is supported by the action of the ferrocene catalyst on $HClO_4$ or its decomposition products in the gas phase. This is further confirmed by studying $\dot{r}$ of the propellant containing tetramethyl ammonium perchlorate oxidizer and n-butylferrocene catalyst. This oxidizer does not form $HClO_4$ like in AP, since no proton transfer occurs and the propellant fails to show large enhancement in $\dot{r}$ in the presence of the catalyst. It may then be concluded that n-butylferrocene catalyst acts in the gas phase. However, there are other views proposing their action in the condensed phase as well. Ferrocene and n-butylferrocene are found to accelerate the thermal decomposition of AP and the products of catalyst decomposition remaining in the condensed phase display catalytic activity; n-butyl ferrocene is particularly found to contribute to the condensed phase reactions in propellant combustion[522]. The heat generated in the solid phase decomposition is implicit in the temperature distribution measurements and photomicrograph study by Kuwahara[535]. Thus, one cannot provide generalized information regarding the site of action of n-butyl ferrocene.

To test the hypothesis whether a catalyst becomes more effective with increasing fluidity, Pittman[419] prepared polyamide, polyesters containing ferrocene and copolymers of vinyl ferrocene and butadiene. These polymers were incorporated into the propellant and $\dot{r}$ values measured. It was observed that the polymeric catalysts became increasingly more effective than their monomeric counterparts, as they become more fluidic. Several polymeric ferrocene catalysts have been reported (Table 5.2). They have a multifunctional role and are good processing aids apart from being good $\dot{r}$ modifiers. Polymeric catalysts have the added advantages of migration resistance, low volatility and reduced crystallization tendency at low temperatures normally encountered in the usual low molecular weight liquid catalysts[529].

5.5.1 Prognosticative Capability of Ferrocene Catalysts

Although ferrocene-based catalysts are known to influence the $\dot{r}$ of AP, the influence of structural features of small amounts of ferrocene-based catalysts on $\dot{r}$ and their prognosticative capability are hitherto unknown. A unique approach of estimating the contribution of groups in the catalysts towards the $\dot{r}$ of catalyzed AP/HTPB in stoichiometric amounts has been attempted[536]. The structure of ferrocene-based catalysts used in the propellant are given in Fig. 5.4; catalyst (DNPHAP) concentration at which $\dot{r}$ is optimum has been found to be 4.8 x 10^{-4} mole % of the propellant. For the same molar concentration of all other catalysts containing different groups, $\dot{r}$ and ΔH_c values (Table 5.3) were determined; these showed significant effect of structure of the catalyst.

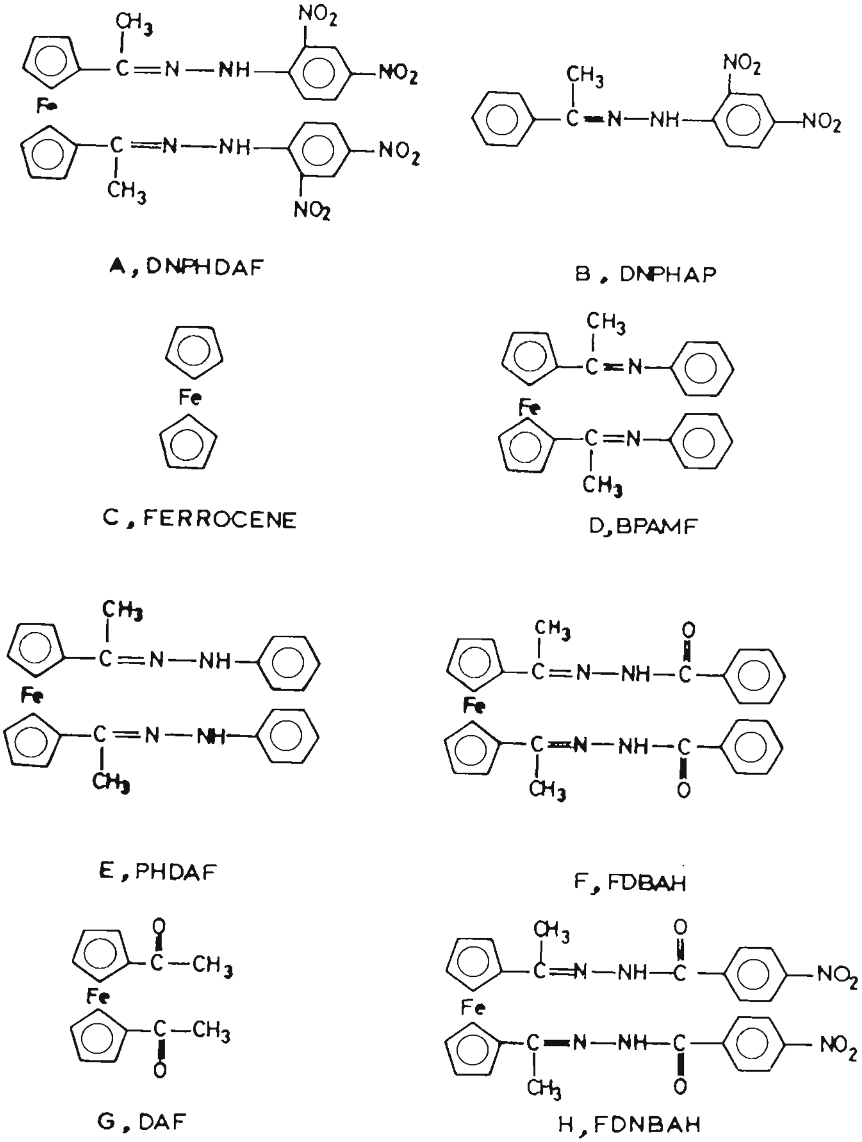

A, DNPHDAF

B, DNPHAP

C, FERROCENE

D, BPAMF

E, PHDAF

F, FDBAH

G, DAF

H, FDNBAH

Figure 5.4. Structure of ferrocene derivatives[534,536].

Table 5.3. Group contribution of ferrocene catalysts towards $\dot{r}$ and ΔH_c values of AP/HTPB propellants

System	$\dot{r}$ *(cm/s)*	ΔH_c *(cal/g)*	*Groups*	*Derivation 1of groups values*	*% contribution per group*	
					$\dot{r}$	ΔH_c
nil	0.120±0.02 (a)	1478.0±7.0	-	-	-	-
A	0.159±0.001(b)	1554.0±6.0	F_c	C	+25.8	+7.24
B	0.130±0.01 (c)	1495.0±7.0		|B-|A-C/2||	+5.0	+2.20
C	0.151±0.01	1585.0±5.0	$-NO_2$	(A-E)/4	+.10	+1.70
D	0.151±0.001 (d)	1471.0±7.0	-NH	[[F-D]/2]	+0.7	-0.55
E	0.153±0.001 (e)	1455.0±7.0	$-CH_3$	[(G-C)/2]-g	-0.5	-
F	0.130±0.002 (f)		-C=N-	|(D-C)/2]-b	-5.0	-9.40
G	0.127±0.002 (g)		>C=O	[[F-E)/2]	-7.5	-
H	0.133±0.001					

F_c : Ferrocene group; AP: HTPB ratio, 87.13 by wt; catalyst concentration, 4.8 x 10^{-4} mol/ 100 g of CSP

By various permutations and combinations, the contributions of various groups in the catalyst structure towards $\dot{r}$ (Table 5.3) were determined. Ferrocene and aromatic groups increase the $\dot{r}$ significantly, while C=N- and C=O groups reduce it. Other groups have only marginal effect on $\dot{r}$ Based on these group values, the calculated increase (14%) in $\dot{r}$ for a test ferrocene compound used as catalyst (FDNBAH) was in fair agreement with the experimentally observed value (11%).

Further, ΔH_c values have been used to understand the catalyst behaviour during combustion of the propellant. DNPHDAF, DNPHAP and ferrocene increase ΔH_c value, while BPAMF and PHDAF decrease the same. This suggests that the ferrocene moiety is not the sole contributing factor for altering ΔH_c. The positive and negative contributions (Table 5.3) impart opposing effects in ΔH_c contributions. The groups which have fuel oxidizing capability (e.g. $-NO_2$) or those themselves getting oxidized energetically, have a positive contribution. The groups which undergo bond breakage process, understandably show a negative contribution; the high negative contribution of C=N- group is suggestive of the fact that this group is more stable compared to others. This has been verified mass-spectrometrically in a typical ferrocene free compound (DNPHAP), which reveals the formation of relatively intense peaks at m/z 103 and m/z 118 corresponding to benzonitrile and its precursor containing the nitrile group, respectively. These species are comparatively stable and conform to higher negative group contribution assigned to (C=N-) towards ΔH_c and $\dot{r}$. The groups identified in the catalyst for contribution estimation have some sort of bearing on the pyrolyzed fragments from the catalyst which puts this approach on realistic footing. This study also suggests that ferrocene-based burning rate catalysts should be with more of nitro, phenyl and imino groups, which enhance the energetics of CSP and should be without nitrile or other groups which are precursors of nitrile. However, the uniqueness of this approach has to be ascertained by working out the structural contributions in more number of ferrocene derivatives.

Thus, the group contribution approach seems to be a powerful tool in predicting the $\dot{r}$ of a propellant based on the structural features of a catalyst. It also helps in the identification of energetic sites and in obtaining mechanistic information of the catalyst action. This method will also evoke considerable interest in the field of combustion, paving a novel way in creative designing of potential catalysts showing anticipated performance.

CHAPTER 6

AGEING OF COMPOSITE SOLID PROPELLANTS

6.1 AN OVERVIEW

The safe storage life of CSP is the period over which a propellant can be stored without undue hazard, such as autoignition, and the useful life is the duration in which it meets all the desired ballistic and mechanical requirements[537]. During storage there may be migration of ingredients, evaporation of plasticizer and gas evolution, resulting in the weight loss, dimensional changes, discoloration etc[538]. The ingredients may interact with one another or with the surrounding atmosphere and cause irreversible changes in the calorimetric value, $\dot{r}$ and the mechanical properties, like, for example changes in the modulus of the propellants leading to case-bond separation, formation of cracks, voids, etc[539]. Such deterioration in the characteristics of the propellant determines the useful shelf-life period and storage temperature limits.

To assess the changes undergone due to ageing during storage, two types of studies are carried out: normal ageing and accelerated ageing. In real time normal ageing studies, the performance parameters during actual prolonged storage are monitored, but this takes a very long time. Accelerated ageing studies are preferred, since they take much short times. In fact, good correlations have been obtained by extrapolating long time mechanical properties of propellants starting from accelerated tests[540]. In this type of study, the samples are maintained at elevated temperatures (30 °C-150 °C) and studied at fixed time intervals with respect to their mechanical properties, $\dot{r}$ dimensional changes, etc. and the results are extrapolated to normal conditions to assess their performance[537,541]. This procedure, however, presupposes that the changes in material properties are caused by a single reaction or multiple chemical reactions, and that the rate-controlling step depends on the frequency of collision of reactive species, the temperature dependence is studied using Arrhenius equation. Very few studies on the ageing of CSP have been reported[541-548].

6.2 CHANGES IN WEIGHT LOSS

Schedelbauer[541] carried out accelerated ageing studies on PU and CTPB based propellants and found that the weight loss was more when the extent of crosslinking in the propellant was more. He ascribed this to the evaporation of solvents from the binder, moisture from AP, decarboxylation of CTPB to produce carbon dioxide and evaporation of the residual compounds at elevated storage temperatures. Korobienichev, *et al.*[549] also observed that first the binder degrades; they attributed weight loss to the loss of binder. Nagamoto[543] observed that PBD/PU binder, when aged under identical conditions, looses weight to the same extent as the corresponding propellant. Change in the calorimetric value (6.5-7.0%) of CTPB/AP propellant has been attributed to the weight loss of the binder[62].

6.3 CHANGES IN MECHANICAL PROPERTIES

Deterioration in the mechanical properties is caused by some chemical reactions. Therefore, knowledge of ageing chemistry is a pre-requisite to understanding the ageing behaviour and is essential for the development of a proper ageing model that fits the measured short time ageing data and predicts the direction of ageing in future recourse.

The effect of ageing on the mechanical properties of CSP was studied by Suzuki, *et al*[541] in dry N_2 atmosphere, dry air and under humid conditions. No change in mechanical properties was observed in N_2 or in dry air, whereas at higher humidity, increase in elongation and decrease in tensile strength were observed, these changes were restored on drying. In CTPB and PU-based CSP's, long term ageing studies[544] (2 yrs, -30 to + 80 ^{0}C) have indicated changes in tensile strength, modulus of elasticity, etc. The mechanical properties have been found to depend on hardener/ binder ratio. Due to shrinkage during storage, density also increases. However, CTPB propellants have better storage stability compared to PU propellants. The mechanical properties of CTPB-AP propellant deteriorate during ageing, CTPB degrades via the decomposition of the carboxyl group with an activation energy of 19.5 kcal/mol[550].

Decrease in compression strength as a function of storage time and temperature has been attributed to polymer ageing[551,552].

revealed that there is a correlation between the changes in U_c and *TD* rate (Fig. 6.1). The activation energy values for the changes in *TD* rate, $\dot{r}$ and U_c of different CSP's have been found to be the same (13$\pm$2 kcal/mole), suggesting that the rate-controlling step for all the changes is the same. Since the rate-controlling step for the change in $\dot{r}$ has been found to be the *TD* of the propellant, it implies that the *TD* rate also controls the change in U_c.

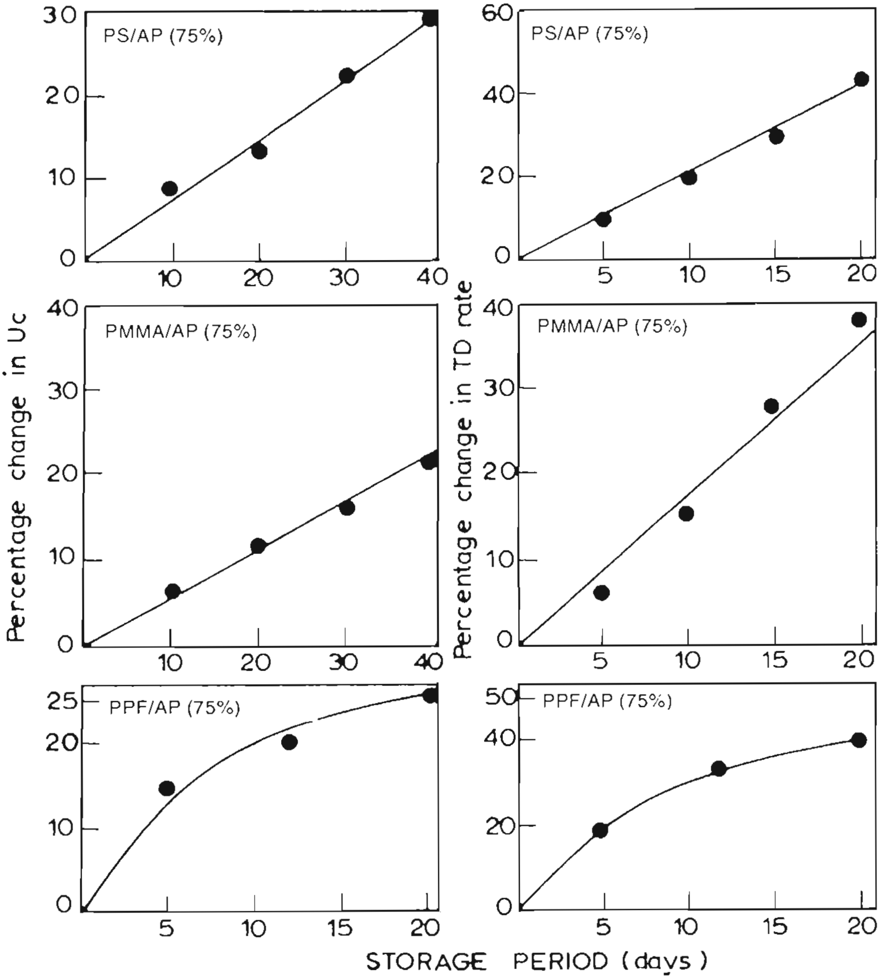

Figure 6.1. **Plots of changes in U_c and TD rate as a function of storage period for different propellant systems aged at 100 °C[179].**

6.4 Ignition Temperature of the Binder and CSP

Depending upon the sample size and heating rate, the propellant ignites after the phase transition temperature of AP. The ignition temperature can, therefore, be used as a parameter to compare the stability of the propellants during ageing[554].

Interestingly, ignition temperature of CTPB increases with storage time, while a reverse trend is observed[59] for the corresponding propellant. Hence, the rate controlling mechanism in the binder and the propellant are different during ageing. This is explained[62] in terms of gasification rate of the products of polymer degradation. Generally, polymers having a higher gasification rate ignite with ease while higher degree of crosslinking leads to a lower rate of gasification and eventually to longer ignition delays. Dynamic TG measurements of aged (20 days) and unaged binder samples have shown that the degradation rate is faster for the unaged binder compared to the aged samples. Thus, desensitization in the ignition temperature of the binder samples occurs during ageing.

Milena[555] has reported that the calorimetric value of aged (1-6 months at 65 -100 °C) propellant does not change. However, it has been found in this laboratory[62] that the calorimetric value (Table 6.1) decreases with ageing and has a direct bearing on our earlier finding[59] that the ignition temprature decreases during ageing. As a result of additional crosslinks at the double bonds, the propellant matrix becomes rigid and the escape of decomposition products of AP/binder is prevented, leading to their exothermic reaction inside the matrix. This condensed phase heat release in the matrix lowers the ignition temperature on ageing. Since the extent of crosslinking increases, consequently the ignition temperature decreases with ageing.

Table 6.1. Effect of ageing on calorimetric values

Temperature (°C)	*Cal. value (cal g⁻¹)*		
	CTPB/AP		*CTPB/AP/Al*
	20 days	*60 days*	*20 days*
Unaged	1010	1010	1365
60	1009	991	1360
70	995	980	1351
80	942	936	1304
100	935	936	1242

6.5 CHANGES IN THERMAL DECOMPOSITION RATE & BURNING RATE

Due to ageing, $\dot{r}$ increases and decomposition temperature of the propellant decreases[556]. Studies on TD rate of aged propellant samples below and above the phase transition temperature of AP have revealed that at 230 °C, $\dot{r}$ is proportional to TD rate while at 260 °C, it is inversely proportional to the TD rate, suggesting that the change in $\dot{r}$ is primarily caused by thermal decomposition of AP. Since ageing takes place in the orthorhombic region, the change in $\dot{r}$ during ageing is governed by the thermal decomposition of the orthorhombic AP[176]. Studies[61,177,178,556,557] have also been made on propellants containing different binder systems. Generally, $\dot{r}$ increases linearly with the storage period at all temperatures. This is explained on the basis of change in porosity and slow decomposition of the propellant.

6.6 MECHANISM OF AGEING

It is necessary to know the mechanism of ageing to increase the longevity of the propellant. By measuring dynamical mechanical properties as a function of ageing time and temperature, the following mechanism has been proposed[558]:

Below 40 °C → Slow physical processes result in slow ageing
40-65 °C → Volatilization of the plasticizer
> 65 °C → Chemical degradation of the propellant

The ageing mechanism of polybutadiene binder involves atmospheric oxidation.[559]

In CTPB propellants, ageing is explained in terms of gel content, crosslink density, ignition temperature and penetration temperature[59]. The gel content initially increases exponentially and remains constant after about 100 h, ensuring complete curing. The trend is the same in the case of the binder and the propellant (Fig. 6.2), suggesting that the curing process remains unaltered in the presence of AP and does not contribute to ageing. Beyond 100 °C-160 °C, the additional increase in the gel content during ageing is attributed to further crosslinking at the double bonds; this is in accordance with the findings of Layton[560] Since there is an increase of 14% in the crosslink density of neat binder and 20% in the case of the propellant, the mechanism of crosslinking must be different in the binder and CSP. It has been shown[57,561] in our laboratory that a free-radical crosslinking mechanism is possible in the case of neat binder and that ageing of a CSP is through a proton transfer process catalyzed by AP. Actually, $HClO_4$ formed as a result of interaction of AP with moisture[544], acts as a crosslinking agent. This is visualized as follows:

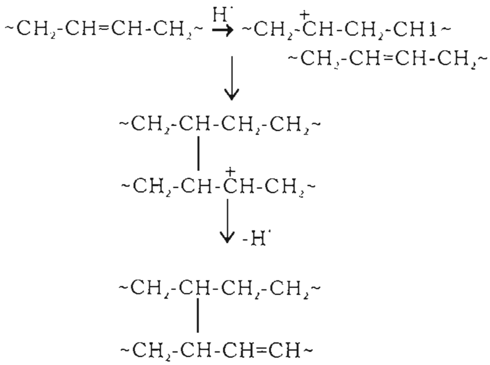

Since crosslinking occurs through the double bonds in the main chain, it leads to increase in the amount of gel. The *E* for the proton transfer process (~13 kcal/mole)[57] is much lower than that anticipated for a thermally initiated free-radical process. Crosslinking hardens the propellant during ageing; the extent of crosslinking in the polymer (crosslink density), determined by DMA and TMA, increases continuously during ageing. A marginal increase in the gel content and a drastic increase in the penetration temperature suggest that increase in the crosslink density need not necessarily increase the gel content, particularly when all the end groups are crosslinked and further crosslinking is only through the double bonds within the crosslinked network. The above facts support the occurrence of thermal crosslinking in CTPB during ageing, while a free-radical process had been proposed earlier[562]. Thermal crosslinking occurs through the double bond and an activation energy of 23 kcal/mole corresponds to opening of the double bond. This energy is approximately equal to the loss of one pi-bond, giving rise to two sigma-bonds[563,564]. Changes in the chemical structure during ageing of CTPB, HTPB and PBAN have been correlated with changes in their mechanical properties[548,559]. Although studies of cure reactions and ageing chemistry of CSP have enabled some understanding of the changes in mechanical properties of the propellant, detailed investigation is still warranted.

Safe-life of the propellant can be increased by removing the double bonds in the binder. OH-terminated cis-polyisoprene was hydrogenated to prepare hydrogenated-hydroxy terminated

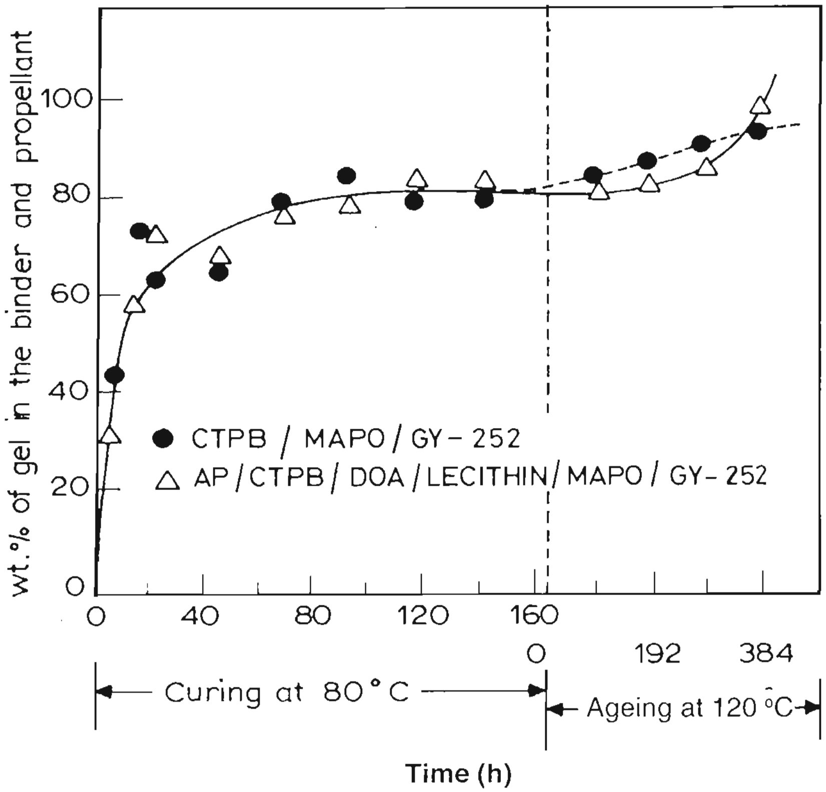

Figure 6.2. Variation in gel content with curing and ageing time[59].

polyisoprene (HHTPI) [(OH (--CH_2 CH $MeCH_2CH_2$ --$)_n$-OH] (mol-wt ~3000) which when used in propellants improves the long-term storage properties[565,566]. HHTPI propellants have poor ignitability, but similar $\dot{r}$. The ageing characteristics and thermal stability, however, are superior to those of HTPB[566].

Other chemical processes which cause ageing are photodegradation and thermal oxidative degradation[567]. Although not much information is available on the former, as regards the thermal oxidative degradation mechanism, ageing (air; 70 °C-130 °C) of model CSP based on PVC/AP plasticized with dibutyl phthalate (DBP) has been elucidated in terms of weight-loss measurements, $\dot{r}$, and calorimetric values[568]. In plasticized PVC, DBP starts oozing out (200 °C) along with the evolution of HCl (60 %) and this continues until carbonaceous residue is formed at 300 °C; the associated weight loss decreases gradually with ageing time and storage temperature.

Although $\dot{r}$ does not change significantly on ageing, isothermal decomposition rates of PVC/AP propellant decrease with ageing and this is reverse of what happens in the case of CTPB/AP propellants. Decrease in the TD rate of PVC/AP propellant is possible if exothermic condensed phase reactions between the decomposition products of the binder and the oxidizer in the porous matrix of the propellant are suppressed due to restricted gasification of the crosslinked binder. Crosslinking results on account of HCl elimination and subsequent unsaturation. Due to this, the calorific values of the binder of the aged propellant increase with ageing, because the resulting hydrocarbon $(-(CH=CH)_n-)$ structure functions as a better fuel than PVC itself. This has been verified by calculating the heats of combustion of PVC (4.2 kcal/g) based on data on heats of formation[339] and the hydrocarbon residue (10.2 kcal/g) on the basis of the following stoichiometry:

$$(\text{-CH}_2\text{-CHCl-})_n + (5/2)n\,O_2 \xrightarrow{298^\circ K} 2nCO_2 + nH_2O(g) + nHCl(g)$$

$$(\text{-CH=CH-})_n + (5/2)n\,O_2 \xrightarrow{298^\circ K} 2nCO_2 + nH_2O(g)$$

The ΔH_f^0 values for PVC (-2.40 kcal/mole repeat unit) and hydrocarbon polymer (+23.5 kcal/mole repeat unit) were calculated by group additivity method. Considering the difference in calorimetric value for oxidizer deficient (25/75 wt.%) and stoichiometric (10/90 wt.%) combustion of HTPB/AP which is 0.39 kcal/g[569], increase in the calorimetric value for PVC/DBP/AP (25/75 wt.%) propellant system was found to be 0.75-0.39 = 0.36 kcal/g of the propellant. Here, 0.75 kcal/g is the increase in the heat of combustion due to complete HCl elimination from the PVC/DBP/AP (1:1:6) propellant system based on stoichiometric combustion. This value agrees with the experimentally observed calorimetric value (0.34 kcal/g) for the complete elimination of HCl during ageing, as explained on the basis of the above mechanism.

The fact that the ageing characteristics are related to the thermal stability of the oxidizer and not of the binder is evidenced by peroxide formation due to the decomposition of AP in aged (100 °C; 25days) PS/AP propellant. Such peroxide formation is not observed in unaged samples and in dummy NaCl/PS propellants[556]. Also, changes in thermal decomposition rate and $\dot{r}$ were similar for samples aged in air, N_2 and vacuum, indicating that the ageing process depends only on the oxidizer in CSP. Easily decomposable ammonium salts increased the stability of the propellants[176] by desensitizing the thermal decomposition[214,230,570] and deflagration rate of AP[262]. This is further supported by the identical E values for the decomposition of the propellant and the oxidizer in the temperature range 200-300 °C. Below 200 °C, the E value (13-20 kcal/mole) for AP decomposition corresponds to the proton transfer process[571]. TD studies of AP[249] were carried out for orthorhombic AP partially decomposed isothermally to various extents; it contains significant amounts of HCl and HNO_3. A similar observation was made at 285 °C in propellant samples previously partially decomposed at 230 °C. Variation in the concentration of $[H^+]$ in AP as well as the propellant follows the same trend for decomposition at 230 °C and 150 °C. It appears that reactive intermediates like $[H^+]$ resulting from decomposition of AP influence ageing of the propellant more than the reactive intermediate species like polyperoxides obtained on decomposition of the binder. From the above facts it may be inferred that ageing in CSP is primarily governed by the decomposition of AP.

6.7 KINETICS OF AGEING PROCESS

It is surprising that not much attention has been paid in the past to gaining an understanding of the kinetics of the ageing process. Layton[548,560] suggested the following equation, which is applicable to CTPB and HTPB propellants for all ageing conditions:

$$P = k\,(\log t) + (bt^n) + P_o \qquad (67)$$

where P is the mechanical property at some ageing time, t and P_0 is the initial value of the property; k is a constant at temperature, T, b and n are dependent on the chemical nature of the propellant.

Change in the mechanical properties (P), followed in terms of gel formation, depends on the ageing time according to the equation

$$P = k \log t + C \qquad (68)$$

where C is a constant representing the value of the mechanical property at the beginning of ageing, and k is rate constant for the gel formation.

It has been shown[60] that change in $\dot{r}$ follows a zero order kinetic law according to the equation:

$$P = k(T)\,P\,Ct + P_o \qquad (69)$$

where P is the changeable propellant property at time t and temperature T, P_o is the initial value of the property; k is rate constant, and constants C and P are functions of the composition and oxidizer particle size in the propellant, respectively. C and P are kept constant for a particular set of experiments. Using Eqn. 69, the kinetics for ageing of the propellant containing different oxidizer loadings has been studied. For HTPB-RDX-AP-Al propellant the first order ageing model of Layton does not give a good fit of the data. The viscoelastic behaviour can be studied on the basis of time-crosslinking density superposition principle[572].

6.8 ESTIMATION OF SAFE-LIFE

In literature, the study of ageing related to mechanical properties is given more emphasis than the changes $\dot{r}$. But in ballistic missiles, estimation of ageing characterized by $\dot{r}$ is more desirable and therefore safe-life estimations are done on the basis of changes in $\dot{r}$, in addition to those in mechanical properties. Safe-life varies from mission to mission and, therefore, it is very difficult to give an exact definition for safe-life. However, using the accelerated ageing process for a specified change in the propellant property and by extrapolation to a lower temperature, safe-life is generally determined[179,538] from the activation energy (E) using Arrhenius equation. After the safe storage life there appears to be a sharp increase in the heat output of the propellant,[573], heat evolved during ageing has been measured by microcalorimetry. In CTPB CSP, useful safe-life data at 21°C have been obtained[545] by following the changes in the gel content, degree of swelling, dilation, creep compliance and crack propagation. Recent studies[176,177] have shown that the changes in TD rate, $\dot{r}$ and ultimate compression strength (U_c) follow zero order kinetic law during ageing. At a particular storage temperature and duration, the rate of change in any property can be used to obtain the following equation:

$$\Delta(\log(dh/dt) = n\Delta\log(h) - (E/2.303R)\ (\Delta 1/T) \qquad (70)$$

where h is a parameter like ΔTD, $\Delta\dot{r}$ and $\dot{r}\,U_c$ and n is the order of reaction. For a zero order kinetic law, n log(h) becomes zero and E can be obtained by plotting ($\log\Delta dh/dT$) against $1/T$. The safe-life data for different propellants for changes in $\dot{r}$ and U_c are given in Table 6.2. The safe-life for mechanical properties for PS and PMMA is higher compared to $\dot{r}$, but it is reverse for the PPF propellant. Meaningful propellant-case bond stress measurements

Table 6.2. Safe-life data of some CSP's

Propellant system	*Safe-life (months)*					
	$\dot{r}$, %			U_c, %		
	5	*1015*	*5*	*10*	*15*	
PS/AP (75%)	1.8	44	56	54	110	164
PMMA/AP (75%)	60	120	128	72	72	230
PPF/AP (75%)	66	138	204	13	13	40

that can eliminate or reduce some uncertainties of service life predictions is now possible in case-bonded CSP's[545]. The service life is also extended[547] by introducing curable barrier lacquers based on polyurethanes and epoxides between the propellant and the insulation, which reduces the rate of migration of the plasticizers. Burning rate catalysts like organo-copper compounds containing tridentate ligand are found to give very high storage life of AP-HTPB propellant–6.5 times more than the conventional copper chromite catalyst[574].

6.9 ACTIVATION ENERGY

The ageing model used to predict the normal ageing properties from accelerated ageing data is based on the activation energy values for the process. Ageing done in air suggests that the changes in $\dot{r}$ and *TD* are almost similar and are unaffected by aerial oxidation[544]. In another study[542], the activation energy (23-27 kcal/mole) for surface, subsurface and bulk material are almost equal and it is found that the primary component getting altered on the surface is the binder, while in the interior, it is the oxidizer. A value of about 6 kcal/mole obtained for both gel formation and change in mechanical properties suggests diffusion-controlled ageing rather than the involved curing and crosslinking reactions during ageing[548,559]. However, it is also felt that this low E value is unlikely for the diffusion-controlled process, as it requires a much higher energy. Recently, it has been found[557] that a value of ~ 9 kcal/mole corresponds to the polymer chain extension process during ageing and the value of 6 kcal/mole may be assigned to additional crosslinking at the double bonds. Thus, there is controversy over *E* values and at present it is difficult to resolve it.

Considering the activation energy values for the dehydrochlorination process in PVC and those for the proton transfer in the decomposition of AP, the activation energy (10 kcal/mole) for reactions responsible for change in calorific value during the ageing of PVC/DBP/AP propellant system has been attributed to the proton transfer during decomposition of AP and not to dehydrochlorination of the binder. The activation energy for change in the calorimetric value has been found to be 15 kcal/mole and is concordant with the corresponding values for changes in TD and $\dot{r}$ during ageing[62].

6.10 EFFECT OF OXIDIZER LOADING

This aspect has not been studied much. According to Schedelbauer[544], propellants with low binder content have better storage characteristics. Kishore, *et al*[61,177] found that in AP/PS propellants, the changes in $\dot{r}$, U_c and *TD* rate get reduced as the oxidizer loading increases (Fig. 6.3); thermal decomposition is sensitized in the cubic region, while it is desensitized in the orthorhombic region. Broadening of IR and X-ray diffraction peaks suggests that the oxidizer in the propellant is under strain. Thus, it is possible to reduce the rate of ageing by taking higher AP loaded propellants.

6.11 EFFECT OF ADDITIVES ON AGEING

Not many studies have been reported on the use of additives to increase the safe-life of CSPs. However, it has been observed that additives like $(NH_4)_2HPO_4$, NH_4F, NH_4Cl and NH_4Br, which desensitize decomposition of AP[213,230,569] and its deflagration[265], increase the safe-life of the propellant for changes in $\dot{r}$ as well as U_c. Desensitization of the ageing process by these additives is explained on the basis of the proton transfer process. Fe_2O_3, a well known $\dot{r}$ modifier, was also found to increase the safe-life of the propellant.

Most of the ageing studies have been on the changes occurring in the binder properties. Certain additives protect the binder from oxidation or other chemical reactions and reduce the ageing rate[575]. Yokoyama, *et al*[576] studied the effects of the hardner and antioxidants on the mechanical properties of CTPB propellants during ageing. Accelerated ageing studies were carried out[575] in the presence of triethanolamine (TEA) and benzaldehyde, as they are more effective antioxidants compared to other conventional antioxidants, N-phenyl naphthylamine and 2,6-diteritiarybutyl-p-cresol. Dynamic TG thermograms of DVB crosslinked polymers with and without antioxidants reveal that oxidative degradation occurs at a slower rate in the presence of antioxidants. The inception of weight loss at a higher temperature in the presence of antioxidants indicates inhibition of the oxidative reactions.

In a simple (AP/PS) model propellant with about 1 wt.% antioxidants, the rate of deterioration of the binder may be suppressed leading to small changes in the $\dot{r}$ of the propellant during ageing. The plot of % change in $\dot{r}$ as a function of storage time was found to follow zero order kinetics. From the plot, for a particular change in $\dot{r}$, storage time *t* could be obtained at different temperatures. The inverse of storage time t^{-1} gives the rate of ageing and the *E* value for the ageing process {13±2 kcal/mole in the temperature range (60-160 °C)}. It was used to estimate the safe-life time of the propellant for ballistic stability Arrhenius equation in the following form was used to calculate the safe-life time for a chosen percentage change in $\dot{r}$ at ambient storage temperature.

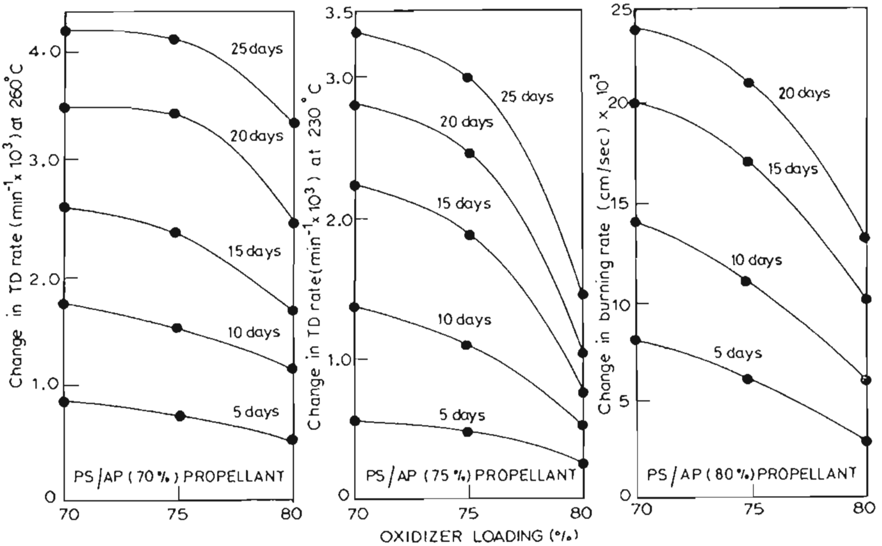

Figure 6.3. Extent of change in thermal decomposition rate and burning rate on AP loading[179].

$$\log t_2 = \log t_1 + (E/2.303R) \times (T_1 - T_2) / (T_1 T_2) \qquad (71)$$

where t_1 is the storage time at T_1 (K) for a particular percentage change in $\dot{r}$ and t_2 is the safe-life time at ambient temperature (T_2). Safe-life data for various systems and for various percentage changes in $\dot{r}$ (Table 6.3), suggest that the incorporation of

Table 6.3. Safe-life data for different propellant systems for the changes in $\dot{r}$

System	Safe life (years) for various % changes in $\dot{r}$			
	2.5%	5%	10%	15%
AP/PS	2.25	5.04	10.08	15.12
AP/PS+DVB	3.13	6.28	12.52	18.78
AP/PS+DVB+TEA	5.21	10.42	20.84	31.26
AP/PS+Benzaldehyde	3.47	6.93	13.84	20.84

antioxidants increases the safe-life. The effect of TEA which is more than that of benzaldehyde, may be attributed to the fact that TEA contains both amine and alcoholic groups known for their antioxidant capabilities, whereas benzaldehyde is not a stabilizer in the conventional sense. However, its mechanism is unique, as it is a product generated from the polymer substrate itself through poly(styrene peroxide) formation. Addition of triphenylphospine, as a stabilizer for HTPB, has been found[577] to effectively prevent the ageing during prolonged storage at ambient temperatures. Tang[578] has shown that styrene volatilization is the major factor which affects the mechanical properties of the propellant during initial ageing. Hence, it is desirable that HTPB propellant composition be without styrene residues.

6.12 EFFECT OF HUMIDITY ON AGEING

Very little work has been done on the humid ageing of CSP[579-580], which is of considerable importance in respect of propellant performance. The effect of humidity on the mechanical properties is more profound compared to thermal effects. It has been observed that in humid atmosphere, the propellant strength is lowered during storage due to the breaking of the filler-binder crosslinking[547], depolymerization[548], etc., resulting in an increase in elongation and decrease in tensile strength and modulus[549]. Sarojini, *et al*[579] studied humid ageing of CSP containing (Al-Mg) alloy to understand how the reactivity of Mg would influence combustion of the metal alloy and other characteristics upon storage. Addition of Mg-Al alloy results in a marked difference in the humid ageing behaviour of CSP compared to its Al-containing counterparts; the samples containing the alloy retained their shape compared to Al-containing CSP. However, visual observations of changes in dimensions, appearance of cracks, and absence of glittering alloy particles, suggest the liberation of gases due to reaction and consumption of metal in such reactions. Weight loss was observed only when the samples were aged under non-humid conditions. Increases in sample weight and moisture absorption are probably due to the presence of Mg and formation of $MgClO_4$. Decrease in the lattice parameter of Al in the alloy, the value becoming almost equal to that of Al alone, has suggested the leaching of Mg out of the alloy and its subsequent reaction with moist AP, leading to the formation of $MgClO_4$. This product is believed to catalyze and enhance thermal decomposition of the propellant. Significant increase in the value of $\dot{r}$ has been observed at higher storage temperatures (60-90 °C) and higher relative humidities(RH).

The mechanical properties deteriorate on ageing of the samples as a function of temperature, RH and storage period. In fact, the propellant becomes soft and the compression modulus decreases, leading to failure. Increase in modulus, when humidity is excluded, is ascribed to the formation of additional crosslinks through the magnesium carboxylate bridge brought about by the reaction of $MgClO_4$ or Mg metal with residual -COOH groups on adjacent polymer chains, as revealed by IR studies. It is, however, felt that by virtue of the slow diffusive character of Mg in the alloy, the modulus decrease can be controlled within the required limits by varying the Mg content in the alloy, but this needs further investigation.

Under humid ageing conditions, decrease in the calorimetric value has been attributed to the formation of $MgClO_4$ and depletion of Mg in the alloy resulting from the diffusion of Mg out of the alloy. Upon excluding humidity, the calorimetric value of CSP containing the alloy increases due to enhanced reactivity and oxidation of Al in the presence of Mg. Thus, inclusion of Al-Mg alloy in CSP formulation seems to improve performance of the propellant in non-humid environment only.

It has also been demonstrated[580] that propellants containing quarternary ammonium salts, stored at an equilibrium condition of 40% RH and room temperature, can retain the mechanical properties stable despite moisture absorption by the salt.

CHAPTER 7

HIGH-PERFORMANCE BINDERS, OXIDIZERS & PROPELLANTS

7.1 AN OVERVIEW

There has always been interest in developing new binders and oxidizers for solid propellants which could provide not only high energy but also could be safely handled during processing. Oxetanes and their derivatives are attracting considerable attention for their potential application as binders in solid propellants due to their molecular weight control, low polydispersity, low glass transition temperature (T_g), high energy and easy handling characteristics. Initial investigations on the use of low molecular weight azido compounds such as 1,7-diazido-2,4,6-trinitrazaheptane (DATH), 1,6-diazido-2,5-dinitrahexane (DADNH) and 1,3-diazido-2-nitrazapropane (DANP) in solid propellant formulations confirmed high energy release during ballistic testing[581]. Having demonstrated the utility of the above organic azido compounds in advanced propellants, it was considered highly desirable to extend the scope further to polymeric azides. Consequently, research was initiated in 1976 on the synthesis of azido polymers with hydroxyl end groups, so that that they could be used in conjunction with the HTPB binder. Among azido polymers known so far, hydroxyl-terminated glycidyl azide polymer (GAP) has been most widely studied due to its hazard insensitiveness and thermal stability characteristics for its potential application in advanced solid propellants. Current research on such new energetic binders is focussed on synthesis and characterization of polymers containing azide groups in the side chain[582,583]. Thermal decomposition of these azide polymers[582-585] is significantly different from that of the conventionally used HTPB binder.

It has been shown that propellant formulations based on AP + ammonium nitrate (AN) + GAP provide chlorine-free exhaust plumes[586]. Such propellants would reduce the harmful contaminants in the upper atmosphere. Ammonium dinitramide (ADN) is a new class of stabilized chlorine-free high energy oxidizer. It considerably reducs HCl production from propellant plumes, thereby reducing wetland stresses near the launch pad[587]. ADN is being seriously considered as a potential replacement for AP in propellant applications. Hydrazinium nitroformate (HNF) is another high energy pollution-free oxidizer.

In this chapter, some of these azide polymers, ADN and HNF, will be discussed.

7.2 GLYCIDYL AZIDE POLYMER (GAP)

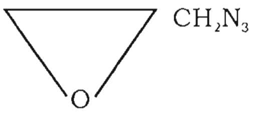

GA monomer

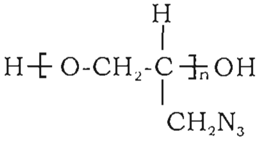

$$H\left[O-CH_2-\underset{CH_2N_3}{\overset{H}{C}}\right]_n OH$$

GA Polymer

Glycidyl azide (GA) is a well known compound made by reacting epichlorohydrin (ECH) with hydrazoic acid followed by cyclization of 1-azido-3-chloro-2-propanol, produced using a base (Eqn 72) . It was found that GA monomer was quite unreactive and did not polymerize to give GAP (Eqn 73).

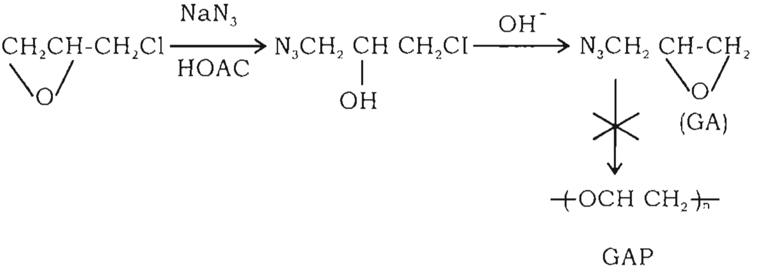

(72)

(73)

Therefore, another approach involving first the polymerization[588] of ECH to polyepichlorohydrin (PECH) (Eqn 74) followed by the reaction of PECH with NaN_3 was adopted. In 1983, Frankel, *et al.*[1589] successfully synthesized GAP containing -OH end groups (Schemes, 1 and 2). When DMSO[590.591] was used as the solvent, complete conversion of PECH to GAP occurred at 90 °C, within 18 h,

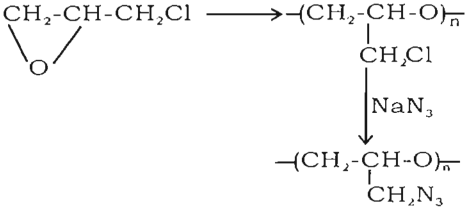

(74)

while in water, complete conversion took 7 days at the same temperature[581] The conversion of PECH to GAP was confirmed by the appearance of a sharp band of -CH_2N_3 group at 2100 cm^{-1} and the total disappearance of CH_2Cl band at 720 cm^{-1} in the IR spectra[592,593]. ^{13}C-NMR of GAP has been studied to find out all resonances due to main chain and terminal groups[594].

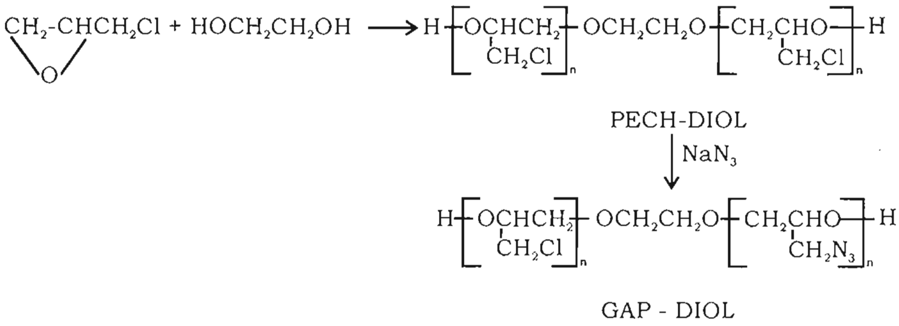

Scheme1. Preparation of GAP-diol.

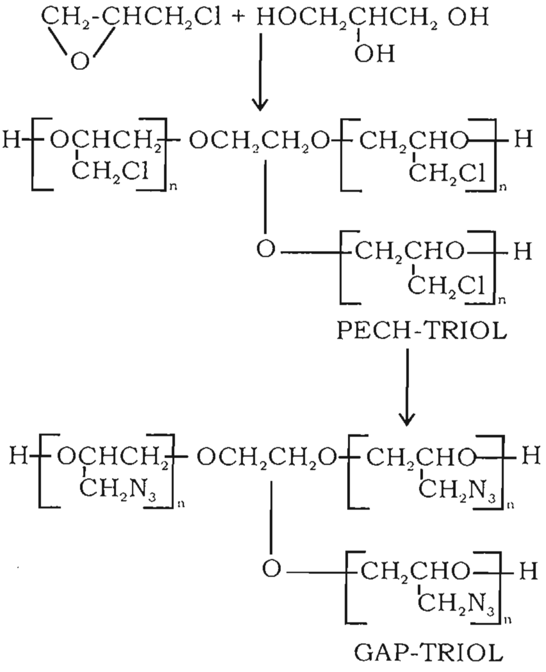

Scheme 2. Preparation of GAP-Triol.

If we replace ethylene glycol (Scheme 1) with glycerol as the initiator for the polymerization of ECH, we get GAP-triol[581] (Scheme 2).

Ampleman developed a new method for the synthesis of GAP which involves preparation of PECH with tosylate end groups as intermediary in the azidation process[595]. He has shown that the functionality (number of -OH terminated chains) of PEACH and GAP can be increased up to four times with a regio-specific epoxidation of low molecular weight linear PECH[595]. Ahad[596-598] reported the synthesis of high molecular weight branched GAP with commercial rubbery PECH as the starting material after the isotactic and chiral PECH was reported. Ampleman, *et al*[595] studied the synthesis and characterization of isotactic and chiral GAP using the respective PECH's as the starting materials. DSC analysis revealed that both isotactic and chiral GAP's were amorphous. It was also observed that during the azidation reaction, the molecular weight decreases. For example, 1150 kg/mol wt PECH, after 89% azidation, produced GAP of 164 kg/mol wt. Furthermore, the extent of degradation depends on the amount of NaN_3 taken as a well as the reaction time. A similar observation of the degradation of PECH was found during other nucleophilic substitution reactions also[595]. Absence of crystallinity in both isotactic and chiral GAP has been attributed to the bulky nature of the azide group, low degree of intermolecular interactions, branching, and crosslinking. By properly choosing the solvent, temperature and time, it is possible to prepare GAP with varied molecular weights.

Recently, a new method for GAP synthesis has been reported which increases the functionality[599,600] of PECHs by a factor of 2–4. It consists in regio-specific epoxidation of linear EPHs under basic conditions and opening of epoxides under different conditions. These new polymers can be used as binders. They can also be reacted with caprolactone or sulfone to produce energetic thermoplastic elastomers[599,600]. Multi-OH functional GAP could be used to modify the surface characteristics of the oxidizer crystals[601]. Recyclable energetic thermoplastic elastomers based on GAP of different molecular weights have been synthesized[602]. Azide-terminated GAP has been synthesized by reacting (-(2-chloroethyl)-ω-benzenesulfonyl polyepichlorohydrin with NaN_3 in DMSO[603]. Minora, *et al*[604] synthesized azide-terminated GAP (Eqn. 75).

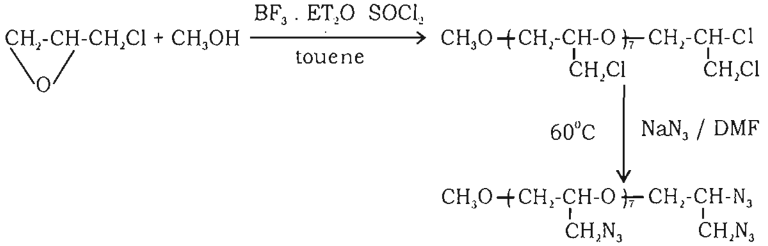

(75)

The physical properties[581,592] of GAP of mol.wt ~2000 are summarized in Table 7.1.

Table 7.1. Physical properties of GAP

E. weight	1132
F_{OH}	1.98
M_w	2097
M_n	1668
Q	1.27
%H_2O	0.007
T_g	-45 °C
Density	1.30 g/cc
Thermal stability	0.88-0.22 ml/N_2 /g after 697 at 50 °C
Impact sensitivity	200 kg-cm
Friction sensitivity	32.4 kg.
Electrostatic sensitivity	6.25 J
ΔH_f (experimental)	+0.28 kcal/g (Difunctional eq. wt=1200)
Burn rate (cured strands)	self-extinguishes at ambient pressure: 1.96 cm/s at 6.89 MPa

7.2.1 Copolymers of GAP

Bui, *et al.*[605] reported the synthesis and properties of glycidyl azide-ethylene oxide(GAP-EO) copolymer. Initially, ECH was copolymerized with ethylene oxide to form the polyepichlorohydrin-ethylene oxide (PEEO) copolymer (Eqn. 76) . PEEO on treatment with NaN_3 in DMSO, using lithium methoxide as the cleaving agent, yielded the GAP-EO copolymer. Since the alcohols used in this study were glycerol, trimethylol propane (TMP) or pentaerythritol, the copolymers obtained were having a branched structure. It was found that the GAP-EO copolymer cured using isophorone diisocyanate (IPDI) had higher elongation at break and lower T_g compared to the polyurethane (PU) made from the GAP homopolymer. The differences in properties are attributed to the presence of EO units in the copolymer which give higher flexibility. It is to be mentioned here

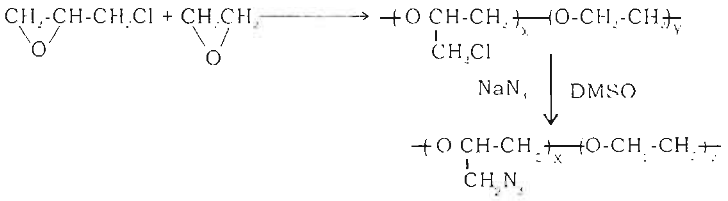

(76)

GAP - EO

that the properties of cured GAP or cured GAP-EO are not only dependent on the type of backbone structure, but also on the type of isocyanate used for crosslinking. For example, an aliphatic diisocyanate, such as hexamethylene diisocyanate (HMDI) gives rise to PU with a lower tensile strength, but a higher elongation at break than PU made using an aromatic diisocyanate like toluene diisocyanate[25] (TDI). In a similar fashion, Cao, *et al*[606] synthesized copolymers of GAP and THF (Eqn 77) which had better mechanical properties and lower hazard sensitivity and possessed similar thermal stability as neat GAP.

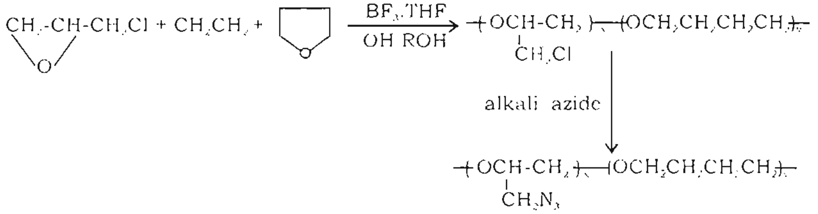

(77)

GAP - THF

Copolymers containing both GAP and BAMO units were reported by Minora *et al*[604] (Eqn. 78). When polyglycidyl nitrate (PGN) polymer is reacted with a metallic azide in an organic solvent in the presence of a phase transfer catalyst substitution of nitrate groups by azide groups occurs, resulting in the formation of GAP-PGN copolymers (Eqn. 79).

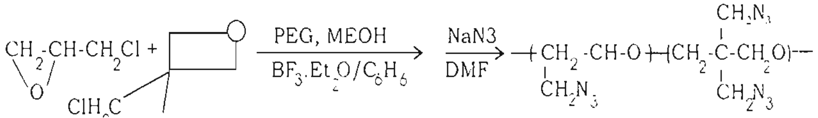

(78)

GAP - BAMO

(79)

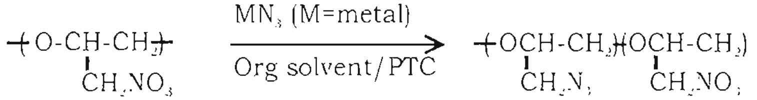

$$-\!\left(O-\underset{CH_2NO_3}{CH}-CH_2\right)\!- \xrightarrow[\text{Org solvent/PTC}]{MN_3\text{ (M=metal)}} -\!\left(O\underset{CH_2N_3}{CH}-CH_2\right)\!\left(O\underset{CH_2NO_3}{CH}-CH_2\right)$$

GAP-PGN

GAP polyester having the formula $R(COCH_2C(CH_2N_3)H)_xOR')_y$, where x=2-10, y=1-4, R, a residue of a monohydric alcohol, diol, triol, or polyol and R', the acyl residue of an organic carboxylic acid, was synthesized and used as an energetic plasticizer[607].

Block polyurethanes, GAP-OH having mol. wt. ~2440 and an OH-terminated polyether having a mol 1000-5000 were coupled using isocyanates. The resultant block polyurethane (Eqn. 80) is suitable as a fuel-binder in rocket propellants, gunpowder, plastic explosives and solid-fuel combustion engines[608].

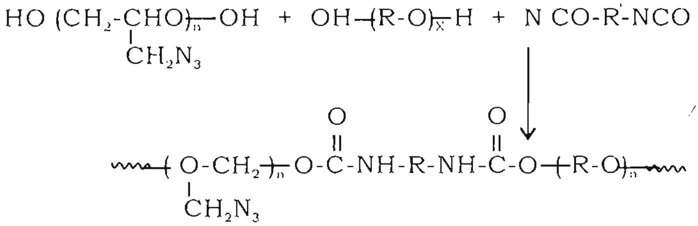

$$HO\,(\underset{\substack{|\\ CH_2N_3}}{CH_2\text{-}CHO})_n\text{-}OH + OH\text{-}(R\text{-}O)_x\text{-}H + NCO\text{-}R'\text{-}NCO \longrightarrow \sim\!\sim(\underset{\substack{|\\ CH_2N_3}}{O\text{-}CH_2})_n\text{-}O\text{-}\overset{\overset{O}{\|}}{C}\text{-}NH\text{-}R\text{-}NH\text{-}\overset{\overset{O}{\|}}{C}\text{-}O\text{-}(R\text{-}O)_n\sim\!\sim$$

(80)

(GAP - polyether) polyurethane

7.2.2 Thermal Decomposition of GAP

Thermal degradation studies[609] on GAP have been carried out using techniques such as DTA, TG, DSC, ARC, MS, etc. The data available in literature are listed in Table 7.2. Recently, Eroglu, *et al*[610] reported a study on the thermal decomposition of GAP-diol.

Table 7.2. Summary of the reported[583,635] thermal decomposition data on GAP

Authors	*Technique used*					*1st stage*	*2nd stage*	E_a
	DSC	*DTA*	*TG*	*ARC*	*MS*	*Decom--position (°C)*	*Decom--position (°C)*	*kcal/mol*
Kubota, *et al*		X	X			202	277	-
Farber, *et al*					X	120		42.2
Leu, *et al*	X		X			240	260	-
Mishra, *et al*	X			X			-	-

The DSC (Fig. 7.1) shows a broad exotherm with the range, 200-300 0C. TG analysis of GAP-diol (Fig. 7.2) reveals a two-step degradation process; the first step, being the major step corresponds to nearly 36% weight loss occurring in the range 210-270 °C.

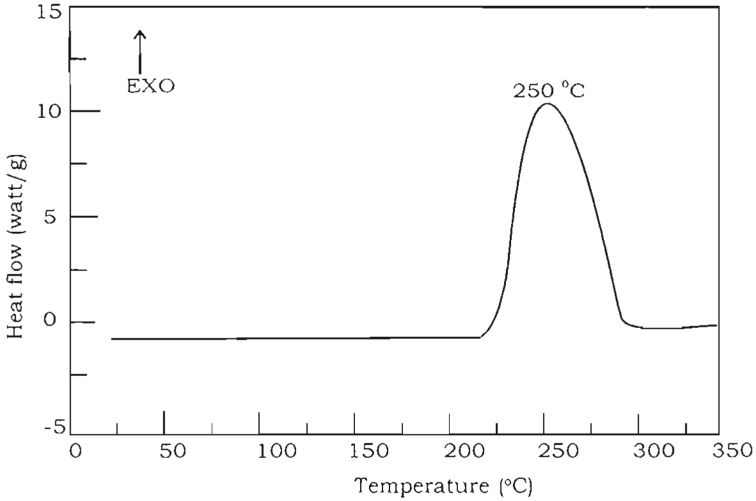

Figure 7.1. DSC thermogram of GAP.

Source: Eroglu *et al.* Thermal decomposition of poly (alycidy azide) as studied by high temperature FTIR and thermogravimetry. *J. Annld. Polym Sci*, 1996, **61**, 201 (Reproduced with permission from John Wiley & Sons Inc. New York and Dr. Mehmet. S. Eroglu, Tubitak-Marmara Research Centre. Turkey).

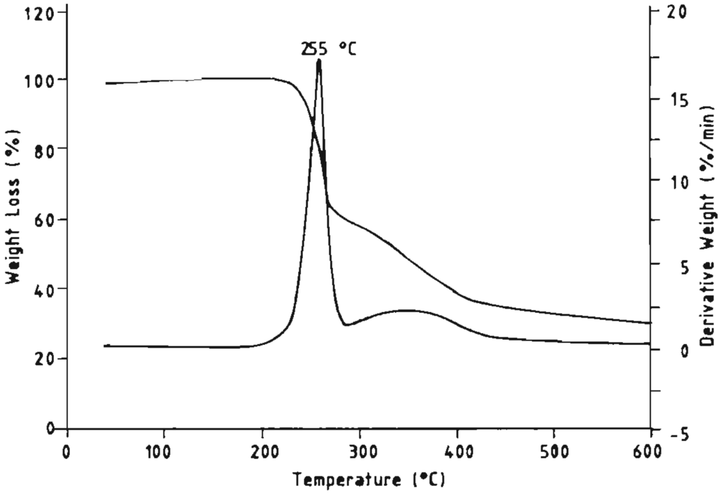

Figure 7.2. TG thermogram of GAP.

Source: Eroglu *et al.* Thermal decomposition of poly (alycidy azide) as studied by high temperature FTIR and thermogravimetry. *J. Annld. Polym Sci*, 1996, **61**, 201 (Reproduced with permission from John Wiley & Sons Inc. New York and Dr. Mehmet. S. Eroglu, Tubitak-Marmara Research Centre. Turkey).

The second stage is completed around 410 ^{0}C. The first step corresponds to the elimination of N_2 from the side methyl azide chain, which constitutes 30% of the repeat unit and is also responsible for high exothermicity (1828 J/g) of the degradation. Apart from N_2, using GC-MS and FTIR techniques, the other major degradation products of GAP were found to be H_2, CH_4, CH_2O, C_2H_2, C_2H_4, NH_3, CO and HCN[583]. The mechanism of degradation of GAP involves the elimination of N_2 molecule from the side chain methyl azide group followed by either intramolecular cyclization or intermolecular crosslinking[609] (Scheme 3).

Like GAP-diol, GAP-triol[611] also undergoes exothermic degradation in the temperature range 217-277 ^{0}C (Fig. 7.3) as well as two-step degradation in TG, the first step corresponds to 36% weight loss (Fig. 7.4) However, in air theTG shows four-step

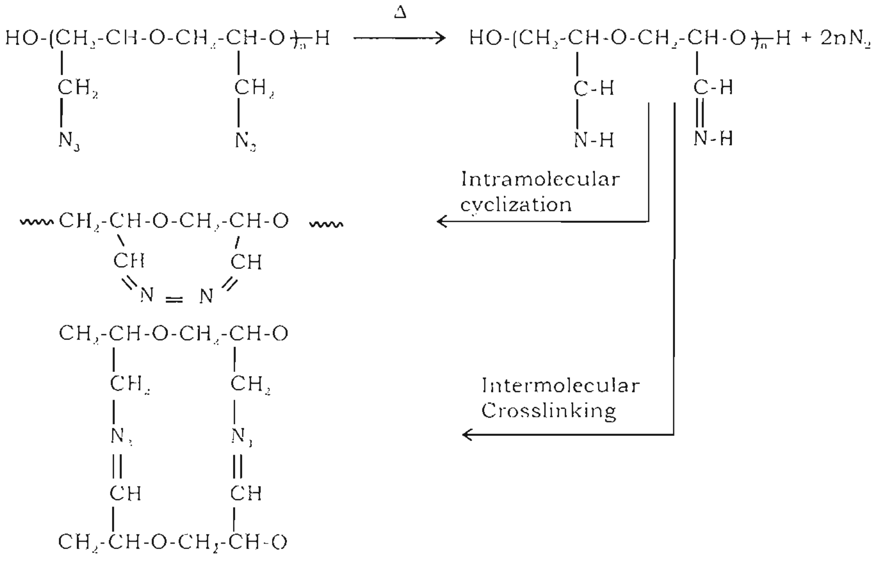

Scheme 3. Mechanism of thermal degradation of GAP-diol.

degradation for GAP-triol (Fig.7.4). Oyumi[612] found that GAP having azide (GAP-N_3) end groups decomposes faster than GAP-OH. However, both the polymers showed the same activation energy (E_a), indicating that the terminal azide groups of GAP-N_3 decompose independent of the pendent azide groups. The heats of

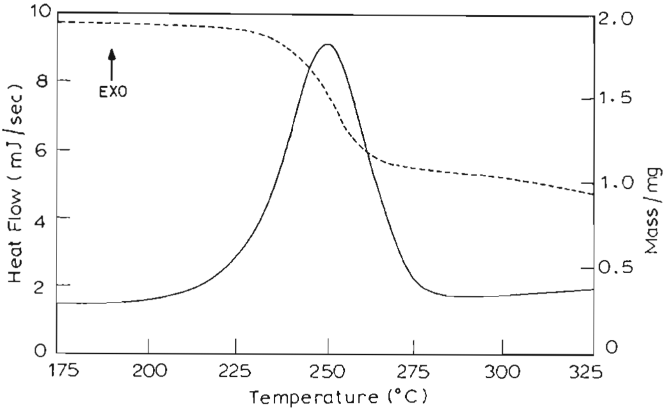

Figure 7.3. DSC and TG (in nitrogen) of GAP-triol at a heating rate of 10°K/min.

Source: Reprinted from *Thermochimica Acta*, Vol. 242, David Jones E.G. Malechaux, L and Rainer Augsten, R. Thermal Analysis of Gaptriol, An energetic azide polymer. P. 187-197. copyright 1994, with permission from Elsevier Science and Dr DEG Jones, Head, R & D Canadian Explosives Research Laboratory.

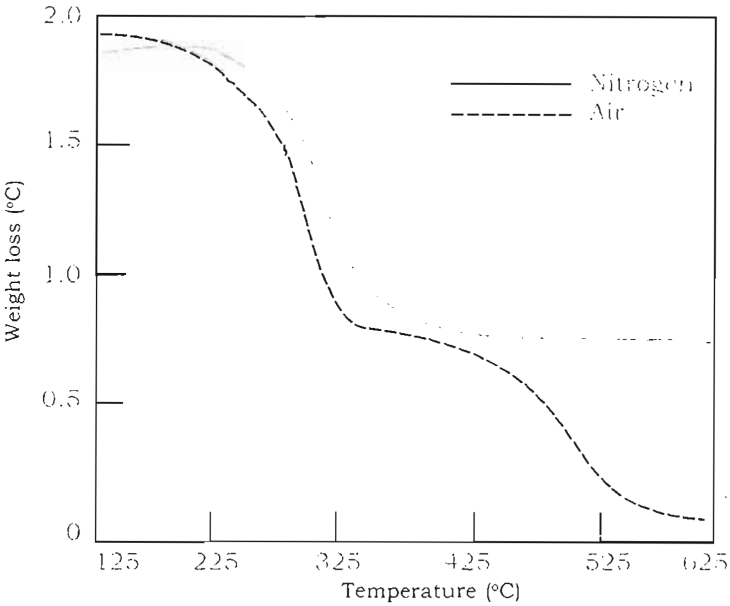

Figure 7.4. TG of GAP-triol in nitrogen and air at a heating rate of 2 °k/min.

Source: Reprinted from *Thermochimica Acta*, Vol. 242, David Jones E.G. Malechaux, L and Rainer Augsten, R. Thermal Analysis of Gaptriol, An energetic azide polymer. P. 187-197. copyright 1994, with permission from Elsevier Science and Dr DEG Jones ,Head, R & D Canadian Explosives Research Laboratory.

decomposition of GAP-OH and GAP-N_3 were found to be 3,100 and 3,500 J/g, respectively. It was also found that addition of 5 wt% catocene ($C_{27}H_{32}Fe_2$) accelerated the decomposition of GAP-OH. When the same sample was aged for 100 days at 70 ^{0}C, the DSC decomposition peak temperature increased from 224^0 C to 232 ^{0}C. The role of catocene in the decomposition of GAP, after ageing, is not clearly understood. On the other hand, neat GAP-OH is stable to accelerate ageing. Brill, *et al*[585] found that among the azide polymers, the rate of thermal decomposition follows the order: GAP>BAMO>AMMO. But the E_a of degradation of all the three polymers were very similar, around 40 kcal/mol.

The decompsition of GAP at -196 ^{0}C was studied using laser-generated shock waves. Comparison of FTIR spectra obtained before and after the shock passage showed that the initial reaction involves elimination of N_2 from the azide functional groups of the polymer[613]. Another study[614] involving laser-induced (pulsed TEA CO_2 laser tunable at 920-1080 cm^{-1}) decomposition of solid GAP, under vaccum, produced N_2, CO, HCN and probably H_2 as the main products. Two products, HCHO and NH_3, which were detected during thermal decomposition, were found to be absent in the present study. In addition, a powdery polymeric material containing CH:NH group was also observed[614].

7.2.3 Combustion of GAP

Argon (Ar) plasma jet ignition and flameless combustion wave propagation of GAP were examined as an upright slab, in air and Ar environment. After an ignition delay of 70-1500 ms, blue and yellow flames were observed in air, but not in Ar. GAP is ignitable, extinguishable and reignitable at 0.1 MPa pressure with measured ignition temperature of 511K in Ar; combustion of GAP is not self-sustainable below 0.3MPa Ar pressure[615].

7.2.4 GAP Propellants

GAP has been used in double base, composite-modified double base, composite and gun propellants. The burning rate characteristics of GAP cured with HMDI/TMP are compared with

Table.7.3. Burning rate characteristics of GAP propellant and a conventional NC/NG propellant (at MPa, T_o = 293 K)

	GAP	*NC/NG*
T_f (K)	1365	2716
$\dot{r}$ x 10^{-3} m/s	10.7	6.9
η	0.44	0.58
σ_p / *K*	0.0103	0.0034

those of conventional double base [nitrocellulose(NC)/nitroglycerine(NG)] propellants in Table 7.3. Burning rate of GAP propellant was found to be significantly higher than that of NC/NG propellant, even though the energy of a unit mass of GAP propellant is smaller. Further, the temperature sensitivity of burning rate of GAP propellant is also higher compared to that of NC/NG propellant[616]. Kubota and Nakashita[617,618] observed that when 12.5% of diethyl phthalate (DEP) plasticizer was replaced by the same amount of GAP in NC/NG propellant, the ballistic parameters increased: adiabatic flame temperature (T_f) from 2557 to 2964 K, specific impulse from 237.2 to 253.3 s and burning rate by ~ 70%. It was also found that the burning rate of neat GAP is much higher than those of NG/NC/GAP and NC/NG/DEP propellants. Here, unlike in DEP, the -OH end groups of GAP-OH can be chemically linked to NC using isocyanates, such as HMDI or IPDI. Thus, addition of GAP can increase not only the combustion performance but also improve the strength of the NC/NG propellant. The basic combustion mechanisms of NC/NG/DEP and NC/NG/GAP propellants in the gas phase were found to be similar.

Kubota, *et al*[616] observed that both burning rate and T_f decrease when GAP was mixed with ammonium perchlorate(AP), cyclotetramethylene tetranitramine (HMX) or triaminoguanidine nitrate (TAGN). Also, GAP/AP propellant produced a large number of streams in the flame structure, indicating a heterogeneous combustion behaviour. On the other hand, GAP/HMX and GAP/TAGN produced no flame streams, indicating a homogeneous combustion behaviour. Kubota, *et al*[619] observed that the burning rate of neat GAP is much higher than that of HMX. Addition of 2.0 wt.% lead citrate +0.6 wt.% carbon mixture increased the burning rate of GAP/HMX(19.4/78) propellants. Leu *et al*[620,621] investigated the thermal behaviour of GAP, GAP/bis-2,2 dinitropropyl acetol (BDNPA)/bis-2,2-dinitropropyl formal (BDNPF) and PEG/BDNPA/BDNPF energetic binder systems using TG, DTG, DSC and Parr bomb calorimetry. It was found that BDNPA/F (BDNPA + BDMPF) is more compatible with GAP than with PEG and also the thermal decomposition of GAP did not change when BDNPA/F was used. The decomposition temperatures for energetic composites of the above three binder systems with HMX were found to be lower than that of pure HMX. The heats of explosion of these energetic composites were found to be proportional to the particle size of HMX. However, the T_g values of the energetic polymer systems were not affected by the addition of the nitroplasticizer BDNPA/F.

Tokui, *et al*[590-592] studied 59-62.5 wt. % AN-based GAP compositions. The pressure exponent (n) value of these compositions was 0.7. The composition having 62 wt. % AN showed unstable combustion in the rocket motor. Similarly, the effect of particle size of AP on the thermal decomposition of GAP was studied by Huang, *et al*[622]. The cured propellant containing AP particles of 400 and 225 μm sizes undergoes two-step decomposition, the first one occurring at 224 ^{0}C, which corresponds to the decomposition of GAP; the second one in the range 359-386 ^{0}C, was attributed to decomposition of AP. But when AP of particle sizes 50 and 5 μm was used, only one-step decomposition was observed at 170-191 ^{0}C. It is well known that by decreasing the particle size of AP, the thermal sensitivity of the propellant increases. Further, since AP particles are surrounded by GAP, the heat liberated by decomposition of GAP supplies enough energy to overcome the barrier of decomposition of AP; as a result, AP decomposes immediately after the decomposition of GAP.

In a recent study[586], it was found that when GAP is used as the binder, the amount of HCl produced is greatly reduced in an AP/AN propellant. Hazardous air pollution by HCl mist from exhaust plumes of a conventional composite propellant is avoided by propellant formulations in which AP is replaced with AN. But decrease in the specific impulse due to the use of AN as a chlorine-free oxidizer can be compensated by the addition of GAP. However, 15-30 wt.% AP is a must to ensure reliable ignition and stable combustion. Successful propellant formulations[623] contained GAP 22-70, AN 0-60 and AP 15-30 wt.%. However, the HCl formed, can be scavenged by the addition of 1:1 Al-Mg alloy powder.

Addition of Fe_2O_3 to GAP/AN/AP propellant is found to increase $\dot{r}$ as well as pressure exponent by catalyzing the thermal decomposition of AP[624]. Duncan[625] studied the effect of strain rate and relaxation response of GAP/PSAN (phase-stabilized ammonium nitrate) propellant. Analysis of the maximum stress and the strain at maximum stress showed that there is a limited range of temperatures for any given strain rate at which the measured strain at maximum stress exceeds 17%. The long-term equilibrium strain capability of GAP/PSAN lies in the range 10-12 wt.%. It was also observed that modulus versus reciprocal of the strain rate had two distinct trends: below 30 ^{0}C, the slope of the curve was notably higher; this was attributed to reduction in the molecular mobility of the GAP chains as the T_g is approached. A change in the slope was also noted in the tensile strength data, but this was restricted to the data at -40 ^{0}C, suggesting that more rigid, brittle-like behaviour begins to affect the tensile modulus more than the tensile strength at higher temperatures.

The influence of GAP-OH, HTPB and cellulose acetate butyrate (CAB) binders on the properties of nitramine propellants, such as RDX, HMX, NG and TAGN was studied by Volk and Bathelt[626]. Due to more positive heat of formation and better oxygen balance of GAP-OH, compared to HTPB, the specific energies of nitramine propellants based on GAP-OH were found to be superior. Table 7.4 depicts both O_2 balance and enthalpy of formation of different plasticizers used in propellants. Nagayama and Oyumi[627] found that the AP-(3,3-bis(azidomethyl)oxetane-3-nitratomethyl-3-methyloxetane (7/3) copolymer, B/N propellant and AP/GAP propellant have much higher specific impulses than AP/HTPB propellant when AP content is below 85 wt.%. The Azide polymers decompose exothermally and improve the performance. However, the less reactive products from the azides, such as N_2 and HCN decrease the specific impulse of the propellant at the higher oxidizer loading (Fig.7.5).

Table. 7.4. Oxygen balance and heat of formation (ΔH_f^o) of various plasticizers

Plasticizer	*O_2-balance (g O_2/ 100g)*	*ΔH_f^o [KJ/kg]*
Diethylphthalate	194.4	-776
Dibutylphthalate	224.2	-843
Dioctylphthalate	258.1	-1122
Ethylphenylurethane	227.7	-464
Triacetin	139.3	-1331
Camphor	283.8	-327
Ethylcentralite	256.4	-105
DBNPA (50 : 50)	57.5	-827
Butylnitratoethylnitramine (BUNENA)	104.3	-140
1, 5-diazido-3,3-nitro-azapentane (DANPE)	79.9	554
2, 4-dinitro-2, 4-Diaza-6-nitroazapentane	36.8	-145
2, 4-dinitro-2, 4-diaza-6 azidohexane	62.1	210
GAP	121.1	1179
PH(HTPB)	323.0	-380
PIB	342.2	-1568
CA	129.6	-5518
CAB	149.2	-4523

Schedlbauer[628] studied the performance of LOVA-gun propellants containing either GAP or HTPB binder. It was found that GAP propellants possessed high energy and a low pressure exponents in contrast to HTPB formulations. However, T_f of GAP propellants is substantially higher, resulting in increased erosion. Due to better O_2 balance, GAP propellants prevent the formation of solid carbon. But the mechanical, chemical and thermal properties of the two types of propellants are nearly the same. In the bullet impact and the sympathetic detonation tests, no deflagration or detonation was observed. Generally, the application of GAP as a binder for nitramine propellants seems to be advantageous for the performance enhancement.

Shyu, *et al*[629] investigated the combustion characteristics of GAP-coated boron particles as well as GAP-boron propellant. It was found that the total combustion time for boron was reduced on coating with GAP. This is attributed to the reaction of degradation

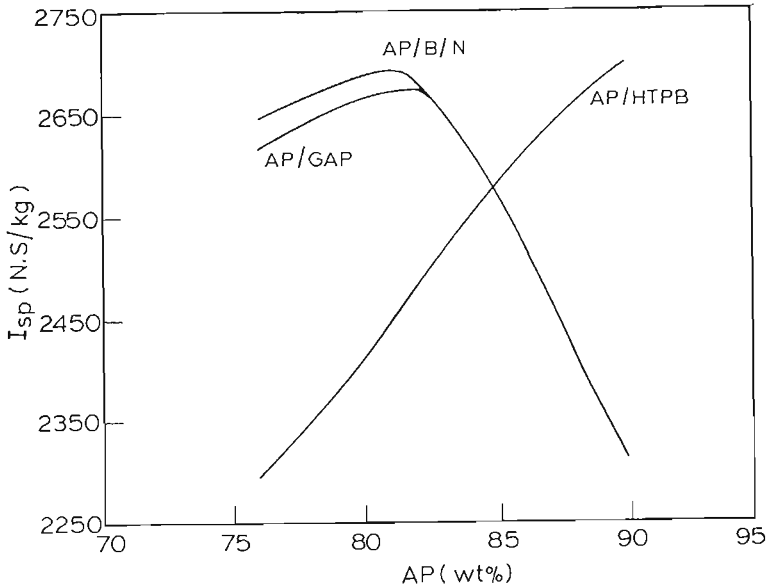

Figure 7.5. Specific impulse (20 Mpa) of propellants as a function of AP content.

Source: Nagayama *et al.* Combustion characteristics of high burn rate azide polymer propellant. Propellants. *Explosives Pyrotechnics.* 1996, **21**(2), 74-78 (Reproduced with permission from Wilcy-VCH Eingang, Weinheim and Dr. Y. Oyumi and Dr. E. Kimura, Japan Defence Agency.

products of GAP, such as H_2O and N_2, with boron and B_2O_3 {Eqns. (81-83)} as also due to the exothermic degradation of GAP in raising

$$\tfrac{1}{2}\, B_2O_3^{(l)} + \tfrac{1}{2}\, H_2O^{(g)} \rightarrow HBO_2(g) \qquad (81)$$

$$3/2\ B_2O_3^{(l)} + 3/2\ H_2O^{(g)} \rightarrow H_3B_3O_6 \qquad (82)$$

$$B + 1/2\ N_2 \rightarrow BN \qquad (83)$$

the temperature of the boron particles, thus promoting the ignition/ combustion process. GAP-coated amorphous boron-based fuel-rich propellant exhibited more vigorous combustion behaviour, higher burning rates and lesser residue agglomeration compared to uncoated boron propellant.

7.2.5 Hazard Characteristics

Due to high energy release from azide polymers, the impact friction and other sensitivity aspects are of major concern. Nazare, *et al*[592] reported the impact, friction and electrosensitivity of GAP, TAGN, GN and AN-based compositions. The friction and impact sensitivity of various GAP formulations containing AP, HMX, TEGDN, etc., have been studied[630]. It was found that certain types of GAP formulations were extremely friction and impact-sensitive. On the other hand, neat GAP was found to be insensitive to impact[631].

7.3 POLY (3-AZIDO METHYL, 3-METHYL OXETANE) (AMMO)

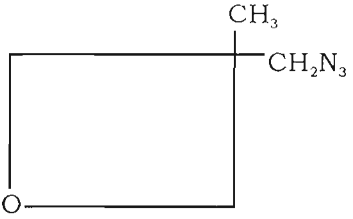

AMMO monomer

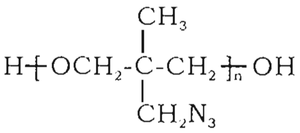

$$H\!+\!OCH_2\text{-}\underset{CH_2N_3}{\overset{CH_3}{C}}\text{-}CH_2\!+_n\!OH$$

AMMO Polymer

AMMO homopolymer is the most stable azide polymer. It is synthesized by stirring AMMO monomer with $BF_3.Et_2O$ in anhydrous methanol for 24 h; this gives a polymer molecular weight 8000-10,000[584] amu. AMMO homopolymer decomposes exothermally around 240 °C, but AMMO binder, cured with IPDI, decomposes exothermally in the temperature range 200-250°C under slow thermolysis conditions. It is accompanied by evolution of N_2 gas from the methyl azide group. The rate of decomposition of these energetic polymers follow the trend: GAP > BAMO>AMMO which is reflected in their T_{max} data (Table 7.5). The heat of decomposition

(ΔH_d) follows the trend of the weight fraction of the azide group in the polymer. Similarity in the activation energy (E_a) values of these alkyl azide polymers suggests that the azide group largely controls the kinetics through the following reaction:

$$RN_3 \rightarrow RN + N_2$$

Table 7.5. Thermochemical and kinetic data for decomposition of some oxetane polymers[585]

Polymer	T_{max} (°C)	ΔH_d (J/g)	E_a (kcal/mol)
AMMO	233	-1550	40-41
BAMO	224	-2670	40-41
GAP	221	-2060	39-40

The nitrene intermediate (RN) is unstable and reacts further to give various products. High energy BAMO and GAP polymers produce small hydrocarbon fragments also along with CO and CH_2O from the backbone. Low molecular weight hydrocarbons are not present among products of decomposition of AMMO polymer. The nitrene functional group is formed in the methylene azide side chain. Formation of HCN and NH_3 indicates that it involves C-C and C-N bond scission followed by hydrogen migration to liberate NH_3. AMMO polymer has the lowest ΔH_d value, and it leads to a somewhat different fragmentation process[585]. H_2O dominates the quantifiable products.

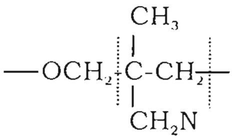

$$-OCH_2-\overset{\displaystyle CH_3}{\underset{\displaystyle CH_2N}{C}}-CH_2-$$

Following the decomposition of azide group of AMMO, backbone cleavage also occurs, as shown above, forming CH_2O and 2-methyl allyl nitrene intermediate. Recombination of coordinately unsaturated N atoms would produce azo compounds. Recombination, after an N atom is eliminated and H is scavenged, would produce a secondary amine. HCN, NH_3 and CO are significant products of decomposition of AMMO polymer which suggests that the backbone degrades into smaller fragments. However, under combustion conditions, 2-methyl nitrene may not completely recombine and may function as a reactant itself in the combustion of AMMO polymer[585].

7.3.1 AMMO/AP Propellant

AMMO/AP propellant[632] containing 20 wt.% AMMO was made by curing the propellant mix with IPDI at 60 °C for 10 days. TMP was used as the crosslinking agent. TG undergoes two-step decomposition, one up to 20 wt.% decomposition followed by rapid decomposition thereafter. Onset of weight loss matches with AMMO decomposition. The DSC thermogram shows an endotherm peak around 250 °C for the phase transition of AP followed by two exothermic peaks at 280 °C and 400 °C. The first exotherm is related to 20% wt loss of AMMO and the second for AP decomposition. These exotherms are strongly related to each other; the heat generated by the decomposition of AMMO accelerates the decomposition of AP.

Propellant containing 2 wt.% 2,2-bis (ethyl ferrocenyl) propane (CFe) and 2 wt.% Fe_2O_3 catalysts accelerates the decomposition of AMMO/AP propellant[632]. Both the exotherms are shifted to lower temperatures. They lower the 400 °C exotherm of decomposition of AP by about 65 °C. But 280 °C exotherm is lowered by 20 °C by Fe_2O_3 and by 70 °C by CFe, suggesting that CFe mainly accelerates the decomposition of AMMO binders. AMMO/AP propellant is thermally stable even after ageing at 75 °C for one year[582].

The effect of energy content of the binder on the AP/(AMMO + poly propylene glycol) has been studied[633]. By increasing the amount of AMMO polymer in the mixed binder, the adiabatic flame temperature, heat of combustion *(ΔH_C)* and $\dot{r}$ increase.

7.4 POLY [3,3 BIS (AZIDO METHYL) OXETANE] (BAMO)[585,621,632-645]

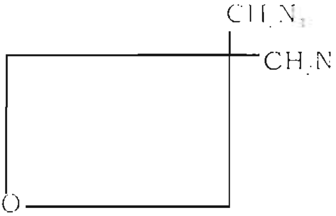

BAMO monomer

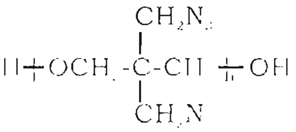

$H+OCH_2-\overset{CH_2N_3}{\underset{CH_2N_3}{C}}-CH_2+_n OH$

BAMO monomer

BAMO is one of the most energetic polymers having two methyl azide groups and contains 50 wt.% nitrogen. It is solid at room temperature and it shows poor mechanical properties because of its crystalline nature. For making liquid polymer, it is copolymerized with tetrahydrofuran (THF) or 3-nitrato-methyl-3-methyloxetane (NMMO) to improve the mechanical properties at low temperatures. Exothermic degradation of the copolymer is caused by the breakage of methyl azide group to produce N_2 gas.

BAMO polymer has been synthesized from 3,3-bis (chloromethyl) oxetane (BCMO) by chlorine exchange reaction in the presence of NaN_3. The reaction was carried out in N,N-dimethyl formamide at 90 °C. Diethylene glycol (DEG)/BF_3. $(C_2H_5)_2O$ initiating system gives good results in terms of safety, yield, molecular weight and functionality. It is purified by passing it through neutral alumina[640]. BAMO polymer has also been synthesized by cationic ring opening polymerization of oxetane using a new Lewis acid initiator, namely 3,3,3,3'-tetrakis (trifluoro methyl)-1,1' (3H,3H') spirobis (1,2-benzoxasilole) [SBS], in CH_2Cl_2 solution of the monomer at 20 °C. This initiator has also been used for polymerizing several oxetanes[642] in the temperature range of -10 to +20 °C. $\overline{M}_n$ of the polymer ranged from 1 to 6 x 10^4 amu. The kinetic parameters are given in Table 7.6.

Table 7.6. Kinetic parameters[642] of oxetans obtained using SBS initiators

Monomer	*AMMO*	*NMMO*	*BAMO*
Temp (°C)	-15	+10	+20
R_p x 10^4 ($M.sec^{-1}$)	1.9	1.2	0.26

BAMO polymer has been characterized from ^1H and ^{13}C NMR spectra[641]. The peak at 3.3 ppm was assigned to the main chain as well as the side chain methylene groups[640].

Primary degradation studied using effusion mass spectrometric method, showed that E_a for the release of N_2 is 42.7 kcal/mol for BAMO polymer[583]. ΔH_d of BAMO, prepared by bulk and solution methods, was found to be 914.5 J/g and 341.2 J/g, respectively[639]. DSC of poly BAMO shows T_g at -22.8 °C and T_m at 92.2 °C. Poly BAMO has been thoroughly investigated for its crystallization behaviour and the ways to prevent it[645]. Copolymerization of BAMO has been attempted as the most effective way to prevent crystallization and depress the T_g.

The main decomposition products of poly BAMO are HCN, CO, CH_2O, NH_3; the product spectrum does not change in the range 275-400 °C. These products come from the residual nitrene intermediate (RCH_2N), after the evolution of N_2 from the methyl azide group. The two decomposition branches are based on the appearance of HCN and NH_3 (C-C and C-N bond cleavage respectively)[643].

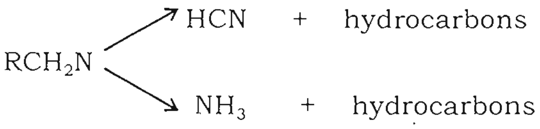

7.4.1 BAMO-NMMO (3-Nitromethyl-3-Methyloxetane) Copolymer

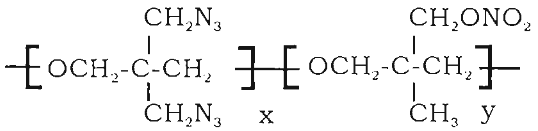

$$-\!\left[OCH_2-\underset{CH_2N_3}{\overset{CH_2N_3}{C}}-CH_2\right]_x\!-\!\left[OCH_2-\underset{CH_3}{\overset{CH_2ONO_2}{C}}-CH_2\right]_y\!-$$

Energetic thermoplastic elastomers have potential application as novel binders in solid propellants. Therefore, multiblock copolymers based on cyclic ether, THF, oxetane and their derivatives have generated considerable interest due to their molecular weight control, low polydispersity, low T_g and energetic characteristics. Block copolyoxetanes are generally synthesized using $BF_3.(C_2H_5)_2O$/ 1,4 butane diol initiating system. However, it has the disadvantage of involving a block linking step and poor molecular weight distribution.

Difunctional BAMO and NMMO were copolymerized in CH_2Cl_2 solution at 25 °C using 1,4-butane diol/$BF_3.(C_2H_5)_2O$ initiating system. The solution of the reactants were stirred for several hours to get the copolymer[634,636.637]. $\overline{M}_n$ and polydispersity of the copolymer were around 3000 and 1.37, respectively. The copolymer was characterized by ^1H and ^{13}C NMR spectra[637]. BAMO-NMMO is the ideal copolymer system in which copolymer composition is approximately the same as the monomer feed. Reactivities of the monomers are similar. The triad microstructures were found to match the theoretical values[637].

In another procedure, difunctional p-bis (α, α–dimethylchloromethyl) benzene (p-DCC) is allowed to react with a cocatalyst, $AgSbF_6$, to generate a carbonium ion, which starts the polymerization of NMMO through formation of the carboxonium ion[640]. Both the ends of p-DCC initiator are allowed to react before BAMO is introduced. It forms a triblock BAMO-NMMO-BAMO copolymer. It may be noted that p-DCC/Ag SbF_6 catalyst system, despite providing narrow polydispersity, does not have the advantage of precise molecular weight control and removal of the residual AgCl impurity[640].

SBS catalyst has been used for living polymerization of oxetane derivatives, such as the following copolymer[644].

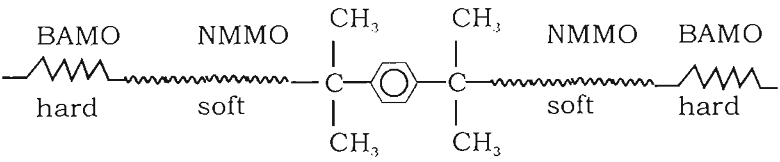

First crystalline and telechelic dihydroxy poly (BAMO), i.e, [HO-(BAMO)$_x$-OH] is made by charging SBS catalyst/1,4 - butane diol /BAMO in a Schlenk reactor for eight days. Poly (BAMO) thus obtained had $\overline{M}_n$=2000 amu and polydispersity 2.4. Similarly, amorphous dihydroxy poly (NMMO), i.e, [HO-(NMMO)$_y$-OH], is made by using SBS and propane diol, the reaction was carried out for three days. It had $\overline{M}_n$=1010 amu and polydispersity 1.85. Poly BAMO - poly NMMO segmented polymer was made by charging poly(NMMO), TDI and dibutyltindilaurate in the Schlenk reactor and carrying out the reaction for 10 h at 50 ^{0}C. Then poly (BAMO) in dioaxane solvent was added and the reaction carried out for 24 h at 80-85 ^{0}C to produce the (BAMO)$_x$-(NMMO)$_y$ copolymer. It was characterized on the basis of ^{1}H NMR spectra. DSC curve of (BAMO)$_x$-NMMO)$_y$ copolymer[644] showed T_g at -3.4 ^{0}C and T_m at 82.2 ^{0}C. Poly (BAMO) shows T_m at 88.1^{0}C and poly(NMMO) shows T_g at -33.2 ^{0}C. The ΔH_f of the copolymer was 17.4 J/g which suggests the presence of 30% BAMO in the copolymer. TG showed a very sharp weight loss which begins at 200 ^{0}C. Most of the polymer pyrolyzed within 1 ^{0}C (224 °C-225 ^{0}C). The sharp decomposition is consistent with the high energy content of the polymer due to the presence of $-N_3$ and $-NNO_2$ groups. Exothermicity of the decomposition was found to be 0.7 kJ/g.

T_g of BAMO-NMMO-BAMO copolymer[640], prepared from p-DCC initiator, was found to be -27 ^{0}C; its T_m was 56 ^{0}C. From TG analysis, the decomposition was found to begin at 170^{0}C, and to be completed at 216 ^{0}C. This shows that this copolymer has good thermal stability. From hazard (impact , friction and electrostatic) point of view, the copolymers are insensitive, but the monomers need to be handled with caution[640]. DSC thermograms of the homopolymers and copolymers prepared using 1,4 butane diol/BF_3. $(C_2H_5)_2O$ initiator, at a heating rate of 10 ^{0}C/min, showed one exothermic peak for the homopolymers and two exotherms for the copolymers in between

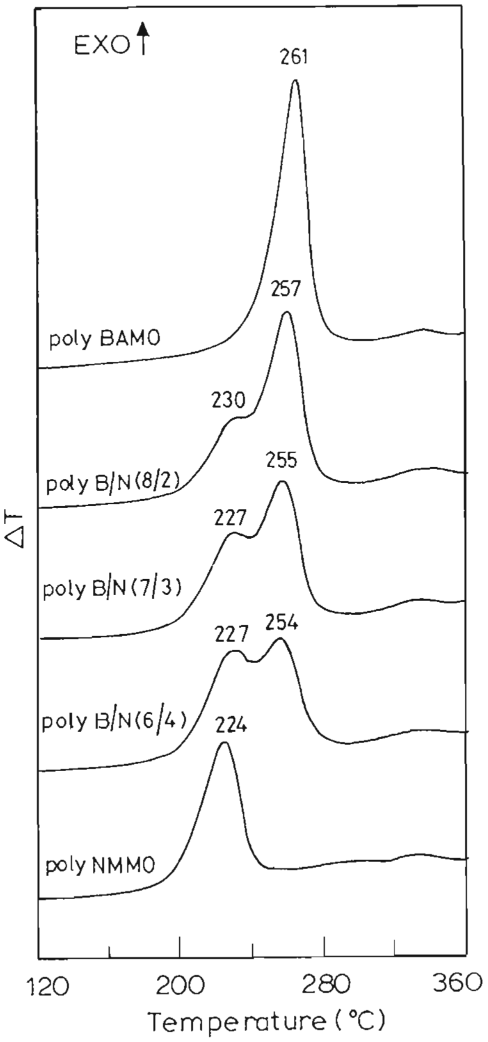

Figure 7.6. DSC thermograms of homopolymers and copolymers.

Source: Characterization of BAMO/NMMO copolymers. Propellants, *Explosives, pyrotechnics*. 1994, **19**, 270-75 (Reproduced with permission from Wiley-VCH Eingang, Weinheim and Dr E. Kimura and Y. Oyumi from Japan Defence Agency)

the temperature range of the homopolymers (Fig. 7.6). From theoretical exothermicity calculations, it was found that decomposition BAMO unit was activated by the heat generated by decomposition of NMMO unit. Poly BAMO-NMMO copolymer 70:30 was found to give maximum ΔH_d. The tensile strength and ΔH_d of the copolymer were higher than those for other copolymers. Poly BMMO - NMMO (70/30) was found to be the best candidate as an advanced energetic binder on the basis of overall sensitivity characteristics[637].

In place of 1,4 butane diol, the soft segment containing an initiating system, namely, OH-terminated polyester (PE)/ BF_3. $(C_2H_5)_2O$, has also been used to improve the mechanical properties of the propellant[64]. The polymerization procedure was the same as used[634.636.637] for 1, 4 butane diol/BF_3. $(C_2H_5)_2O$ system. The CH_2Cl_2 solution of BAMO/NMMO was added to the intitiator for 3 h. The reaction was accomplished at 25 ^{0}C in 6 h. The BAMO/ NMMO/PE molar ratio was 7/ 3/0.33. The $\overline{M}_n$ was 3300 and polydispersity, 1.42. The copolymer was characterized from ^{1}H and ^{13}C NMR spectra. Copolymer samples, containing 29 wt.% DOP, were cured with 1,3,5-tris (6-isocyanate hexyl/-1,3,5-triazine-2,4,6-(1H, 3H, 5H)-trione/IPDI (0.3/0.7 molar ratio, NCO/OH=1.0) at 60 °C for three days. Values of dynamic modulus of BAMO/NMMO/PE elastomer were lower than those for BAMO/NMMO elastomer showing that the former is more elastic[634].

The low temperature mechanical properties of BAMO/NMMO/PE containing propellant were found to be superior to those of BAMO/NMMO propellant due to the presence of PE. Theoretical I_{sp} (at 10 MP_a) of BAMO/NMMO/PE and BAMO/NMMO propellants were found to be 2545 N-S and 566 N-S, respectively. Tensile elongation of BAMO/NMMO/PE at 20 °C was found to be larger than that of BAMO/NMMO propellant. Improvement in tensile elongation at low temperatures played an important role in case-bonding processability and propellant grain design[634].

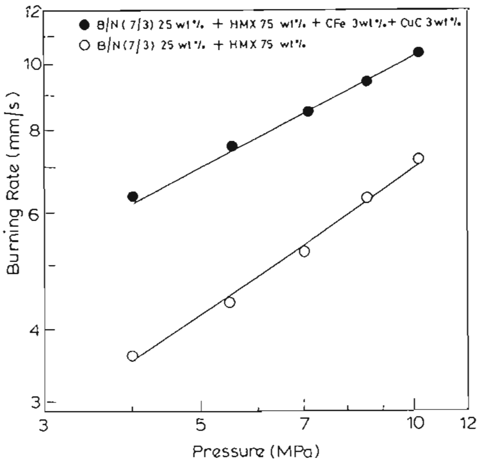

Figure 7.7. Relationship between pressure and burning rate of propellant at 20 °C.

Source: Kimura, E *et al.* Effects of copolymerization ratio of BAMO/NMMO & catalysts on sensitivity and burning rate of HMX propellant. *Propellants, Explosives, Pyrotechnics.* 1995, **20**, 215-25 (Reproduced with permission from Wiley-VCH Eingang, Weinheim and Dr E, Kimura and Dr Y. Oyumi from Japan Defence Agency).

HMX propellant has been made from BAMO/NMMO copolymer, which was prepared using 1,4 butanediol /$BF_3 \cdot (C_2H_5)_2O$ initiator[636]; IDPI and TMP were used as curing and crosslinking agent, respectively. Propellants containing B/N (7/3)/HMX (25/75) were prepared[636] with and without catalysts, B/N (7/3) /HMX/

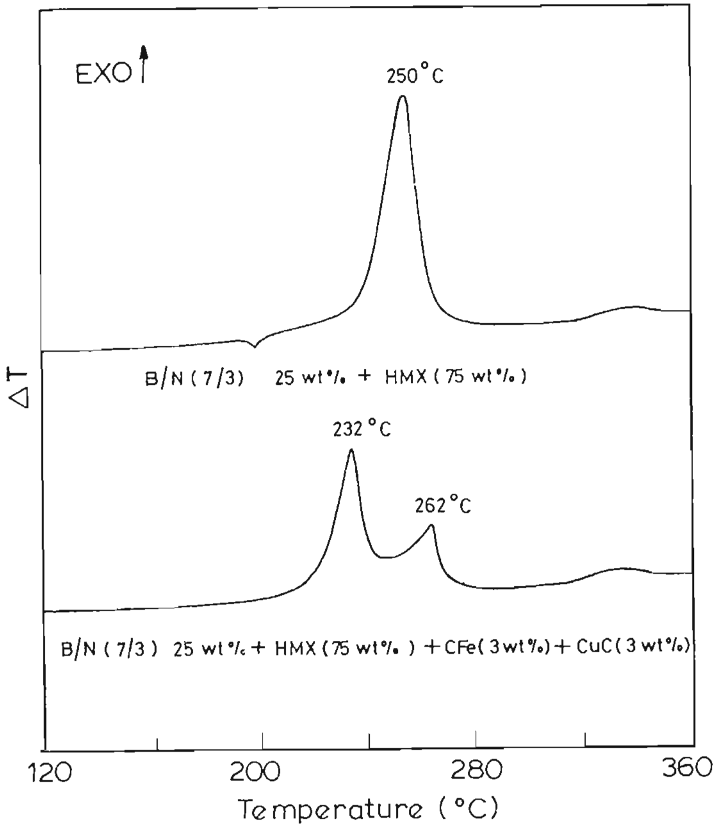

Figure 7.8. DSC thermogram of propellant samples.

Source: Kimura, E *et al* Effects of copolymerization ratio of BAMO/NMMO & catalysts on sensitivity and burning rate of HMX propellant. Propellants, Explosives, Pyrotechnics. 1995, **20**, 215-25 (Reproduced with permission from Wiley-VCH Eingang, Weinheim and Dr E, Kimura and Dr Y. Oyumi from Japan Defence Agency).

catocene (CF_e)/copper chromite ($Cu (CrO_2)_2$) in the proportion 25/75/3/3. The $\dot{r}$ *vs* pressure plot, at 20 °C, is shown in Fig. 7.7. It is seen that the catalysts increase the value of $\dot{r}$ by 1.6 times. DSC thermogram of the propellant is shown in Fig.7.8.

The catalyst mixture splits the main exotherm into two peaks; the exotherm is lowered by 18 °C in the presence of the catalyst mixture. However, DSC exothermicity decreased from 2440 mJ/mg to 1890 mJ/mg on the addition of the catalyst. The catalyst was found to be contributing to the interaction between the products of HMX and the binder. The burning rate equation in the absence and presence of catalyst was found to be:

$$\dot{r} = 1.3\ P^{0.73}\ ;\ \dot{r} = 3.0\ P^{0.53}\ \text{(catalyst)} \qquad (84)$$

Generally speaking the actual application of HMX propellant is difficult because of the low $\dot{r}$ value and high value of pressure exponent. But combination of azide polymer and catalyst significantly improved the $\dot{r}$ characteristics of HMX propellants[636].

7.4.2 BAMO-THF (Tetrahydrofuran) Copolymer[636,639]

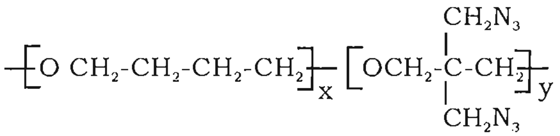

$$-\left[O\ CH_2\text{-}CH_2\text{-}CH_2\text{-}CH_2\right]_x\left[OCH_2\text{-}\overset{CH_2N_3}{\underset{CH_2N_3}{C}}\text{-}CH_2\right]_y$$

THF is known to polymerize as a living system by cationic polymerization; trifilic anhydride (CF_3SO_2) is the most suitable bifunctional initiator for this living polymerization. Synthesis of the energetic thermoplastic copolymer of THF/BAMO[639] involves cationic ring opening polymerization of THF and BAMO with CF_3SO_2 initiator. Triblock copolymers are based on PolyTHF as the centre block and poly BAMO or poly THF-co-BAMO as the end blocks; these are characterized on the basis of IR and ^1H NMR spectra. The reactivities of THF and BAMO, determined from Fineman-Ross plot, were found to be 0.33 and 1.12, respectively. The azide groups of BAMO would offer a higher electron density on the oxygen atoms. This effect makes the BAMO monomer more nucleophilic. BAMO is therefore even more active than THF, which is actually shown by the reactivity ratio data. The oxonium propagating chain ends may possibly be the active species for polymerization of BAMO.

The TG of BAMO-THF-BAMO shows two-step weight loss at 243.5 ^0C and 341.6 ^0C. The first stage of weight loss is the result of decomposition of the methyl azide groups. The same result is seen from DSC also. Exothermicity of the copolymer is a result of decomposition of the methyl azide groups. ΔH_d of THF/BAMO (50/50) copolymer was found to be 298.4 J/g compared to 341.2 J/g for neat poly BAMO.

7.5 AMMONIUM NITRONITRAMIDE OR AMMONIUM DINITRAMIDE NH_4 $[N(NO_2)_2]$ (ADN)

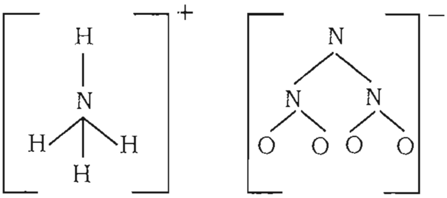

Ammonium salts of strong acids-nitrate (NO^-_3, AN), perchlorate (ClO^-_4, AP), and dinitramide [$N(NO_2)^-_2$, ADN]$^-$ find use in explosives and propellants. Recent synthesis of ADN has provided an example of a new class of stabilized energetic inorganic compound[587]. ADN is a chlorine-free high energy oxidiser, it gives reduced HCl production from propellant plumes and is considered a potential replacement for AP in propellant applications. Its use in propellants leads to significantly reduced levels of harmful contaminants in the upper atmosphere as well as wetland stresses near the launch pad. Hence, there has been intensive interest in the energetics and burning characteristics of ADN[646].

Both AP and AN are produced in bulk and have been the subject of major accident investigations in this century . But synthesis of ADN has been reported only recently and it is not yet widely available. It forms two types of crystals: prismatic and needle type. The former is less sensitive to ignition, friction, impact and electrostatic spark. With a view to preventing major accidents during manufacture, formulation and storage, thermal decomposition studies on ADN have been carried out and the results compared with those for other energetic ammonium salts[648-652].

DSC trace[547] of ADN (in a sealed glass tube) shows an endotherm at 94 °C, exotherm at 189 °C, exotherm at 274 °C and again an endotherm at 301 °C (Fig.7.9). The first endotherm at 94 °C is due to melting of ADN . The exotherm at 274 °C is attributed to the decomposition of AN formed during decomposition of ADN. The endotherm at 301 °C is due to the formation and vaporization of H_2O during decomposition of AN. The major decomposition occurs at 189 °C. The enthalpies of decomposition at 189 °C and 274 °C are; 1.7 kJ/g and 0.2 kJ/g, respectively. In another study[650], DSC was done in aluminium pans, but not under sealed conditions to

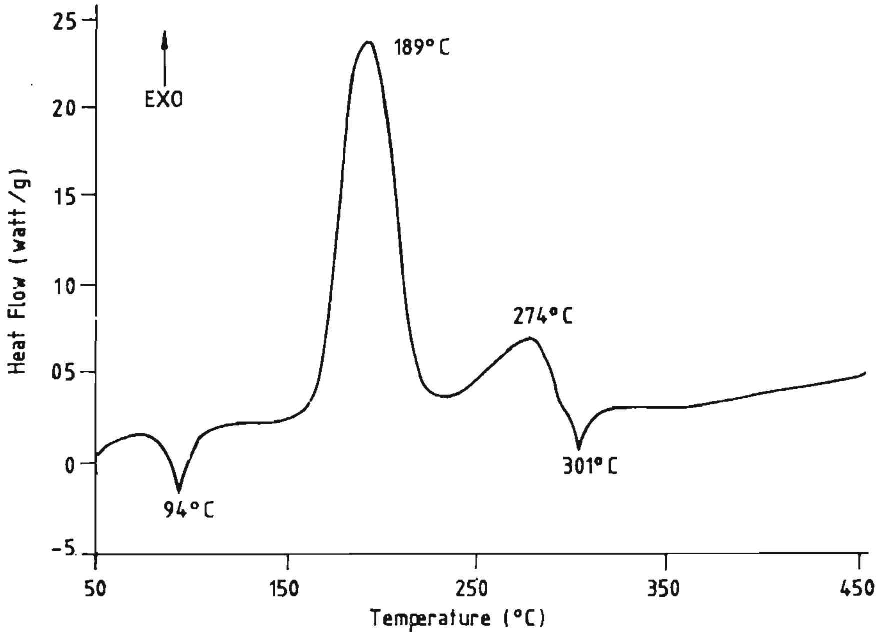

Figure 7.9. DSC trace of ADN at a heating rate of 20 °C/min.

Source: Oxley *et al.* Thermal decomposition studies on ADN ^{15}N and ^{2}H Isotopomers. *J. Phys. Chem.* A 1997, 101, P-5630-58 (Reproduced with permission from American Chemical Society, copyright 1997 and Prof. J. C. Oxley, University of Rhode Island).

avoid the build up of excessive gas pressure during decomposition. T_m was observed at 92 °C. Russel, *et al*[649] reported T_m to be 95°C Variation in T_m could be due to the AN impurity[650] present in the sample . Molten ADN decomposes over the temperature range 130-230 °C. The process is highly exothermic [ΔH_d = 1.96 ± 0.35 kJ/g]. Brill, *et al*[651] reported a low ΔH_d (0.92 kJ/g).

For analysing the decomposition products, ADN was decomposed in a sealed glass tube and heated in a constant temperature bath; the products were analysed in a gas chromatograph[647]. At 230 °C, ADN formed N_2 and N_2O in an approximate ratio of 0.6:0.8. Mass spectral analysis of the gases obtained on decomposition of ^{13}N-labelled ADN showed that 90 % of N_2 comes from the interaction of ammonium nitrogen with the nitrogen of one of the nitro groups. N_2O is formed from one nitrogen coming from nitro group and another from the amino nitrogen. NO was observed in some experiments and it came mostly from the nitro groups on the amino nitrogen[647].

TG-MS experiments give products at lower temperatures and higher pressures favouring the condensed phase reaction mechanism[650]. The formation of gaseous products appears to occur in two stages. The first products detected are N_2O, NO and NO_2. At a later stage, H_2O, HONO, NH_3 and HNO_3 are formed. No evidence was found for O_2 or N_2.

Decomposition of ADN has also been carried out in an IR gas cell in N_2 atmosphere from 20 °C to 250 °C at a heating rate of 0.5-20 °C/min. Major gaseous products detected were N_2O, NO_2, NO, NH_3 and HNO_3. The first decomposition product detected at 50 °C was NO_2, which is followed by the formation of HNO_3. Most of N_2O is formed at a somewhat later stage. Formation of NO and NH_3 is observed[652] only above 100 °C.

Thin film laser pyrolysis of ADN has also been studied. A thin film of ADN, sandwiched between two CsI windows, was placed in a Dewar cell cooled at 77 °K. The sample was then irradiated by pulses from a CO_2 laser; N_2O, N_2O_4 and $(NO)_2$ were detected[652].

Gas cell and TG-MS data show NO_2 and N_2O as the primary decomposition products. Decomposition of molten ADN follows an ionic mechanism involving the formation of NH_4NO_3. One channel of decomposition of ADN seems to be oxygen transfer from NO_2 group to the N atom of another NO_2 group followed by the dissociation of an N-N bond[650].

$$NH_4\,N(NO_2)_2 \rightarrow N_2O + NH_4^+ + NO_3^- \qquad (85)$$

This pathway is consistent with a recent report[649] according to which the pressure-temperature reaction phase diagram, for the solid-state molecular rearrangement reaction, shows the formation of NH_4NO_3 and N_2O. AN is reported to decompose to $N_2O + 2H_2O$ via a mechanism involving the formation of NH_3 and HNO_3 as intermediates. However, the above reaction cannot account for the observation of NO and NO_2 early during decomposition prior to the appearance of NH_3.

The second high temperature channel of decomposition begins with N-N bond rupture and the formation of NO_2 and mononitramide. It starts with proton transfer forming NH_3 and dinitramide followed by N-N bond scission[652] liberating NO_2.

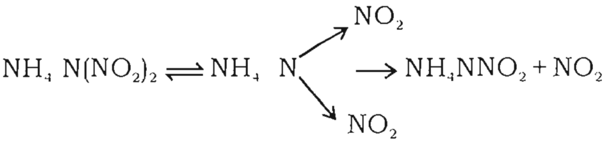

$$NH_4\,N(NO_2)_2 \rightleftharpoons NH_4\,N\begin{matrix}\nearrow NO_2\\ \searrow NO_2\end{matrix} \longrightarrow NH_4NNO_2 + NO_2 \qquad (86)$$

In fact, ADN structure of $[NH_3].[HN(NO_2)_2]$ has been shown to be a more stable structure compared to the structure $[NH_3].[HON(O)NNO_2]$[653]. The mononitride dissociates as follows:

$$NH_4NNO_2 \rightarrow NH_4NO + NO \qquad (87)$$

The net reaction is:

$$(NH_4)\ N\ (NO_2)_2 \rightarrow NO_2 + NO + NH_4NO \qquad (88)$$

N-N bond dissociation requires 184 kJ/mol. This is consistent with the experimental value of 175 ± 20 kJ/mol for the initial step of the reaction. HNO_3 is observed in ADN decomposition experiments, but it appears at a much lower temperature than NH_3. Most probably, HNO_3 is a secondary product of the reaction of NO_2 and H_2O in the heated gas cell. AN could be formed during ADN decomposition in the liquid state at temperatures below its melting point because of the formation of a eutectic with ADN[652].

Laser pyrolysis experiments have shown that at higher temperatures initially, N_2O and NO_2 are formed simultaneously and NO is formed at a much later stage; it is a product of the secondary reaction. The gas cell and laser pyrolysis experiments unequivocally show that N_2O and NO_2 are the primary products followed by the formation of NO at a later stage[652]. These results are in agreement with those of TG-MS experiments, which explains theformation of NO, N_2O and NO_2 in the early stages of decomposition (below 170 ^{0}C). In the later stages, gasification of the remaining ammonium salts results in the formation of NH_3 and H_2O through a combination of ionic and free radical reactions[650]. N_2 has not been detected in the MS study. This is consistent with the formation of AN as an intermediate in the thermal decomposition of ADN. The overall conversion can be represented as[650]:

$$\begin{aligned} 2\ NH_4\ N(NO_2)_2 \rightarrow\ & 3NH_3 + 10\ N_2O + 6\ NO_2 + 15\ H_2O \\ & + 2NO + 6N_2 + HNO_3 + 2NH_4\ NO_3 \qquad (89) \end{aligned}$$

ADN has been proposed as a powerful oxidant for propellants and explosives[654]. Using ADN-paraffin (90:10) mixture corresponding to a maximum I_{sp}, $\dot{r}$ value of 50 mm/s was obtained at 7 MPa and a pressure exponent of 0.8 was obtained. The flame temperature, determined spectroscopically, was found to be 2960 K.

7. 6 HYDRAZINIUM NITROFORMATE (HNF)[655,656]

$N_2H_5\ [C\ (NO_2)_3\ ]$

HNF is a highly efficient high energy oxidizer. It is chlorine-free and produces smokeless and less polluting exhaust gases. HNF is a salt of hydrazine and nitroform. It was discovered in 1951. Attempts have been made to develop a safe method for the synthesis of HNF. HNF is found to be stable when gas evolution from its decomposition is less than 5 cc/g. Use of stabillizers has been attempted to increase its stability, but pure HNF is more stable and does not require the addition of a stabilizer. The products of decomposition of HNF are: CO_2, CO, N_2O , NO and H_2O. HNF is not compatible with HTPB; it attacks its double bond. Therefore, earlier attempts to make HNF propellants were not successful. However, combustion of HNF/Al/GAP has been claimed to be very promising. Its performance appears to be approximately 7% better than that of the corresponding standard propellant. AP/Al/HTPB. Besides, HNF propellants do not produce any Cl_2 or HCl in the exhaust plumes. Therefore, they cause less pollution. HNF propellants ignite very easily at low pressures and give higher values of $\dot{r}$ and pressure exponent. The friction and impact sensitivities of HNF are within acceptable limits, but it is more sensitive than AP.

CHAPTER 8

FUTURE DIRECTIONS

A realistic prognosis of future developments would be to gain more fundamental knowledge about the characteristic properties of individual components through studies on simple model propellant systems. This would allow a better understanding of the combustion phenomena of real propellant systems.

As a prelude, it is first of all, necessary to understand the pressure and temperature-influenced burning surface structure of deflagrating AP, which happens to be the major constituent. Such an analysis of the surface structure permits understanding of the decomposition of AP during its deflagration. These studies should be followed by examination of the vitiated deflagration of AP in the presence of polymeric fuels. Another important aspect of AP deflagration is LPL. An understanding of the decomposition mechanism operative in controlling deflagration-non deflagration at LPL is imperative.

Attempts should also be made to establish a correlation between the structure of the binder and combustion of CSP; parametrical representation of the role of fuel in the overall burning of CSP may be obtained and incorporated in the modelling studies. The effect of molecular weight and its dispersity, functionality of the end groups, crosslinking (which is a processing variation) on the burning behaviour of CSP need to be studied systematically. Analysis of intermittent burning and intermediate pressure extinction seems to be a consequence of the role of the binder at the surface. Analysis should be made to explain both the phenomena on the basis of fuel characteristics.

Most of the studies on the effect of catalyst and its mechanism of action are made under the presumption that CSP can be formulated with predictable $\dot{r}$. However, since the mechanism of action of the catalyst is not very clear it has not permitted such an objective to be achieved. Under the belief that studies on catalyst decomposition cannot be safely extrapolated to burning conditions, a concerted approach of group contribution must be made in predicting the $\dot{r}$ of CSP, based on the characteristics of the catalyst.

It is clear that in ageing studies, inadequate attention has been paid to understanding the ageing mechanism. There is need to understand the degradation of the binders under humid conditions. For development of longevity conferring additives, attention must be focussed on adopting a unified approach that takes into account the effect of humidity besides averting unfavourable changes in ballistic and mechanical properties.

The conventional $\dot{r}$ theories do not adequately explain the chemical effects associated with plateau burning. Perhaps, new experimental techniques which could probe transient burning phenomena may help in gaining an understanding of the underlying chemical processes. Another area that has come into prominence is the combustion chemistry in the presence of oxidizer-deficient formulations of relevance in solid fuel ramjets. The $\dot{r}$ theories for such propellants, their ignition processes, extinction phenomena, etc. may need a renewed look.

Thermophysical properties of propellants and their ingredients in a theoretical model may vary a great deal from author to author. There is a need for reliable experiments and analyses for obtaining authentic thermophysical data.

Just as high pressure decomposition and combustion of AP are relevant in understanding CSP combustion, there is need to study polymer combustion at high pressures, particularly the associated condensed phase characteristics. Such studies may be useful in the combustion modelling of CSP. It is known that decomposition of the binder and the oxidizer is drastically affected by their mutual presence. More quantitative studies are required in this direction to understand the behaviour of individual components under a more realistic situation.

Although the solid propellant field has advanced significantly during the last 50 years, there are still many unresolved problems of significant relevance as far as the new applications are concerned. In some specialized applications, one may encounter pressure larger than 100 atm and, therefore, propellant chemistry has to be re-examined at pressures at least 10-fold higher than those encountered in conventional solid propellants. It would be interesting to see as to how the combustion and ignition theories could be extrapolated to a situation of high pressure performance.

Figure 8.1 shows the distribution of papers and patents on various aspects of GAP. It is obvious that very little work has been

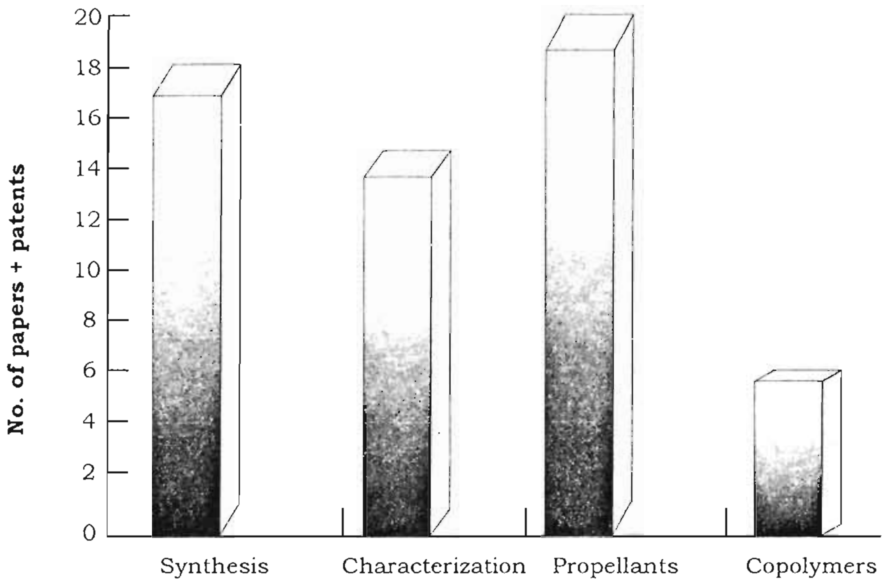

Figure 8.1. Bar diagram showing the number of patents and papers on GAP.

done on copolymers of GAP and hence there is lot of scope for carrying out studies on various GAP copolymers from the points of view of high energy output, easy handling, processing and providing maximum energy. In brief, either by varying the comonomer composition or using different comonomers, one can prepare a wide range of GAP copolymers having specific properties, thus opening a new horizon for the vast applicability of high energy binders. For example, although BAMO possesses more energy than GAP, the former could not find much application due to its crystalline nature. By synthesizing GAP-BAMO copolymer, the energy of this binder will be much more than that of neat GAP,due to the presence of BAMO units. Besides, keeping BAMO concentration at low levels in the copolymer, T_g can also will be kept below room temperature, so that the copolymer remains in liquid state for easy processibilty. In this context, a block copolymer of HTPB and GAP could also provide a wide range of tailored propellant properties for a desired application.

As to the synthesis of GAP, it may be noted that the azidation reaction of PECH results in decrease in molecular weight and hence there is a need to develop new reactive catalysts which could polymerize GA monomer. This would provide a better synthetic approach for developing high molecular weight GAP in one step.

Although thermal degradation of azide-containing high energy polymers has been studied extensively, we do not yet have sufficient knowledge on their primary degradation products as well as the primary degradation mechanism. It is worthwhile to undertake direct pyrolysis-mass spectrometric (DP-MS) and Py-GC-MS studies to establish the mechanism of thermal degradation of these high energy polymers.

CHAPTER 9

REFERENCES

1 Williams, F.A.; Barrere, M. & Huang, N.C. Fundamental aspects of solid propellant rockets. No.116, Technovision Services, Slough, England, 1969, pp. 3-202.

2 Holzmann, R.T. Chemical rockets, flame and explosives technology. Marcell Dekker Inc., New York, 1969, pp. 1-54.

3 Kubota, N. Fundamentals of solid propellant combustion. Prog. Astron. Aeron., AIAA Inc., New York, **90**, 1984, pp. 1-52.

4 Kumar, N.R.R. Fundamentals of solid propellant combustion. Prog. Astron. Aeron., AIAA Inc., New York, **90**, pp. 1984, pp. 409-77.

5 Summerfield, M.; Sutherland, G.S.; Webb, M.J.; Taback, H.J. & Hall, K.P. The burning mechanism of ammonium perchlorate propellant. Prog. Astron. Rocketry, Solid Propellant Rocket Research. 1960, **4**, pp. 141-82.

6 Mastrolia, E.J. & Klager, K. Propellants manufacture: Hazards and testing. Adv. Chem. Ser. (ACS,Washington DC), No.88, 1969, pp. 122-64.

7 Fan, C. The optimization of composite solid propellant. *J. Propulsion Technology,* 1990, 53-8.

8 Gardiner, W.C.(Jr). Combustion chemistry. Springer Verlag, New York, 1984, p. 509.

9 Bernard, J.A. & Bradley, J.N. Flame and combustion (Ed. II). Chapman and Hall Publications, New York, 1985, p. 328.

10 Kuo, K. Principles of combustion. AIAA Publications, New York, 1986, p. 810.

11 Williams, F.A. Combustion theory (Ed. II). The Nikkau Kogyo Shimbum Ltd., Tokyo, Japan, 1987, p. 728.

12 Miller, J.A. & Fisk, G.A. Combustion chemistry. *Chem. Eng. News,* 1987, **65**(35), 22-31, 34-46.

13 Zeldovich, Yu. B.; Librovich, V.B. & Merzhanova, A.G. Combustion: A modern look at an age old process. Priroda (Moscow), 1985, **2**, 30-43.

14 Wagner, H.G. Chemistry and kinetics of combustion process. *EPE, Rev. Energ. Primaire,* 1984, **18**(4), 47-54.

15 Shen, R. & Chen, S. Combustion characteristics of the regional composite propellant. Proc. 20th It. Pyrotech. Semin, 1994, pp. 879-90. Chem. Abstr. 1995.122, 34511v,

16 Brown, R.S.; Anderson, R. & Shannon, L.J. Ignition and combustion of solid rocket propellants. *Adv. Chem. Eng.,* 1968, **7**. 1-69.

17 Waesche, R.H.W.; Wenograd, J. Calculation of solid propellant burning rate from condensed phase decomposition kinetics. *AIAA*, 1969, Paper No. 69-145, New York.

18 Sammons, G.D. Study of the thermal behaviour of solid propellants by differential scanning calorimeter. Analytical Calorimetry, Plenum Press, New York, 1968, p. 305-11.

19 Kishore, K.; Pai Verneker, V.R. & Nair, M.N.R. Condensed phase reactions in solid propellants. *AIAA. J,* 1975, **13**(9), 1230-42.

20 Kishore, K.; Pai Verneker, V.R.; Chaturvedi, B.K. & Gayathri, V. Mechanistic studies on composite solid propellants. *AIAA. J,* 1977, **15**(1), 114-16.

21 Kishore, K.; Pai Verneker, V.R.; Sunitha, M.R. & Prasad, G. Contribution of the condensed phase reaction in the combustion of solid rocket fuels. *Fuel,* 1977, **56**(3), 347-48.

22 Pai Verneker, V.R.; Kishore, K. & Krishna Mohan, V. Correlation between combustion and decomposition of solid propellants. *AIAA. J,* 1975, **13**(10), 1415-16.

23 Kishore, K. & Pai Verneker, V.R. Thermal decomposition studies on ammonium perchlorate-based composite solid propellants. *AIAA. J,* 1976, **14**(7), 966-68.

24 Rastogi, R.P.; Kishore, K. & Singh, G. Solid propellant decomposition studies by differential scanning calorimetry. *Thermochimica Acta,* 1975, **12**(1), 89-96.

25 Kishore, K.; Pai Verneker, V.R. & Sunitha, M.R., Role of condensed phase reactions during the ignition of composite solid propellants. *Thermochimica Acta,* 1977, **19**(2), 232-35.

26 Pai Verneker, V.R.; Kishore, K. & Nair, M.N.R. Importance of condensed phase reactions in solid propellant combustion. AIAA/SAE 11th Propulsion Conf., Anaheim, California, Paper No.75-1202, 1975, pp. 9.

27 Pai Verneker, V.R.; Kishore, K. & Prasad, G. Is ammonium perchlorate in composite solid propellant under strain. *Propellants and Explosives*, 1978, **3**(4), 127.

28 Kishore, K.; Kashyap, A.K. & Prasad, G. Kinetics of propellant decomposition. *J. Chemical Technol. Biotechnol.*, 1978, **29**, 116-19.

29 Kishore, K.; Pai Verneker, V.R. & Nair, M.N.R. Thermal degradation of polystyrene. *J. Appl. polym. Sci.*, 1976, **20**, 2365-66.

30 Pai Verneker, V.R. & Kishore, K. Combustion and thermal decomposition characteristics of composite solid propellants. *Thermochimica Acta*, 1976, **17**(1), 73-93.

31 Kishore, K.; Pai Verneker, V.R. & Subhash, C.B.V. Assessment of the thermal decompositon and combustion behaviour in double base propellants. *J.Spacecraft and Rockets*, 1983, **20**(4), 398.

32 Kishore, K.; Pai Verneker, V.R. & Gayathri, V. Reaction intermediates during combustion and decomposition of some model solid rocket fuels. *Fuel*, 1981, **60**(2), 164-67.

33 Mukundan, T. & Kishore, K. Recent advances in exploring the physicochemical properties of polyperoxides. *Current Science*, 1991, **60**(6), 355-62.

34 Kishore, K.; Pai Verneker, V.R.; Shubha, K. & Sankaralingam, S. Some features of solid propellant chemistry. *Combustion and Flame*, 1982, **46**(1), 323-24.

35 Kishore, K.; Ravindran, K. & Sankaralingam, S. Intermediary analysis during propellant decomposition. *Combustion Science &-Technology*, 1982, **27**(3-4), 155-57.

36 Kishore, K.; Gayathri, V. & Ravindran, K. Formation and degradation of polymeric peroxides. *J. Macromol. Sci. Chem.*, 1981, **A16**(8), 1359-83.

37 Kishore, K. & Ravindran, K. Thermal reactivity of polystyrene peroxide: a thermodynamic approach. *Macromolecules*, 1982, **15**(6), 1638-39.

38 Kishore, K.; Pai Verneker, V.R. & Gayathri, V. Kinetic studies on thermal decomposition of polystyrene peroxide. *J. Anal. Appl. Pyrolysis*, 1980, **1**(4), 315-22.

39 Kishore, K. & Ravindran, K. Effect of temperature, pressure and additive on the pyrolysis of polystyrene peroxide. *J. Anal. Appl. Pyrolysis*, 1983, **5**(4), 363-70.

40 Kishore, K. Mechanism of the thermal decomposition of polystyrene peroxide. *J. Therm. Anal.*, 1981, **21**(1), 15-19.

41 Mukundan, T.; Bhanu, V. & Kishore, K. First report of a polymeric peroxide initiated room temperature radical polymerization of vinyl monomers. *Chemical Communications*, 1989, **12**, 780-81.

42 Kishore, K. Spectral and thermal data on polystyrene peroxide. *J.Chem. Eng. Data.*, 1980, **25**(1), 92-94.

43 Mukundan, T. & Kishore, K. Synthesis, characterization and reactivity of polymeric peroxides: a review. *Prog. Polym. Sci.*, 1990, **15**, 475-505.

44 Mukundan, T. & Kishore, K. Structure and pyrolysis of poly (methylmethacrylate peroxide): a thermochemical approach. *Macromolecules*, 1987, **20**(10), 2382-85.

45 Mukundan, T. & Kishore, K. Poly(vinyl naphthalene peroxide): synthesis characterization and thermal reactivity. *Macromolecules*, 1989, **22**(21), 4430-33.

46 Mukundan, T. & Kishore, K. Synthesis of poly(1,4-divinyl benzene peroxide). *J. Polym. Sci. Polym. Lett.* (Ed)., 1989, **27**(11), 455-56.

47 Jayanthi, S. & Kishore. K. Synthesis and characterization of poly(vinylacetate peroxide). *J. Appl. Polym. Sci.*, 1996, **59**, 1887-90.

48 Kishore. K.; Paramasivam S. & Sandhya, T.E. High pressure kinetics of vinyl polyperoxides. *Macromolecules*, 1996, **29**(22), 6973-78.

49 Murthy. K.S.; Kishore. K. & Krishnamohan, V. Vinyl monomer based polyperoxides as potential initiators for radical polymerization: an exploratory investigation with poly (-methyl styrene peroxide). *Macromolecules*, 1994, **27**(23), 7109-14.

50 Jayanthi. S. & Kishore, K. Oxidative copolymerization: Microstructure analysis of the terpolymer of styrene methyl

methacrylate and oxygen. *Macromolecules,* 1993, **26**(8), 1985-89.

51 Jayanth, S. & Kishore. K. Microstructure of copolyperoxides of (-methyl styrene with styrene and methylmethacrylate. *Macromolecules,* 1996, **29**(14), 4846-52.

52 Murthy, K.S.; Kishore. K. & Krishnamohan, V. Synthesis and characterization of terpolymer of styrene, methylmethacrylate, (-methylstyrene and oxygen). *Macromolecules,* 1996, **29**(14), 4853-58

53 Kishore. K. & Murthy, K.S. Vinylpolyperoxide (oxygen copolymerization). The Polymeric Materials Encylopedia, CRC Press Inc., Florida, 1996, 11, 8378-83.

54 Kishore. K. & Murthy. K.S. Vinyl polyperoxide: a unique class of weak-link polymers. *Ind. Nat. Sci. Acadamy.* 1996, **62A**(2).

55 Kishore, K. & Mukundan, T. Poly(styreneperoxide): an autocombustible polymer fuel. *Nature,* 1986, **324**, 130-31; cited in Chem. & Engg. News, 1986, 17, 32.

56 Mukundan, T.; Annakutty, K.S. & Kishore, K. A novel solid fuel system based on autopyrolyzable polymer. *Fuel,* 1993, **72**(51), 688-89.

57 Kishore, K.; Pai Verneker, V.R. & Prasad, G. Mechanism of aging of composite solid propellants. *Combustion and Flame,* 1979, **36**(1), 79-85.

58 Prasad, G.; Kishore, K. & Pai Verneker, V.R. Effect of aging on ballistic and mechanical properties of propellants. *Combustion and Flame,* 1980, **37**(2), 197-99.

59 Kishore, K.; Pai Verneker, V.R.; Gayathri, V.; Shubha, K.R. & Sridhara, K. Aging Studies on carboxyterminated polybutadiene (ctpb) binder and propellant. *J. Spacecrafts and Rockets,* 1983, **20**(4), 371-75.

60 Kishore, K.; Prasad, G. & Mohandas, K.. Some observations on the aging of composite solid propellants. *Fuel,* 1980, **59**(6), 451-54.

61 Kishore, K.; Pai Verneker, V.R. & Prasad, G. Storage stability of solid rocket fuels: part-II, effect of oxidizer loadings. *Fuel,* 1978, **57**(1), 22-24.

62 Kishore, K.; Sankaralingam, S. & Sameena Begum, A. Changes in the calorometric value of ignition temperature of composite

solid propellants during aging: a note. *Def. Sci. J,* 1986, **36**, 389-94.

63 Kishore, K.; Prasad, G. & Gayathri, V. On increasing the longevity of composite solid propellants. *Ind. J. Technology*, 1981, **19**(6), 212-14.

64 Kishore, K. & Prasad, G. Kinetics of the aging process of composite solid propellants. *Ind. J. Technology*, 1980, **18**(10), 426-28.

65 Kishore, K. & Prasad, G. Survey of solid propellant aging studies. *J. Spacecrafts and Rockets*, 1978, **15**(5), 261-62.

66 Kishore, K.; Pai Verneker, V.R. & Sunitha, M.R. Influence of electric field on the low temperature thermal decomposition of ammonium perchlorate polystyrene propellants. *Combustion and Flame*, 1982, **46**(1), 1-6.

67 Waich, R.E.(Jr). & Strauss, R.F. Fundamentals of rocket propulsion. Reinhold Space Technology Series, Reinhold Publishing Corporation, New York, 1960, p. 30.

68 Barrere, M. Research in the field of solid propellant rockets (a survey). AGARD Conf. Proc., 259, 1979, pp.1-28.

69 Timnat, Y.M. Advanced chemical rocket propulsion. Academic Press, London, UK, 1987, p. 286.

70 Kishore, K. Comprehensive view of the combustion models of composite solid propellants. *AIAA. J,* 1979, **17**(11), 1216-24.

71 Kishore, K. & Sunitha, M.R. Effect of transition metal oxides on decomposition and deflagration of solid propellant system: a survey. *AIAA. J,* 1979, **17**(10), 1118-25.

72 Kishore, K. & Rajalingam, P. Polymer-Filler interactions in HTPB/AP system in the presence of a bonding agent. *J. Appl. Polym. Sci.*, 1989, **37**(10), 2845-51.

73 Crawford, B.L.; Hugget, C.(Jr).; Daniels, F. & Wilfong, R.E. Direct determination of burning rates of propellant powders. *Anal. Chem.*, 1947, **19**, 630-33.

74 Grune, D.; Kegler, W.; Nicolas, M. & Benhaim, P. Studies of the combustion of solid propellants at high pressures. Proc. Int. Symp. Ballist., 3rd Paper.A2, 1977, pp. 12.

75 Osborn, J.R.; Murphy, J.M. & Kershner, S.D. Photographic measurement of the burning rates in solid propellant rocket motors. *Rev. Sci. Inst.*, 1963, 34, 305-30.

76 Osborn, J.R.; Brunick, R.J. & Ho, P.Y. Ind. Report No. I-65-2, Purdue Univ., Lefayette., 1965.

77 Caveny, L.H.; Pokrocos, L.M. & Lelshain, G.R. High pressure burning rates of multibase propellants. Report AMS-1377, Order No.A.D-A060027, 1977, pp. 75.

78 Cauty, F. & De'maraus, J.C. Ultrasonic measurement of the uncured solid propellant burning rate. 21st International Congress, Karlsruhe, FRG, ONERA, TP No.1990-90, 1990, pp. 15.

79 Osborn, J.R. & Bethal, H.E. Technique for measuring burning rates of solid propellants. *Rev. Sci. Intstr.,* 1964, **35**(9), 1130-34.

80 Phung, P.V. & Hardt, A.P. Burning rates of solid propellants by a variable pressure method. *Explosive Stoffe*, 1968, **12,** 274-80.

81 An Fang Lui. A new method for measurement of burning rate of propellant and explosives, *In.* Combustion and detonation phenomena. Proceedings of the 19th International Annual Conference of ICT, Karlsruhe, FRG, (A89-19501 06-28), 1988, pp. 49-1 to 49-11.

82 Richard, B.C. High pressure solid propellant combustion studies using a closed bomb. NASA Accession No.N65-34852. Report No. AD.471575, 1965, pp. 63.

83 Boggs, T.L. & Kraeutle, K.J. Role of the scanning electron microscope in the study of solid rocket propellant combustion. *In.* Ammonium Perchlorate Decomposition and Deflagration. *Combustion Science and Technology,* 1969, **1**(2), 75-93.

84 Muraor, H. Etude Des Lois De Combustion des poudres Colloidates. Sur La Validite de La loi V=a+bP', *Chemie and Industreis,* 1942, **47**(6), 602-06.

85 Hall, A.R. & Pearson, G.S. Ammonium perchlorate; a review of its role in composite propellant combustion. RPE Technical Report, No. 67/1, 1967, pp. 164.

86 Steinz, J.A., Stang, P.L. Summerfield, M.The burning mechanism of ammonium perchlorate based composite solid propellant. AIAA Paper. No. 68-658, 1968.

87 Penner, S.S. Chemical rocket propulsion and combustion research. Gordon and Breach Science Publishers, New York, 1962, p. 132-37.

88 Von Elbe, G.; King, M.K.; McHale, E.T.; Macek, A.; Friedman, R. & Levy, J.B. Chemical kinetics and physical process in composite solid propellant combustion. Atlantic Research Corp. Rept. No. 66307, 1967.

89 Rosen G. Burning rates of solid propellants. *J. Chem. Phys.* 1960, **32**(1), 89-93.

90 Hermance, C.E. A model of composite propellant combustion including surface heterogeneity and heat generation. *AIAA. J*, 1960, **4**(9), 1629-37.

91 Beckstead, M.W.; Derr, R.L. & Price, C.F. A model of composite solid propellant combustion based on multiple flames. *AIAA. J*, 1970, **8**(12), 2200-07.

92 Fenn, J.B. A phalanx model for the combustion of composite solid propellant. *Combustion and Flame*, 1968, **12**(3), 201-16.

93 Kumar, R.N. A new look at AP/composite propellant combustion. *JPL Quarterly Tech. Rev.*, 1973, **3**(2), 53-77.

94 Kumar, R.N. Condensed phase details in the time independent combustion of AP/composite propellants. *Combustion Science and Technology*, 1973, **8**(3), 133-48.

95 Rastogi, R.P.; Singh, H.J.; Deepak, D. & Srivatsava, A.K. Pressure dependence of burning rate of composite solid propellants. *AIAA. J*, 1978, **16**(5), 534-36.

96 Rastogi, R.P.; Singh, R.R. & Rao, A.P. Dependence of burning data of composite solid propellants on pressure. *Combustion and Flame*, 1982, **45**(1), 205-07.

97 Miller, R.R.; Hartman, K.O. & Myers, R.B. Prediction of ammonium perchlorate particle size effect on composite propellant burning rate, Vol.I, CPIA Publication No.196, 1970, p. 567-91.

98 Zaehringer, A.J. & Shorr, M. Solid rocket technology. John Wiley and Sons, Inc., New York, 1967, p. 11-52.

99 Herrick, J.W.; Burgess, E. & Lanford, W. Rocket encyclopedia illustrated. Aeropublishers Inc., Los Angeles, Calif., 1959, p. 348-484.

100 Landers, L.C.; Cohen. J. & Lou, R.L. Negative exponent propellant technology and applications. Int. Jahrrestag. Fraunhofer-Inst-Trieb-Explosivst, 1981, pp. 305-20.

101 Xu, W.; Li, B. Wang, K. Mechanism of steady state burning of composite solid propellant including those with negative pressure exponent. *Acta Astronautica,* 1987, **15**(2), 83-96.

102 Maruizumi, H.; Kosaka, K.; Suzuki, S.; Fukuma, D. & Yamamoto, A. Development of HTPB binder for solid propellant. AIAA, ASME, SAE, and ASEE, 24th Joint Propulsion Conference, Boston, MA, USA, AIAA Paper No. 88-3352, 1988, pp. 6.

103 Powling, J. The combustion of ammonium perchlorate based composite propellant; a discussion on some recent experimental results, ERDE Report, 15/R/15, 1965.

104 Webb, M.J. The dependence of linear burning rate upon pressure for ammonium perchlorate-polyester resin composite propellants. M.S. Thesis, Princeton Univ., Princeton, 1958.

105 Silla, H. Burning rate of composite solid propellants at sub atmospheric pressure. *ARS. J,* 1961, **31**, 1277.

106 Bernard, M.L.; Lallemand, M. & Bourreau, A. Ammonium perchlorate based propellants combustion: behaviour at low pressure. 7th Proc. Int. Pyrotech. Semi., 1980, 2, pp. 934-38.

107 Heath, G.A. & Hirst, P. Some characteristics of the high pressure combustion of double base propellants. 8th Symp.(Int.) on Combustion, The Williams and Wilkins Co., Baltimore, 1962, pp. 711-20.

108 Adams, G.D.; Newman, B.M. & Robins, A.B. The combustion of propellants based upon ammonium perchlorate. 8th Symp. (Int.) on Combustion, Williams and Wilkins Co., Baltimore, 1962, pp. 693-705.

109 Arden, E.A.; Powling, J. & Smith, W.A. Observations on the burning of ammonium perchlorate. *Combustion and Flame,* 1962, **6**(1), 21-33.

110 Barrere, M. & Nadaud, L. Les domaines de combustion des poudres composites. *Rech. Aerospatiale,* 1964, (98), 15-31.

111 Renie, J.P.; Barger, M.E. & Osborn, J.R. Effect of errosive burning on pressure and temperature sensitivity of propellant. CPIA Publication 308 (JANNAF Combust. Meet., 16th V2; ADA 084681), 1979, pp. 153-70.

112 King, M.K. Predicted and measured effects of pressure and crossflow velocity on composite propellant burning rate. Atlantic Research Corpn. Report No. AFOSR-TR-81-0393,

Order No. AD-A098090, Alexandria, Virgina, U.S.A., 1980, pp. 26.

113 Strand, L.D. & Cohen, N.S. Characterization of heterogeneity of composite propellants and its effect on combustion behaviour. CPIA Publications, 412, 1984, pp. 139-52.

114 Jian, Z.Q & Osborn, J. R. Oxidizer size effect on dynamic combustion of AP/HTPB composite propellants. 41st IAF International Astronautical Congress, Dresden, FRG, IAF Paper, No. 90-243, pp. 8.

115 Bloomshield, F.S. & Osborn, J.R. Effect of variable solid phase thermal properties on combustion. CPIA Publication 412, 1984, p. 233-40.

116 King, M.K. Modelling of pressure-coupled response function of solid propellants. 19th Symp. (Int). Combustion, 1982, pp. 707-15.

117 Cherng Lui, A. Effects of composition on combustion instability of composite solid propellants. *J. Chinese Society of Mechanical Engineers,* 1988, **9**, 327-32.

118 Bruno, C.; Riva, G.; Zanotti, C.; Donde, R.; Grimaldin, C.; Deluca, L.; Experimental and theoretical burning of solid rocket propellant near the pressure deflagration limit. *Acta Astronaut.*, 1985, **12**(15), 351-60.

119 Shannon, L.J. Composite propellant ignition by radiant energy. *AIAA. J,* 1970, **8**, 343-46.

120 Lengelle, B.; Brulard Z. & Moutet, M. Combustion mechanism of composite solid propellants. 16th Symp. (Int) on Combustion, Pittsburgh, pa, 1976, pp.1257-69.

121 Boggs, T.L.; Derr, R.L. & Beckstead, M.W. The surface structure of AP composite propellants. *AIAA.J,* 1970, **8**(2), 370-72.

122 Sarner, S.F. Propellant chemistry. Reinhold Publishing Corporation, New York, 1966, pp. 328-29.

123 Irwin, O.R.; Salzman, P.K. & Anderson, W.H. Mechanism of the accelerated burning of ammonium perchlorate at high pressure. *AIAA. J,* 1963, **1**(5), 1178-80.

124 Siefert, J.G. & Kuo, K.K. Crack propogation in burning solid propellants. Prog. Astronaut. Aeronaut. (Dyn. Shockwaves, Explosives, Detonations), 1984, pp. 575-95.

125 Kuo, K.K. & Moreci, J.A. Crack propagation and branching in burning solid propellants. 21st Symp.(Int.) on Combustion, Munich, West Germany, 1988, pp. 1933-41.

126 Kishore, K.; Sridhara, K & Srikanthan, D. Combustion studies on magnesium containing fuel-rich solid propellants: A thermodynamic approach. Unpublished results.

127 Bouck, L.S. A high heating rate thermal analysis of solid propellant reactions. Ph.D. Thesis, Dept. of Chemical Engg., Univ. of Utah, 1971.

128 Waesche, R.H.W.; Wenograd, J. & Feinauer, L.R. Investigations of solid propellant decomposition characteristics and their relations to the observed burning rate. ICRPG/AIAA, Second Solid Propulsion Conference, Preprint, 1967, pp. 26-37.

129 Eisenreich, N. & Pfeil, A. Thermal analysis of double base propellants by pressure DSC. Proc. Ist European Symp. on Thermal Anal. Edt, Dolimore, 1976, pp. 452-54.

130 Warren, F.A. Rocket propellants. Reinhold Publishing Corp., New York, 1958, pp. 93-94.

131 Hugget, C.; Bartley, C.E. & Mark, M.M. Solid propellant rockets. No.2. Princeton Aeronautic Paperbacks, Princeton, New Jersey, 1960, p. 33-130.

132 Cohen, N.S. & Flanigan, D.A. Mechanism and models of solid propellant burn rate temperature sensitivity; A review. *AIAA. J*, 1985, **23**(10), 1538-47.

133 Schoyer, H.F.R. & Korting, P.A.O.G. Combustion behaviour of composite propellant at sub-atmospheric pressure. *Acta Astronaut.*, 1986, **13**(2), 55-61.

134 Schoyer, H.F.R. & Korting, P.A.O.G. Propellant combustion at low pressures. *Combustion and Flame.* 1986, 63(3), 317-27.

135 Xu, W., Hamke, R.E. Osborn, J.R. Motor temperature sensitivity for negative exponent composite propellants. AIAA, 26th Aerospace Sciences Meeting, Reno, NV, USA, AIAA Taper No. 88-0244. pp. 8.

136 Hamke, R.E & Osborn, J.R. The effect of aluminium concentration on motor temperature sensitivity. AIAA, 26th Aerospace Sciences Meeting, Reno, NV, USA, AIAA Paper No.88-0245, pp. 6.

137 An-Lu Leu Ru-Jau Wu. Formulation effects on the burning rate of aluminized solid propellant. *J. Propulsion and Power*, 1988, **4**, 22-26.

138 Bernard, F. Initial temperature sensitivity of the combustion rate of AP-based solid composite propellants and fuel-rich propellants. La Recherche Aerospatiale, 1989, (6), 67-76.

139 Kubota, N. & Miyazaki, S. Temperature sensitivity of burning rate of ammonium perchlorate propellants. *Propellants Explosives Pyrotechnics,* 1987, **12**(6), 183-87.

140 Cornelisse, J.W.; Schoyer, H.F.R. & Wekker, K.F. Rocket propulsion and spaceflight dynamics. Pitman Publications, 1979, p. 174-77.

141 Takashi, H. Effects of particle diameter on burning rate at various pressure and initial temperature. *Kogyo Kayaku Kyokaishi,* 1961, **22**(3), 132-37.

142 Lukashenya, C.V.; Malinenko, C.H.; Bakhmann, N.N. & Belayaev, A.F. Temperature coefficient of the combustion rate of condensed mixtures at varying component ratios. Fiz. Goreniya i Vzryva, 1966, 3, 59-66.

143 Kishore, K. & Sridhara, K. Effects of temperature on the burning rate of solid propellants. *J. Propul. Power,* 1986, **2**(3), 193-94.

144 Blair, D.W. Initial temperature and pressure effects on composite solid propellant burning rates: comparisons with theory. *AIAA.J,* 1970, **8**(8), 1439-43.

145 Northam, G.B.; Pellet, C.L. & Cofer III, W.R. Effects of low temperature ammonium perchlorate decomposition on the ballistic properties of a CTPB propellant. *AIAA, J,* 1972, **10**(8), 1068-72.

146 Ewing, D.L. & Osborn, J.R. Burning rate temperature sensitivity of composite solid propellants. *J. Spacecrafts and Rockets*, 1971, **8**(3), 290-92.

147 Ebenzer, J.; Cole, R.B. & McAlevy, R.F. Steady state burning of ammonium perchlorate composite solid propellants. US. Natl., Tech. Inform. Serv., AD Report No.762600, 1973, pp. 146.

148 Cohen Nir, E. Temperature sensitivity of the burning rate of composite solid propellants. *Combustion Science and Technology,* 1974, **9**(5-6), 183-94.

149 Trittmater, R.C.; Holmes, H.E. & Ward, J.R. Sensitivity of burning rate to initial temperature for a binary magnesium-

sodium nitrate mixture. ARBRL-NE-02589, AD-E480186, Report Order No.A066119, 1978, pp. 22.

150 Renie, J.P.; Condon, J.A. & Osborn, J.R. Oxidizer size distribution effects on propellant combustion. *AIAA. J,* 1979, **17**(8), 877-83.

151 Condon, J.A.; Renie, J.P. & Osborn, J.R. Temperature sensitivity of propellant burning rates. *Combustion and Flame,* 1977, **30**(3), 267-76.

152 Nakagawa, T.W. & Rudy, T.P. Solid composite propellant composition containing carboxy terminated polymers. US Patent No. 3,837, 939, 1974, pp. 7.

153 Osborn, J.R.; Renie, J.P. & Murphy, J.M. Effect of errosive burning on pressure and temperature sensitivity. *Acta Astronaut.,* 1984, **11**(7-8), 459-67.

154 Miyazaki, S. & Kubota, N. Temperature sensitivity of AP based composite propellants. *Kogyo Kayoku,* 1983, **44**(6), 341-46.

155 Glick, R.L. & Condon, J.A. Statistical analysis of polydisperse, heterogeneous propellant combustion: steady state, 13th JANNAF Combust. Meet., CPIA Publication 281, Vol.II, 1976, pp. 313-45.

156 Glassman, I. The plateau region of composite propellants Chem. Phys. Processes. Combust. 1994, 211-13.; Chem. Abstr. 1995, 122, 137590 z,

157 Ishihara, A. & Brewater, M.Q. Combustion studies of B, Mg and Al Composite propellants. *Combust. Sci. Technol,* 1993, **87**(1-6), 275-90.

158 Zhao, Y. Tian, D. Simulating computation of temperature sensitivity of burning rate of composite solid propellant. *J. Propulsion Technology,* 1990, 48-51.

159 Schroeder, M.A.; Fifer, R.A.; Miller, M.S.; Pesce-Rodriguez R.A & Selawski, C.J. Solid propellant combustion. Preliminary depth profiling studies on XM39, JA2, M 9, M 30 and HMXL. Report 1994, ARL-TR-346 Gov. Rep. Announce. Index (4.5) 1994, Vol.94, No.13. ; Chem. Abstr., 1995, 123, 261215 r.

160 Hamke, R.E.; Gaunce, M.T. & Obsorn, J.R. The effect of pressure exponent on temperature sensitivity. *Acta. Astronautica,* 1987, **15**(6-7), 377-82.

161 Martynyuk, V.F.; Khasainov, B.A.; Sulimov, A.A. & Sukoyan, M.K. Evaluation of heat evolution in detonation of non-

compacted ammonium perchlorate. *Fiz. Goreniya i Vzryva,* 1987, **23**(1), 64-67.

162 Zhao, Y.; Tian. D. & Jisuanj, Yu. Simulation study of explosive combustion of ammonium perchlorate. *Yingyong Huaxro,* 1987, **4**(1), 77-78.

163 Jacobs, P.W.M. & Whitehead, H.M. Decomposition and combustion of ammonium perchlorate. *Chem. Rev.*, 1969, 69, 551-90.

164 Boldyrev, V.V. Mechanism of the thermal decomposition of ammonium perchlorate. *Dok1. Akad, Nauk.* SSSR, 1968, **181**(6), 1406-9.

165 Keenan, A.G. & Siegmund, R.F. Thermal decomposition of ammonium perchlorate. Quart. Rev., 1969, **23**(1), 430-52.

166 Hagihara, Y & Bankid, M. Effect of porous ammonium perchlorate on burning rate & slurry viscosity of AP-HTPB composite propellants. *Kogyo Kayaku,* **51**(2), 65-69.; Chem. Abstr., 1990. 113, 62296 m.

167 Leu, A.L. & Yeh, T.F. Thermal characteristics of residual ammonium perchlorate and the role of the same in the burning of solid propellant. Int. Ann. Conf. ICT (Combust. React. Kinet.) Vol. 51, No.12, pp. 1-51.; Chem. Abstr 115, 1991, 23587u .

168 Chang, C.; Huang, T.F.; Yeh, Liu, C.S. & Len, A.L. Characteristics of porous ammonium perchlorate. *Len Prop. Explos. Pyrotech.*1990, **15**(6), 261-65.; Chem. Abstr 114, 65310t, 1991.

169 Min, K.J. & Kelly, F.N. Structure - property relationships of highly filled elastomeric composites as model solid propellants. Int. Annu. Conf. ICT 21, 1990 Techno. Polym. Compd. Energy. Mater.) **28**, No.17, 1-28.; Chem. Abst 199, 1114, 26753v.

170 Ninan, K.N.; Mahadevan, A. & Ramasubramanium, T.S. A direct and rapid volumetric estimation of AP as a process check in propellant manufacture. Int. Annn. Conf. ICT. 1994, 25th energetic materials analysis, characterization and test techniques , Vol.68, No.7, pp. 1- 68.; Chem. Abstr 1995, 122, 13155 s.

171 Kohga, M. Hagihara, Y. AP-HTPB composite propellant using ultrafine ammonium perchlorate prepared by freeze-dry method. *Kogyo Kayaka,* 1993, **54**(2), 64-69. Chem. Abstr., 1993, 119, 229461z.

172 Pai Verneker, V.R.; McCarty, M.(Jr) & Maycock, J.N. Sublimation of ammonium perchlorate. *Thermochimica Acta*, 1971, **3**(1), 37-48.

173 Pai Verneker, V.R.; Kishore, K. & Kannan, M.P. Sublimation and thermal decomposition of ammonium perchlorate. *Chem. Eng. Sci.*, 1977, **32**, 1114-15.

174 Pai Verneker, V.R.; Kishore, K. & Kannan, M.P. Effect of pretreatment on the sublimation of ammonium perchlorate. *J. Appl. Chem. Biotechnol.*,1977, **27**(6), 309-17.

175 Pai Verneker, V.R.; Kishore, K.; Chaturvedi, B.K. & Ramanath, M. Some observations on sublimation and decomposition of ammonium perchlorate. *Propellants and Explosives*, 1981, **6**, 158-60.

176 Prasad, G. Mechanistic studies on aging behaviour of composite solid propellant. Ph.D. Thesis, Indian Institute of Science, Bangalore, India, 1978.

177 Kishore, K.; Pai Verneker, V.R. & Prasad, G. Storage stability of solid rocket fuels. 1. effect of temperature. *Fuel*, 1977, **56**(3), 292-94.

178 Pai Verneker, V.R.; Kishore, K. & Prasad; G. Effect of preheating on the burning rate of solid propellants. *AIAA. J*, 1976, **14**(9), 1330-31.

179 Kishore, K. & Prasad, G. Aging of composite solid propellants. *J. Sci. Ind. Res.*, 1979, **38**(8), 414-23.

180 Guirao, C. & Williams F.A. A model of ammonium perchlorate deflagration between 20 atm and 100 atm. *AIAA. J*, 1971, **9**(7), 1345-56.

181 Manelis, G.S. & Strunin, V.A. The mechanism of ammonium perchlorate burning. *Combustion and Flame*, 1971, **17**(1), 69-78.

182 Price, C.; Boggs, T.L. & Derr, R.L. Modelling of solid monopropellant deflagration. AIAA, 16th Aerospace Sci. Meet., Huntsville, Alabama, 16-18, Pap. 78-219, 1978, pp. 12.

183 Sohn, H.Y. A unified theory of ammonium perchlorate deflagration and the low pressure deflagration limit. *Combustion Science and Technology*, 1975, **10**(3-4), 137-54.

184 Hertzberg, M., Oxid. Combust. Rev., 1971, 5, 1.

185 Rosser, W.A, (Jr.), Inami, S.H., Wise, H. Thermal diffusivity of ammonium perchlorate. *AIAA. J.*, 1966, **4**, 663.

186 Caveny, L.H.; Pittman, C.U. (Jr). Contribution of solid phase heat release to AP composite propellants burning rate. *AIAA. J,* 1968, **6**(8), 1461-67.

187 Beckstead, M.W.; Derr, R.L. & Price, C.F. The combustion of solid monopropellants and composite propellants. 13th Symp.(Int.) on Combustion, The Combustion Institute, Pittsburg, Pa, 1971, pp. 1047-56.

188 Rajeshwar, K. Effect of prior treatment on the chemical reactivity of inorganic perchlorate. Ph.D. Thesis, Indian Institute of Science, Bangalore, 1975.

189 Luca, L.D.; Galfelli, L. & Zanoti, C., Ignition and extinction of solid rocket propellants. Symp. Solid Rocket. Motor Technol., 53rd AGARD Meeting, 1977, pp. 12.

190 Kishore, K.; Pai Verneker, V.R. & Krishnamohan, V. Differential scanning calorimetric studies on ammonium perchlorate. *Thermochimica Acta,* 1975, **13**(3), 277-92.

191 Markowitz, M.M. & Boryta, D.A. Aspects of crystallographic transition of ammonium perchlorate. *Am. Rocket. Soc. J,* 1962, 32, 1941-42.

192 Cohen, N.; Fleming, R.N. & Derr, R.L. Role of binders in solid propellant combustion. *AIAA. J,* 1974, **12**(2), 212-18.

193 Inami, S.H.; Rosser, W.A. & Wise, H. Dissociation pressure of ammonium perchlorate. *J. Phys. Chem.,* 1963, **67**(5), 1077-79.

194 Kishore, K. & Pai Verneker, V.R. Enthalpy and activation energy for the sublimation of solids involving proton transfer process. *J. De Chimie Physique,* 1977, **74**(10), 997-1000.

195 Waesche, R.H.W. & Wenograd, J. The effect of pressure and additives on the kinetics of decomposition of ammonium perchlorate. United Aircraft Research Lab., East Hartford, Conn., Report No. WSCI-67-8. 1967, pp. 1-16.

196 Beachell, H.C. & Hackman, E.E. Combustion characteristics of crystalline oxidizer. *AIAA. J,* 1968, 16, 561-64.

197 Wenograd, J. Shinnar, R. Combustion of ammonium perchlorate; some negative conclusions. *AIAA. J,* 1968, **6**(5), 964-66.

198 Pai Verneker, V.R.; Kishore, K. & Kannan, M.P. Effect of doping on the sublimation of ammonium perchlorate. Phys. Chem., 1976, **80**(15), 1735-36.

199 Kishore, K.; Pai Verneker, V.R. & Pitchaiah, K. Studies on vacuum pyrolysis of ammonium perchlorate and ammonium perchlorate/polystyrene propellants in the presence of transition metal oxides. *J. Anal. Appl. Pyrolysis*, 1980, **2**, 45-52.

200 Kraeutle, K.J. The thermal decomposition of ammonium perchlorate. Western State Section, The Combustion Institute, 1969.

201 Boldyrev, V.V.; Savintsen Yu.P.; Mulina, T.V. & Chehetinina, G.V. Physicochemical causes of the formation and growth of reaction nucleii during the thermal decomposition of ammonium perchlorate. *Kinet. Katal.*, 1970, **11**(5), 1131-39.

202 Kishore, K. & Gayathri, V. Chemistry of ignition and combustion of ammonium perchlorate-based propellants. (Chp 2), *In* Fundamentals of Solid Propellant Combustion, K.K. Kuo & M. Summerfield (Eds) Prog. Astron. Aeron., AIAA Inc., New York, Vol. 90, 1984, pp. 53-119.

203 Bircumshaw, L.L. & Phillips, T.R. Kinetics of thermal decomposition of ammonium perchlorate. J. Chem. Soc., Part IV, 1957, 4741-47.

204 Jacobs, P.W.M. & Jones, R.A. Sublimation of ammonium perchlorate. *J. Phys. Chem.*, 1968, **72**(1), 202-07.

205 Galway, A.K. & Jacobs, P.W.M. High temperature thermal decomposition of ammonium perchlorate. J. Chem. Soc., (Part I), 1959, 837-44.

206 Simchen, A.E. Decomposition equations of ammonium perchlorate. *J. Appl. Chem.,* 1963, 13, 369-74.

207 Oxley, J.C.; Smith, J.L. & Velenzuela, B.R. Ammonium perchlorate decompostion: heat and solution. *J. Energ. Mater.*, 1995, **13**(1&2), 57-91.

208 Stone, R.L. Differential thermal analysis by the dynamic gas technique. *Anal. Chem.*, 1962, **32**(12), 1582-88.

209 Morisaki. S. & Komamiya, K. Differential thermal analysis and thermogravimetry of ammonium perchlorate at pressures upto 51 atm. *Thermochimica Acta,* 1975, **12**(3), 239-51.

210 Schmidt, W.G. The effect of solid phase reaction on the ballistic properties of propellants. Aerojet Solid Propul. Co., Sacromento, Calif., 1) NASA Contract NAS 1-7816, NASA CR 66757, 1969, pp. 49.

211 Sammons, G.D. Dynamic calorimetric solid propellant combustion studies. AIAA. 5th Propulsion Joint Specialists Conf. Colarado, USA, No.69-504, 1969, pp. 10.

212 Kraeutle, K.J. Decomposition of ammonium perchlorate below the phase transition temperature. ICRPG, 3rd Combustion Conf., CPIA Publication 138, Vol.1, 1967, pp. 45.

213 Osada, H. & Sakamoto, E. Thermal decomposition of ammonium perchlorate. *Kogyo Kayaka Kyokaishi,* 1963, **24**(5), 236- 44.

214 Mayer, S.W.; Weinberg, E.K. & Schieler, L.R. Procedures for suppressing premature exothermic decomposition in ammonium perchlorate. *AIAA. J,* 1970, **8**(7), 1328-34.

215 Rajeshwar, K.; Rosenvold, R. & Dubow, J. Electric field effects in the thermal decomposition of solids. *Nature* (London). 1983, **301**(5895), 48-49.

216 Galwey, A.K. & Jacobs, P.W.M. The thermal decomposition of ammonium perchlorate at low temperature Proc. Roy. Soc., A., 1960, 254, pp. 455-69.

217 Maycock, J.N. & Pai Verneker, V.R. Role of point defects in the thermal decomposition of ammonium perchlorate Proc. Roy. Soc. A., 1968, 307, 303-15.

218 Boldyrev, V.V.; Savintsev, Yu.P. & Mulina, T.V. Mechanisms of formation and growth of the nuclii in the thermal decomposition of ammonium salts. Proc. 7th Intern. Symp. On the Reactivity of Solids, Bristol, 1972, pp. 421-30.

219 Pai Vernekar, V.R. & Varadaraju, U.V. Chemistry of the incomplete decomposition of ammonium perchlorate(AP). *J. Solid State Chem.,* 1970, **29**(2), 215-20.

220 Davies, J.V.; Jacobs, P.W.M. & Russel-Jones, A. Thermal decomposition of ammonium perchlorate. *Trans. Faraday. Soc.,* 1967, **63**(Pt 7), 1937-1748.

221 Varadaraju, U.V. Mechanism of incomplete decomposition of ammonium perchlorate. Ph.D. Thesis, Indian Institute of Science, Bangalore. India, 1979, pp. 115-23.

222 Pearson, G.S. & Jacobs, P.W.M. Mechanism of the decomposition of ammonium perchlorate. Clearinghouse Fed. Sci. Tech. Inform., AD.NO.702569, 1969, pp. 28.

223 Koroban, V.A.; Guk, V.P. & Svetlov, B.S. Study of the formation and decomposition of perchloric acid in ammonium perchlorate. Tr. Mosk. Khim. Teckhnol. Inst. Im. DI-Mendeleeva, 1980, 112, 63-66.

224 Koroban, V.A. & Guk, V.P. Thermal decomposition of deuterated ammonium perchlorate. Tr. Mosk. Khim. Teckhnol. Inst. Im. DI- Mendeleeva, 1980, 112, 51-58.

225 Pai Verneker, V.R.; Kishore, K. & Sunitha, M.R., Effect of electric field on ammonium perchlorate decomposition. *J. Solid State Chem.,* 1978, **26**(2), 203-07.

226 Rubtsov, Yu, I. & Manelis, G.B. Mechanism of the thermal decomposition of ammonium perchlorate. Makhanism Term. Razlozheniya. Perkhlorata. Ammoniya, Chernogolovka. 1981, pp. 123-29.

227 Khairetidinov, E.P.; Mulina, T.V. & Boldyrev, V.V. Mechanism of nucleation during the low temperature decomposition of ammonium perchlorate. Makahanizm Term. Razlozheniya. Perkhlorata Ammoniya, Chernogolovka, 1981, pp. 101-23.

228 Koroban, V.; Svetlov, B.S.; Guk, V.P. & Smirnova, T.I. Mechanism of the thermal decomposition of ammonium perchlorate. Mekhanizm. Term. Razlozheniya Perkhlorata, Ammoniya, Chernogolovka, 1981, pp. 5-29.

229 Bircumshaw, L.L. & Newman, B.H. The thermal decomposition of ammonium perchlorate. ERDE Report No.8/EMR/50, 1951.

230 Bircumshaw, L.L. & Newmann, B.H. The thermal decomposition of ammonium perchlorate. *In.* Introduction, Experimental, Analysis of Gaseous Products and Thermal Decomposition Experiments, Proc. Roy. Soc.A., 1954, 227, pp. 115-32.

231 Bircumshaw, L.L. & Newmann, B.H. The thermal decomposition of ammonium perchlorate II. the kinetics of the decomposition, the effect of the particle size, and discussion of the results., Proc. Roy. Soc. A., 1955, 27, 228-41.

232 Isaev, R.N.; Zakhanov, Yu. A. & Bordachev, V.V. Mass spectrometry of gaseous products of ammonium perchlorate thermolysis. *Z. Fiz. Khim.,* 1970, **44**(2), 302-5.

233 Boldyrev, V.V.; Aleksandrov, V.V.; Boldyreva, A.V.; Gritsan, V.I.; Karpenko, Yu.Ya.; Korobenichev, P.P.; Panifilov, V. & Khanetidenov, F. Mechanism of the thermo decomposition of ammonium perchlorate. *Combustion and Flame,* 1970, **15**(1), 71-77.

234 Khairetidinov, E.F.; Medvinskii, A.A. & Boldyrev, V.V. Initial stage of the thermal decomposition of ammonium perchlorate. Kinet. Katal., 1970, **11**(5), 1343-45.

235 Khairetidinov, E.F.; Boldyrev, V.V. & Burshtem, I. I. On the mechanism of conductivity of ammonium salts. *J. Solid State Chem.,* 1974, **10**(3), 288-93.

236 Khairetidinov, E.F.; Mulina, T.V.; Boldyrev, V.V. Nucleation mechanism during low temperature decomposition of ammonium perchlorate. *J. Solid State Chem.,* 1976, **17**(1 & 2), 213-19.

237 Kaidimov, B. Effect of ammonia on the thermal decomposition of orthorhombic and cubic ammonium perchlorate. *Thermochimica Acta,* 1983, **62**(1), 87-89.

238 Tang, S.P. & Fenn, J.B. Vacuum sublimation of ammonium perchlorate. *J. Phys. Chem.,* 1973, **77**(7), 940-44.

239 Thomas, D.; Bregeon, B.; Cointol. A. & Hardy, Bernard, M.L. Effect of the gaseous phase and catalysts on the thermal decomposition of ammonium perchlorate. Prog. Vac. Microbalance. Tech., 1975, 3, 281-92.

240 Solymosi, F. & Borcsok, S. Pyrolysis of ammonium perchlorate in a stream of perchloric acid vapour. *Combustion and Flame,* 1975, **25**(1), 135-36.

241 Osada, H. & Kakinouchi, N. Initiation of ignition of solid composition propellants. *Kogyokayuku Kyokaishi,* 1965, **26**(4), 200-11.

242 Maycock, J.N. & Pai Verneker, V.R. Kinetics and mechanism of the thermal decomposition of nitronium perchlorate. *J. Phys. Chem.,* 1968, **72**(12), 4004-9.

243 Dedgaonkar, V.G. & Sarwade, D.B. Radiation effects on the thermal decomposition of ammonium perchlorate. *J. Radional. Nucl. Chem.,* 1992, **165**(5), 269-75.

244 Kishore, K.; Pai Verneker, V.R. & Sridhara, K., Thermoanalysis of ammonium perchlorate and sodium nitrate mixture. *J. Solid State Chem.,* 1983, **46**(2), 209-14.

245 Solymosi, F. Structure stability of salts of the halogen oxyacids in the solid phase. Wiley, London, 1977.

246 Galwey, A.K. & Mohamed, M.A. Nitrylperchlorate as the essential intermediate in the thermal decomposition of ammonium perchlorate. *Nature* (London), 1984, **311**(5987), 642-45.

247 Galwey, A.K. & Mohamed, M.A. The low temperature thermal decomposition of ammonium perchlorate: nitrylperchlorate

as the reaction intermediate. Proc. Roy. Soc. London A., 1984, **396**(1811), 425-40.

248 Galwey, A.K. & Mohamed, M.A. The formation of nitryl perchlorate as an intermediate during the low temperature decomposition of ammonium perchlorate. *J. Chem. Soc. Chem. Commun.*, 1984, (18), 1197-98.

249 Pai Verneker, V.R.; Kishore, K. & Varadaraju, U.V. Chemical changes during the aging and decomposition of composite solid propellant. *Combustion and Flame*, 1982, **45**(2), 137-46.

250 Khairetidinov, E.F. & Boldyrev, V.V. The mechanism of the low-temperature decomposition of NH_4ClO_4. *Thermochemica Acta,* 1980, **41**(1), 63.

251 Dode, M. & Sur, la. Decomposition thermique du perchlorate d'ammonium influence de la temperatures sur la nature des produits qui se Forment lors del'oxydation de l' ammoniac. *Bull. Soc. Chim. Fr,* 1938, **5**(5), 170-76.

252 Pearson, G.S. Perchlorates: A review of their thermal decomposition and combustion with an appendix on perchloric acid. RPE, Westcott. Tech. Report. No.68/11, 1968, pp. 67-76.

253 Rosser, W.A.; Inami, S.H. & Wise, H. Decomposition of ammonium perchlorate. 3rd ICRPG Combustion Conference, CPIA Publication, Vol.I, No.138, 1967, pp. 27-28.

254 Pellet, G.L. & Saunders, A.R. Mass spectrometric study of ammonium perchlorate at low pressure. 3rd ICRPG Combustion Conference, CPIA Publication, Vol.1, No.138, 1967, pp. 29-38.

255 Jacobs, P.W.M. Pearson, G.S. Mechanism of the decomposition of ammonium perchlorate. *Combustion and Flame,* 1969, **13**(4), 419-30.

256 Kishore, K. & Sankaralingam, S. Effect of pressure on the ignition of ammonium perchlorate. *Propellants, Explosives and Pyrotechnics,* 1985, 10, 158.

257 Demazeau, G.; Maestro, P.; Plante, T.; Pouchard, M. & Hagen Mullar, P. Generation of high oxygen pressure by the decomposition of oxidizing acids or ammonium perchlorate under hydrothermal conditions: application to the preparation of chromium oxide. High Pressure Sci., Technol. Proc. Zust., 7th AIRAPT Conf., 1979 (Publ. 1980), pp. 572-75.

258 Cohen, Nir, E. Effect of initial temperature on the burning rate and on the low pressure deflagration limit of ammonium perchlorate. La Recherche Aerospatiale, 1972, (2), 75-84.

259 Boggs, T. L.; Zurn, D.E. & Netzer, D.W. Ammonium perchlorate combustion: effects of sample preperation; ingredient type and pressure, temperature and acceleration environments. *Combustion Science and Technology,* 1973, **7**(4), 177-83.

260 Shannon, L. J. & Petersen, E.E. Burning velocity of ammonium perchlorate strand and crystals. *AIAA. J,* 1968, **6**(8), 1594-95.

261 Glaskova, A.P.; Zenin, A.A. & Balepin, A.A. Effect of the initial temperature on the characteristics of the combustion zone of ammonium perchlorate. *Arch. Procsow Spalania,* 1970, **1**(3-4), 261.

262 Glaskova, A.P. & Bobolev, V.K. Effect of temperature on the deflagration of ammonium perchlorate. *Explosifs,* 1971, **24**(2), 37-41.

263 Shannon, L.J. Effect of particle size and initial temperature on the deflagration of AP strands. Ph.D. Thesis University of Berkely, California, 1963.

264 Boggs, T.L.; Zurn, D.E. & Cordes, H.F. The combustion of ammonium perchlorate and various inorganic additives. AIAA 13th Aerospace Sci. Meet., Calif., AIAA Paper No.75-233, 1975, pp. 9.

265 Glaskova, A.P. Three possible ways to inhibit the ammonium perchlorate combustion process. *AIAA. J,* 1975, **13**(4), 438-42.

266 Shadman-Yazdi, F. & Petersen, E.E. The effect of catalysts on the deflagration limits of ammonium perchlorate. *Combustion Science and Technology,* 1972, **5**(2), 61-72.

267 Sankaralingam, S. The effect of pressure and temperature on the reactivity of composite solid propellants. Ph.D. Thesis, Indian Institute of Science, Bangalore, India, 1983, pp. 300.

268 Hightower, J.D. & Price, E.W. Combustion of ammonium perchlorate. 11th Symp. (Int.) on Combustion, The Combustion Institute, Pittsburgh, 1967, pp. 463-72.

269 Derr, R.L. & Boggs, T.L. Role of SEM in the study of solid propellant combustion 3. The surface structure and profile characteristics of burning composites propellants. *Combustion Science and Technology,* 1970, **1**(5), 369-84.

270 Boggs, T.L.; Kraeutle, K.J. & Zurn, D.E. Decomposition pyrolysis and deflagration of pure and isomorphous doped ammonium perchlorate, *AIAA. J*, 1972, **10**(1), 15-16.

271 Beckstead, M.W. & Hightower, J.D. Surface temperature of deflagrating ammonium perchlorate crystals. *AIAA. J*, 1967, **5**(10), 1785-90.

272 McGurk, J. L. Crystallographic changes in AP related to different rate of heating. Proc.of 3rd ICRPG Combustion Conf. Chemical Propulsion Information Agency, Laurel. Md., Pub. No.138, 1967, pp. 51-62.

273 McGurk, J.L. Microscopic determination of propellant combustion surface temperature. Proc. 1st ICRPG Combustion Instability Conf. Chemical Propulsion Information Agency, Laurel, Md., CPIA Publ. No.68, 1965, pp. 345-59.

274 Kishore, K.; Sridhara, K. & Sankaralingam, S. A thermodynamic protocol for explaining subcriticability and other subtle features in self-deflagrating solids. *Curr. Sci.*, 1995, **65**(5), 406-13.

275 Kishore, K. & Sridhara, K. A thermodynamic proposal for the exploration of criticability and other subtle features in self-deflagrating ammonium perchlorate systems. Proc. Roy. Soc. Lond. A 1993, 440, 55-76

276 Korobeinichev, O.P. & Kuibida, L.V. Study of condensed system flames by molecular beam mass spectrometry. Prog. Astronat. Aeronat., 1983, 88 (Flames, Lasers, React Syst.) 197-207.

277 Ermolin, N.E.; Korobeinichev, O.P.; Tereshchenko, A.G. & Fomin, V.M. Measurement of concentration profiles of reacting components and temperature in an AP flame. Fiz Goreniya. Vzryva, 1982, **18**(1), 46-49.

278 Ermolin, N.E.; Korobeinichev, O.P.; Teresheheuko, A.G. & Fomin, V.M. Kinetic calculations and mechanism determination for chemical reactions in an AP flame. *Fiz Goreniya Vzryva,* 1982, **18**(2), 61-70.

279 Ermolin, N.E.; Korobeinichev, O.P.; Tereshchenko, A.G. & Fomin, V.M. Modelling of the kinetics and mechanism of chemical reactions in an AP flame. Khim. Fiz., 1982, 12, 1711-17.

280 Freidman, R.; Levy, J.B. & Rumbel, K.E. The mechanism of deflagration of pure ammonium perchlorate. Atlantic Research Corporation, Alexandria, Virgina, AFOSR. TW59-173, AD 211313, 1959.

281 Chaiken, R.F. Implications of a steady state solid propellant combustion model to a low pressure deflagration limit. West states. Sect. Combust Inst., WSS/CI-69-5, 1969, pp. 10.

282 Freidman, R.; Nugent, R.G.; Rumbel, K.E. & Scurlock, A.C. Deflagration of ammonium perchlorate. 6th Symp.(Int.) on Combustion, Reinhold Publ. Corp., New York, 1957, pp. 612-18.

283 Krishnan, S. & Jeenu, R. Combustion characteristics of AP/HTPB propellants with burning rate modifiers. *J. Propul. Power*, 1992, **8**(4), 748-55.

284 Boggs, T.L. Deflagration rate, surface structure, and subsurface profile of self-deflagrating single crystals of ammonium perchlorate. *AIAA. J,* 1970, **8**(5), 867-73.

285 Bobolev, V.K.; Glaskova, A.P.; Zenin, A.P. & Leypunskii,O.I. A study of the temperature distribution in the combustion of ammonium perchlorate. Zh.Prikl Mekhi-i-Tekh. Fiz., 1964, (3) 153-58.

286 Shannon, L.J. & Petersen, E.E. Deflagration characteristics of ammonium perchlorate strands. *AIAA. J,* 1964, **2**(1), 168-69.

287 Watt, D.M.(Jr). Petersen, E.E. The deflagration of single crystals of ammonium perchlorate. *Combustion and Flame,* 1970, **14**(3), 297-312.

288 Levy, J.B. & Friedman, R. Further studies of pure ammonium perchlorate deflagration. 8th Symp.(Int) on Combustion, Williams and Wilkins, Baltimore, 1962, 663-72.

289 Glaskova, A.P. On influence of pressure on the combustion of ammonium perchlorate. Zh. Prikl. Mekh-i-Tekh. Fiz. SSSR, 1963, (5), 121-25.

290 Irwin, O.R.; Salzman, P.K. & Andersen, W.H. Deflagration characteristics of AP at high pressures. 9th Symp. (Int.) on Combustion, Ithaca, New York, 1962, pp. 358-65.

291 Cordes, H.F. Estimate of the melting point of ammonium perchlorate, *AIAA. J,* 1969, **7**(6), 1193-95.

292 Hermance, C.E. Phase transition line shift in ammonium perchlorate during quenching of burning single crystals. 7th JANNAF Combustion Meeting, Chemical Propulsion Information Agency, Laurel, Md., 1971.

293 Melik, Gaikazov, G.V. & Marshakov, V.N. Electrical conductivity of ammonium perchlorate. *Fiz.Goreniya Vzryva,* 1987, **23**(4), 15-20.

294 Powling, J. & Smith, W.A.W. The surface temperature of ammonium perchlorate burning at elevated pressures. 10th Symp.(Int.) on Combustion, The Combustion Institute Pittsburgh. Pa. 1969, pp. 1373-80.

295 Powling, J. & Smith, W.A.W. The surface temperature of burning ammonium perchlorate. *Combustion and Flame,* 1963, **7**, 269-75.

296 Zenin, A.A. Study of temperature distribution during combustion of condensed substances. Dissertation, Moscow, 1962.

297 Bobolev, V.K.; Glaskova, A.P.; Zenin, A.A. & Lupunskii, O.T. Temperature distribution in ammonium perchlorate when burning. Dokl. Acad. Nauk. SSSR, 1963, 151, 604-07.

298 Glaskova, A.P. & Bobolev, V.K. Effect of the initial temperature on the combustion of ammonium perchlorate. *Dokl. Akad. Nauk. SSSR.,* 1969, **185**(2), 346-48.

299 Maksimov, E.I.; Grigerev, Yu. M. & Merzhanov, A.G. Conditions and mechanism governing the combustion of ammonium perchlorate. Izv, Akad. Nauk. SSSR. Ser., Khim., 1966, (3), 422-29.

300 Watt, D.M.(Jr). & Petersen, E.E. Relationship between the limiting pressure and the solid temperature for the deflagration of ammonium perchlorate. *J. Chem. Phys.*, 1969, **50**(5), 2196-98.

301 Cohen, Nir, E. Experimental study of the low pressure limit for steady deflagration of ammonium perchlorate. *Combustion and Flame,* 1973, **20**(3), 419-35.

302 Strunin, V.A. & Manelis, G.B. Temperature coefficient of the burning rate of condensed substances. *Fiz. Goreniya Vzryva,* 1975, **I**(5), 797-99.

303 Friedman, R. & Levy, J.B. Research on solid propellant combustion, AFOSR Tech. Report No. 2005, Atlantic Res. Corpn., Alexendria, Virginia, 1961.

304 Boggs, T.L.; Petersen, E.E. & Watt, D.M. Comment on the deflagration of single crystals of ammonium perchlorate. *Combustion and Flame,* 1972, **19**(1), 131-33.

305 Johnson, W.F. & Nachbar, W. Deflagration limits in the steady linear burning of a monopropellant with applications to ammonium perchlorate. 8th Symp.(Int.) on Combustion, The Williams & Wilkins Co., Baltimore, 1962, pp. 678-89.

306 Waesche, R.H.W. & Wenograd, J. Calculation of solid propellant burning rate from condensed phase decomposition kinetics. AIAA, 7th Aerospace Sci. Meet., New York, 1969.

307 Sohn, H.Y.Closed form solution for the adiabatic laminar-flame theory applied to monopropellant burning rate. Chem. Eng. Commun., 1979, 3, 135.

308 Gordan, J.C. Model of AP self deflagration. Rech. Aerosp., 1982, 207, 101-7.

309 Steinz, J.A. & Summerfield, M. Propellants manufacture; hazards and testing. Amer. Chem. Ser., Washington DC. No.88, 1969, pp. 244-95.

310 Pai Verneker, V.R.; Kishore, K. & Gayathri, V. Thermal reactivity of ammonium perchlorate crystallized from solutions having different pH. *J. Appl. Chem. Biotechnol.*, 1978, 28, 660-62.

311 Kishore, K.; Pai Verneker, V.R. & Chaturvedi, B.K. Effect of preheating on thermal decomposition of ammonium perchlorate. *Ind. J. Technol.*, 1979, **70**(12), 483-85.

312 Sabadell, A.J.; Wenograd, T. & Summerfield, M. Measurement of temperature profile through solid propellant flame using fine thermocouple. *AIAA. J.*, 1965, (3), 1580-87.

313 Belyaev, A.F. & Lukashenya, G.V. Temperature coefficient of the rate of flameless combustion of a powder. *Zh. Fiz. Khim.*, 1966, **40**(9), 2066-70.

314 Kishore, K. & Sridhara, K. Effect of surface microstructure on the temperature sensitivity of burning rate of ammonium perchlorate. *Def. Sci. J.*, 1997, **47**(2), 177-84.

315 Boggs, T.L & Zurn, D.E. Temperature sensitivity of the deflagration rate of pure and doped ammonium perchlorate. *Combustion Science and Technology,* 1972, **4**(5), 227-32.

316 Stacer, R.G. & Husband, M.D. Molecular structure of the ideal solid propellant binder. *Propellants, Explosives, Pyrotechnics*, 1991, **16**(4), 167-76.

317 Nazare, A.N.; Deshmukh, S.M.; Ghorpade, V.G.; Asthana, S.N. & Shrothri, P.G. Influence of crosslinking curatives on HTPB based binder and propellant system. *J. Polym. Mater.*, 1992, **9**(4), 321-23.

318 Bhagawan, S.S.; Prabhakaran, N.; Rao, S.S. & Ninan, K.N. Visco elastic behaviour of solid propellants based on various polymeric binders. *Def. Sci. J*, 1995, **45**(1), 17-23.

319 Hartman, K.O. & Bohrer, E.K. Synthesis and characterization of PIB propellant binders. *Poly. Bull.* (Berlin), 1987, **18**(5), 403-10.

320 McGuchan, R. & Spickernell. CTPB cure studies-effect of experimental variables on epoxide cure and properties of gumstocks. *Propellants Explosives and Pyrotechnics,* 1976, **1**(2), 33-34.

321 Fukuma, D.; Shirota, K.; Suzuki, S.; Iwama, A. & Saitoh, A. Effect of HTPB polymer characteristics on propellant performance. Inst. Jahrestag-Fraunhofer-Inst. Treib-Explosivst, 1982, pp. 121-36.

322 Gusachenko, L.K. & Zarko, V.E., Analysis of contemporary models of steady state combustion of composite solid fuels. *Fiz. Goreniya, Vzryva,* 1986, **22**(6), 3-15.

323 Oberth, A.E. & Bruenner, R.S. Propellant manufacture testing and hazards. Amer. Chem. Ser., No.88, Washington DC, 1969, pp. 84-121.

324 Almeida, W.A. The utilization of a brazilian polymer acquired for solid propellant used in space vehicles. Inst. Pesqui. Espaniais. Report No. INPE-1473-RPE/024, 1979, pp. 20.

325 Krammer, A. & Reich, H.V. Study of the effect of binders on the combustion characteristics of composite solid propellants, Verbrennungs. Vorgaenge, Treib-Brennst., Jahrestag. Inst. Chem. Treib-Explosivst. Fraunhofer Ges., 1975 (Publ.1975), pp. 115-27.

326 Thomas, T.J.; Krishnamurthy, V.N. & Nandi, U.S. Thermogravimetric and mass spectrometric study of the thermal decomposition of PBCT resin. *J. Appl. Poly. Sci.,* 1979, **24**(8), 1797-808.

327 Powers, R.J. Rapid pyrolysis of polymeric solid propellant binders. (Georgia Institute of Technology, Atlanta, GA, USA), 1986, pp. 180, Diss. Abstr. Int.B, 1987, 47, (7), 3007.

328 Beck, W.H. Pyrolysis studies of polymeric materials used as binders in composite propellants: a review. *Combustion and Flame*, 1987, **70**(2), 171-90.

329 Varney, A.M. & Strahle, W.C. Thermal decomposition studies of some solid propellant binders. *Combustion and Flame,* 1971, **16**(1), 1-7.

330 Bouck, L.S.; Baer, A.O. & Ryan, N.W. Pyrolysis and oxidation of polymers at high heating rates. 14th Symp. (Int.) on Combustion, Penn. State. Univ., 1972 (Publ. 1973), pp. 1165-76.

331 Brazier, D.W. & Schwartz, N.V. The effect of heating rate on the thermal degradation of polybutadiene. *J. Appl. Polym. Sci.*, 1978, **22**(1), 113-24.

332 Chen, J.K. & Brill, T.B. Chemistry and kinetics of HTPB and isocynate-HTPB polymers during slow decompostion and combustion like conditions. *Combust.Flame*, 1991, **87**(3-4), 217-32.

333 Rabanovich, B. Regression rate and kinetics of polymeric degradation, 10th Symp. (Int.) on Combustion, 1965, pp. 1395-404.

334 Kishore, K. & Mohandas, K. Polymer gasification process: a thermodynamic approach. Ph.D thesis. Indian Institute of Science, Bangalore, 1984.

335 Kumar, R.N. Solid propellant combustion, lecturer notes for a short term course held at Vikram Sarabhai Space Centre, Trivandrum, India., Indian Institute of Science/ISRO Educational Programme, 1978, pp. 16-29.

336 Kumar, R.N. & Stickler, D.B. Polymer degradation theory of pressure sensitive hybrid combustion. 13th Symp. (Int.) on Combustion, The Combustion Institute, Pittsburgh, Pa., 1971, pp. 1059-72.

337 Ingredient list for JPL performance programme thermodynamic data. Tape No.1079, 1977.

338 Brandrup, J. & Immergut, E.H. Polymer hand book. Interscience Publishers, John Wiley & Sons, USA, 1966, pp. 373.

339 Karapetyants, M. Kh. & Karapet'yants, M.L. Thermodynamic constants of inorganic and organic compounds. Ann Arbor Humphrey Science Publishers, London, 1970, pp. 303-6.

340 Ninan, K. N. & Krishnan, K. Thermal decomposition kinetics of polybutadiene binders. *J. Spacecraft and Rockets,* 1982, **19**(1), 92-94.

341 Kishore, K.& Pai Verneker, V.R. Correlation between heats of depolymerization and activation energies in the degradation of polymers. *J. Polym. Sci. Letters,* 1976, 14, 761-65.

342 Kishore, K. & Bhanu, V.A. Maximum degradation rates in vinyl polymers. *J. Polym. Sci. Letters,* 1985, 23, 567-71.

343 Chaiken, R.F.; Anderson, W.H.; Barsh, M.K.; Mischuk, E.; Moe, G. & Schultz, R.O. Kinetics of the surface degradation of polymethylmethacrylate. *J. Chem. Phys.,* 1960, **32**(1), 141-46.

344 McAlevy III, R.F.; Lee, S.Y. Smith, W. Linear pyrolysis of Poly (Methylmethacrylate) during combustion. *AIAA. J,* 1968, **6**(6), 1137-42.

345 Hansell, J.G. & McAlevy III, R.F. Energetics and chemical kinetics of polystyrene surface degradation in inert and chemically reactive environments. *AIAA. J.,* 1966, **4**(5), 841-48.

346 Madorsky, S.L. Thermal degradation of organic polymers. Wiley (Interscience), New York, 1964.

347 Radhakrishnan, T.S.; Rao, M.R. Thermo-oxidative degradation of polybutadiene binders. *Prop. Explos.Pyrotech.,* 1995, **20**(1), 32-35.

348 Carvalheira, P.; Gadiot, G.M.H.; J.L. Klerk, W.P.C. Thermal decomposition of phase stabilized ammonium nitrate (PSAN) hydroxy terminated polybutadiene (HTPB) based propellants. The effect of iron (III) oxide burning rate catalyst Thermochemica. Acta.,1995, 269, (27), 273-93.

349 Adolph, H.G., Evidence for rate-determining C-C bond heterolysis in the condensed phase thermal decomposition of polynitroethyl compounds. *Combustion and Flame,* 1987, **70**(3), 343-47.

350 McAlevy III, R.F. & Hansell, J.G. Linear pyrolysis of thermoplastics in chemically reactive environments. *AIAA. J,* 1965, **3**(2), 244-49.

351 Price, E.W. Comment on thermal decomposition kinetics of polybutadiene binders. *J. Spacecraft and Rockets,* 1983, **20**(3), 320.

352 Kishore, K. & Nagarajan, R. Polymer combustion: a review. *J. Polym. Eng.*, 1987, **1**(4), 319-47.

353 Yano, Y. Miyata, K. Kubota, N. Sakamoto, S., Combustion wave structure of ammonium perchlorate composite propellants. Propellants, Explosives, Pyrotechnics, 1987, 12, 137-40.

354 Stacer, R.G.; Eisele, S.; Senreich, N.E.; Eisele, S. & Eisenreich, N. Polymer binders and the combustion of propellants. Int.Annn.Conf. ICT 1990, 21st (Technal.Polym.Compd.Energy.Mater.) Vol. 80, No.15, 1-80. Chem.Abstr 114, 26763y 1991.

355 Bazaki, H. Combustion mechanism of high energy composite propellant. *Kayaka Gakkaishi,* 1995, **56**(3), 105-11: Chem. Abstr., 123, 148303 e, 1995

356 Pfeil, A.; Krause, H.H. & Eisenreich, N. The consequence of beginning slow thermal decomposition on the molecular weight of nitrate cellulose. *Thermochimica Acta*, 1985, 85, 395-98.

357 Colodny, P.C. Degradation studies of polybutadiene type propellant binders by chomorheological techniques. Int-Jahrestag-Fraunhofer, Inst. Trieb-Explosivst, 1984, pp. 293-314.

358 Fong, C.W. & Hamshere, B.L. The mechanism of burning rate catalysis in composite HTPB-AP propellant combustion. *Combustion and Flame.* 1986, **65**(1), 61-90.

359 Anikeev, V.I.; Korobeinichev, O.P. & Shuneleev, A.S. Combustion of heterogeneous system with constituents capable of evaporating in the condensed and gas phases. *Fiz. Goreniya Vzryva,* 1979, **15**(2), 80-88.

360 Xu, W.; Li, J.; Li, B. & Wang, K. Covering of the molten binder over the oxidizer surface. Combustion and Detonation Phenomena 1988, pp. 66-113.

361 Trubert, J.F.. Analysis of the degradation gases of energetic binders in the condensed phase. La Recherche Ae'rospatiale, 1989, (2), 69-79.

362 Smith, J.M. Burning rates of solid propellants. *A.I.Ch.E. J.*, 1960, **6**, 299-304.

363 Jones, H.E. & Strahle, W.S. Effects of copper chromite and iron oxide catalysts on AP/CTPB sandwiches, 14th Symp. (Int.) on Combustion, Pittsburgh, Pa, 1972, pp. 1287-95.

364 Strunin, V.A.; Firsov, A.N.; Shkadinskii, K.G. & Manelis, G.B. Stationary combustion of decomposing and evaporating condensed substances. *Fiz.Goreniya Vzryva*, 1977, **13**(1), 3-7.

365 Kishore, K.; Pai Verneker, V.R. & Sunitha, M.R. Thermal decomposition and combustion studies on KP/PS propellant systems, *AIAA. J,* 1980. **18**(8), 966-67.

366 Fishman, N. Surface exotherm during ignition of ammonium perchlorate, *AIAA. J.,* 1967, 5, 1500-01.

367 Wise, S. & Rocchio, J. J., The relationship between polymer decomposition and the thermal sensitivity of energetic materials. Org. Coat. Appl. Polym. Sci. Proc., 1982, 47, 130-35.

368 Kumar, K.K. Importance of surface reactions during radiation ignition of composite solid propellants. *Combustion and Flame*, 1985, **59**(1), 63-80.

369 Kishore, K. & Sankaralingam. S. Effect of pressure on polymer ignition. *J. Fire. Sci.,* 1986, **4**(2), 94-99.

370 Kishore, K. & Sankaralingam, S.; Nagarajan, R. & Mohandas, K. Some observatons on the ignition of composite solid propellants. *Def. Sci. J.,* 1995, **45**(3) 243-54.

371 Kishore, K.; Nagarajan, R. & Mohandas, K. Polymer ignition: a review. *Polymer. Eng. Reviews*, 1983, **2**(3), 257-93.

372 Kishore, K.; Mohandas, K. & Anna Kutty, K.S. ls gasification rate controlling step in polymer ignition. *Combustion Science & Technol.,* 1983, 31, 203-6.

373 Kishore, K. & Mohandas, K. Effect of additives on the ignition behaviour of polystyrene, *J. Fire Retardant Chemistry,* 1982, (9), 115-34.

374 Garn Butcher. A propellant response to cook off as influenced by binder type. 26th AIAA, SAE, ASME and ASEE Joint Propulsion Conference, Orlando, Florida, 1990, AIAA Paper No. 90-2524, p. 7.

375 Trubert, J.F., Analysis of the degradation gas of energetic binders in the condensed phase. La Recherche Aerospatiale, No. 2, 1989, 69-79.

376 Zhang, R. Thermal decomposition characteristics of binder and its effect on combustion behaviour of propellant. *J. Propulsion Technology*, 1988, 39-49.

377 Zhang, D. Systematical studies on thermal decomposition of HTPB. IAF, 39th International Astronautical Congress, Bangalore, India, IAF Paper No. ST-88-05, 1988, pp. 5.

378 Kubota, N.; Kuwahara, T.; Miyazaki, S.; Uchiyama, K. & Hirata, N. Combustion wave structure of ammonium perchlorate composite propellants. *J. Propul. Power*, 1986, **2**(4), 296-300.

379 White, K. J.; McCoy, D.G.; Doali, J.D.; Anugst, W.D. & Juhasz, A.A. Closed chamber burning characteristics of very high burning rate propellants. Int. Jahrestag. Fraunhofer-Inst. Trieb-Explosivst., 16th (Pyrotech. Basic. Prime. Technol. Appl.) 18/1-18/19, 1985.

380 Kuwahara, T. & Kubota, N. Combustion of RDX/AP composite propellant at low pressure. *J. Spacecraft Rockets*, 1984, **21**(5), 502-7.

381 Kraeutle, K.J.; Read, R.(Jr).; Atwood, A.I. & Mathes, H.P. Effect of binder type on aluminium combustion and aluminium oxide formation. CPIA Publication No. 308 (JANNAF Combust. Meet. 16th., V2; ADA 084681). 1979, pp. 225-36.

382 McGuhan, R. Spickernell. CTPB Cure studies- effect of experimental variables on epoxide cure and properties of gumtocks. *Propellants Explosives and Pyrotechnics*, 1976, **1**(2), 33.

383 Koenig, J.L. Chemical microstructure of polymer chains. John Wiley and Sons, New York, 1980, p. 1-2.

384 Kishore, K. & Sridhara, K. Influence of structure of polymeric fuels on the combustion behaviour of composite solid propellants. *Fuel*, 1996, **75**(7), 912-18.

385 Petrov, A.P. & Fomin, V.M. Combustion of mixed solid propellant under conditions of static mechanical tensile stresses. *Fiz. Govenya.Vzoyva* 1993, **29**(4), 20-28; Chem. Abstr., 1993, 119, 229463b,

386 Nazare, A.N.; Deuskarm, V.D.; Asthana, S.N. & Shrotri, P.G. Influence of characteristics of HTPB on mechanical properties and ballistic behaviour of composite propellants. *J. Polym. Mater.* 1993, **10**(3), 213-15.

387 Petrella, R.V. Mass burning rate and relative fire hazard of polymers and other fuels, Proc. Int. Conf. Fire. Saf., Vol.5, 1980, pp. 250-69.

388 Kuwahara, T. & Kubota, N. Low pressure burning of ammonium perchlorate composite propellants. *Combustion Science and Technology,* 1986, **47**(1-2), 81-91.

389 Ivanov, G.V.; Shibaev, G.I.; Komarov, V.F.; Boldyrev, V.V. Burning of mixtures of ammonium perchlorate and various organic substances. Fiz.Goreniya i Vzryva., 1967, p. 3, 315.

390 Cohen, N.S. Review of composite propellant burn rate modelling, AIAA Pap. No.79-0160, 1979, pp. 7.

391 Pai Verneker, V.R. & Rajeshwar, K. Effect of prior mechanical and thermal treatment on the thermal decomposition of orthorhombic ammonium perchlorate. *J. Solid State Chem.,* 1976, **17**(1-2), 27-33.

392 Manelis, G.B. Strunin, V.A. Mechanism and elementary theory of burning of composite solid propellants. Proc., Int. Symp. Space. Technol. Sci., 1975, pp. 97-104.

393 Pantoflicek, J. Lebr, F. Burning of solid propellant at low pressure, Sb-Ved. pr. Vgs.Sr. Chemikotechnol. Pardubice, 1970, 23, (Pt 2), 97-110.

394 Kaper, H.G.; Leaf, G.K.; Margolis, S.B. & Matkowsky, B.J. On non adiabatic condensed phase combustion. *Combustion Science and Technology,* 1987, **53**(4-6), 289-314.

395 Braginskii, V.I. & Bakhmam, N.N. Relation between the heat of gasification of fuels and the burning rate of condensed mixtures. *Fiz Goreniya Vzryva,* 1971, **7**(3), 376-79.

396 Brown, R.S.; Muzzy, R.J. & Steinle, M.E., surface reaction effects on the acoustic response of composite solid propellants. *AIAA. J,* 1968, **6**(3), 479-87.

397 Lengelle, G. Thermal degradation kinetics and surface pyrolysis of vinyl polymers. *AIAA. J,* 1970, **8**(11), 1989-98.

398 Nachbar, W. & Parks, T.M. A sandwich burner model for the composite solid propellant. LMSO, 2191, AFOSR, TNDD, 132-497, Calif., 1957.

399 Schultz, R.D. & Decker, A.D. Aerojet General Corporation, Report No.576, Vol.I., Azusa, Calif., 1952, pp. 6-10.

400 Chaiken, R.F. & Anderson, W.H. The role of binder in composite propellant combustion. Solid Propellant Rocket

Research. Prog. Astronaut. Rocketry, Academic Press, New York, Vol. I. 1960, p. 227-47.

401 Ebenezer, J.; Cole, R.B. & McAlevy, R.F. Steady state burning of ammonium perchlorate composite solid propellant. NJ1US Nat. Tech. Inform. Serv. A.D. Report No.73004, 1973, pp. 146.

402 Bernard, M.L.; Gistin, J.L. & Martin, J.L. Combustion of propellants based on ammonium perchlorate. C.R. Acad. Sci. Soc., 1971, **272**(26), 2122-115.

403 Bernard, M.L. Formulation of the law of combustion velocity of composite explosives as a function of pressure. *C.R. Acad. Sci. Ser.,* 1971, **273**(25), 1700.

404 Rice, O.K. The theory of burning of rocket powders. US RD Report No.5574, 1955.

405 Hur, B.K. & Mok, Y.I. A new approach to the burning rate correlation of solid propellant. *Hwahak Konghak*, 1984, **22**(1), 51-58.

406 Horton, M.D. & Rice, D.W. Effect of compositional variables upon oscillatory combustion of solid rocket propellants. *Combustion and Flame*, 1964, **8**(1), 21-28.

407 Kerstein, A.R. Percolation model of polydisperse composite solid propellant combustion. *Combustion and Flame,* 1987, **69**(1), 95-112.

408 Beckstead, M.W. & McCarty, K.P. Modelling calculation for HMX composite propellants. *AIAA. J.*, 1982, **20**(1), 106-15.

409 Beckstead, M.W. A model for solid propellant combustion. 18th Symp. (Int). Combustion, Waterloo, Canada, 1980, pp. 175-85.

410 Cohen, N.S. & Strand, L.D. An improved model for the combustion of AP composite propellants. *AIAA.J.*, 1982, **20**(12), 1739-46.

411 Strunin, V.A.; Firsov, A.N.; Shkadinskii, K.G. & Manelis, G.B. Combustion regimes of volatile substance decomposing in condensed and gas phase. *Fiz Goreniya Vzryva,* 1986, **22**(11), 40-47.

412 Barton, T.J.; Griffiths, T.T.; Charsley, E.L. & Rumsey, J. The influence of binders pyrotechnic reactions. II. Titanium-oxidant systems, 9th Proc. Int. Pyrotech. Semin., 1984, pp. 743-58.

413 Bernard, M.L.; Brassy, C. & Boyset, E. Study on properties of explosive active molecules in an active state part.IV. Activation volumes and molecular structures. *Explosifs,* 1981, **34**(3), 50-55.

414 Afamanenko, M.E.; Pikhienko, V.V.; Taisumov, Kh.A. & Taradaiko, V.P., Effect of the molecular size and structure of combustible on the fire extinguishing effectiveness of powder composition, Gorenie. Probl. Tushomiya, Pozharon, Mater. Vscs. Nainchno-Prokt. Konf., 7th, 1981, pp. 32-35.

415 Barton, T.J.; Griffiths, T.T.; Charsley, E.L. & Ramsey, J. The role of organic binders in pyrotechnic reactions, Proc. Int. Pyrotech. Semin., 8th, 1982, pp. 83-98.

416 Barton, T.J.; Griffiths, T.T.; Charsley, E.L. & Ramsey, J., The influence of binders in pyrotechnique reaction, *1n.* Magnesium-oxidant systems, Proc. Int. Pyrotech. Semin., 9th, 1984, pp. 723-41.

417 Burnside, C. H. Correlation of ferric oxide surface area and propellant burning rate. AIAA Paper. No.75-234, 1975.

418 Kishore, K.; Pai Verneker, V. R. & Sunitha, M.R. Effect of catalyst concentration on the burning rate of composite solid propellants. *AIAA. J,* 1977, **15**(11), 1649-51.

419 Pittman, C.U. Location of action of burning rate catalysts in composite propellant combustion. *AIAA. J,* 1969, **7**(2), 328-34.

420 Handley, J.C. An experimental investigation of catalysis in the combustion of composite solid propellants (Georegia Inst. Technol. Atlanta, GA) Microfilms, No.76-16, 449, 1976, pp. 214.

421 Dyagileva, L.M. & Andreev, B.Ya. Products of the thermal decomposition of ferrocenes. Tr. Khim. Khim. Tekhnol., 1973, 2, 126-27.

422 Glaskova, A.P. & Popova, P.P. Inhibitors of the burning of ammonium nitrate, ammonium perchlorate and their mixtures. *Dokl. Akad. Nauk. SSSR.,* 1967, **177**(6), 1341-44.

423 Kishore, K.; Pai Verneker, V.R.; Pitchaiah, K. & Sridhar, K. Mechanisms of catalyst activity of metal oxides and chromites on ammonium perchlorate pyrolysis. *Fuel,* 1986, **65**(8), 1169-71.

424 Dubey, B.L.; Singh, G. & Shukla. C. Effect of copper chromite and copper chromate/copper oxide mixture catalyst on the

thermal decomposition of ammonium perchlorate and composite solid propellant. *Fuel,* 1982, **61**(2), 929-32.

425 Langlet, A., Sanden, R. Ostermark, H. Study of the effect of Fe_2O_3 on the degradation of HTPB. Int. Annn. Conf. ICT, 1991, 22nd (Comst. React. Kinet)1991, Vol.52, No.8, pp. 1-52.; Chem. Abstr 115, 235788 v,

426 Oyumi, Y.; Mitrasi, Y. & Bazaki, H. Thermal decomposition of AMMO/AP composite propellants. *Propell. Explos. Pyrotech.*, 1993, **18**(3) 168-72.

427 Santacesaria, E. Thermal decomposition of ammonium perchlorate in the presence of manganese dioxide. *Rivista dei. Combustibili,* 1973, **21**(10), 468-73.

428 Jacobs, P.W.M. & Russel-Jones, A. The thermal decomposition and ignition of mixtures of ammonium perchlorate and copperchromite. 11th Symp. (Int.) on Combustion. The Combustion Intitute, Discussion 462, 1967, pp. 457-61.

429 Pellet, G.L. Heterogeneous ammonium perchlorate decomposition using isothermal and pulsed laser mass spectrometry. *AIAA. J,* 1970, **8**(9), 1560-66.

430 Longachev, V.S.; Donitriev, A.S. & Pokhil, P.F. Mechanism of action of catalyst on ammonium perchlorate. Dokl. Acad. Nauk. SSSR, 1974, 214, 1113-16.

431 Kuratani, K. Some studies on solid propellants. *In* kinetics of thermal decomposition of ammonium perchlorate, Aeronautical Res. Inst., Univ. of Tokyo. Report, Vol.28, No.372, 1962, P. 79.

432 Solymosi, F. Revesz, L., Catalysis of reactions in solid phase: thermal disintegration of ammonium perchlorate in the presence of ferric oxide, kinetics and catalysis, 1963, **4**(1), 73-89.

433 Kishore, K.; Pai Verneker, V.R. & Sunitha, M.R. Effect of manganese dioxide on the thermal decomposition of ammonium perchlorate. *J. Appl. Chem. Biotechnol.*, 1977, **27**, 415-22.

434 Solymosi, F. & Dobo, K., The effect of impurities on the thermal decomposition and explosion of ammonium perchlorate. Magyar Kemaiai Folyoirat, 1966, (3), 124-29.

435 Korobeinichev, O.P.; Boldyrev, V.V.; Karpenko, Yu, Ya. & Lyakhov, V.Z., Rapidly proceeding processes during the thermal decomposition of ammonium perchlorate studied with

the aid of a time of flight mass spectrometer. Izv. Akad Nauk, SSSR, Ser. Khim., 1969, 4, 778-81.

436 Rosser, W.A.; Inami, S.H. & Wise, H. Thermal decomposition of ammonium perchlorate. *Combustion and Flame*, 1968, **12**(5), 427-35.

437 Yang, R. & Ma,Q. Catalytic combustion of ammonium perchlorate, Int. Annn. Conf. ICT 1990, 21st (Technol. Polym. Compd. Energ. Mater). Vol.82, No.8, pp. 1-82.; Chem Abst 114, 26765 a, 1991.

438 Rastogi, R.P.; Rao, A.P. & Syal, V. Unified model of catalysed and inhibited decomposition of ammonium perchlorate. *Combustion and Flame*, 1983, **51**(2), 177-82.

439 Rastogi, R.P.; Rao, A.P. & Syal, V. Mechanism of catalyzed and inhibited decomposition of ammonium perchlorate. *Indian J. Chem. Sect.A.*, 1986, **25A**(6), 521-25.

440 Ivashchenko, Yu. S.; Sadynin, A.L. & Pavlenko, V.L. Study of the electric conductivity of the combustion surface of AP. *Fiz. Goreniya Vzryva*, 1986, **22**(4), 30-33.

441 Shadman, Yazdi, F. Experimental and theoretical studies of combustion of solid fuels. Proceedings 1st Iranian Congress On Chemical Engineering., Arya Melv University of Technology, Teheran, 1973.

442 Shadman, Yazdi, F. Petersen, E.E., The effect of catalysts on the deflagration limits of ammonium perchlorate. *Combustion Science and Technology*, 1972, **5**(2), 61-67.

443 Shadman, Yazdi, F. Effect of catalysts on the pressure limits of ammonium perchlorate. Cah. Therm. 1974, 4, 47-50.

444 Mitani, T. A model for lower deflagration limit and burning rate of catalyzed ammonium perchlorate, *In*: mathematical modelling in combustion sciences. Proceedings of the Conference. Juneau, AK, 1987, (A89-36376 15-25) Berlin and New York, Springer-Verlag, 1988, pp. 78-89.

445 Boggs, T.L.; Zurn, D.E.; Cordes, H.F. & Covino, J. Combustion of ammonium perchlorate and various inorganic additives. *J. Propul. Power*, 1988, **4**(1), 27-40.

446 Al Fakir, M.S. & Joulan, P. Kinetics parameters of solid propergol combustion in flammable flow. Collog. Int. Berthelot-Vieilli-Mullard- LeChatelier [Actes] 1st, Vol.2, 1981, pp. 31-36.

447 AlFakir, M.S.; Joulan, P. & Most, J.M., Combustion of $LiClO_4$-NH_4Cl-NH_4ClO_4 solid mixtures. Prog. Astronaut. Aeronaut., 1983, 8 (Flames, Lasers, React Syst.), 167-81.

448 Landel, R.F. & Rembaum, A., (Eds) Chemistry in space research. American Elsevier Publishing Co., Inc. New York, p. 411.

449 Reich, L. & Stivala, S.C. Auto-oxidation of hydrocarbons and polyolefins. Marcel Dekker Inc., New York, 1969.

450 Kishore, K.; Polymer flame inhibition in presence of transition metal oxides. Colloid and Polym. Sci., 1979, **257**(9), 984-86.

451 Vuga, S. Effect of liquid combustion rate catalysts the thermal decompostion of AP-HTPB composite propellant. *Naucho-Tech. Pregl.,* 1992, **41**(10), 16-21.; Chem. Abstr 1992, 117, 174564 m.

452 Kishore, K. Mohandas, K. Oxygen index and flammability of polymeric materials: A review. *J. Sci. Ind. Res.*, 1983, **42**(2), 76-78.

453 Fong, C.W. & Hamshere, B.H. The mechanism of burning rate catalysis in composite propellants by transition metal complexes. *Combustion and Flame*, 1986, **65**(1), 71-78.

454 Martin, F.J. & Rice, K.R. Flammability of epoxy resins, *J. Appl. Polym. Sci.,* 1968, **12,** 143.

455 Fennimore, C.P. & Jones, C.W. Modes of inhibiting polymer flammability. *Combustion and Flame,* 1968, **10**, 295.

456 Kishore, K.; Pai Verneker, V.R. & Sunitha, M.R. Mechanistic studies on the pyrolysis and combustion of PS/AP propellant in the presence of transition metal oxides. *J. Anal. Appl. Pyrolysis,* 1980, **2**(2), 169-74.

457 Kishore, K.; Pai Verneker, V.R. & Sunitha, M.R. Action of transition metal oxide on composite solid propellants. *AIAA. J,* 1980, **18**(11), 1404-05.

458 Kishore, K. & Sunitha, M.R. Mechanism of catalytic activity of transition metal oxides on solid propellant burning rate. *Combustion and Flame,* 1978, **33**, 311-14.

459 Kishore, K. & Sunitha, M.R. Effect of oxidizer particle size on the burning rate and thermal decomposition of composite solid propellant. *Defence Sci. J.,* 1982, **32**(3), 251-57.

460 Krishna, S. & Periaswamy, C. Low pressure burning rate of catalyzed composite propellant,. *AIAA. J*, 1986, **24**(10), 1670-75.

461 Price, E.W. & Sambamurthi, J.K. Mechanism of burning rate enhancement by ferric oxide. CPIA. Publ. No. 412, 1984, pp. 213-31.

462 Ramaprabhu, R. & Bhaskaran, K.A. Role of catalyst on the ignition mechanisms of composite solid propellant. Energy Res., 1983, 3 (Altern. Energy Sources 5, Part D), 333-42.

463 Eisenreich, N. & Pfeil. A. The influence of copper and lead compounds on the thermal decomposition of nitrocellulose in solid propellants. *Thermochemica Acta* 1978, **27**, 339-46.

464 Kubota, N. Role of additives in combustion waves & effect on stable combustion limit of double-base propellants. *Propellants and Explosives*, 1978, **3**, 163- 68.

465 Hewkin, D.J.; Hicks, J.A.; Powling, J. & Watts, H., Combustion of nitric based propellants: ballistic modification by lead compounds. *Combustion Science and Technology,* 1971, 2, 307-27.

466 Lengelle, G.; Duterque, J.; Verdiar, C.; Bizot, A. & Trubert, J. Combustion mechanisms of double base solid propellants. 17th Symp.(Int.) on Combustion, 1978, pp. 1443-51.

467 Fifer, R.A. & Lannon, J.A. Effect of pressure & some lead salts on the chemistry of solid propellant combustion. *Combustion Flame,* 1975, 24, 369-80.

468 Kishore, K.; Sankaralingam, S.; Nagarajan, R. & Mohandas, K. Some observations on the ignition of composite solid propellants. *Def. Sci. J.,* 1995, **45**(3), 243-54.

469 Kishore, K.; Prasad, G. & Nagarajan, R. Flammability of polystyrene in the presence of transition metal ions. *J. Fire and Flammability*, 1979, **10**(4), 296-307.

470 Kishore, K. & Nagarajan, R. High temperature oxidative degradation of polystyrene in the presence of transition metal salicylates. (Unpublished results).

471 Inami, S.H.; Rajapakse, Y.; Shaw, R. & Wise, H. Solid propellant kinetics, Pt.1. The ammonium perchlorate-copper chromite fuel system. *Combustion and Flame*, 1971, *17*, 189-96.

472 Yoo, Y.J. Burning rate catalytic effect of ferric oxide and chromic oxide in composite propellants. Hwadhak Konghak, 1987, **25**(5), 442-46.

473 Pearson, G.S. The role of catalysts in ignition and combustion of solid propellants. *Combustion Science and Technology*, 1971, **3,** 155-63.

474 Nadaud, L. Model used at ONERA to interpret combustion phenomenon in heterogeneous solid propellants. *Combustion and Flame,* 1968, **12,** 177-95.

475 Zhang, R. An important role of condensed phase interphase reaction heat in combustion process of composite propellant. *J. Aerospace Power,* 1989, **4**, 286-88 & 296.

476 Krishnan, S. & Jeenu, R. Surface reaction model for catalysed composite propellant. *AIAA. J.*, 1992, **30**(11), 2788- 91.

477 Kishore, K. & Mohandas, K. Fire retardancy of polymers in the presence of ammonium phosphates. VI National Conf. on I.C. Engines and Combustion, IIT, Bombay, 1979, C307-13.

478 Kishore, K. & Mohandas, K. Effect of ammonium halides on the combustion of polystyrene. *J. Fire Sciences,* 1983, 1, 81-95.

479 Engen, T.K. & Johannessen, T.C. The effects of two types of iron oxide on the burning rate of a composite propellant. Int. Ann. Conf. ICT, 21st (Technol. Polym. Compl. Energ. Mater) Vol.81, No.12 , pp. 1-81.; Chem. Abst 1991, 114, 26764 Z,

480 Oyumi, Y.; Anan, T.; Bazaki, H. & Harada, T. Plateau burning characteristics of AP based azide composite propellants. *Prop. Explos. Pyrotechn.,* 1995, **20**(3), 150-55.

481 Kishore, K. & Mohandas, K. Mechanistic studies on the action of ammonium phosphate on polymer fire retardancy. *Combustion and Flame,* 1981, 43, 145-48.

482 Tonkai, T.; Iida, A. & Fugisawa, T. Burning rate reduction of ammonium perchlorate composite propellants. *Kogyo Kayaku,* Asahi Chem. Ind. Co. Ltd., Vol.51, No.5, pp. 286-91.; Chem. Abstr 1991, 114, 210014 f,

483 Suzuki, S. & Morimoto, K., Thermal analysis of ammonium perchlorate modified by adding the carbonates of alkali and alkaline earth metals and application of AP-HTPB -Al propellants containing SrCO3 and oxamide to 140 mm motor. *Kogyo Kayaka,* 1990, **51**(5), 292-301; Chem.Abstr 1991, 114, 210015 g,

484 Shen Shin-Ming; Chen, Sun-I. & Wu, Bor-Hormg. The thermal decomposition of AP containing burning rate modifiers. *Thermochem. Acta*, 1993, **223**(1-2), 135-43.

485 Yin, J.; Li, B.; Wang,W. & Chem, B. Combustion mechanism of a negative pressure exponent composite solid propellants. *J. Prop. Power,* 1992, **8**(1), 37-44.

486 Zhang, R. Lu,Z., Cao, F. Zhang, Y., Investigation on catalytic thermal decomposition of AP/HTPB composite propellant. *J. Propulsion Technology*, 1989, 46-51, 72.

487 Yum, Y.J. & Rho, M.K. Comparison of two burning rate catalysts, Fe_2O_3 and Cr_2O in composite propellant, *In* Combustion and detonation phenomena. Proceedings of the 19th International Annual onference of ICT, (A89-19501 06-28), Karlsruhe, FRG, 1988, pp. 73-1 to 73-9.

488 Zhang, W.; Zhn, H. & Zhang, R. Correlation between thermal decomposition and burning rate in AP/HTPB propellant. Int. Annn. Conf. ICT 1991 22nd (Combust. React. Kinet), Vol.62, No.6, pp. 1-62.; Chem.Abst. 115, 259397A

489 Harmoni, A. & Salmon, A. The catalytic decomposition of ammonium perchlorate. 8th Symp.(Int.) on Combustion, William and Wilkins Co., Baltimore, Md., 1962, pp. 656-62.

490 Stammler, M. & Schmidt, W.C. Oxidizer properties that affect combustion rate of solid propellants. Paper WSCI-66-26, The Combustion Institute, Pittsburgh, Pa. 1966.

491 Howard, B.C. & Powling, J. The use of the catalytic surfactants in plastic propellants. ERDE. Report No.TM/15/M/65, 1965.

492 Krishnan, S. & Jeenu, R. Subatmospheric burning characteristics of AP/CTPB composite solid propellant with burning rate modifiers. *Combustion and Flame*, 1990, **86**, 1-6.

493 Pearson, G.S.; Composite propellant catalyst: copper chromate and copper chromite. *Combustion and Flame.* 1970, **14**, 73-84.

494 Rosser, W.A.; Inami, S.H. & Wise, H. Kinetics of decomposition of ammonium perchlorate. Stanford Res. Inst., Manlopark, Report No.29, 1966.

495 Jones, H.E. & Strahle, W.C. Effect of copper chromite and iron oxide catalysts and AP/CTPB sandwich. 14th Symp.(Int.) on Combustion, The Combustion Institute, Pittsburgh, Pa, 1972, pp. 1287-95.

496 Iwama, A.; Hasue, K.; Takhashi,T.; Matsui, K. & Ishiura, K. Hydrogenated hydroxy-terminated polisopropane as a fuel binder for composite solid propellants. *Prop. Explos. Pyrotech.,* 1996, **21**(1), 43-50.

497 Strahle, W.C.; Handley, J.C.; Milkie, T.T. Catalytic effect in the combustion of AP/HTPB sandwich upto 3200 Psia. *Combustion Science and Technology,* 1974, **8**, 297-304.

498 Bakhman, N.N.; Genkin, M.V.; Kushnerev, M.Ya.; Labanov, I.N.; Sadanikov, V.V.; Sakhanov, M.M. & Slaskin, D.P. Variation of the dispersity and phase composition of a ferrous oxide catalyst in the burning of an ammonium perchlorate-poly (methylmethacrylate) mixture. Reaction Kinetics and Catalysis Letters, 1979, 13, 123-30.

499 Powling, J. & Smith, W.A.W. Measurement of burning surface temperature of propellant compositions by infra-red emissions. *Combustion and Flame,* 1962, 6, 173-81.

500 Wang, S.Y.; Wang, S.S.; Liu, F. Chiu, H.S. An investigation of catalysis in the combustion of iron catalyzed composite propellants. *In:* combustion and detonation phenomena. Proceedings of the 19th International Annual Conference of ICT, (A89-19501 06-28), Karlsruhe, FRG, 1988, pp. 8-1 to 8-14.

501 Bobolev, V.K.; Gen, M.Ya.; Maltsev, V.M., Melesov, G.P.; Pokhil, F.F.; Seleznev, V.A.; Stasenko, A.N. & Chuiko, S.V. Mechanism of action of iron containing catalytic additives on the burning of mixed composite systems. *Fiz. Goreniya Vzryva,* 1971, **3**(7), 366-75.

502 Nielsen, A.T. Monofunctional diferrocenyl compounds. US. Pat 3,878,233, 1975, pp. 4.

503 Wang, J.; Zhang, P.; Yang, Y.; He, Y. The comparison of volatility and migration of some derivatives of gem-bis (ferrocenyl) alkane. *J. Propulsion Technology,* 1990,.43-47.

504 Proebster, M.; Strecker, R.; Harrer, I. Improvement of the processibility of rapid burning composite propellant. Int. Jahrestag. Fraunhofer-Inst. Treib-Explosivst., 18th (Technol. Energ. Mater.) No.65/1-65/9, 1987.

505 Sarden, R. Extension of Pot Life of HTPB-Based Composite Propellants, Report No. FOA-C-20436-D1, 1982, pp. 27.

506 Ma, Q Liang, J., The effect of chemical structure of ferrocene derivatives on the burning rate of ammonium perchlorate. *Acta Armamentarii,* 1990, 51-57.

507 Huang, G.; Tang, S. & Ding, H. Recent advances in the research of ferrocene derivatives as burning rate catalysts. *J. Propulsion Technology,* 1989, 46-50, 75.

508 Iyanar, K.; Prema, S. & Kishore, K. Synthesis and characterisation of ferrocene bonding agents. *J. Chem. and Eng. Data,* 1988. **33**(2), 220-21.

509 Kishore, K. & Rajalingam, P. The bonding ability and bonding site of a new ferrocene based silicon compound in composite solid propellants. *J. Poly. Sci., Poly. Lett.* Ed., 1986, **24**, 471-76.

510 Sayles, D.C. Propellant composition containing triferrocenyl methyl perchlorate as catalyst oxidzer. 1975, US 3,860,463., pp. 3.

511 Sayles, D.C., Solid propellant composition and method of modifying propellant burning rate using ferrocene derivatives. US. 3,447,981., 1969, pp. 2.

512 Huskins, C.W. & Thomas, A.T., Composite propellants with a difunctional modifier curing agent. US.3,781,179, 1971, pp. 3.

513 Van Landyut, D.C. & Ayers, O.E. Propellant composition with a ferrocene compound as bonding agent and ballistic modifier. US.3,765, 965., 1973, pp. 3.

514 Van Landyut, D.C. & Ayers, O.E., 1-Pyrrolidinyl methylferrocene, US, 3.955,410, 1975, pp. 3.

515 Stephens, W.D. & Ashmore, C.I. Solid propellant containing diferrocenyl ketone. US. 4,318,760, 1982, pp. 3.

516 Johnson, N.C.; Gotzmer, C. & Graff, M. Piperazine derivative of ferrocene potential propellant burning rate modifier. US. 351,711, 1982, pp. 9.

517 Ayers, O.E. & Van Landyut, D.C. 2-Ferrocenyl tetrahydrofuran. US.3,745,177., 1973, pp. 1.

518 Norris, W.P. Ferrocence derivatives as burning rate catalysts in solid rocket propellants. US. 3.968, 126., 1974, pp. 5.

519 Kishore, K.; Pai Verneker, V. R. & Varghese Dharumaraj, G. Crosslinking reactions of 1,1-bis(glycidoxy methyl) ferrocene with carboxyl-terminated polybutadiene and its wetting effect. *J. Poly. Sci., Poly. Lett.* Ed., 1984, **22**, 607-10.

520 Sayles, D.C. Combination burning rate catalysts and curing agents. US.3,762,969, 1973, pp. 3.

521 Propellants for rocket igniters. Nissan Motor Co., Ltd., Japan, Kokai Tokkyo Koho, JP.5864,298., 1983, pp. 7.

522 Nakamura, H.; Hatanakal S.; Hara, Y. & Osada, H. Studies of the thermal decomposition of AP, IV effect of n-butyl ferrocene or ferrocene on the thermal decomposition of AP. Kogya Kayaku, 1981, **42**(5), 309-15.

523 Vuga, S. Composite rocket fuels with high combustion rates. Naucno-Teh Progl., 1986, **36**(7), 13-16.

524 Corley, R.C. & Dewey, E.M. Use of 1,1'-Bis(1-glycidoxyalkyl) ferrocence in rocket propellants. US.3,874,957., 1975, pp. 8.

525 Reed, S.F.(Jr)Propellant composition using carboxyterminated copolymers of butadiene and ferrocene derivatives. US.3,813,302, 1974, pp. 2.

526 Reed, S.F.(Jr). Propellants containing copolymers of dienes and polymerizable ferrocenes or carborane compounds. US.3,813,304., 1974, pp. 3.

527 Stevens, T.E. & Reed, S.P.(Jr). Ferrocene containing monomers and copolyers. US.3,867,213., 1975, pp. 5

528 Baldwin, M.G., Hydroxyterminated copolymers of butadiene and acrylates. US.3,847,882, 1974, pp. 2.

529 Baldwin, M.G. & Reed, S.F.(Jr). Solid propellant with hydroxyterminated butadiene-ferrocenyl acrylate copolymer binder. US. 3,881,969., 1975, pp. 3.

530 Huskins, C.W. & Thomas, A.J.(Jr). Ferrocenyl hydroxybutenes, US.3,770, 786, 1973, pp. 2.

531 Gotzmer, C.(Jr). & Cziesla, M.J., Nonmigrating ferrocene containing solid propellant binders. US,4.168.362., 1976, pp. 4.

532 Len, A.L. & Wu, R.J. Formulation effects on the burning rate of aluminized solid propellants. *J. Propul. Power.* 1988, **4**(1), 22-26.

533 Tompa, A.S. DSC and TG study of the stability in vacuum of ferrocenyl compounds and their compatibility with ammonium perchlorate.. *Thermochemica Acta,* 1984, **77**(1-3), 133-50.

534 Kishore, K.; Prema, S.; Iyanar, K. & Pandurang , L.P. Mechanistic studies on the effect of ferrocene bonding agents in composite solid propellants. *Fuel,* 1994, **73**(10), 1583-93.

535 Kuwahara, T. Mechanism of n-butylferrocene catalyst action on burning rate of AP composite propellants. *Kogyo Kayaku,* 1986, **47**(2), 61-65.

536 Kishore, K.; Sridhara, K. & Rajalingam, P. Prediction of performance of burning rate catalysts: a group contribution approach. *Fuel,* 1993, **72**(6), 902-3.

537 Boyars C. Surveillance of solid propellant rockets. *J. Am. Rocket Soc.*, 1959, **29**, 148-50.

538 Volk. F. Determining the shelf life of solid propellants. *Propellants and Explosives*, 1976, **1**(3), 59-65.

539 Kelly, I.N. Propellant Manufacture, *In* hazards and testing. edited by F.G. Robert, (ACS, Washington) 1969.

540 Sbriccoli, E.; Saltarelli, R. & Martinuca, S. Comparison between accelerated and natural aging in HTPB composite propellant, *In*: environmental testing in the 90's. Proceedings of the 20th International ICT Annual Conference and 18th GUS Annual Technical Meetings, Karlsruhe, FRG (A90-2947611-28), 1989, pp. 15-1 to 15-9.

541 Suzuki, K.; Omura,I.; Iizuka,T. & Harda, T. Effects of aging on the mechanical properties of composite propellants. *Kogyo Kayaku,* 1969, **30**(3), 126-30.

542 Kuletz, E. & Pakulak, J.M,(Jr). Effects of thermal aging on a cast-composite propellant. U.S. Dept. Com., Office Tech. Serv., AD 291,792, 1962, pp. 18.

543 Nagatomo, M., Effects of space environment on the burning rate of composite propellants. *Kogyo kayaku,* 1969, **30**(3), 114-21.

544 Schedelbauer, F. report on the problems of determining the life-time of composite solid propellants and new results. Proceedings of the Institute Fur Chemie Der Trieb Und Explosivstoffe (ICT) Annual Conference, Karlsruhe, Germany, 1971 (Pub 1972), pp. 275-303.

545 Myers, G.E. Chemical structural aging effects. U.S.N.T.I.S, AD/A Report No. 000538/9GA, 1975, pp. 82.

546 Francis, G & Buswell, J. Service life prediction and testing of composite propellant rocket motors, *In*: Environmental testing in the 90's. Proceedings of the 20th International ICT Annual Conference and 18th GUS Annual Technical Meetings, Karlsruhe, FRG, (A90-2947611-28), 1989, pp. 12-1 to 12-14.

547 Probster, M. Service life extension of composite propellant grain by reducing the migration of plasticizer, *In*: environmental testing in the 90's; Proceedings of the 20th International ICT Annual Conference and 18th GUS Annual Technical Meetings, Karlsruhe, FRG,(A90-2947611-28), 1989, pp. 48-1 to 48-13.

548 Layton, L.H. Chemical aging effects on composite solid propellants. AIAA/SAF 11th Propulsion Conference, Anaheim/ California/ Sept. 29-Oct.1, 1975, AIAA Paper No. 75-1281, New York, USA.

549 Korobeinichev, O.P. & Anisiforov, G.I. Effect of an oxidant on the degradation rate of a polymer binder. *Fiz. Goreniya i Vzryva,* 1973, **9**(4), 599.

550 Rhyu, H.J.; Kim, K.Y.; Yim, Y.J. & Hwahak Konghak. Mechanical properties of CTPB propellant deteriorates on ageing. 1989, **27**(2), 183-187.; Chem. Abstr. 1990, 112, 219917u,

551 Kishore, K.; Pai Verneker, V.R. & Prasad, G. Mechanism of the oxidative degradation of the binder during ageing of composite solid propellants. *J. Appl. Polym. Sci.,* 1979, 24, 589-93.

552 Wewerka, E.M.; Loughran, E.D. & Williams, J.M. Effects of long-term storage at elevated temperatures on small cylinders of PBX 9501, Los Alamos Sci. Lab., N. Mex., Report No. LA-6302-MS, 1976, pp. 15.

553 Kishore, K.; Pai Verneker, V.R. & Prasad, G. Effect of storage temperature on the mechanical properties of composite solid propellants. *Combustion Science and Technol.,* 1979, **19**(7), 107-13.

554 Kishore, K. & Sankaralingam, S. Studies on the pyrolysis of composite solid propellants leading to ignition. *Def. Sci. J.* 1987, **37**(3), 333-38.

555 Milena, N., Useful life of composite rocket fuels. *Naucno-Tech. Pregl.,* 1982, **31**(1), 33-38.

556 Prasad, G.; Kishore, K. & Verneker, Pai V.R. Proceedings of the 4th national conference on IC engines and combustion. 9-11 December 1977, Madras, India, Dec. pp. C4-7-14.

557 Okunaga, H.Y.I. & Nakamura, H. Aging effects on burning characteristics of ammonium nitrate composite propellants. *Kogyo Kayaku,* 1991, **52**(6), 406-11.; Chem. Abstr. 116, 109577h, 1992

558 Husband, D.M. Use of dynamic mechanical measurements to determine the aging behaviour of solid propellants. *Prop. Explos. Pyrotech.* 1992, **17**(4), 196-201.

559 Bunyan, P.; Cunliffe, A.V.; Davis, A. & Kirby, F.A. The degradation and stabilization of solid rocket propellants. *Polym. Degrad. Stab.*, 1993, **40**(2), 239-50.

560 Layton, L.H. Chemical aging studies on ANB-3066 and TP-H1011 propellants, AFRPL-TR-74-77. Final Technical Report, 1974, 53. Thiokol/Wasatch Division, Thiokol Corporation, Utah, USA,

561 Kishore, K.; Verneker, P.V.R.; & Vasantha Kumari, R. Curing reactions in plastic prepolymers and propellants, I. polystyrene. J.Applied Polym. Sci., 1979, 24, (7), 1603-08.

562 McGreedy, K., & Keskkula, H. Effect of thermal crosslinking on polybutadiene decomposition. *Polymer*, 1979, 20, 1155-59.

563 Kishore, K. & Vasanthakumari, R. Thermal crosslinking of CTPB', (Unpublished work).

564 Kishore, K.; Verneker, Pai V.R. & Dharumaraj, V.G. DTA studies on the thermal oxidative and thermal crosslinking reactions of CTPB. *J. Polym. Sci., Chem*, (Ed.), 1984, **22**, 1481-86.

565 Iwana, A.; Saito, T.; Yamaya, T.; Fujiko, T. & Matmi, K. Solid propellant based on hydrogenated hydroxyl terminated polyisopropene as a fuel binder prepolymer realizing high thermal stability performance. Int. Annn. Conf.ICT 1993 24th energetic materials insensitivity and environmental awareness, 14(1) 14-17.; Chem. Abstr., 120, 302688 f, 1994.

566 Iwama, A.; Takahashi, T.; Saito, T.; Hasur, K.; Matsui, K. & Yoneda. J. New fuel binder hyrogenated hydroxy terminated polyisopropene for composite propellents and plastic bonded explosives. 19th, Proc. Int. Pyrotech. Semin 1994, 276-87.; Chem. Abstr., 1995, 122, 34513x.

567 Kishore, K. & Nagarajan, R. High temperature degradation of polystyrene in presence of transition metal salicylates (Unpublished work).

568 Kishore, K & Begum, A.S. Studies on the aging behaviour of PVC/AP composite solid propellant. *Fuel*, 1989, **68**(11), 1476.

569 Kishore. K., Sankaralingam Begum, A.S. Studies on the aging behaviour of PVC/AP. *Fuel*, 1989, 68, 1476-82.

570 Munson, W.O & Reed, R, (Jr). Fifth specialist propulsion conference AIAA Paper No. 69-505, USAF Academy, Colorado Spring Co., 1969, AIAA, New York, USA.

571 Verneker, Pai V.R & Mohan, V.K. *Propellants and explosives*, 1977, **2**(6), 115-19.

572 Tsou, J.D. & Perng, H.C. Effect of aging at elevated temperature on relaxation modules of HTPB propellant. *Muryado Jishu*, 1991, **7**(3), 1-10.; Chem. Abstr., 1993, 119, 163542t.

573 Volk, F. Aging behaviour of solid propellants by measurement of heat evolution and stabilizer degradation, Symp. Chem. Probl. connected stab. Eplos., [proc] 8th, 1988, pp. 91-123.; Chem. Abstr. 113, 81629p, 1990.

574 Hamshree, B.L. & Rawson, P. Aging studies on a composite propellant containing a new organo-copper burn rate catalyst' Mater. Res. Lab Technical Note MR2-TN (Australia) MR2-TN-627, pp. 22.; Chem. Abstr. 119, 229475g, 1993.

575 Kishore, K.; Gayathri, V. & Dharumaraj, G.V. Effect of triethanolamine and benzaldehyde on the storage stability of polystyrene-ammonium perchlorate propellant. *Def. Sci. J.*, 1986, **36**, 389-94.

576 Yokoyama, A.; Sumi, K. & Kiname, S. Aging properties of carboxyl-terminated polybutadiene propellants. Part I. in Aging and Crosslinking Characteristics. *Kogyo kayaku*, 1978, **39**(4), 189-95.

577 Hinney, H.R & Murphy, J.R. Suppression of reactivity changes in poly BD, R - 45M. *In*: Environmental testing in the 90's; Proceedings of the 20th International ICT Annual Conference and 18th GUS Annual Technical Meetings, Karlsruhe, FRG, (A90-2947611-28), 1989, pp. 49-1-12.

578 Tang, H. An investigation of effects of styrene on the storage-mechanical properties of HTPB propellant. *J. Propulsion Technology*, 1988, 50-54.

579 Sarojini Devi; Kishore, K. & Verneker, Pai V.R. Role of aluminium-magnesium alloys in humid aging of composite solid propellants. *J. Propulsion Power*, 1989, **5**(4), 411-20.

580 Lee, W.G.; Tsai, J.Y.; Bai, G.C. & Chiu, H.S. The environmental effect on HTPB-AP propellant containing a quaternary ammonium salt modifier. *In* environmental testing in the 90's. Proceedings of the 20th International ICT Annual Conference

and 18th GUS Annual Technical Meetings, 1989, Karlsruhe, FRG, (A90-2947611-28), pp. 65-1-14.

581 Frankel, M.B.; Grant, L.R. & Flanagan, J.E. Historical development of glycidyl azide polymer. *J. Propul. & Power.*, 1992, **8,** 560-63.

582 Oyumi, Y.; Mitarai. & Bazaki, H. Thermal decomposition of AMMO/AP composite propellants. *Propellants Explosives & Pyrotechnics*, 1993, 18, 166-72.

583 Farber, M.; Harris, S.P. & Srivastava, R.D. Mass spectrometric kinetic studies on several azide polymers. *Combust. Flame,* 1984, 55, 203-10.

584 Oyumi, Y. & Brill, T.B. Thermal decomposition of energetic materials Infrared spectral and rapid thermolysis studies of azide containing monomers and polymers. *Combust. and Flame,* 1986 , 65, 127-35.

585 Chen, J.K. & Brill, T.B. Thermal decomposition of energetic materials 54: kinetics and near surface products of azide polymers AMMO, BAMO, and GAP in simulated combustion. *Combust. Flame,* 1991, 87, 157-68.

586 Suzuki, S. Composite propellants. Jpn. Kokai Tokkyo Koho JP 05,294,773 [93,294,773] (Cl.C06D5/00), 09 Nov.1993, Appl. 92/104,769, 23 Apr. 1992 ; 6 pp; Chem.Abstr., Vol.120, 1994, 274690e.

587 Bottaro, J.C.; Schmidt, R.J.; Renwell, P.E. & Ross, D.S. World intellectual property organization. International application number DCT/4s91/04268, December 26, 1991.

588 Johannessun, B. Hydroxyl-terminated epichlorohydrin polymers. U.S. patent 4,879,419, (Cl.568-606 ; C07C43/12) 07 Nov.1989, Appl. 750, 910, 01 Jul. 1985; Chem.Abstr ; Vol.112, 1990, 199408y.

589 Frankel, M.B. & Flanagan, J.E. Energetic hydroxy terminated azide polymers. Cand. Patent, 1,140,296, 25 Jan. 1983 ; and Aqueous process for the quantitative conversion of polyepichlorohydrin to glycidyl azide polymer. U.S. Patent, 4,379,894, 2 April, 1983.

590 Tokoui, H.; Saitosh, T.; Hori, K., Notono, K. & Iwama, A. Synthesis and physicochemical properties of glycidyl azide polymer (GAP) and the application of GAP/ammonium nitrate-based propellants to a small motor'; 21st Int. Annu. Conf.

ICT 1990 on Technol. Polym. Compd. Energ. Mater. 7/1-7/14 ; Chem. Abstr., Vol.114, 1991, 26751t.

591 Tokoui, H. & Iwama, A. Synthesis and characterization of glycidyl azide polymer. *Kogyo kayaku* 1990, **51**(4), 207-15 Japan ; Chem. Abstr., Vol.114, 1991, 188534b.

592 Nazare, A.N.; Asthana, S.N.; Singh, H. Glycidyl azide polymer (GAP) - an energetic component of advanced solid rocket propellants - a review. *J. Energ. Mater.*, 1992, **10**, 43-63.

593 Eroglu, M.S., & Guven, O. Thermal decomposition of poly (glycidyl azide) as studied by high temperature FTIR and thermogravimetry. J. *Appld. Polym. Sci.*, 1996, **60,** 1361-67

594 Nissan, R.A.; Chan, M.L.; Ciaramitaro, D.A.; Harris D.J.; Freyer, A.J. GAP analyses: NMR methods; Report 1993, NAWC-WPNS- TP-8127; Order No.AD-A270 611, pp. 16; Chem. Abstr., Vol.123, 1995, 203794t.

595 Brochu, S. & Amplemann, G. Synthesis and characterization of Glycidyl azide polymers using Isotactic and chiral poly(epichlorohydrin). *Macromolecules,* 1996, 29, 5539-45.

596 Ahad, E. Branched hydroxy-terminatd aliphatic polyethers having alkyl azide substituents; U.S. Pat. 4,882,395 (Cl.525-407 ; C08G65/24), 21 Nov.1989, CA Appl. 571, 721, 04 Jul 1988 , pp. 6 ; Chem. Abstr., Vol.112,1990,159265t.

597 Ahad, E. Branched hydroxy-terminated aliphatic azido ether polymers. PCT Int. Appl. WO 94 00,507 (Cl.C08G65/32), 06 Jan 1994, Appl. 92/CA267, 2 Jun. 1992 ; 36 pp; Chem. Abstr., Vol.121, 1994, 234056s.

598 Ahad, E. Branched hydroxy-terminated aliphatic polyethers. Eur. Pat. EP-A-0,350,226, 10 Jan.1990 ; and Cand. Patent, 1,300,171 5 May, 1992 ; U.S. Patent. 5, 130, 381, Preparation and use of branched hydroxy terminated azide rubbers, (Cl.525-407 ; C08G65/24), 14 Jul.1992, Appl. 680,927, 05 April 1991 (Chem. Abst. Vol.117, 1992, 113319p).

599 Ampleman, G.; Desilets, S. & Marois, A. Energetic thermoplastic elastomers based on glycidyl azide polymers with increased functionality. Proc. 27th Int. Annu. Conf. ICT 1996, on energetic materials, 132.1-132.12.; Chem. Abstr., Vol.125, 1996, 172448t .

600 Ampleman, G. 'Glycidylazide polymer for propellant binder'; Can. Pat. Appl. CA 2,052,728 (Cl.C08G65/24), 04 Apr 1993,

Appl.03 Oct 1991 ; 19pp ; Chem. Abstr., Vol.120, 1994, 11328k.

601 Wang, P.; Xia, Z.; Zhou, Y.; Li, C. `Investigation of high molecular weight GAP'. Proc.26th Int. Annu. Conf. ICT 1996, on energetic materials. 25.1-25.10 ; Chem.Abstr., Vol.125, 1996, 172463u.

602 Ampleman, G. & Beaupre, F. 'Synthesis of linear GAP-based energetic thermoplastic elastomers for use in HELOVA gun propellant formulations'. Proc. 27th Int. Annu. Conf. ICT 1996, on energetic materials; 24.1-24.11.; Chem. Abstr., Vol.125, 1996, 172462t.

603 Frankel, M.B.; Cunningham, M.A. & Wilson, E.R. Energetic glycidyl polymer azide. Brit. U.K. Pat. Appl. GB 2,285,624 (Cl. C07C247/04), 19jul 1995, US Appl.150,590, 01 Feb 1988; 9 pp. ; Chem. Abstr., Vol.123, 1995, 318126u.

604 Minora, H.; Kato, K.; Takano, Y. Azide containing polyethers as binders and plasticizers. JPN Kokai Tokkyo Koho JP 04,39,328, [9239,328] (Cl.C08G65/32), 10Feb 1992, Appl.90/146,287, 06 Jun.1990; Chem. Abstr., Vol.117, 1992, 49484j.

605 Bui, V.T.; Ahad, E.; Rheaume, D.; & Raymond, M.P. Energetic polyurethanes from branched glycidyl azide polymer and copolymer. *J. Appld. Polym. Sci,* 1996, **62,** 27-32.

606 Cao, Y.; Zhang, J. Study on the tetrahydrofuran copolymerized GAP binder. *Guti. Huojian Jishu,* 1997, 20, 45-50 ; Chem. Abstr., Vol.126, 1997, 295250a.

607 Flanagan, J.E.; Wilson, E.R. Glycidyl azide polymer esters as plasticizer of propellants. U.S. Pat 4,938,812 (Cl. 149-19.1; C06B45/10), 03 Jul 1990, Appl. 364,753, 12 Jun 1989 ; pp 2; Chem. Abstr., Vol.113, 1990, 155374a.

608 Pearson, D.; Lundgren,R. Glycidylazido polymer-containing energetically hardenable compositions. Swed. SE 503,997 (Cl.C06B45/06), 14 Oct.1996, Appl. 95/660, 22 Feb. 1995 pp. 1; Chem. Abstr., Vol.126, 1997, 77033r.

609 Zhang. X. & Cheng, X. Investigation of decomposition kinetics and reaction mechanism of organic azide polymer GAP. Proc. 17th. Int. Pyrotech. Semin. 1991, **1**, 542-6; Chem. Abstr., Vol.116,01992, 177220m.

610 Eroglu, M.S.; Guven,O. 'Thermal decomposition of poly (glycidyl azide) as studied by high temperature FTIR and thermogravimetry. *J. Appld. Polym. Sci.,* 1996, **61**, 201-06.

611 David Jones, E.G.; Malechaux, L. & Rainer Augsten, R. Thermal analysis of GAPTRIOL, an energetic azide polymer. *Thermochimica Acta,* 1994, **242**, 187-97.

612 Oyumi, Y. Thermal decomposition of azide polymers. *Propellants, Explosives, Pyrotechnics,* 1992, **17,** 226-31.

613 Ling, P.; Sakata, J.; Wight Charles, A. Detonation chemistry of glycidyl azide polymer. Proc. Mater. Res. Soc. Symp. Roc. 1996, pp. 363-71. Chem. Abstr., Vol.124, 1996, 236470h.

614 Hass, Y.; Eliahu, Y.B. & Welner, S. Characterization of shock waves in the decomposition of GAP by pulsed laser radiation. Proc. 25th Int. Annu. Conf. ICT 1994, on energetic materials-analysis, characterization and test techniques, 24/1-24/14; Chem. Abstr., Vol.122, 1995, 110197q .

615 Hommura, S.; Katoh, T.; Hori, K.; Hasebe, A. & Iwama, A. Plasma jet ignition and flame combustion wave propagation on the slab of glycidyl azide polymer (GAP). Proc. 22nd Int. Annu. Conf. ICT 1991, on Combust. React. Kinet., 46/1-46/15 ; Chem. Abstr., Vol.115, 1995, 235785s

616 Kubota, N. Sonobe, T. Yamamoto, A. & Shimizu, H. Burning rate characteristics of GAP propellants. *J.Propulsion,* 1990, **6**, 686-89.

617 Nokashita, G. & Kubota, N. Energetics of nitro/azide propellants. *Propellants, Explosives, Pyrotechnics,* 1991, **16,ss** 77-181.

618 Nakashita, G. & Kubota, N. Energetics of nitro/azide propellants; Proc. 21st Int. Annu. Conf. ICT 1990, on Technol. Polym. Compd. Energ. Mater.), 37/1-37/10 pp. 251-68; Chem. Abstr., Vol.114 , 1991, 46033p, pp. 251-68 .

619 Kubota, N.; & Sonobe, T. Burning rate catalysis of azide/nitramide propellants. 23rd Symposium (International) on Combustion/The combustion Institute, 1990, pp. 1331-37.

620 Shen, S.M. & Leu, A.L., Thermal characteristics of GAP, GAP/BDNPA/BDNPF and PEG/BDNPA/BDNPF and the energetic composites thereof. *Thermochimica. Acta,* 1991, **180,**251-68.

621 Leu, A.L.; Shen, S.M.; Wu, B.H.; Chen, S.I.; Yeh, H.C. & Bai, G.C. Thermal characteristics of GAP, GAP/BDNPA/BDNF, PEG/BDNPA/BDNF and energetic composites. 21st Int. Annu. Conf. ICT 1990., 6/1-6/14., Chem. Abstr., Vol.114, 1991, 26750s.

622 Shen, S.M.; Wang, S.W.; Chiu, Y.S.; Chen, S.I.; Chang, F.M. & Huang, C.C. Thermal decomposition of cured-GAP-AP propellants containing decomposition of cured GAP-AP propellants containing catocene. *Thermochimica Acta,* 1993, 126, 255-66.

623 Iwama, A.; Saito, T.; Yamaya, T.; Shimoda, M. & Hori, K. GAP/AN/AP/aluminium-magnesium propellants for low pollution and waste cost and their application to *Φ* 70mm motor; Proc. 23rd. Int. Annu. Conf. ICT. 1992, on Waste Manage. Energ. Mater. Polym. 26/1-26/14 ; Chem. Abstr., Vol.118, 1993, 1055902d.

624 Kato, K.; Nakashita, G. Burning rate characteristics of GAP/ AN propellant. *Kayaku Gakkaishi,* 1995, **56**(3), 130-34; Chem. Abstr., Vol.123, 1995, 174350n.

625 Duncan, E. J. S. Characterization of a glycidyl azide polymer composite propellant, strain rate effects and relaxation response. *J. Appld. Polym. Sci.,* 1995, 56, 365-75.

626 Volk, F. & Bathelt, H. Influence of energetic materials on the energy-output of gun propellants. *Propellants, Explosives, Pyrotechnics,* 1997, 22, 120-24.

627 Nagayama, K. & Oyumi, Y. Combustion characteristics of high burn rate azide polymer propellant. *Propellants, Explosives, Pyrotechnics,* Vol. 21, 1996, pp. 74-78.

628 Schedlbauer, F. Lova gun propellants with GAP binder. *Propellants, Explosives, Pyrotechnics,* 1992, **17**, 164-71.

629 Shyu, I.M.; & Liu, T.K. Combustion characteristics of GAP-coated boron particles and the fuel-rich solid propellant. *Combustion and Flame.* 1994, 634-44.

630 Lusby, C.A.; Ferguson, D.C. & Husband, D.M. Friction and impact of formulations containing glycidyl azide polymer. *Propellants, Explosives, Pyrotechnics,* 1995, **20**, 27-31.

631 Agrawal, J.P.; Walley, S.M. & Field, J.E. High speed photographic study of the impact response of ADN and GAP. *J. Propul. Power,* 1997, **13**, 63-470.

632 Zhang, Wei.; Zhu, Hui. Progress in research on AMMO azide polymer. Chem. Abstr., **125**, 1996, 118894x ,

633 Bazaki, H., Kai, T., & Anan, T. Combustion mechanism of high energy composite propellants. IV. Effect of energetic binders. Chem. Abst., Vol.127, 1997, 222622 j.

634 Kawasaki, H.; Anan, T.; Kimura, T. & Oyumi, Y. BAMO/NMMO copolymer with polyester initiation. *Propellants, Explosives, Pyrotechnics,* 1997, **22**, 87-92.

635 Bando, K.; Sato, K.; Inokami, K.; Kawasaki, T.; Yamazaki, K. & Matsumoto, K. '3,3-bis(azido methyl) oxetane (BAMO)- based propellants.1997, *In,* Synthesis and characterization of BAMO-based polymers. Chem. Abstr., Vol.114, 1991, 231541r .

636 Kimura, E.; & Oyimu, Y. Effects of copolymerization ratio of BAMO/NMMO and catalyst on sensitivity and burning rate of HMX propellant. *Propellants, Explosives , Pyrotechnics,* 1995, 20, 215-25.

637 Kimura, E.; Oyumi, Y.; Kawasaki, H.; Maeda, Y. & Anan, T. Characterization of BAMO/NMMO copolymers. *Propellants, Explosives, Pyrotechnics,* 1994, **19,** 270-75.

638 Kubota, N. & Miyazaki, T. Combustion and decomposition of azide polymers. Chem. Abstr. 1992, 116, 132284 u .

639 Gingho, H.; Yingling, L. & Yieshun, C. Triblock copolymers based on cyclic ethers preparation and properties of THF-BAMO triblock copolymers. *J. Polym. Sci.* Part A Polym. Chem, 1994, **32**, 2155-59.

640 Talukher, M.H.H. & Lindsay, G. K. Synthesis and the preliminary analysis of block copolymers of BAMO-NMMO. *J. Polym. Sci.* Part A Polym. Chem., 1990, 28, 2393-401.

641 Cheradane, H. & Gojon, E. Synthesis of polymers containing pseudohalide groups by cationic polymerization 2. Copolymerization of BAMO with substituted Oxetans containing azide group. *Macromol.Chem,* 1991, **192,** 919-29.

642 Xu, B.; Lillya, P. & Chen, J.C.W. Spiro (benzoxasilole) catalysed polymerization of oxetane derivatives. *J. Polym. Sci.* Part A Polym. Chem., 1992, 30, 1899-909.

643 Brill, T. B. & Brush, P. J. Condensed Phase Chemistry of explosives and propellants at high temperature: HMX, RDX and BAMO. Proc. Roy. Soc. Lond., A339, 1992, pp. 377-85.

644 Xu, B.; Lin,Y. G. & Chien, J. C. W. Energetic ABA and (AB)n thermoplastic elastomers. *J. Appld. Polym. Sci,* 1992, 46, 1603-11.

645 Hardenstine, K.E.; Henderson, G.V.S.; Sperling, L.H.; Murphy, C.J. & Manser, G.E. Crystallization behaviour of poly (3,3-bisethoxy methyl oxetane) and poly (3,3-bis azido methyl oxetane). *J. Polym. Sci.* Part B Physics. Ed, 1985, **23,** 1597-605.

646 Borman, S. Advanced energetic materials energy for military and space applications. *Chem. Engg. News*, 1994, 72, 18.

647 Oxley, J.C.; Smith, J.L.; Zhang, W.; Rogers, E. & Cobura, M.D. Thermal decomposition studies on ADN and 15N and 2H isotopomers, *J. Phys. Chem.*, 1997, A(101), 5646-52, and references therein.

648 Mebel, A.M.; Lin, M.C.; Morokuma, K. & Melins, C.F. Theoretical study of the gas phase structure, thermochemistry and decomposition mechanism of NH_4NO_2 and NH_4 $N(NO_2)_2$,. *J. Phys. Chem.,* 1995, 99, 6842-48.

649 Russel, T.P.; Piermarini, G.J.; Block, S. & Miller, P.J. Pressure temperature reaction phase diagram of ADN. *J. Phys. Chem.,* 1996, **100**, 3248-51.

650 Vyazovkin, S. & Wight, C.A. ADN: Kinetic and mechanism of thermal decomposition, *J. Phys. Chem.*, 1997, **A**(101), 5653-58.

651 Brill, T.B.; Brush, P.J. & Patil, D.G. Thermal decomposition of energetic materials 58. Chemistry of AN and ADN near the burning surface temperature. *Combust. and Flame,* 1993, **92**, 187-96.

652 Vyazovkin, S. & Wight, C.A. Thermal decomposition of ADN at moderate and high temperature. *J. Phys. Chem.,* **A**(101), 1997, 7217-21.

653 Politzer, P. & Seminario, J.M. Computational study of the structure of dinitramide acid (HN(NO2)2 and the energetics of some possible decomposition steps. *Chem. Phys. Lett.,* 1993, **216**, 348-52

654 Weiser, V.; Eisenerich, N.; Bayer, A.; Weindel, M. & Menke, K. Burning behaviour of ADN-mixtures. 28th Int. Ann. Conf. ICT 1997; Chem. Abstr., 1997, 127, 163977d

655 Louwers, J. Hydazinium nitroformate: a high performance next generation oxidizer. *J. Pyrotechnics,* 1997, **6**, 36-42.

656 William, G.K. & Brill, T.B. Thermal decomposition of energetic materials 67, hydrazinium nitroformate (HNF) rate and pathways under combustion like conditions. *Combust. Flame,* 1995, **102**, 418-26.

Index

ISBN: 81-86514-02-6

Defence Scientific Information & Documentation Centre
Defence Research & Development Organisation
Ministry of Defence
Metcalfe House, Delhi – 110 054
India